



This is to certify that the
dissertation entitled

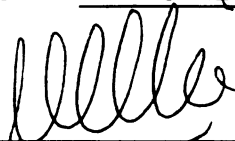
**INSTRUMENTED PERMEABLE BLANKETS FOR
ESTIMATING SUBSURFACE HYDRAULIC CONDUCTIVITY
AND CONFIRMING NUMERICAL MODELS USED FOR
SUBSURFACE LIQUID INJECTION**

presented by

MOUMITA MUKHERJEE

has been accepted towards fulfillment
of the requirements for the

Ph.D. degree in CIVIL ENGINEERING



Major Professor's Signature

12/9/08

Date

PLACE IN RETURN BOX to remove this checkout from your record.
TO AVOID FINES return on or before date due.
MAY BE RECALLED with earlier due date if requested.

DATE DUE	DATE DUE	DATE DUE

**INSTRUMENTED PERMEABLE BLANKETS FOR ESTIMATING
SUBSURFACE HYDRAULIC CONDUCTIVITY AND
CONFIRMING NUMERICAL MODELS USED FOR
SUBSURFACE LIQUID INJECTION**

By

Moumita Mukherjee

A DISSERTATION

**Submitted to
Michigan State University
in partial fulfillment of the requirements
for the degree of**

DOCTOR OF PHILOSOPHY

Civil Engineering

2008

ABSTRACT

INSTRUMENTED PERMEABLE BLANKETS FOR ESTIMATING SUBSURFACE HYDRAULIC CONDUCTIVITY AND CONFIRMING NUMERICAL MODELS USED FOR SUBSURFACE LIQUID INJECTION

By

Moumita Mukherjee

Recirculation of leachate into municipal solid waste landfills is routinely practiced to: (1) enhance waste settlement for gain in landfill volume; (2) increase landfill gas generation rate for cost-effective energy recovery; and (3) potentially reduced post closure maintenance and environmental liability period. In order to better design the leachate recirculation system and model hydraulics of landfills, numerical models are used. The key objectives of this dissertation included: 1) confirmation of numerical model predictions; and 2) develop a new method to estimate vertical hydraulic conductivity of the porous medium underlying an instrumented permeable blanket in real-time. A lab-scale physical model of a landfill (85 cm long x 30 cm wide x 55 cm high) was constructed and instrumented to simulate liquid recirculation system consisting of a permeable blanket. A 2-cm thick permeable blanket made up of pea gravel was built in the landfill model. Uniform fine sand, coarse sand and structured heterogeneous sand comprised of homogeneous blocks of fine, coarse and coarser sands were tested in separate experiments as porous media underlying the blanket. The blanket and the porous media below the blanket were instrumented with pressure transducers and water content sensors to monitor the migration of injected water in the blanket and in the underlying sand. Liquid injections in the blanket were carried out at flow rates ranging from 20 to 150 cm³/s in continuous or on/off modes. For continuous injection, it was observed that the initial wetted width of the blanket

gradually decreased as the degree of saturation of the underlying soil increased. The entrapped air bubbles influenced the pressure heads in the underlying sand(s) and the blanket. The air pressure exceeded the hydrostatic pressure at any point in the system during the liquid injection experiments. During continuous injection, the air pressures gradually decreased as injected water gradually removed or dissolved the air. The pressure heads in the blanket and the soil water content distributions predicted by HYDRUS-2D and Vadose/W, agreed relatively accurately with the data at steady-state when the entrapped air within the underlying sand was minimal. The single phase unsaturated flow models do not consider positive air pressures in the pores. The vertical hydraulic conductivity of the soil located below the permeable blanket was accurately estimated from an analytical approach termed ACRES (Analysis of Conductivity in Real-time using Embedded Sensors) using pressure heads measured in the blanket at steady-state during continuous injection. The horizontal hydraulic conductivity and the unsaturated hydraulic properties of the soil below the blanket have no effect on the vertical hydraulic conductivity estimated using ACRES. The vertical hydraulic conductivity of waste estimated through ACRES was found to be lower than the waste hydraulic conductivity in the presence of low conductivity cover soil layers in a simulated landfill.

Keywords: Bioreactor landfills, leachate recirculation system, permeable blanket, hydraulic conductivity, landfill model, instrumentation, HYDRUS-2D, Vadose/W.

DEDICATION

I thank God for giving me strength to complete this work.

*I dedicate this dissertation to my son - Soham Sinha, husband - Prantik Sinha,
parents - Dilip Kumar and Nibedita Mukherjee.*

*I also dedicate this thesis to all those women in my country who cannot pursue
their dream of higher education inspite of their huge potentials.*

ACKNOWLEDGMENTS

I am grateful to my husband Prantik and son Soham for their continued encouragement. I would not have been able to sustain this effort over the last four years, had it not been for their sacrifice and support.

More than anything else, I would like to extend my sincere gratitude and appreciation to my advisor, Dr. Milind V. Khire, for his mentoring, support and guidance, without which I would not have been able to complete this work. Dr. Khire not only helped me with his vast repertoire of knowledge and expertise, but also continuously inspired me to achieve more. His innovative inputs were critical to clearing roadblocks encountered during the work.

My special thanks to the members of my Ph.D. committee: Dr. Roger Wallace, Dr. Thomas Wolff, Dr. Farhad Jaber, and Dr. Xuede Qian for their valuable comments and suggestions during the whole research tenure.

My sincere appreciation goes to the Department of Civil and Environmental Engineering, Michigan State University, for partially funding my graduate tenure through assistantship and fellowship.

I am indebted to National Science Foundation, who funded this project work through their Grant No. CMS-0510091. I appreciate the support from Jason Ritter of Campbell Scientific for his programming help for the data acquisition system, and James Brenton and Mike Mclean for their help with the fabrication of the landfill model. I would also like to express sincere gratitude to Dr. Jirka Simunek for his input related to HYDRUS simulations and Dr. Greg Newman for his input related to Vadose/W simulations.

I also thank other faculty, colleagues, friends, and family who constantly supported me.

TABLE OF CONTENTS

LIST OF TABLES	xii
LIST OF FIGURES	xiii
KEY TO ABBREVIATIONS.....	xix
KEY TO SYMBOLS	xx
INTRODUCTION.....	1
BACKGROUND ON BIOREACTOR LANDFILLS	1
LEACHATE RECIRCULATION METHODS.....	2
NUMERICAL MODELS	3
FIELD-SCALE HYDRAULIC CONDUCTIVITY OF WASTE.....	4
Effect of Heterogeneity.....	4
Effect of Vertical Stress.....	5
Effect of Aging/Degradation	5
Effect of Gas	6
ESTIMATION OF HYDRAULIC CONDUCTIVITY	6
CONVENTIONAL METHODS FOR ESTIMATION OF HYDRAULIC	
CONDUCTIVITY	8
Field Leachate Pumping Test /Slug Test.....	8
Limitations	8
Borehole Permeameter Test.....	9
Limitations	9
Large-scale Percolation Test.....	9
Limitations	10
Large Diameter Permeameters in the Laboratory.....	10
Limitations	10
Analysis of Conductivity in Real-Time Using Embedded Sensors (ACRES)	11
Permeable Blanket Concept.....	12
Technical Approach.....	12
OBJECTIVES	13
METHODOLOGY	14
DISSERTATION ORGANIZATION	15
 PAPER NO. 1: LEACHATE INJECTION USING VERTICAL WELLS IN	
BIOREACTOR LANDFILLS	17
ABSTRACT.....	17
INTRODUCTION	18
BACKGROUND	19
NUMERICAL MODELING METHODOLOGY	21
HYDRUS-2D Computer Model	21
Conceptual Model and Assumptions	22
Boundary Conditions and Mass Balance.....	25

Design Parameters	26
Hydraulic Properties	27
Vertical Well Dimensions.....	29
RESULTS AND DISCUSSIONS.....	30
Liquid Pressure Head on Liner	31
Due to Injected Liquid	31
Due to Uniform Impingement of Percolation	38
Soil versus Geocomposite Drainage Layer.....	41
Wetted Width of Waste	42
Effect of Hydraulic Conductivities	42
Time to Reach Steady-State.....	45
Effect of Well Diameter, Screen Height, and Well Height.....	46
Effect of Hydraulic Conductivity of Drainage Pack.....	48
Transient Condition	49
Well Spacing.....	51
MODEL VALIDATION	51
Jain <i>et al.</i> (2005)	52
Haydar and Khire (2005)	53
SUMMARY AND PRACTICAL IMPLICATIONS.....	54

PAPER NO. 2: INSTRUMENTED LARGE SCALE SUBSURFACE LIQUID INJECTION MODEL FOR LANDFILLS

ABSTRACT.....	58
INTRODUCTION	59
OBJECTIVES	60
Field-Scale Testing of Permeable Blankets	61
MATERIALS AND METHODS.....	63
Model Dimensions.....	63
Waste Representation	66
Fabrication	66
Sensors in Landfill Model	66
Pressure Transducer	68
Water Content Sensors.....	68
Flow Sensor	69
Laboratory Testing and Calibration.....	70
Calibration of Pressure Transducers and Flow Sensor	70
Calibration of TDR Water Content Sensor	71
Signal Drift in Pressure Transducers	71
Pump.....	71
Materials	72
Saturated Hydraulic Conductivity.....	73
Soil Water Characteristics Curves	73
Fabrication of Instrumented Landfill Model	74
Leachate Collection System.....	74
Sand Layer Simulating Waste.....	74
Permeable Blanket	75
Falling Head Tests	76
RESULTS AND DISCUSSION	77

Effect of Hydraulic Conductivity of Underlying Soil on Pressure Head	77
Effect of Injection Rate on Pressure Head.....	79
Effect of Hydraulic Conductivity on Degree of Saturation	81
Effect of Injection Rate on Degree of Saturation	82
Effect of Hydraulic Conductivity and Injection Rate on Wetted Width	83
On/Off Dosing	86
SUMMARY AND PRACTICAL IMPLICATIONS.....	88

PAPER NO. 3: NUMERICAL MODELING OF SUBSURFACE INJECTION IN AN INSTRUMENTED LANDFILL MODEL91

ABSTRACT.....	91
INTRODUCTION	92
PHYSICAL MODEL.....	93
Landfill Components	95
Hydraulic Properties of Materials.....	95
Saturated Hydraulic Conductivity.....	95
Soil-Water Characteristic Curves	96
Unsaturated Hydraulic Conductivity	98
Instrumentation and Calibration	100
Pressure Transducer	100
TDR Water Content Sensor	101
Flow Sensor	102
Pump	102
Fabrication of Instrumented Model Landfill	103
Falling Head Tests	104
NUMERICAL MODEL.....	105
HYDRUS-2D and Vadose /W	105
Input Parameters for HYDRUS-2D.....	106
Mesh Discretization	106
Material Properties.....	107
Initial and Boundary Conditions.....	107
Other Input Parameters	108
Input Parameters in Vadose/W	109
Mesh Discretization	109
Material Properties.....	110
Initial and Boundary Conditions.....	111
RESULTS	111
Continuous Injection in Coarse Sand	111
Pressure Heads in Blanket	111
Water Content of Sand.....	114
Observed versus Simulated Results.....	115
Air Compression in the Physical Model	116
Effect of Entrapped Air Bubbles.....	117
Single Phase Approach	119
Supporting Experiments.....	120
Continuous Injection in Coarse Sand	129
Pressure Heads in Sand.....	129
Continuous Injection in Fine Sand	131

On and Off Dosing in Coarse Sand	134
PRACTICAL IMPLICATIONS	139
SUMMARY AND CONCLUSIONS	141

**PAPER NO. 4: INSTRUMENTED PERMEABLE BLANKETS FOR
ESTIMATION OF SUBSURFACE HYDRAULIC CONDUCTIVITY 144**

ABSTRACT.....	144
INTRODUCTION	145
ESTIMATION OF HYDRAULIC CONDUCTIVITY OF WASTE	147
Reported Field Studies.....	151
Analysis of Conductivity in Real-time using Embedded Sensors (ACRES)	152
OBJECTIVES	153
MATERIALS AND METHODS.....	154
Landfill Components	154
Hydraulic Properties of Materials.....	156
Saturated Hydraulic Conductivity.....	156
Soil-Water Characteristic Curves	156
Instrumentation and Calibration	158
Pressure Transducer	159
TDR Water Content Sensor	160
Flow Sensor	160
Pump	161
Fabrication of Model Landfill	161
Falling Head Tests	163
Vadose/W 2007 Numerical Model	163
Input Parameters for Numerical Model	164
Mesh Discretization	164
Material Properties.....	165
Initial and Boundary Conditions.....	166
Input Parameters for Field-scale Simulations.....	166
Conceptual Model.....	166
Material Properties and Assumptions	167
Mesh Discretization	169
Initial and Boundary Conditions.....	169
RESULTS	170
ACRES	170
Approach.....	170
Application to the Data from Landfill Model	172
Comparison with Falling Head Conductivities.....	175
Inverse Numerical Modeling	181
Tracer Test	184
Performance of ACRES Method	187
Numerical Simulation of Field Application of ACRES Method	190
Effect of Anisotropy Ratio.....	198
Effect of Unsaturated Properties of Waste.....	200
LIMITATIONS.....	202
SUMMARY AND CONCLUSIONS	204

**PAPER NO. 5: INSTRUMENTED PERMEABLE BLANKET FOR
ESTIMATION OF HYDRAULIC CONDUCTIVITY OF HETEROGENEOUS
SUBSURFACE.....206**

ABSTRACT.....	206
INTRODUCTION	207
Analysis of Conductivity in Real-time using Embedded Sensors (ACRES)	208
OBJECTIVES	209
Materials and Methods.....	209
Representation of Heterogeneity	211
Materials	213
Saturated Hydraulic Conductivity.....	214
Soil-Water Characteristic Curves	215
Instrumentation and Calibration	216
Pressure Transducer.....	216
TDR Water Content Sensor	217
Flow Sensor	217
Fabrication of Instrumented Model Landfill	218
LCS	218
Heterogeneous Subsurface Soils.....	218
Blanket	221
Falling Head Tests	221
NUMERICAL MODELS	222
HYDRUS-2D and Vadose /W	222
HYDRUS-2D Input	223
Mesh Discretization and Material Properties.....	223
Initial and Boundary Conditions.....	224
Other Input Parameters	225
Input Parameters in Vadose/W for Field-scale Simulations.....	225
Conceptual Model for Field Scenario	225
Material Properties and Assumptions	228
Mesh Discretization	230
Initial and Boundary Conditions.....	230
RESULTS AND DISCUSSION	231
Pressure Heads in Blanket Due to Continuous Injection.....	231
Homogeneous and Isotropic Sand	231
Heterogeneous and Isotropic Sand.....	234
Average Degree of Saturation of Sand Due to Continuous Injection.....	236
Homogeneous and Isotropic Sand	236
Heterogeneous and Isotropic Sand.....	237
Pressure Heads in Sand Due to Continuous Injection	240
Homogeneous and Isotropic Sand	240
Heterogeneous and Isotropic Sand.....	241
Pressure Heads in Blanket Due to On and Off Injection	243
Homogeneous and Isotropic Sand	243
Heterogeneous and Isotropic Sand.....	245
Average Degree of Saturation of Sand Due to On/Off Injection.....	247
Homogeneous and Isotropic Sand	247
Heterogeneous and Isotropic Sand.....	248

Pressure Heads in Sand Due to On/Off Injection	250
Homogeneous and Isotropic Sand	250
Heterogeneous and Isotropic Sand.....	251
Hydrostatic Pressure Heads in Sand	253
ACRES (Analysis of Conductivity in Real-time using Embedded Sensors)	255
Analytical Equations.....	256
Field-Scale Simulations	260
SUMMARY AND CONCLUSIONS	263
 SUMMARY AND CONCLUSIONS	 265
REFERENCES.....	267

LIST OF TABLES

Table 1-1:	Saturated and unsaturated hydraulic parameters input to HYDRUS-2D to simulate leachate recirculation system consisting of vertical well.....	24
Table 2-1:	Specifications of the sensors used in the landfill model	67
Table 2-2:	Grain size distribution and hydraulic properties of soils used in the landfill model.....	72
Table 3-1:	Saturated and unsaturated hydraulic properties of soils used in the landfill model.....	96
Table 4-1:	Previous studies reporting various methods used for estimating hydraulic conductivity of waste.....	148
Table 4-2:	Saturated and unsaturated hydraulic properties of soils used in the landfill model.....	158
Table 4-3:	Saturated and unsaturated hydraulic properties used in field-scale simulations.....	168
Table 4-4:	Comparison between the hydraulic conductivities estimated through ACRES and falling head tests.....	178
Table 5-1:	Saturated and unsaturated hydraulic properties of soils used in the landfill model.....	214
Table 5-2:	Saturated and unsaturated hydraulic properties for field-scale simulations.....	229
Table 5-3:	Comparison between heterogeneous and homogeneous sand.....	256
Table 5-4:	Comparison of hydraulic conductivities.....	258

LIST OF FIGURES

Figure 1-1:	Conceptual model for numerical simulation of leachate recirculation in municipal solid waste landfill using a vertical well: (a) cross section AA;' and (b) Plan view Section BB'.....	23
Figure 1-2:	Simulated shape of wetted areas for various degrees of saturation for a vertical injection well at steady-state.	32
Figure 1-3:	Simulated pressure head on the liner for a 17 m-deep single vertical well for leachate collection system slope equal to 3.5%.	33
Figure 1-4:	Simulated pressure head on the liner for a 17 m-deep single vertical well for leachate collection system slope equal to 10%.	34
Figure 1-5:	Simulated pressure heads on the liner as a function of leachate injection rate at steady-state for leachate collection pipe spacing equal to 30 m.....	36
Figure 1-6:	Simulated pressure heads on the liner as a function of vertical distance between the bottom of well screen and top of leachate collection at steady-state	36
Figure 1-7:	Simulated wetted width as a function of leachate injection rate at steady-state.....	43
Figure 1-8:	Simulated average injection pressure head versus leachate injection rate at steady-state.....	45
Figure 1-9:	Simulated increase in wetted width as a function of leachate injection flux.	46
Figure 1-10:	Effect of well diameter on wetted width at steady-state.	47
Figure 1-11:	Effect of screen height on wetted width at steady-state.....	47
Figure 1-12:	Effect of dosing frequency on wetted width for transient state.	50
Figure 1-13:	Simulated leachate flux at steady-state versus leachate injection pressure head for a horizontal trench for $k_w = 10^{-7}$, 10^{-6} and 10^{-5} m/s.....	54
Figure 2-1:	Responses of pressure transducers embedded in a field-scale blanket in Michigan showing increase or decrease in pressure heads.....	62
Figure 2-2:	Schematic of the lab-scale landfill model.	62
Figure 2-3:	Photo of the setup of the instrumented laboratory scale landfill model.....	65

Figure 2-4:	Sensors used in the landfill model	67
Figure 2-5:	Pressure heads in injection pipe, blanket, LCS and in fine sand simulating waste.....	78
Figure 2-6:	Decrease in pressure heads in blanket with increase in average degree of saturation.....	80
Figure 2-7:	Increase in average degree of saturation of underlying fine sand due to continuous injection.....	82
Figure 2-8:	Transient water content profiles in coarse sand due to continuous injection at: (a) 120 cm ³ /s; and (b) 150 cm ³ /s.....	83
Figure 2-9:	Wetted width at various injection rates in coarse sand.	84
Figure 2-10:	Simulation of on/off dosing cycles in the landfill model for a larger time interval.	87
Figure 2-11:	Snap shot of few on/off dosing cycles showing the pressure distribution in various sensors in the blanket.....	88
Figure 3-1:	Schematic of the lab-scale landfill model.....	97
Figure 3-2:	Soil-water characteristics curves for fine sand (a); and coarse sand (b).....	97
Figure 3-3:	Typical mesh used for modeling in HYDRUS-2D.	107
Figure 3-4:	Typical mesh used for modeling in Vadose/W.....	109
Figure 3-5:	Measured and HYDRUS-2D predicted pressure heads in the blanket due to continuous injection with coarse sand underlying the blanket.	112
Figure 3-6:	Measured and Vadose/W predicted pressure heads in the blanket due to continuous injection with coarse sand underlying the blanket. ..	113
Figure 3-7:	Measured and Vadose/W simulated water content at different depths within the coarse sand below the blanket due to continuous injection.	115
Figure 3-8:	Measured pressure heads in the blanket with coarse sand underlying the blanket: (a) with pre air injection; and (b) without pre air injection.....	121
Figure 3-9:	Measured pressure heads in the coarse sand underlying the blanket: (a) with pre air injection; and (b) without pre air injection.....	122

Figure 3-10:	Measured and simulated rise in water content in coarse sand due to an average upward injection rate of $95 \text{ cm}^3/\text{s}$	124
Figure 3-11:	Measured and simulated pressure heads in coarse sand due to an average upward injection rate of $95 \text{ cm}^3/\text{s}$	125
Figure 3-12:	Measured and estimated hydrostatic pressure heads from ponding events for: fine sand (a); and coarse sand (b).	127
Figure 3-13:	Measured hydrostatic pressure heads in coarse sand.	129
Figure 3-14:	Measured and simulated pressure heads at different depths within coarse sand underlying the blanket.	130
Figure 3-16:	Simulated and measured pressure heads in fine sand underlying the blanket for different injection rates.....	133
Figure 3-17:	Measured and numerically simulated average pressure heads in the blanket due to various rates of injection with fine sand underlying the blanket.....	134
Figure 3-18:	Measured and simulated: (a) peak pressure heads; and (b) snap shot of few cycles showing the pressure distribution in blanket due to on/off dosing cycles.	135
Figure 3-19:	Average pressure heads in the blanket for different dosing frequencies.	135
Figure 3-20:	Measured and simulated pressure heads with snap shot of few cycles showing the pressure distribution in blanket due to on/off dosing cycles with 100% saturation as initial condition.....	135
Figure 3-21:	Measured and simulated pressure heads with snap shot of few cycles showing the pressure distribution in sand due to on/off dosing cycles with 100% saturation as initial condition.....	139
Figure 3-22:	Measured pressure heads in the field-scale blanket in Michigan Landfill.....	141
Figure 4-1:	Hydraulic conductivity values for waste as estimated by various researchers.....	150
Figure 4-2:	Schematic of the lab-scale landfill model.	155
Figure 4-3:	Conceptual model for field-scale simulations (adapted from Haydar and Khire 2007).	167
Figure 4-4:	Measured pressure heads in blanket showing decrease in pressure heads with increase in average degree of saturation of underlying sand.	173

Figure 4-5:	Estimation of hydraulic conductivity function using ACRES method from continuous and on/off injection experiments for coarse sand.	177
Figure 4-6:	Ratio of K_{ACRES}/K_{FH} for various dosing frequencies for coarse sand.	181
Figure 4-7:	Estimation of hydraulic conductivity of underlying sand using inverse numerical simulation for continuous injection.	183
Figure 4-8:	Estimation of hydraulic conductivity of underlying sand through inverse numerical simulation for 6 min on and 10 s off injection duration.	184
Figure 4-9:	Breakthrough curve of tracer in fine sand.	186
Figure 4-10:	Correlation of the hydraulic conductivity values obtained from ACRES method, falling head tests, inverse numerical modeling, tracer tests and constant head permeameter tests.	188
Figure 4-11:	Hydraulic conductivity functions obtained from two models.	189
Figure 4-12:	Simulated wetted width and average pressure heads of injected leachate in field-scale blanket for various continuous leachate injection rates.	191
Figure 4-13:	For different injection rates and dosing frequencies: simulated average pressure heads in the blanket (a); the ratio of K_{ACRES}/k_w (b).	195
Figure 4-14:	Transient water content profiles in waste due to injection rates at: (a) 400 m ³ /d; and (b) 550 m ³ /d.	196
Figure 4-15:	Simulated time to reach quasi steady-state as a function of the initial degree of saturation of waste (S).	198
Figure 4-16:	Effect of anisotropy ratio on the ratio of K_{ACRES}/k_w	199
Figure 4-17:	Soil water characteristics of waste.	200
Figure 4-18:	Effect of unsaturated properties of waste on the ratio of K_{ACRES}/k_w	201
Figure 5-1:	Schematic of the lab-scale landfill model.	210
Figure 5-2:	Typical spatial distribution of hydraulic conductivities with stochastic parameters: $\lambda_x = 2$ m, $\lambda_z = 0.5$ m and $\sigma^2 = 0.42$	212

Figure 5-3:	Soil-water characteristics curves for all the soils in the landfill model.	215
Figure 5-4:	Photo of the structured heterogeneous soil below the blanket.....	219
Figure 5-5:	Schematic of structured heterogeneous sand.	220
Figure 5-6:	Conceptual model for field-scale simulations showing waste with no daily cover soil layers (adapted from Haydar and Khire 2007).	226
Figure 5-7:	Conceptual model for field-scale simulations showing waste with (a) continuous daily cover soil layers; (b) breached daily cover soil layers.	227
Figure 5-8:	Conceptual model for field-scale simulations showing waste with staggered breached cover soil layers.....	228
Figure 5-9:	Measured and simulated pressure heads in blanket in homogeneous coarse sand.	233
Figure 5-10:	Measured and simulated increase in water content of homogeneous sand due to continuous injection.....	233
Figure 5-11:	Measured and simulated pressure heads in blanket in heterogeneous sand	233
Figure 5-12:	Measured and simulated water content in different blocks of heterogeneous sand due to continuous injection.....	238
Figure 5-13:	Measured and simulated pressure heads within homogeneous sand.	241
Figure 5-14:	Measured and simulated pressure heads in various blocks of heterogeneous sand with different hydraulic conductivities.....	242
Figure 5-15:	Measured and simulated: (a) peak pressure heads; and (b) snapshot of few on/off cycles in blanket for homogeneous sand for 6 min on and 10 s off injection.....	244
Figure 5-16:	Measured and simulated: (a) peak pressure heads; and (b) snapshot of few cycles in blanket for heterogeneous sand for 6 min on and 10 s off injection.	246
Figure 5-17:	Measured and simulated water content of homogeneous sand due to 6 min on and 10 s off injection.	248
Figure 5-18:	Measured and simulated water content in different blocks of heterogeneous sand due to 6 min on and 10 s off injection.	249

Figure 5-19:	Measured and simulated pressure heads in homogeneous sand due to 6 min on and 10 s off injection.	250
Figure 5-20:	Measured and simulated pressure heads in different blocks [(a) and (b)] of heterogeneous sand due to 6 min on and 10 s off injection.....	252
Figure 5-21:	Comparison of measured versus estimated hydrostatic pressure heads at different locations in the heterogeneous sand due to static ponding.	254
Figure 5-22:	Equivalent overall hydraulic conductivity determination.	261
Figure 5-23:	Simulated wetted width and average pressure heads of injected leachate in blanket for various dosing frequencies.	261
Figure 5-24:	K_{ACRES} for various configurations of daily cover layers within waste for various dosing frequencies	263

KEY TO ABBREVIATIONS

RCRA	= Resource Conservation and Recovery Act
DI	= deionized water
GT	= geotextile
KCl	= potassium chloride
LCS	= leachate collection system
LR	= leachate recirculation
LRS	= leachate recirculation system
LRSs	= leachate recirculation systems
MSW	= Municipal solid waste
SWCC	= soil water characteristic curve
TDR	= time domain reflectometry
CS	= coarse sand
FS	= fine sand
DS	= driller sand
ACRES	= Analysis of conductivity in real-time using embedded sensors
HELP	= Hydrologic Evaluation of Landfill Performance
VW	= vertical well

KEY TO SYMBOLS

C_ψ = correction function and a , n , and m are the Fredlund Xing (1994) fitting parameters

C_c = coefficient of curvature

C_u = coefficient of uniformity

D_{50} = average particle size diameter

G_s = specific gravity

D = vertical depth of porous medium between the blanket and LCS

D_a = Apparent dielectric constant of soil used in Topp's equation

d = spacing between leachate collection system pipes

d_v = Distance between the bottom of the well and top of leachate collection system

d_w = Diameter of well

h_p = Head on the liner at steady-state condition for a single vertical well

h_m = measured hydraulic pressure head

h_{av} = arithmetic mean of pressure heads, h_m recorded by all the pressure transducers embedded in the blanket.

h_s = simulated hydraulic pressure head

h_{PB} = measured leachate pressure head in instrumented blanket in a real landfill in Michigan

H_i = Liquid injection pressure head

H_s = Screen Height

H_w = Well Height

$k(\psi)$ = unsaturated hydraulic conductivity as a function of matric suction head

k_{dp} = saturated hydraulic conductivity of vertical well drainage pack

k_{LCS} = saturated hydraulic conductivity of the drainage material in leachate collection system

k_w = saturated hydraulic conductivity of municipal solid waste

K_s = saturated hydraulic conductivity of soils used in the landfill model from falling head tests

$K_{cover\ soil}$ = saturated hydraulic conductivity of daily cover soil layers used in the field-scale simulations

K_z = equivalent vertical hydraulic conductivity

K_x = equivalent horizontal hydraulic conductivity

K_{eq} = resultant hydraulic conductivity

K_{ACRES} = saturated vertical hydraulic conductivity of underlying soil estimated from ACRES (Analysis of Conductivity in Real-time using Embedded Sensors) method

K_{Tracer} = saturated vertical hydraulic conductivity of underlying soil estimated from tracer test

K_{FH} = unsaturated hydraulic conductivity function from falling head test

K_w = saturated hydraulic conductivity of porous medium underlying the blanket used in numerical simulation

m_v = coefficient of volume compressibility

p_b = pressure in air bubble

p_w = pore-water pressure

p_a = pore-air pressure

r = radius of air bubble

T_s = surface tension of liquid.

v_s = advective seepage velocity

t = breakthrough time

n_e = effective porosity

i = hydraulic gradient

α = fitting parameter for van Genuchten (1980) fitting function for soil-water characteristic curve

m = dimensionless fitting parameter for van Genuchten (1980) fitting function for soil-water characteristic curve

n = dimensionless fitting parameter for van Genuchten (1980) fitting function for soil-water characteristic curve

q_i = Liquid impingement rate in Giroud's Equation

Q_s = Leachate flux that was injected over the entire screened portion of the well

Q = Injection rate in permeable blanket.

S = degree of saturation

S_w = Sink term in Richards equation

S_e = Effective degree of saturation

S_d = Screen Depth measured from the surface to the centre of the screen height

t = time

t_{LCS} = thickness of leachate collection system

W_w = Wetted width

z = vertical spatial dimension through the landfill model domain

β = slope angle of leachate collection system with respect to horizontal

ψ = matric suction head

θ = volumetric water content

θ_r = residual volumetric water content

θ_s = saturated volumetric water content

θ_m = measured water content

θ_s = simulated water content

Q = Injected flow rate

L = Length of the blanket parallel to the length of the injection pipe

ΔH = difference in total (elevation and pressure) heads at blanket and LCS

λ_x = correlation length of waste hydraulic conductivity in the horizontal direction

λ_z = correlation length of waste hydraulic conductivity in the vertical direction

σ^2 = variance in waste hydraulic conductivity

ρ_d = dry density

x = horizontal distance from the injection well along the liner.

x_{max} = horizontal distance from the watershed point.

INTRODUCTION

BACKGROUND ON BIOREACTOR LANDFILLS

In the United States and many other countries, landfilling is the most common method for the management of municipal solid waste (MSW). Conventional landfills in United States are designed and operated according to the regulations promulgated under Subtitle D of the Resource Conservation and Recovery Act (RCRA). RCRA requires minimizing the potential for groundwater contamination by encapsulating the waste in hydraulic barriers such as landfill liners and low permeability caps. Due to restriction to infiltration from the landfill cap, decomposition of waste entombed in the modern landfill proceeds at suboptimal rates and the waste may remain practically “intact” for long periods of time, possibly in excess of the life of the hydraulic barriers (Reinhart and Al-Yousfi 1996; Reinhart *et al.* 2002). This results in concerns for long-term environmental impacts from landfills.

In order to reduce long-term risks from landfills, waste degradation and stabilization can be enhanced when landfills are operated as bioreactors. The bioreactor landfill concept is to introduce water or recirculate leachate which stimulates the microbial activity for decomposition of the organic fraction of waste. The introduction of water and/or recirculation of leachate is relatively common (Pacey *et al.* 1999; Reinhart *et al.* 2002).

Leachate recirculation (LR) is an on-site leachate management alternative consisting of injecting leachate into MSW and collecting it using leachate collection system (LCS) located above the lining system at the bottom of the landfill. Leachate recirculation plays an important role in successful operation of the bioreactor landfill (Pohland 1980; Pohland *et al.* 1985; Chang and Gagnard 1995; Townsend *et al.* 1996; Miller and Emge 1997; El-Fadel 1999; Komilis *et al.* 1999; Warith 2002; Mehta *et al.*

2002; Morris *et al.* 2003; Hossain *et al.* 2003; Benson *et al.* 2007). In addition to potential reduction in the post-closure care period and associated maintenance costs, the expected benefits of bioreactor landfills are: (1) reduced leachate treatment costs (Pohland 1980; Reinhart *et al.* 2002); (2) reduced leachate strength (Barber and Maris 1983); (3) enhanced landfill gas production (Findikakis *et al.* 1988; Mehta *et al.* 2002); and (4) increase in the rate of MSW settlement (El-Fadel 1999; Hossain *et al.* 2003) resulting in an airspace gain and limiting potential for settlement-induced damage of the final cover (Benson 2000).

LEACHATE RECIRCULATION METHODS

Leachate recirculation or liquid injection can be performed using multiple techniques, both surface and subsurface. The surface methods consist of: (1) direct application of leachate or spray irrigation of leachate on the landfill surface; or (2) constructing leachate pond (Townsend *et al.* 1995; Landva *et al.* 1998; Warith 2002). Advantages of surface application include potentially uniform infiltration of leachate into the waste. Disadvantages of surface application include odor problems, direct leachate exposure and potential runoff of applied leachate into storm water management system.

The subsurface application techniques are: (1) vertical wells (Kilmer 1991; Merritt 1992; Watson 1993; Jain *et al.* 2005); (2) horizontal trenches (Reinhart and Carson 1993; Chang and Gagnard 1995; Maier and Vasuki 1996; Miller and Emge 1997; Townsend and Miller 1998); and (3) permeable blankets (Haydar and Khire 2006, 2007; Khire and Haydar 2007).

Due to the lack of specific design guidelines, design of the conventional systems is done on an ad hoc basis with no clear understanding of the effect of design

parameters on the long-term performance of the leachate recirculation system (Haydar 2005). Haydar and Khire (2005) and Haydar and Khire (2007) have presented design guidelines for horizontal trenches and permeable blankets, respectively, through numerical studies. There are no guidelines for vertical wells. Hence, in this dissertation, one of the tasks consisted of performing a numerical parametric study to provide specific design guidelines for subsurface leachate recirculation system consisting of vertical wells.

NUMERICAL MODELS

A number of models were developed to study the moisture movement within landfills such as hydrologic water routing (Schroeder *et al.* 1984), unsaturated flow models (Straub and Lynch 1982; Korfiatis *et al.* 1984) but none of these models are capable of providing essential insight into the design of leachate recirculation devices (McCreanor 1998). McCreanor & Reinhart (2000) employed a two-dimensional finite element model for groundwater flow and transport under saturated and unsaturated conditions (SUTRA) to model leachate recirculation in a landfill. Haydar and Khire (2005), Haydar and Khire (2007) and Khire and Mukherjee (2007) used saturated/unsaturated finite element model HYDRUS-2D to simulate the flow of injected leachate using horizontal trenches, permeable blankets and vertical wells for bioreactor landfills. Vadose/W is another common code which simulates water flow under unsaturated and saturated conditions by solving a modified form of Richards' equation. Khire and Mijares (2008) have used Vadose/W to predict the overall water balance of earthen caps. In this study, HYDRUS-2D and Vadose/W were chosen to mathematically simulate the hydraulics of landfill.

FIELD-SCALE HYDRAULIC CONDUCTIVITY OF WASTE

Powrie *et al.* (2000) and Stoltz and Gourc (2008) stated that one of the main uncertainties concerning the practicality of operating a landfill as a bioreactor is hydraulic conductivity of waste because it governs the ease with which liquids may be introduced into and extracted from landfill. Hence, knowledge of in-situ hydraulic conductivity of waste and an understanding of the factors that control it are essential.

Hydraulic conductivity is a property of porous medium which permits the passage of any fluid through its interconnecting pores. It is a function of both the fluid properties and the physical properties of the medium. The fluid properties of the leachate that affect the hydraulic conductivity of MSW are its viscosity and density which are functions of temperature of leachate. The physical properties that affect the hydraulic conductivity of MSW are particle shape, size and particle size distribution and characteristics of fissures and joints.

Effect of Heterogeneity

Ettala (1987) from his study on Lahti and Hollola landfills in Finland, reported variability in hydraulic conductivity between the two landfills and in different parts of the same landfill indicating the heterogeneity of MSW. Landfill operation practices such as, compaction of refuse in thin lifts (horizontal stratification), application of daily and intermediate cover, the type and thickness of cover material, watering prior to compaction of waste, daily variations in compaction and cell construction practices, and variations in MSW composition lead to anisotropy and heterogeneity (Korfiatis *et al.* 1984; Zeiss and Major 1993; Haydar and Khire 2004) within the landfill and therefore impact the hydraulic conductivity of the MSW.

Effect of Vertical Stress

As the landfill is filled vertically, immediate and time-dependent settlement of waste occurs. The compression of waste due to vertical stress leads to change in porometric structure and increase in density of MSW (Stoltz and Gourc 2008; Zekkos *et al.* 2008; Chen *et al.* 2008). Hydraulic conductivity decreases with decrease in pore size, with increase in density of MSW (Chen and Chynoweth 1995; Reddy *et al.* 2008) and with increase in the strain (Bleiker *et al.* 1995).

Increase in density increases effective stress on MSW (Powrie and Beaven 1999). The hydraulic conductivity of waste tends to decrease with increasing stress and burial depth in the landfill (Oweis *et al.* 1990; Bleiker *et al.* 1993; Bleiker *et al.* 1995; Landva *et al.* 1998; Powrie and Beaven 1999). The stress dependency of waste hydraulic conductivity has major implications for the operation of leachate extraction and recirculation systems, and basal and side slope drainage design which all influence the pore water pressure distributions within the waste body, and hence the effective stresses and shear strength (Dixon and Jones 2005).

Effect of Aging/Degradation

The waste deposited at different depths in a landfill is generally at different stages of degradation. Zhan *et al.* (2008) conducted laboratory tests which revealed that MSW deposited at different depths in the landfill have different values of hydraulic conductivity as a result of change in waste composition with depth – a decreasing trend with embedded depth. Hossain *et al.* (2008) indicated that with advance in degradation phase, the increase in percent of fines in the waste increases and hence increases the probability for fines to enter the pore spaces and thus increasing density and decreasing the hydraulic conductivity. Chen and Chynoweth (1995) also reported a time-dependent decrease in hydraulic conductivity of MSW.

Effect of Gas

Powrie *et al.* (2008) reported that gas accumulation can significantly reduce the hydraulic conductivity of waste, especially at lower pore water pressures. Merry *et al.* (2005) while analyzing the failure of Payatas landfill in Philippines, accounted for the excess pore pressure due to formation of gas within saturated MSW by considering that the linear increase in steady-state excess pore pressure distribution in combination with hydrostatic pressure can be replaced with the pressure exerted by pore fluid of equivalent unit weight. The authors reported that this equivalent unit weight of pore fluid increases significantly with decrease in hydraulic conductivity and stated the need to measure field-scale hydraulic conductivity of the waste to provide appropriate input for unit weight of pore fluid in slope stability programs.

The hydraulic conductivity varies spatially and temporally as a result of settlement, gas content, temperature, age and state of waste decomposition, and other operational variables (Oweis *et al.* 1990). It will be an important contribution to develop a method to measure and monitor changes in the field-scale hydraulic conductivities of landfilled waste and develop strategies to improve overall performance of bioreactor landfills and prevent catastrophic failures (Hendron 1999).

ESTIMATION OF HYDRAULIC CONDUCTIVITY

The proper assessment of field-scale hydraulic characteristics of the landfilled waste is important for:

1. Modeling leachate migration through waste (McCreanor 1998; Bou-Zeid and El-Fadel 2004);
2. Design of liquid injection system to achieve uniform and optimal wetting of the waste (Khire and Mukherjee 2007);

3. Design of an effective leachate collection system including the sizing of pump and leachate collection pipes;
4. Estimating the water balance of landfills to estimate the leachate generation rates and potential storage capacity of the waste. Water balance predictions are sensitive to hydraulic conductivity (Demetrocopoulos *et al.* 1986). A slight change in the magnitude of the hydraulic conductivity results in a relatively large change in the predicted leachate production rate or maximum head on the landfill liner (Khire *et al.* 1997; Giroud *et al.* 2000);
5. U.S. EPA's Hydrologic Evaluation of Landfill Performance (HELP) model that is most commonly used for modeling the water or leachate balance of a landfill requires hydraulic conductivity of waste as an input (Khire *et al.* 1997);
6. Estimating the maximum leachate pressure head on the liner and potential impacts related to uncontrolled migration of leachate on ground water quality (Oweis *et al.* 1990). The U.S. landfill regulations (Subtitle D) require that the maximum leachate head on the liner must not exceed 300 mm. It is only possible to accurately estimate the leachate head on the liner only if we know the representative hydraulic conductivity (Khire and Mukherjee 2007) and also monitor the changes in the hydraulic conductivity as the waste undergoes physical, chemical and biological changes; and
7. Analyzing failure related to slope stability, shallow slope liner stability, steep slope liner stability, leachate / gas wells integrity (Dixon and Jones 2005).

CONVENTIONAL METHODS FOR ESTIMATION OF HYDRAULIC CONDUCTIVITY

The conventional methods used for estimation of hydraulic conductivity of waste in the field and laboratory are as follows:

Field Leachate Pumping Test /Slug Test

Ettala (1987) conducted pump tests and applied Jacob's method to estimate the hydraulic conductivity of waste. Oweis *et al.* (1990) conducted pump tests at an unlined MSW landfill in New Jersey and used Theis method to estimate the hydraulic conductivity of waste. Shank (1993) conducted slug tests in flooded gas wells at an unlined MSW landfill in Florida and used Bouwer and Rice method to estimate the hydraulic conductivity of waste. Jang (2000) conducted pumping and slug tests in Kimpo landfill in Korea and employed all the above methods to estimate hydraulic conductivity of waste.

Limitations

- Sufficient water may not exist in the wells installed in the waste to represent conditions of saturated aquifer;
- Wells may penetrate zones of perched water which may form due to low permeability cover soils. Layers with low hydraulic conductivities such as daily cover soils, may lead to a significant amount of perched leachate within the waste (Koerner and Soong 2000; McCreanor and Reinhart 2000);
- Specific yield may not be representative of the waste as whole (Oweis *et al.* 1990);
- Gas pressures may represent additional driving force for flow of leachate to the wells;

- Horizontal flow through the upper layers of MSW which are of lower density due to lower overburden pressure may bias the estimations of hydraulic conductivity (Bleiker *et al.* 1993); and
- Difficulties can be encountered during monitoring of leachate levels due to gas flow into wells.

Borehole Permeameter Test

Jain *et al.* (2006) employed the borehole permeameter technique similar to that designed for measuring the hydraulic conductivity of a soil in vadose zone where a constant head of water is maintained in a borehole excavated into unsaturated media until a steady infiltration rate is reached.

Limitations

- Numerous point measurements are required to characterize the heterogeneity of waste;
- Gas phase is ignored in analysis. In reality, the production of gas impacts the liquid flow; and
- Clogging due to biological growth and waste decomposition during the relatively long time required to achieve steady-state can impact the measurements.

Large-scale Percolation Test

Townsend *et al.* (1995) applied Zaslavsky's method to estimate the hydraulic conductivity of waste for vertical flow through horizontal strata of waste of different hydraulic conductivities from infiltration pond at a landfill. Landva *et al.* (1998) constructed flow nets to evaluate the hydraulic conductivity of waste from the test pits in landfills at Canada.

Limitations

- Formation of hard-pan deposits can limit infiltration;
- Safety and air emission concerns; and
- These tests should be carried out during dry weather conditions to minimize interference from rain and storm water.

Large Diameter Permeameters in the Laboratory

Many researchers have determined the hydraulic conductivity of waste through laboratory tests (Korfiatis *et al.* 1984; Noble and Arnold 1991; Bleiker *et al.* 1993; Beaven and Powrie 1995; Chen and Chynoweth 1995; Landva *et al.* 1998; Jang *et al.* 2002; Olivier and Gourc 2007; Reddy *et al.* 2008; Hossain *et al.* 2008; Zhan *et al.* 2008). Laboratory determined hydraulic conductivity values for soils are often lower than those obtained in the field (Benson *et al.* 1997).

Limitations

- The size of the sample is often insufficient to represent the mean degree of heterogeneity of waste (Korfiatis *et al.* 1984; Zeiss and Major 1993; McCreanor and Reinhart 2000; Haydar and Khire 2004) and the effect of cover soil layers, fissures and stratifications (Shank 1993; Jain *et al.* 2006);
- The disturbance and decompression of the sample when retrieved from the field, formation of desiccation cracks thereafter and the method of compaction adopted in the laboratory, and changes in the pore structure of the sample may not be representative of field conditions (Oweis and Khera 1990);
- Anisotropy in hydraulic conductivity will yield erroneous values if the direction of flow in the laboratory does not correspond to the field flow direction (Oweis and Khera 1990);

- Smaller specimens do not adequately represent the network of pores controlling the field-scale hydraulic conductivity and hence erroneous conclusions can be drawn if these specimens are used to estimate the field-scale hydraulic conductivity (Benson *et al.* 1997). In the field, small zones of higher hydraulic conductivities govern the overall hydraulic conductivity of landfilled waste;
- Higher confining pressures and the use of much higher gradients in the laboratory are among the factors contributing to lower values for hydraulic conductivity of the waste sample tested in the laboratory (Oweis and Khera 1990); and
- Physical and biochemical processes keep the waste material as well as the entire landfill structure in a state of ongoing change. The conventional laboratory methods restrict the testing to the “same sample” as the waste ages to experimentally study the impact of various parameters.

Field tests integrate the effects of heterogeneity in MSW, discontinuities, irregularities etc., which are typical of landfills (Shank 1993). Hence developing field-scale methods to measure and monitor changes in the hydraulic conductivities of landfilled waste on a continuous and real time basis would be an appropriate contribution.

Analysis of Conductivity in Real-Time Using Embedded Sensors (ACRES)

Haydar and Khire (2006, 2007) developed the permeable blanket leachate recirculation system as an alternative to the conventional leachate recirculation methods. Haydar and Khire (2006) instrumented field-scale permeable blankets to demonstrate the hydraulic performance of permeable blankets for bioreactor landfills. They studied the feasibility of using an automated geotechnical sensing system

consisting of water content, temperature and pressure sensors to monitor the migration of recirculated leachate in permeable blankets. Three permeable blankets made up of crushed recycled glass (15 cm thick), shredded tires (60 cm thick), and a geocomposite drainage layer (0.5 cm thick), each of which is about 60 m long by 10 m wide, were installed at a landfill located in Jackson, Michigan in Summer 2003. Haydar and Khire (2006) and Haydar and Khire (2007) have reported the responses of the thermistor and pressure transducer sensors embedded in the glass blanket at 0.5, 4.5 and 14 m distances from the leachate injection pipe due to leachate injection events in the blanket and demonstrated that the pressure responses are a function of the underlying waste.

Permeable Blanket Concept

The permeable blanket consists of placing a relatively thin and high hydraulic conductivity material on a relatively flat waste surface in a landfill. A perforated pipe is embedded in the blanket in the direction parallel to the shorter or longer plan view dimension of the permeable blanket where leachate is injected under a positive pressure. The relatively high permeability of permeable blanket results in preferential travel of injected leachate within the blanket before the leachate infiltrates through the underlying waste. The blanket acts as an engineered heterogeneity and reduces the effect of spatial variation of waste properties when wetting the waste resulting in a relatively uniform distribution of leachate in the landfill.

Technical Approach

The inert permeable blanket if instrumented can be used as a platform to estimate the field-scale vertical hydraulic conductivity of waste in real-time which may eliminate the need to place sensors in waste. If the flow and distribution of water within a

landfill were uniform, then several point measurements would have been meaningful but preferential flow is (Zeiss and Major 1993; Zeiss and Uguccioni 1995; Rosqvist and Destouni 2000; Fellner *et al.* 2003) probably a dominant process in most landfills. Hence, it significantly decreases the value of point measurements. While the conventional methods used for quantifying water in the pore space work very well in soils, they typically produce inaccurate measurements when embedded directly in waste (Imhoff *et al.* 2003). Also, due to the heterogeneous nature of solid waste, the composition of material next to a probe will vary depending on the probe's location and development of separate calibration curves for each location is not feasible and a single calibration is inadequate.

Due to high transmissivity of the blanket, the sensors embedded in the blanket measure regional or average conditions within the landfill which are more representative of the overall average condition. Hence, the use of an instrumented permeable blanket was explored to measure the in-situ vertical hydraulic conductivity of waste. The changes in hydraulic conductivities of waste estimated continuously over a period of time could be potentially correlated with settlement, changes in bulk density and more.

OBJECTIVES

In order to use the instrumented permeable blanket as for estimation of hydraulic conductivity, the hypothesis was tested in the laboratory. Waste was not used and neither the factors affecting hydraulic conductivity of waste as discussed earlier were studied. The key objectives of this dissertation were to: (1) design a landfill hydraulic model for simulating hydraulic scenarios to improve the understanding of liquid injection or leachate recirculation systems for landfills; (2) confirm the numerical

models using data collected from the physical model in homogeneous and structured heterogeneous porous media; (3) develop a new method named Analysis of Conductivity in Real-time using Embedded Sensors (ACRES) for estimation of hydraulic conductivity using the pressure head and flow data from the sensors embedded in the blanket and evaluate both in laboratory scale and in field scale numerical simulations.

METHODOLOGY

Laboratory-scale tests were conducted in a large-scale physical model of a landfill to achieve the stated objectives. A transparent plexi-glass box for housing the landfill model was designed by simulating the landfill model in saturated/unsaturated numerical model HYDRUS-2D (Simunek *et al.* 1999). Preliminary numerical modeling was conducted to evaluate the sensitivity of pressure heads generated in the blanket and underlying porous medium to the hydraulic properties of the system for various magnitudes of rates of liquid injection, duration of injection, and frequency of liquid dosing, and initial conditions for steady-state as well as transient conditions. The landfill model was 85 cm long x 30 cm wide x 55 cm high. A 50 cm long x 30 cm wide x 2 cm thick horizontal permeable blanket made up of pea gravel was built in the model for subsurface liquid injection.

Homogeneous fine sand, coarse sand and a structured heterogeneous sand consisting of block shaped regions comprised of homogeneous fine, coarse and coarser sand were used as different porous media in separate setups. Total eight water content sensors and twelve pressure transducers were embedded in the blanket and underlying sand. Liquid injection in the blanket was carried out at varying rates ranging from 20 to 150 cm³/s either continuously or in on/off mode using a magnetic

drive pump or a gear pump. The injected flow was monitored by flow sensor and a pressure transducer. The data collected from the model (pressure head and flow) was used to study hydraulics of bioreactor landfills, to confirm numerical models that are commonly used to design various liquid injection systems and to develop the ACRES method.

DISSERTATION ORGANIZATION

This dissertation has been organized into five sections. Each section is written in the form of a technical paper.

The first paper presents a parametric study, using numerical modeling, for the design of vertical wells used for leachate recirculation. From this numerical study, it was observed that hydraulic conductivity is the key parameter that influences the key design parameters- the injection pressure and the wetted widths.

The second paper addresses the design of a lab-scale physical model of a landfill with an automated sensing system consisting of pressure sensors and water content sensors. The landfill model was able to mimic the responses from a field-scale instrumented permeable blanket and was able to demonstrate the findings from the numerical studies on leachate recirculation systems.

The third paper compares the measured responses of the sensors due to injection with numerically simulated pressure heads and water content using numerical models HYDRUS-2D and Vadose/W which are commonly used for subsurface injection studies. This paper assesses these models for sub-surface liquid injection.

The fourth paper presents the Analysis of Conductivity in Real-time using Embedded Sensors (ACRES) method developed for estimation of vertical hydraulic conductivity of porous medium underlying the blanket using pressure and flow data

from the sensors embedded in the blanket. The hydraulic conductivity estimated using ACRES method was independently confirmed by falling head tests, tracer tests and inverse numerical modeling. Field-scale simulations were carried out to study the applicability of ACRES method at field-scale. The effects of anisotropy, unsaturated hydraulic properties of waste, degree of saturation, injection dosing frequencies on the estimation of vertical hydraulic conductivity using ACRES were evaluated.

The fifth paper describes the structured heterogeneous porous medium in the landfill model and compares the hydraulics of flow between homogeneous and heterogeneous porous medium through experimental observations and numerical simulations. The hydraulic conductivity estimated using ACRES method was independently confirmed by falling head tests and analytical equations from soil mechanics. Field-scale simulations were carried out to simulate homogeneous and isotropic waste with different configurations of cover soil layers distributed within the waste of a simulated landfill. The vertical hydraulic conductivity of waste estimated through ACRES was lower than the waste hydraulic conductivity in the presence of low conductivity cover soil layers.

PAPER NO. 1: LEACHATE INJECTION USING VERTICAL WELLS IN BIOREACTOR LANDFILLS

ABSTRACT

Leachate recirculation or liquid injection in municipal solid waste landfills offers economical and environmental benefits. The key objective of this study was to carry out numerical evaluation of key design variables for leachate recirculation system consisting of vertical wells. In order to achieve the objective, numerical modeling was carried out using the finite-element model HYDRUS-2D. The following design parameters were evaluated by simulating liquid pressure head on the liner and the wetted width of the waste under steady-state flow conditions: (1) hydraulic conductivities of the waste and vertical well backfill; (2) liquid injection rate and dosing frequency; (3) well diameter, screen height and screen depth; and (4) hydraulic conductivity of the leachate collection system, slope of the leachate collection system and spacing of the leachate collection pipes. The key findings of this study are as follows. The well diameter, hydraulic conductivity of the well drainage pack, and screen height and screen depth of the well have very little effect on the wetted width for a given liquid flux. The wetted width and the injection pressure for a given liquid flux decrease with the increase in the hydraulic conductivity of the waste. The pressure head on the liner increases with the decrease in the vertical distance between the bottom of the well screen and the top of leachate collection system. The liquid injection flux increases with the decrease in hydraulic conductivity of the leachate collection system. Unlike sand ($k \sim 10^{-4}$ m/s), pea gravel ($k \sim 0.01$ m/s) resulted in less than 0.3 m pressure head on the liner for all simulations carried out in this study.

INTRODUCTION

Leachate recirculation is a leachate management alternative that is commonly used for municipal solid waste landfills. In most developed countries, environmental regulations require containment, collection, and treatment of leachate before it is released into the environment. Leachate recirculation operation consists of injecting leachate into municipal solid waste and collecting it using leachate collection system located above the lining system at the bottom of the landfill. Leachate recirculation offers many environmental and economical benefits (Mehta *et al.* 2002) to municipal solid waste landfills including: (1) reduction in leachate treatment and disposal costs; (2) greater flexibility in leachate management and treatment; (3) faster biodegradation of waste resulting in increased gas production and quicker waste stabilization and settlement; (4) reduction in the risk associated with contamination from spills during off-site transportation, treatment, and disposal of leachate; and (5) potential reduction in the post-closure care period of the landfill. Trucking and leachate treatment costs in the U.S. range from approximately \$5 to \$25/m³ (Leachator 2004). Depending upon size-specific volume of leachate, leachate recirculation can save hundreds of thousands of dollars for a typical medium size landfill over its design life.

Leachate recirculation also has few disadvantages. These disadvantages include (Haydar and Khire 2005): (1) reduction in the shear strength of municipal solid waste potentially reducing the factor of safety for slope stability of the landfill; (2) potential leachate breakouts from the sides of the landfill; and (3) increase in the liquid pressure head on the liner potentially increasing the risk for ground water contamination. Hence, designers and landfills owners are expected to weigh the advantages and disadvantages on a site-specific basis before a leachate recirculation system is implemented.

Leachate recirculation can be performed using multiple techniques. These techniques are divided into surface and subsurface application (Haydar and Khire 2005). Surface application consists of: (1) direct application of leachate or spray irrigation of leachate on the landfill surface; or (2) surface ponding of leachate. Odor problems, poor aesthetics, and potential runoff of applied leachate into storm water management system are key drawbacks of these surface application techniques.

Conventional subsurface application techniques are (Haydar and Khire 2005; Qian *et al.* 2002): (1) vertical wells; (2) horizontal trenches; (3) horizontal piping; and (4) permeable blankets. Unlike surface application of leachate, subsurface leachate recirculation system does not cause odors and direct leachate exposure unless leachate seeps out from the landfill side slopes. Horizontal trenches are more commonly used in modern lined landfills. Vertical wells are relatively common in retrofit landfills where it is not cost effective or possible to install horizontal trenches (Haydar and Khire 2005). Currently, there are no specific design guidelines available for designing subsurface leachate recirculation system consisting of vertical wells. Hence, the key objective of this study is to carry out numerical evaluation of design parameters to assist designers.

BACKGROUND

Kilmer (1991) and Watson (1993) have presented a study where vertical wells were constructed from a series of perforated manhole sections ranging in diameter from 0.60 m to 1.20 m stacked vertically. The bottommost well section was not perforated. Leachate was injected in the landfill by filling each section of the manhole individually by using pipes running into to the top of the manhole section. The key problems associated with this design are: (1) limited recharge or wetted areas; (2)

landfill subsidence and damage to the liner due to the weight of the vertically stacked manhole sections and the downdrag force acting on the shaft of the vertical manhole due to waste settlement; and (3) short circuiting of the injected leachate to the leachate collection system. Watson (1993) used 1.2 m diameter wells and pumps rated at 108 to 1,080 m³/d at the Delaware landfill. These wells were operated using fill and drain cycles. Merritt (1992) used 0.7 m diameter wells and leachate injection rates ranged from 5 to 15 m³/d per well at the Owens-Corning landfill. Daily recirculation rates ranged from 0.01 to 0.1 m³/d per square meter of the plan area of the waste at a Delaware landfill (Watson 1993) and 0.07 m³/d/m² at the Owens-Corning Landfill (Merritt 1992).

Jain *et al.* (2005) have presented a field study at the full-scale bioreactor landfill located in Florida where preliminary leachate injection tests were carried out using vertical wells. Leachate was recirculated in eleven injection wells having diameter equal to approximately 5.0 cm and depths ranging from 6.1 to 18.3 m. The screen heights ranged from 3.0 to 6.1 m. The recirculation trials consisted of continuous pumping for about 400 hours. The mean specific capacity of each well, which is defined by the authors as the ratio of average flow rate to average injection head measured at the center of the screen height was different for shallow wells, intermediate wells, and deep wells. The shallow wells had the highest mean specific capacity and it decreased as the well depth increased. The reason for a lower specific capacity for deep wells was attributed by the authors to a lower hydraulic conductivity of the waste in deeper sections due to higher overburden pressure. The results of the injection tests at this site indicate that higher leachate flow rate could be achieved through shallow wells than deep wells.

McCreanor (1998) and Reinhart *et al.* (1997) simulated horizontal trenches and vertical wells using the numerical model SUTRA2D. A radial coordinate system was used to simulate vertical wells. The authors simulated recirculation rates of 0.2, 0.4 and 0.8 m³/day for waste hydraulic conductivity equal to 10⁻⁵ m/s for a landfill that was 15-m-deep for a total time period equal to 44 days. The simulated wetted area was represented by isoclines of the degree of saturation of waste. At a field site, Reinhart *et al.* (1997) also state that leachate infiltration from the well can be enhanced if the leachate injection is done in on/off dosing cycles.

NUMERICAL MODELING METHODOLOGY

HYDRUS-2D Computer Model

HYDRUS-2D is a computer model that can simulate water, heat, and solute movement in unsaturated, partially saturated, or fully saturated porous media (Simunek *et al.* 1999). The program numerically solves the Richards' Equation for saturated/unsaturated water flow. A 2-D form of Richards' equation can be expressed as follows:

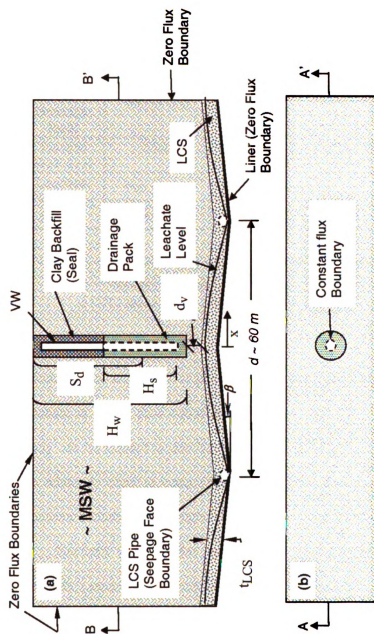
$$\frac{\partial \theta}{\partial t} = -\frac{\partial}{\partial x}\left[k(\psi)\frac{\partial \psi}{\partial x}\right] - \frac{\partial}{\partial z}\left[k(\psi)\frac{\partial \psi}{\partial z}\right] + \frac{\partial k(\psi)}{\partial z} - S_w \quad (1-1)$$

where θ = volumetric water content [dimensionless]; ψ = matric suction head [L]; k = hydraulic conductivity of the porous material which is strongly dependant on the matric suction or water content [L/T]; z = vertical dimension [L]; S_w = volume of water removed per unit time per unit volume of soil by plant water uptake or evaporation (sink term) [1/T]; and t = time [T].

HYDRUS-2D was selected for this study due to its diverse capabilities. HYDRUS-2D can be used to simulate flow regions delineated by irregular boundaries. The boundaries can be selected as constant or time-variable prescribed head, flux, or controlled by atmospheric conditions. The flow region can be simulated with an arbitrary degree of local anisotropy and heterogeneity. The radial vertical flow option is particularly useful for simulating vertical wells. The model also has a built-in database for hydraulic properties of soils and can incorporate hysteresis in the soil-water characteristic curves. The numerical modeling approach followed in this study is very similar to that followed by Haydar and Khire (2005) for horizontal trenches.

Conceptual Model and Assumptions

The conceptual model used for simulating leachate recirculation system consisting of a vertical well is presented in Figure 1-1. The simulated problem domain was about 100-m-wide and 20-m-deep for all simulations unless otherwise specified. The axisymmetric vertical flow option (radial flow) available in HYDRUS-2D was selected to simulate the problem. These key components of the leachate recirculation system were simulated: municipal solid waste, vertical well backfill and drainage pack, and the leachate collection system. Around the screened portion of the vertical well was a drainage pack having hydraulic properties similar to those for pea gravel. The hydraulic properties of the drainage pack were kept constant for all simulations conducted in this study except when the effect of hydraulic conductivity of drainage pack on the wetted width was evaluated. The portion of vertical well from the top of the screened portion to the ground level was simulated as a hydraulic seal having properties similar to those of clay. The hydraulic properties of the various simulated components input to the model are presented in Table 1-1.



Notes:

1. VW = Vertical Well; LCS = Leachate Collection System; MSW = Municipal Solid Waste.
2. H_s = Screen Height; Height of well
3. S_d = Screen Depth (measured from the surface to the centre of the screen height)
4. d_v = Vertical distance between the bottom of the well encasing and the top of the liner

Figure 1-1: Conceptual model for numerical simulation of leachate recirculation in municipal solid waste landfill using a vertical well: (a) cross section AA' and (b) Plan view Section BB'.

Table 1-1: Saturated and unsaturated hydraulic parameters input to HYDRUS-2D to simulate leachate recirculation system consisting of vertical well.

Simulated landfill unit	Material	van Genuchten fitting parameters				Hydraulic conductivity, (m/s)
		θ_r	θ_s	α (1/m)	n	
Municipal Solid Waste	Silt loam	0.078	0.45	2	1.41	10^{-5} , 10^{-6} , & 10^{-7}
Vertical Well Drainage Pack	Pea gravel	0.01	0.3	57.44	2.44	10^{-2}
Vertical Well Seal	Clay	0.068	0.38	0.8	1.09	10^{-8}
Leachate Collection System	Pea gravel	0.01	0.3	57.44	2.44	10^{-2}
	Sand	0.01	0.3	57.44	2.44	10^{-4}

Note: θ_s = saturated volumetric water content [dimensionless];
 θ_r = residual volumetric water content [dimensionless]; and
 α [1/L] and n are van Genuchten's fitting parameters (van Genuchten 1980)

Leachate was simulated as pure water in this study. Henceforth, any reference to leachate or liquid flow corresponds to water flow. Nevertheless, the results of this study can be applied to any liquids as long as the liquid has physical properties that are relatively close to water. The effects of gas flow, temperature, and biochemical reactions including precipitation occurring within a landfill were ignored.

Korfiatis et al. (1984) have demonstrated success when the authors applied Richards's equation for saturated and unsaturated flow to a lab-scale municipal solid waste sample having 0.5 m diameter and 1.5 m height. A wide variety (size and composition) of organic and inorganic materials deposited in landfills results in waste that exhibits heterogeneity and anisotropy in its hydraulic properties. Hence, the soil-water characteristic curves for waste can vary significantly. McCreanor (1998)

simulated the effect of daily cover on the spread of recirculated leachate and found that daily cover having lower hydraulic conductivity than waste can enhance lateral spreading but restrict vertical spreading of leachate. The flow pattern of leachate is also affected by channeling (Zeiss and Uggucioni 1995). In this numerical study, waste was assumed as a homogeneous and isotropic porous medium. Effect of channeling was not considered in this study. Even though this assumption may not be completely in line with field conditions, the results from this numerical study can be useful in comparing designs or to investigate alternatives during an iterative design phase of a leachate recirculation system (Straub and Lynch 1982). Leachate flow as a result of percolation from the cap or waste above the model domain was neglected since the objective of this study was to evaluate the subsurface hydraulics of recirculated leachate. The head losses in pipes, joints, manifolds, and pumps used for the leachate recirculation system were also neglected.

Boundary Conditions and Mass Balance

All external boundaries were simulated as zero-flux boundaries (Figure 1-1). The screened length of the well for leachate injection was simulated as a constant flux boundary. Leachate collection pipes embedded in the leachate collection system were simulated as seepage face boundaries.

The minimum size of the finite-elements used for discretization of the problem domain, the time step, and the error tolerances for pressure head and water content were selected such that cumulative water balance error did not exceed 0.1%. In order to achieve such a low mass balance error, the problem domain was divided into triangular finite elements having maximum dimensions ranging from 1 mm to 25 mm. An error tolerance of 0.1% for the volumetric water content and 10^{-4} m for the matric

suction were used. A minimum time step of 10^{-8} d and a maximum time step of 0.1 d were used. HYDRUS-2D gradually increases the time step automatically if mass balance and error tolerance criteria are met. Typically it took about 2 to 10 days for completing a simulation on a Pentium 2.5 MHz processor. The initial condition was entered in the form of volumetric water content. The initial volumetric water content of the waste was assumed equal to about 25% of its volumetric water content at saturation. This initial volumetric water content represents the typical volumetric water content of MSW in landfills that are not subjected to any liquid injection (SWANA 2002).

Design Parameters

The key parameters incorporated in the design of vertical wells are: well diameter (d_w), screen height (H_s), screen depth (S_d), vertical distance between the bottom of the well and top of leachate collection system (d_v), and hydraulic conductivities of the waste, well drainage pack, and the leachate collection system. These parameters or the materials associated with these properties are presented in Figure 1-1. In order to maintain the pressure head on the liner below the regulatory criterion (0.3 m in the U.S.), the design of the leachate collection system needs to be coupled with the design of the liquid injection system. The leachate collection system design also requires input of the slope of the leachate collection system and the horizontal center to center spacing of the leachate collection pipes. In this numerical study, the influence of the above listed design parameters were evaluated on the wetted width of waste (W_w) and pressure head on the liner (h_p). The reason for selecting W_w as one of the key evaluation parameters was because achieving the greatest possible wetted width for a

given capital and operational cost is one of the key design criteria when liquid injection systems are designed for bioreactor landfills (Haydar and Khire 2005).

The input parameters selected in this study are primarily based on a range of values reported in the literature for field studies. There are no analytical equations available for the results presented in this study. Hence, designers are expected to carry out site-specific modeling if the range of values used in this study is not adequate.

Hydraulic Properties

Three material types were selected for simulating the key components of the leachate recirculation system. These three components included municipal solid waste, vertical well backfill, drainage pack, and the leachate collection system. The materials were simulated as homogeneous and isotropic porous materials. The saturated and unsaturated hydraulic properties of these materials are presented in Table 1-1.

The hydraulic conductivities of municipal solid waste (k_w) were selected based on the typical values published by Hughes *et al.* (1971), Fungaroli and Steiner (1979), Korfiatis *et al.* (1984), Oweis *et al.* (1990), and Bleiker *et al.* (1993). The hydraulic conductivities of the leachate collection system drainage material (k_{LCS}) were selected based on the values for pea gravel or coarse sand which is commonly used for constructing leachate collection system of municipal solid waste landfills (Doran 1999). The unsaturated hydraulic properties for the materials listed above consisted of the van Genuchten (van Genuchten 1980) fitting parameters for the soil-water characteristic curves and unsaturated hydraulic conductivity function (Table 1-1).

The soil-water characteristic curves for the materials simulated are represented by the van Genuchten model (van Genuchten 1980) as follows:

$$\theta = \theta_r + \frac{\theta_s - \theta_r}{\left(1 + |\alpha\psi|^n\right)^m} \quad (1-2)$$

where ψ = matric suction head [L]; θ = volumetric water content [dimensionless]; θ_s = saturated volumetric water content [dimensionless]; θ_r = residual volumetric water content [dimensionless]; and α [1/L], n , and m ($m = 1 - n^{-1}$) are fitting parameters.

HYDRUS-2D model uses the van Genuchten-Mualem (Mualem 1976) function to predict the unsaturated hydraulic conductivities using the van Genuchten fitting parameters and the saturated hydraulic conductivities. The unsaturated hydraulic conductivities are estimated by using the van Genuchten-Mualem model (Mualem 1976) presented in Equation 1-3:

$$k(\psi) = k_s S_e^{0.5} \left[1 - \left(1 - S_e^{\frac{1}{m}} \right)^m \right]^2 \quad (1-3)$$

where S_e is effective degree of saturation [dimensionless]; k_s is saturated hydraulic conductivity [L/T]; $k(\psi)$ is unsaturated hydraulic conductivity function [L/T]; ψ is the matric suction [L]; and m is the fitting parameter for the soil-water characteristic curve.

The unsaturated hydraulic properties for the materials were selected from the database built into HYDRUS-2D for soils having saturated hydraulic conductivities closest to the assumed saturated hydraulic conductivities. Except for the saturated hydraulic conductivity, rest of the parameters presented in Table 1-1 does not have any influence on the wetted width or pressure head on the liner predicted by the model at steady-state flow condition. However, output corresponding to a transient

condition that is achieved before the steady-state is reached is a function of the initial conditions and all saturated and unsaturated hydraulic parameters presented in Table 1-1. The time to reach steady-state is primarily a function of the initial moisture content, the injection pressure head, and the hydraulic properties of the waste. The unsaturated hydraulic properties also influence the water content profile in the capillary zone where degree of saturation is less than 100%. In this paper, the steady-state flow condition is primarily focused.

Vertical Well Dimensions

The diameter of the vertical well ranged from 0.05 to 0.1 m. These dimensions were selected based on the most common designs used at the existing landfills (Jain *et al.* 2005). The thickness of the leachate collection system layer (t_{LCS}) was assumed equal to 0.3 m. The hydraulic conductivity of the leachate collection system drainage material (k_{LCS}) ranged from 10^{-2} to 10^{-4} m/s. The spacing between the adjacent leachate collection pipes (d) ranged from 30 to 60 m (Figure 1-1a). The slope ($\tan \beta$) of the leachate collection system was assumed equal to 3.5% to 10%. The leachate head on the liner was continuously monitored using observation points distributed along the liner. When pea gravel ($k_{LCS} = 10^{-2}$ m/s) was used to simulate the leachate collection system, the simulated pressure head on the liner was always insignificant. The vertical distance, d_v , between the row of vertical wells and the top of the leachate collection system was varied from 2.5 m to 14.5 m. Distance from the top of the well screen to the upper zero flux boundary was in most cases maintained greater than the injection pressure (≥ 10 m) to contain all leachate flow within the problem domain and prevent artesian conditions under the simulated values of leachate injection rates.

The simulated leachate injection rates ranged from $5.5 \text{ m}^3/\text{day}$ (1 gal/min) to $55 \text{ m}^3/\text{day}$ (10 gal/min) to accommodate typical and relatively high liquid injection rates (Merritt 1992).

RESULTS AND DISCUSSIONS

In this study, over 50 simulations using HYDRUS-2D were carried out. The leachate flux was assumed to have reached steady-state when the injected leachate flux equated the total leachate flux seeping from the leachate collection pipes located within the leachate collection system (Figure 1-1a). Note that Q_s in m^3/d represents the leachate flux that was injected over the entire screened portion of the well. Leachate recirculation in the field is often carried out in on/off dosing cycles. Hence, steady-state flow condition can be rarely achieved in the field. In the field, when leachate recirculation system is turned off, gravity drainage of leachate creates storage space in the voids of the waste. Until steady-state is reached, leachate flux greater than Q_s can be recirculated in the landfill for a given injection head or lower injection pressure can be used to achieve a given Q_s . Thus, at steady-state, the injection pressure corresponding Q_s represents an upper limit of injection pressure required to achieve the given Q_s for the given set of design parameters. In addition, steady-state represents the worst-case scenario for pressure head on the liner. Hence, a leachate recirculation system designed using the design values presented in this manuscript under steady-state condition would be conservative. Transient analysis would require reliable values of unsaturated hydraulic properties of waste which do not exist and may not yield conservative results suitable for design.

Figure 1-2 presents the typical isoclines for 60% to 90% degrees of saturation (S) of the waste due to continuous leachate injection in the vertical well at steady-state. Similar isoclines of S ranging from 40% to 100% are presented by McCreanor (1998). The saturation isoclines indicate that the wetted area has a range of saturations propagating outwards from a saturated zone near the screen of the well. The simulated wetted widths for a combination of design parameters are presented in the subsection entitled Wetted Width of Waste. The simulated pressure heads on the liner for a combination of design parameters are presented below.

Liquid Pressure Head on Liner

Due to Injected Liquid

The effect of the following parameters was evaluated on the liquid pressure head (h_p) on the liner: (1) liquid injection rate (Q_s); (2) hydraulic conductivity of the leachate collection system (k_{LCS}) and waste (k_w); (3) slope of the leachate collection system (β); (4) center to center distance between leachate collector pipes (d); (5) vertical distance between the bottom of the well screen and top of leachate collection system (d_v). Unless otherwise specified differently, for all simulations, the thickness of the leachate collection system (t_{LCS}) was assumed constant equal to 0.3 m, the diameter of the well was assumed equal to 0.1 m, the screen height was assumed equal to 3 m, the distance between the bottom of the well and the top of the leachate collection system (d_v) was assumed equal to 5 m, the well height (H_w) was assumed equal to 17 m, and the drainage pack was simulated as pea gravel having hydraulic properties listed in Table 1-1.

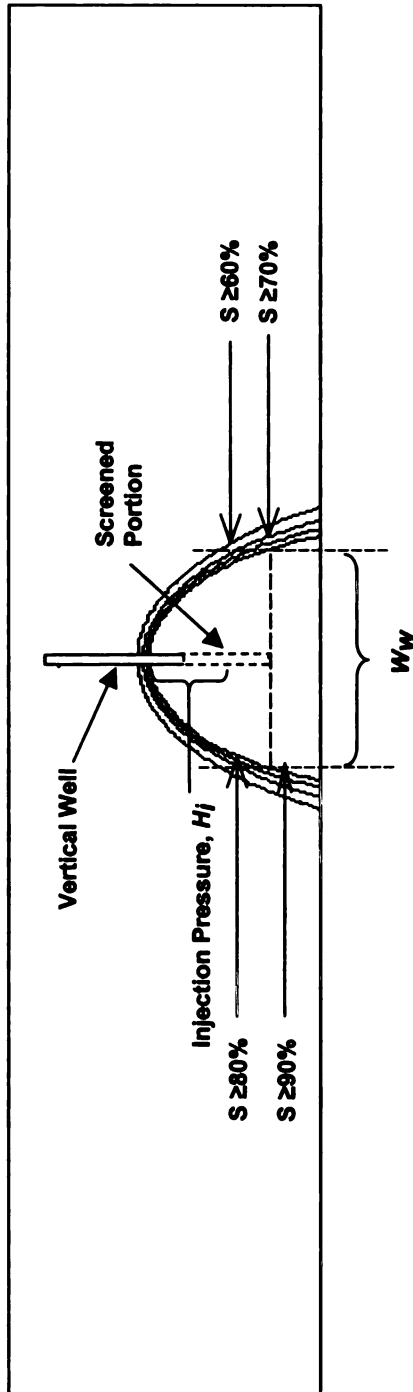


Figure 1-2: Simulated shape of wetted areas for various degrees of saturation for a vertical injection well at steady-state

Figure 1-3 presents h_p on the liner at steady-state for $Q_s = 5.5$ to $55 \text{ m}^3/\text{d}$ and $k_w = 10^{-5}$ and 10^{-6} m/s for leachate collection system simulated using sand and pea gravel.

The simulated pressure heads are greater when k_w is higher, k_{LCS} is lower, Q_s is higher, and/or the observation point is located closer to the vertical well. The simulated pressure heads under equivalent conditions are smaller for a steeper slope of the leachate collection system as shown in Figure 1-4. Similarly, the simulated pressure heads are smaller when the horizontal distance between the leachate collection pipes (d) is reduced from 60 to 30 m (Figure 1-5).

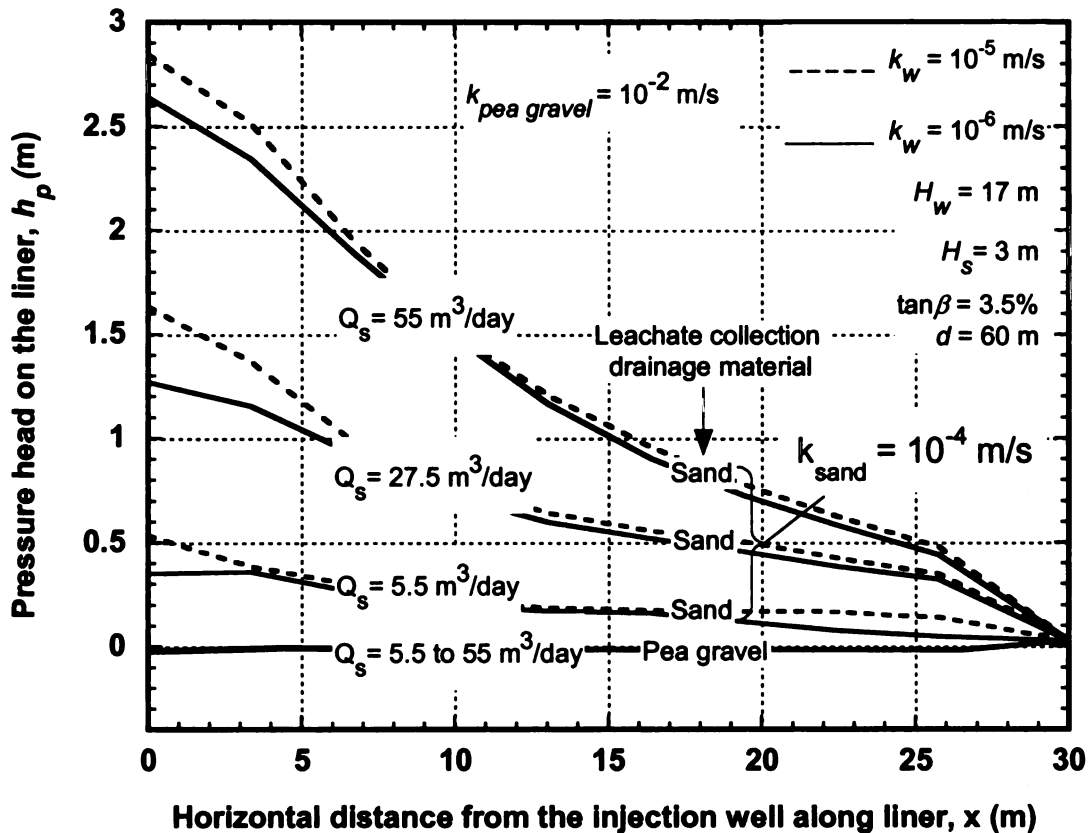


Figure 1-3: Simulated pressure head on the liner for a 17 m-deep single vertical well for leachate collection system slope equal to 3.5%.

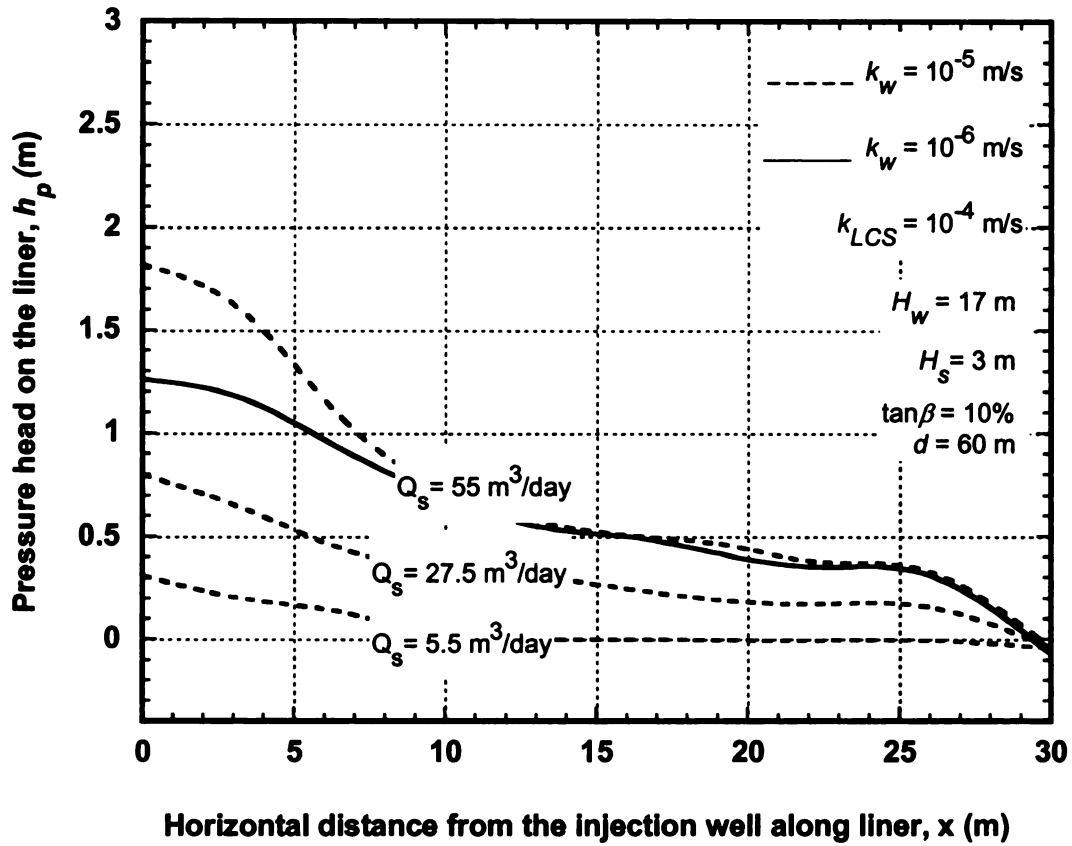


Figure 1-4: Simulated pressure head on the liner for a 17 m-deep single vertical well for leachate collection system slope equal to 10%.

Giroud and Houlihan (1995) have developed Equation 1-4 to estimate the maximum liquid pressure on the liner when subjected to uniform impingement.

$$h_p(\text{max}) = j \frac{d}{2} \frac{\left\{ \sqrt{4\left(\frac{q_i}{k_{LCS}}\right) + \tan^2 \beta} - \tan \beta \right\}}{2 \cos^2 \beta} \quad (1-4)$$

where h_p (max) [L] is the maximum liquid pressure head on the liner under uniform liquid impingement on the leachate collection system equal to q_i [L/T] and j is corrective coefficient [dimensionless] calculated as shown in Equation 1-5.

$$j = 1 - 0.12 \exp \left[- \left[\log \left(\frac{8(q_i / k_{LCS})}{5 \tan^2 \beta} \right)^{5/8} \right]^2 \right] \quad (1-5)$$

Equation 1-4 is only applicable for uniform impingement acting on a horizontal plane that is infinitely wide. Liquid impingement rate from a vertical well is not uniform across the wetted width and acts on a finite width of the leachate collection system. Hence, Equation 1-4 cannot be used to estimate pressure head due to liquid injection using vertical wells. However, the findings presented in Figures 1-3 to 1-5 are in general agreement with the effect of the same parameters on the pressure head when subjected to uniform impingement as described by Equation 1-4. For liquid injection rate equal to 55 m³/d and $k_w = 10^{-5}$ m/s, the maximum pressure head was about 2.8 m for leachate collection system slope equal to 3.5% (Figure 1-3). When the leachate collection system slope was steepened to 10%, the maximum pressure head dropped to about 1.8 m (Figure 1-4) and when the slope was further steepened to 20%, the maximum pressure head dropped to about 1 m (not shown in Figure 1-3).

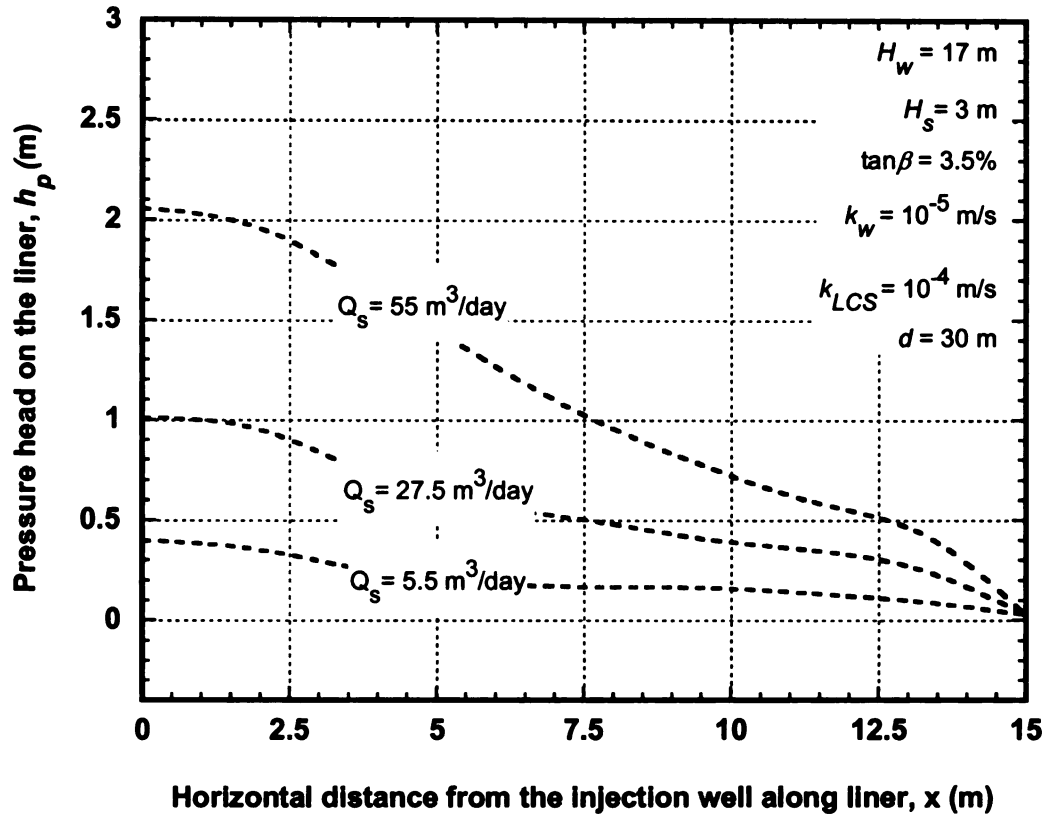


Figure 1-5: Simulated pressure heads on the liner as a function of leachate injection rate at steady-state for leachate collection pipe spacing equal to 30 m.

Figure 1-6 presents the pressure head on the liner for screen depth (S_d) equal to 6 to 18 m (assuming $H_s = 5$ m) for $Q_s = 55 \text{ m}^3/\text{d}$. Sand was used to simulate the drainage material of the leachate collection system.

The key finding of the numerical results presented in Figures. 1-3 to 1-6 is that when sand ($k_{LCS} = 10^{-4} \text{ m/s}$) was used to simulate leachate collection system, for all simulations including the one for the lowest injection rate equal to $5.5 \text{ m}^3/\text{d}$ (1 gpm), the pressure head on the liner exceeded the U.S. regulatory criterion of 0.3 m. However, the pressure head on the liner remained less than 0.3 m when pea gravel ($k_{LCS} = 10^{-2} \text{ m/s}$)

was used to simulate the leachate collection system. Hence, pea gravel or drainage material having $k_{LCS} \geq 10^{-2}$ m/s would be an appropriate choice for leachate collection system if the landfill is expected to receive injected liquids anytime during its active or post-closure life. For all simulations discussed in the forthcoming sections, pea gravel was used to simulate the leachate collection system.

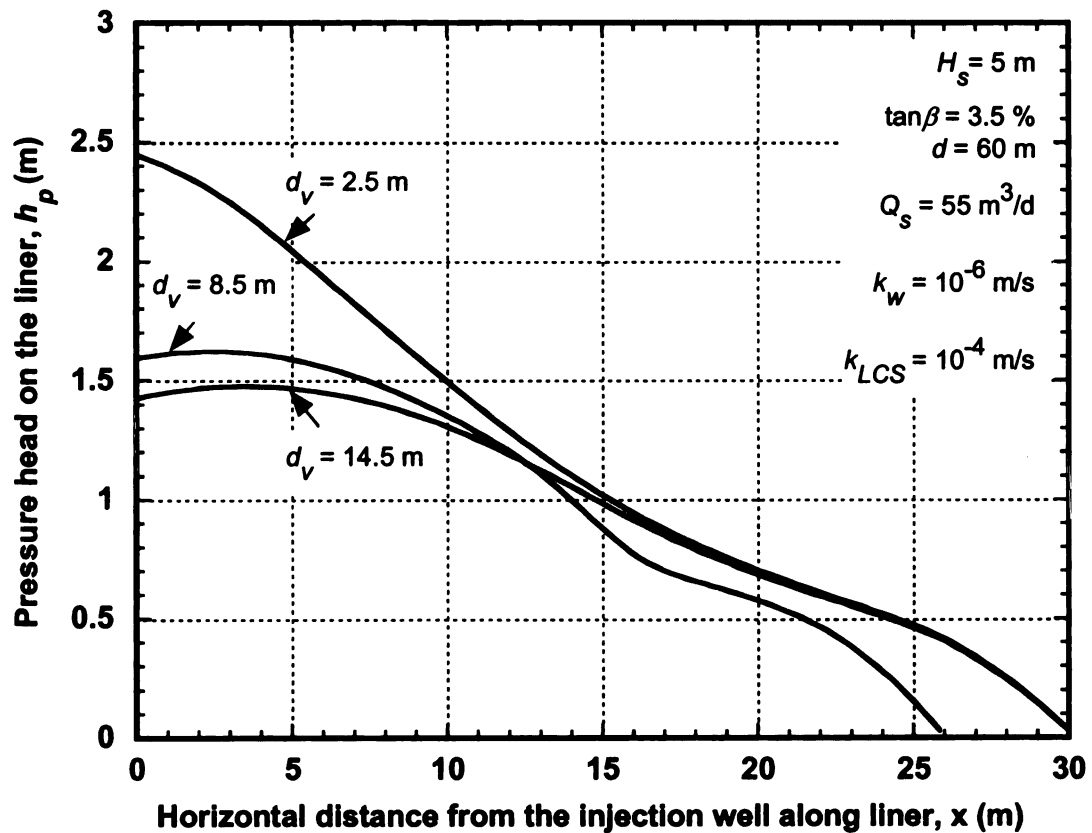


Figure 1-6: Simulated pressure heads on the liner as a function of vertical distance between the bottom of well screen and top of leachate collection system at steady-state.

The vertical distance (d_v) between the bottom of the well and the top of the leachate collection system varied from 14.5 m (for $S_d = 6$ m) to 2.5 m (for $S_d = 18$ m). The

pressure head on the liner was more for $d_v = 2.5$ m compared to for $d_v = 14.5$ m. Thus, closer the screened portion of the well to the leachate collection system, greater the pressure head on the liner. When the screened portion of the well is closer to the leachate collection system, the wetted width immediately above the leachate collection system is narrower. Hence, for a given flux, the leachate impingement rate across the wetted width is more which results in a greater pressure head. When pea gravel was used to simulate the leachate collection system for the parameters presented in Figure 1-6, the pressure head on the liner was insignificant (~ 0).

Due to Uniform Impingement of Percolation

The liquid pressure heads plotted in Figures 1-3 to 1-6 are due to the liquid injected in the vertical well and does not include the additional head due to the impingement of percolation which results from the infiltration of rainfall through the cap and waste. According to the principle of superposition, the total liquid leachate head on the liner or within the leachate collection system is the sum of the liquid head due to the impingement of percolation and the liquid head due to liquid injection. Hence, liquid pressure head due to the impingement of percolation needs to be added to the pressure heads plotted in Figure 1-3 to 1-6 estimated based on site-specific design parameters.

In order to evaluate the additional liquid head in the leachate collection system due to the impingement of percolation, we considered two U.S. cities that represent typical high and average precipitation to simulate relatively high and average leachate impingement rates, respectively. The precipitation records for 30 yrs were considered. The annual average precipitation for Miami, Florida is 145 cm whereas it is 90 cm for Kansas City, Missouri. Here, Miami represents the relatively high precipitation location

and Kansas City represents the average precipitation location. Figure 3a shows that, greater the k_w , greater the liquid pressure head. Hence, $k_w = 10^{-5}$ m/s was input to the HELP model (Schroeder *et al.* 1994) to estimate the liquid impingement rate (q_i) for the leachate collection system design parameters used in Figures 1-3 to 1-6. In order to obtain conservative values for q_i , the thickness of the waste was assumed equal to 4.5 m, the waste surface was assumed without cover (active state) with no surface runoff, $\tan \beta$ was assumed = 3.5%, and $d = 60$ m. Based on this input, the 30-yr average monthly maximum q_i values obtained from the HELP model for Miami and Kansas City were 0.2 m and 0.09 m, respectively. Even though we have simulated typical high and average leachate impingement scenarios here, it may be necessary to carry out an impingement rate analysis for site-specific design conditions. These impingement rates when inserted into Equations 1-4 and 1-5 result in maximum liquid pressure heads equal to: (1) Miami: 0.368 m and zero m for $k_{LCS} = 10^{-4}$ m/s (sand) and $k_{LCS} = 10^{-2}$ m/s (pea gravel), respectively; and (2) Kansas City: 0.182 m and zero m for $k_{LCS} = 10^{-4}$ m/s (sand) and $k_{LCS} = 10^{-2}$ m/s (pea gravel), respectively. Giroud and Houlihan (2000b) have presented Equation 1-6 for estimating the location of maximum leachate thickness.

$$x_{\max} = \frac{k_{LCS} \sin \beta \cdot h_p (\max)}{q_i} \quad (1-6)$$

where x_{\max} [L] is the horizontal distance from the watershed point. For Miami and Kansas City, the maximum liquid head location according Equation 1-6 is at the

watershed point. Hence, for the typical maximum and average impingement rate scenarios we simulated, the total liquid head in the leachate collection system will be maximum at the watershed point (i.e., where $x = 0$ as per Figure 1-1).

According to Equation 1-6, it is also possible that the maximum liquid head location may be anywhere between the watershed point and the leachate collection pipe. Hence, numerical simulations using HYDRUS-2D were carried out where the vertical well was placed at $1/3^{\text{rd}}$ and $2/3^{\text{rd}}$ of the distance between the watershed point and the leachate collection pipe. These simulations yielded lower liquid pressure heads anywhere on the leachate collection system compared to when the vertical well was placed at the watershed point. Hence, the maximum total liquid head on the liner will be: (1) the greater of the maximum liquid head due to a vertical well placed at the watershed point or the head due to the impingement of percolation when the maximum head location according to Equation 1-6 is somewhere between the watershed point and the leachate collection pipe; or (2) the summation of the maximum head due to a vertical well placed at the watershed point and the head due to the impingement of percolation when the maximum head location according to Equation 1-6 is near the watershed point.

If the horizontal distance between the adjacent vertical wells is less than the distance d between the adjacent leachate collection pipes, site-specific numerical modeling will be necessary to estimate the liquid head due to multiple wells. Nevertheless, the maximum liquid heads presented in this section indicate that the maximum liquid heads when pea gravel ($k_{LCS} = 10^{-2}$ m/s) is used as the leachate collection drainage material are 2 to 3 orders of magnitude lower than when sand ($k_{LCS} =$

10^{-4} m/s) is used. Hence, pea gravel is a superior choice for leachate collection drainage material when leachate injection is anticipated as a leachate management strategy.

Soil versus Geocomposite Drainage Layer

Often geocomposite drainage layers are used as an alternative to sand or pea gravel leachate collection drainage layers. Geocomposite drainage layer is commonly used on the side-slope leachate collection systems due its ease of installation compared to natural porous drainage materials and relatively high hydraulic transmissivity. In this study, we have numerically simulated the liquid pressures in sand and pea gravel drainage layers having a thickness equal to 0.3 m. If a geocomposite drainage layer is used in lieu of sand or pea gravel leachate collection drainage layers, the users are recommended to estimate the minimum required transmissivity for geocomposite drainage layer using Equation 1-7 presented by Giroud *et al.* (2000a). The equation is as follows.

$$E = \frac{1}{0.88} \left[1 + \left(\frac{t_{prescribed}}{0.88L} \right) \left(\frac{\cos \beta}{\tan \beta} \right) \right] \quad (1-7)$$

where E is the equivalency factor [dimensionless] to be used in Equation 1-8 to estimate the equivalent minimum transmissivity for the geocomposite drainage layer; $t_{prescribed}$ is the prescribed minimum thickness for natural porous materials like sand or gravel (say equal to 0.3 m or $h_{p(max)}$ presented in Figures 1-3 to 1-5) [L], L is the leachate collection system slope length (equal to $d/2$ in Figure 1-2) [L]; and β is the leachate collection system slope angle [dimensionless].

$$\theta_{GDL} = E \theta_{soil} \quad (1-8)$$

where θ_{GDL} is the equivalent minimum transmissivity [L^2/T] of geocomposite drainage layer; and θ_{soil} is the required transmissivity [L^2/T] for leachate collection drainage layer made up of sand, gravel, or any soil layer.

Wetted Width of Waste

In this study, the wetted width (W_w) was measured along the bottom of the screened portion of the well between the degree of saturation isoclines corresponding to 90%. Figure 1-2 shows how W_w was measured. By selecting W_w corresponding to $S \geq 90\%$ it was not suggested that saturation of waste to degree of saturation $\geq 90\%$ during leachate recirculation. Target degree of saturation to achieve optimum bioreactor performance is beyond the scope of this study. The degree of saturation to achieve optimum bioreactor performance was believed to vary based on composition, density, organic fraction, waste temperature, and meteorological factors. The design engineer and landfill operators are recommended to select a target degree of saturation based on site-specific factors. The wetted width corresponding to degree of saturation, $S \geq 90\%$ can be used to design the center to center spacing between wells. However, the rate and duration of leachate injection and the dosing frequency will ultimately influence the average degree of saturation for the given waste mass (Haydar and Khire 2005) which may require transient modeling of the system.

Effect of Hydraulic Conductivities

The effect of hydraulic conductivity of the waste, k_w , was evaluated for a 17-m-deep well having screen depth equal to 3 m. The hydraulic conductivity of the waste was varied

from 10^{-7} to 10^{-5} m/s while maintaining all other input parameters constant. Figure 1-7 presents the wetted widths at steady-state. Figure 1-7 shows that, for a given hydraulic conductivity of the waste, the wetted width increases as leachate injection rate increases. Figure 1-7 also shows that, for a given leachate injection rate, the wetted width increases as the hydraulic conductivity of the waste decreases.

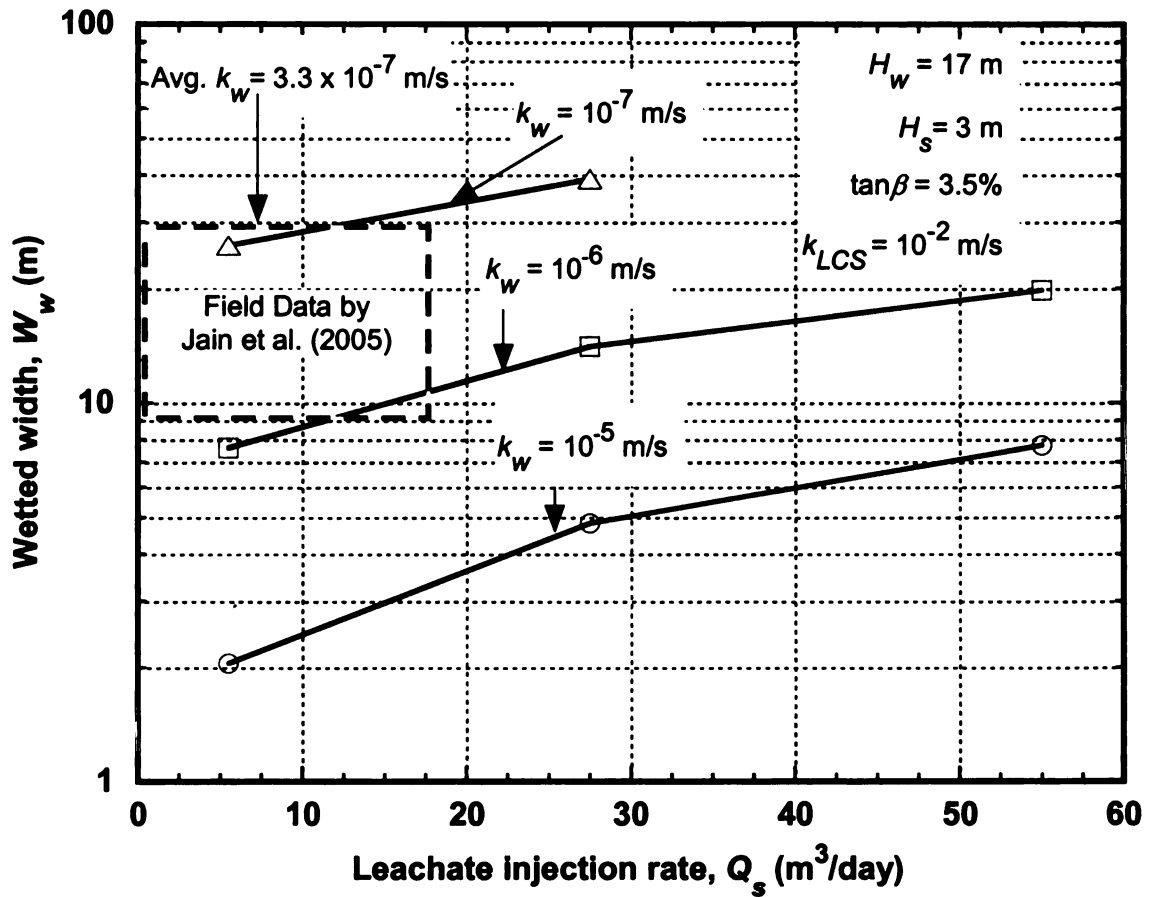


Figure 1-7: Simulated wetted width as a function of leachate injection rate at steady-state.

These findings can be explained using the simulated liquid injection pressures. Figure 1-8 presents the liquid injection pressure near the center of the screened portion of the well at steady-state for the simulations presented in Figure 1-7. In order to maintain a given leachate injection rate, the injection pressure in the well increases as the hydraulic

conductivity of the waste decreases. Similarly, for a given hydraulic conductivity of the waste, the injection pressure increases as the injection rate increases (Figure 1-8). Thus, when injection pressure increases, it results in a greater wetted width. This finding is consistent with the finding for vertical wells presented by McCreanor (1998) and for horizontal trenches presented by Haydar and Khire (2005).

Figure 1-8 also presents results that can be used for sizing the pump for leachate injection. The maximum flow and the total head that a pump needs to deliver are based on these factors: (1) hydraulic conductivity of waste; (2) injection rate; and (3) possibility of artesian condition and slope instabilities. Excessive injection pressure can result in artesian conditions, “splitting” of waste, and slope stability failures. For example, if the hydraulic conductivity of the waste is equal to 10^{-6} m/s, it will require an injection pressure equal to about 4 m in the vertical well to achieve an injection rate equal to $5.5 \text{ m}^3/\text{d}$ (Figure 1-8). For achieving an injection rate equal to $55 \text{ m}^3/\text{d}$, the injection pressure will need to be about 50 m. However, if the depth of the well is less than 50 m and if site-specific slope stability analysis indicates unacceptable factor of safety at 50 m injection pressure, the injection pressure would need to be reduced for a lower injection rate. Once the injection pressure and injection rate are decided, the spacing between the wells can be designed based on the wetted widths presented in Figure 1-7 corresponding to the injection rate.

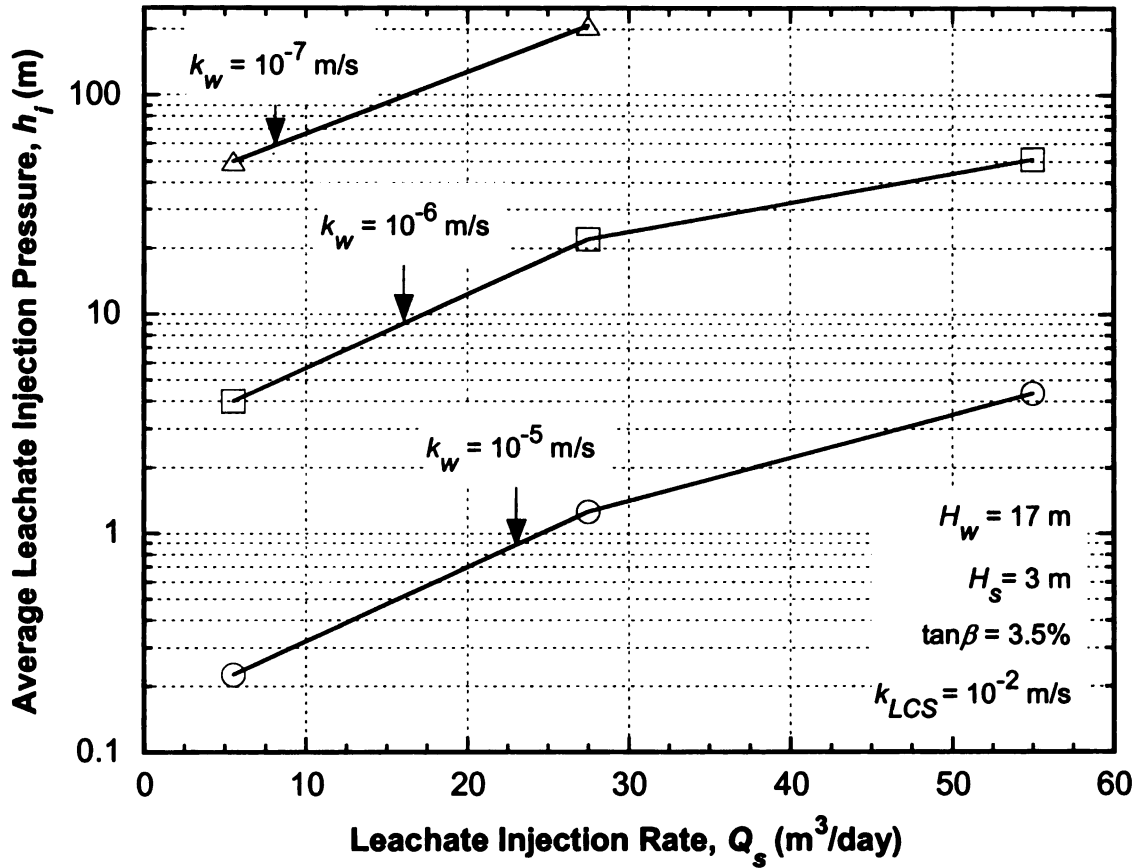


Figure 1-8: Simulated average injection pressure head versus leachate injection rate at steady-state.

Time to Reach Steady-State

Figure 1-9 presents time required to reach the maximum wetted width once continuous leachate injection was started at flux values ranging from 5.5 to 55 m³/d and for $k_w = 10^{-6}$ and 10^{-5} m/s for a single vertical well having screen height equal to 3 m. The initial degree of saturation for the waste was assigned equal to 25%. After the simulated leachate injection was started, the wetted width increased until a steady-state was reached after which the wetted width did not increase. Figure 1-9 shows that for a given flux, for

$k_w = 10^{-5}$ m/s, steady-state is attained more quickly compared to when $k_w = 10^{-6}$ m/s. For a smaller value of Q_s , steady-state reaches sooner compared to for a larger value of Q_s .

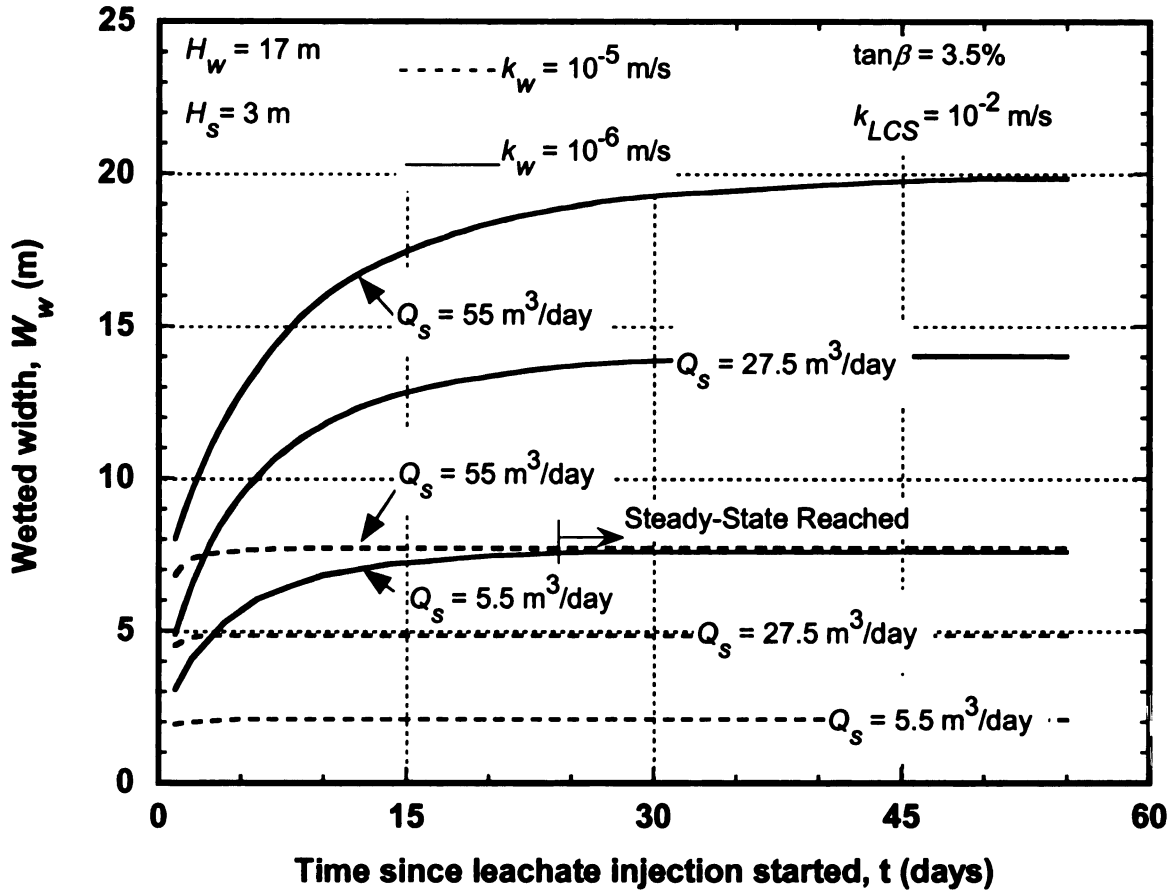


Figure 1-9: Simulated increase in wetted width as a function of leachate injection flux.

Effect of Well Diameter, Screen Height, and Well Height

The diameter of the simulated vertical well was varied to evaluate the effect of d_w on the wetted width at steady-state. Figure 1-10 presents the wetted width for well diameters equal to 0.05 and 0.1 m for $Q_s = 55 \text{ m}^3/\text{d}$. The wetted width did not change when the well diameter was varied but the leachate flux was maintained constant.

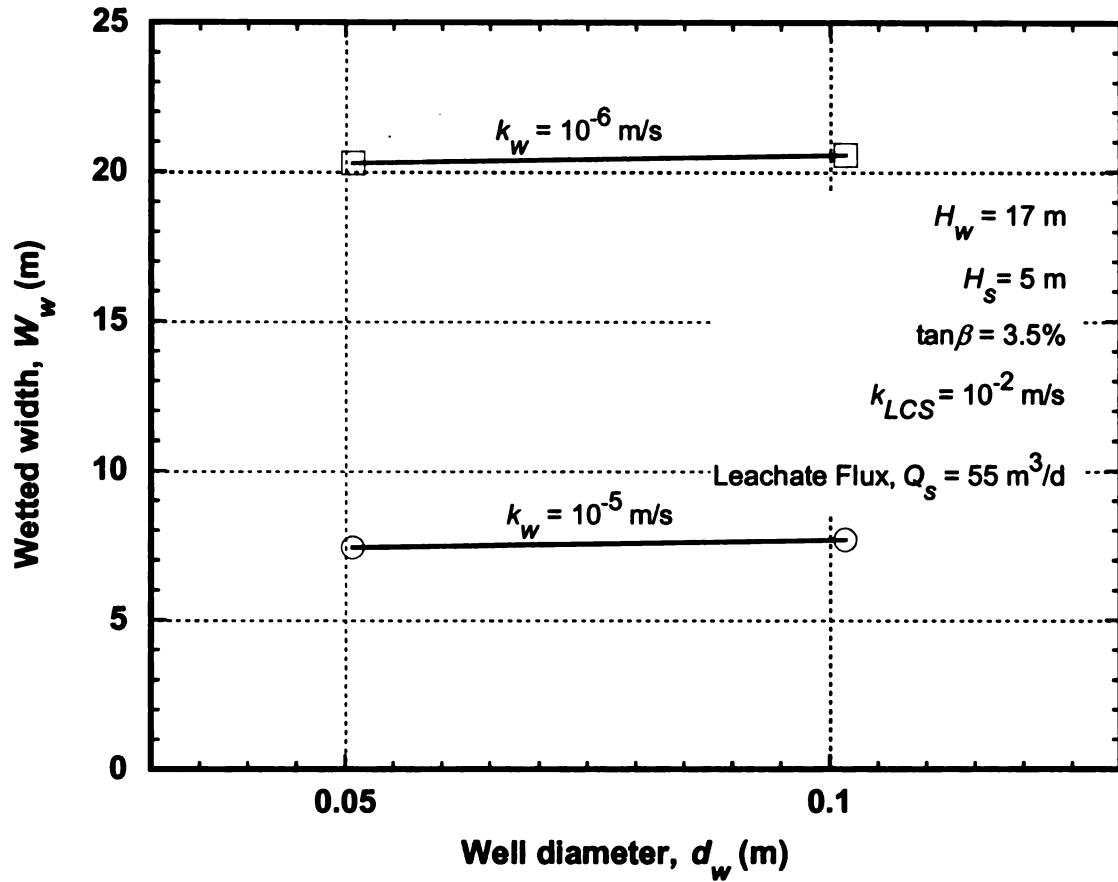


Figure 1-10: Effect of well diameter on wetted width at steady-state.

Similarly, the screen height (H_s) of the simulated vertical well was varied from 3 to 10 m to evaluate the effect of H_s on the wetted width at steady-state. The wetted width did not change when the screen height of the well was varied but the leachate flux and the total height of the well were maintained constant (Figure 1-11). When the well height (H_w) of the simulated vertical well was varied from 8.5 to 20.5 m for a constant screen height equal to 5 m and $Q_s = 55 \text{ m}^3/\text{d}$, the wetted width at steady-state remained constant as well.

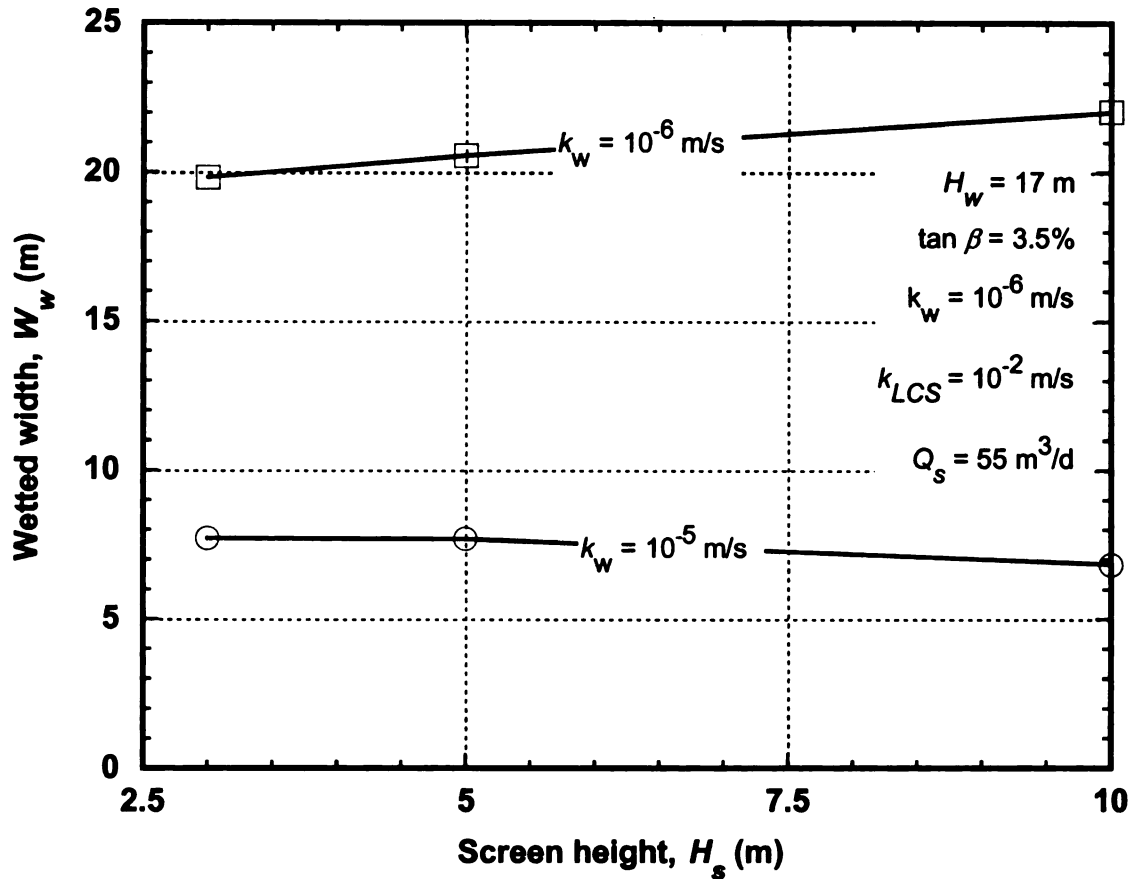


Figure 1-11: Effect of screen height on wetted width at steady-state.

Effect of Hydraulic Conductivity of Drainage Pack

The annular space surrounding the screened portion of vertical wells is typically backfilled with drainage pack made up of gravel or sand. The rest of the annular space around the well is backfilled with hydraulic seal consisting of soil-bentonite or clay-cement slurry. The key functions of the drainage pack are: prevent well clogging by excluding fines from the surrounding waste, to enhance the hydraulic distribution of leachate, and to protect the well by providing a bedding layer for a relatively uniform support. In order to evaluate the effect of hydraulic conductivity of drainage pack (k_{dp})

on the wetted width, k_{dp} was varied from 10^{-4} to 10^{-2} m/s for $k_w = 10^{-5}$ m/s and $Q_s = 55$

m^3/d . The simulated wetted width at steady-state was unaffected by increase in the hydraulic conductivity of the drainage pack. This finding is consistent with the finding by Haydar and Khire (2005) for horizontal trenches. Haydar and Khire (2005) concluded that for $k_{dp} > k_w$, W_w and shape of the wetted area are unaffected. It is because the equivalent hydraulic conductivity of the system is not affected when $k_{dp} > k_w$.

Transient Condition

In order to reduce: (1) pore water pressure increase in the waste; (2) leachate breakouts; and (3) liquid pressure heads on the liner resulting in possible slope instabilities, leachate is not continuously injected in landfills. Instead, leachate is injected in on/off dosing cycles. The dosing volume and frequency for leachate injection may vary depending on the daily leachate generation volume and the operational needs of the landfill.

Hence, steady-state flow condition can be rarely achieved in the field. We evaluated the effect of dosing frequency for $Q = 5.5 \text{ m}^3/\text{d}$ on W_w by simulating leachate injection for 2 hours on/22 hours off, 5 hours on/19 hours off, and 10 hours on/14 hours off for a vertical well having screen height = 3 m. Figure 1-12 presents the effect of dosing frequency on W_w for $k_w = 10^{-5} \text{ m/s}$ and when the initial degree of saturation of the waste is 25%. Figure 1-12 indicates that W_w is a function of the ratio of on to off leachate injection duration. The wetted width of waste was greater for a dosing cycle where the ratio of on to off durations was greater. For a given dosing frequency, W_w progressively increased as the number of leachate dosing days increased until W_w reached a constant

maximum value ranging from 1.3 to 1.9 m depending on the on to off duration ratio. It took about five days for the W_w to reach a constant value.

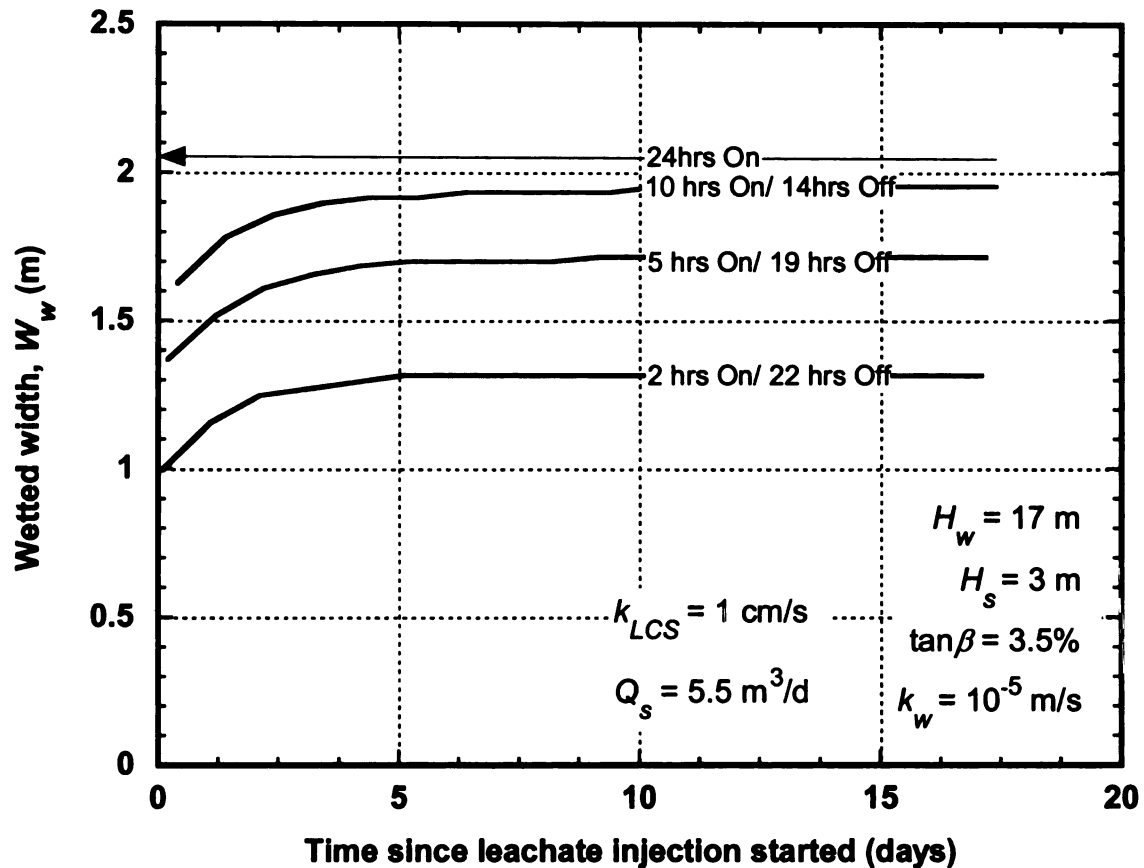


Figure 1-12: Effect of dosing frequency on wetted width for transient state.

For continuous leachate injection, the wetted width would be around 2.05 m. Thus, as the on to off duration ratio approached one (which corresponds to continuous injection), the maximum W_w approached the steady-state value. Thus, W_w can be increased to an appropriate design value by either increasing Q_s or by increasing the on to off duration ratio.

Well Spacing

The wetted widths presented in Figures 1-7 and 1-12 can be used to design the center to center spacing for vertical wells. Due to relatively high cost of drilling in the waste, we believe that well spacing shall not be less than 10 m. In order to achieve uniform wetting, for a spacing of 10 m, the minimum liquid flux in the well needs to be maintained between $15 \text{ m}^3/\text{d}$ for $k_w = 10^{-6} \text{ m/s}$ or greater than $60 \text{ m}^3/\text{d}$ if $k_w = 10^{-5} \text{ m/s}$. The spacing can be increased by increasing the liquid flux values as long as excessive liquid injection pressures are not generated which may jeopardize the slope stability of the landfill (Figure 1-8). Site-specific values of k_w are rarely measured. Hence, designer would need to assume an appropriate value of k_w . Jain *et al.* (2005) have tabulated k_w values measured in many lab and field studies. The geometric mean k_w for waste is about $3 \times 10^{-6} \text{ m/s}$. Hence, in the absence of any site-specific data, $k_w = 3 \times 10^{-6} \text{ m/s}$ can be used to design flow rates, dosing frequency, and well spacing. Selective wells shall be instrumented with moisture content sensors to monitor the wetted widths to allow making changes to an existing design or to use the data during any future design phases.

MODEL VALIDATION

The numerical study presented in this paper is primarily based on numerical modeling conducted using HYDRUS-2D. Municipal solid waste is a highly heterogeneous and anisotropic material consisting of pore fluid (leachate) having complex geochemical properties. Heterogeneity and anisotropy of waste may not ever be fully characterized or the cost of characterization using conventional field methods would exceed the benefits

of such characterization in design or operation of a municipal solid waste landfill. Hence, it may not be possible to measure the representative values of water content and hydraulic properties of municipal solid waste (Oweis *et al.* 1990; McCreanor 1998). Due to these reasons, majority of the modeling results presented in this paper have not or cannot be accurately validated in the field for municipal solid waste landfills. However, the HYDRUS-2D model, which is based on the Richards partial differential equation (Equation 1-1) has been validated for saturated/unsaturated liquid and solute transport through porous media in several lab and field-scale studies (Scanlon *et al.* 2002; Henry *et al.* 2002; Pang *et al.* 2000; Rassam *et al.* 2002). The same model was used for modeling horizontal trench leachate recirculation system by Haydar and Khire (2005). Jain *et al.* (2005) have presented findings from a field study of leachate recirculation system consisting of vertical wells. In this section, we have presented the results from these studies as a validation of our modeling work.

Jain *et al.* (2005)

Jain *et al.* (2005) have presented a field-scale study consisting of vertical wells for moisture addition in a full-scale municipal solid waste landfill cell over duration of 17 months. Specific capacity of vertical wells, extent of lateral movement of moisture away from the vertical wells monitored by moisture content sensors, and leachate generation in response to moisture addition have been reported in this study. The wells have approximate depths of 6, 12 and 18 m. The bottom 6 m of the 12-m and 18-m injection wells and the bottom 3 m of the 6-m injection lines were screened. The flow rates through individual injection wells ranged from 0.09 to 16.5 m³/d. The specific capacities of the

vertical wells ranged from 0.02 to 0.65 m³/d-m-per meter screen length having a mean of 0.09 m³/d-m².

Based on the changes in the water contents of sensors embedded in the waste, the wetted zone ranged from about 8 to 30 m from the center of the vertical wells. It was not possible to accurately establish the degree of saturation of the waste accurately as it would need sensor location specific calibration. Jain *et al.* (2006) have carried out borehole permeameter tests using the vertical wells in the same bioreactor landfill cell. Based on the field tests, Jain *et al.* (2006) have estimated the saturated hydraulic conductivity of the waste. The estimated values of k_w ranged from 5.4×10^{-8} – 6.1×10^{-7} m/s. The average k_w was about 3.3×10^{-7} cm/s. We have presented the range of flow rates and corresponding wetted distances measured by Jain *et al.* (2005) in Figure 1-7. The field data obtained by Jain *et al.* (2005) agrees relatively well with the range of wetted widths we have simulated in this study for the corresponding range of k_w values.

Haydar and Khire (2005)

Haydar and Khire (2005) simulated the hydraulics of liquid injection in landfills for horizontal trenches using the same numerical model (HYDRUS-2D) that was used in this study. The conceptual models for these two studies are also similar. Haydar and Khire (2005) compared the simulated liquid flux values for various liquid injection heads and k_w values. Figure 1-13 shows that the model predictions agreed reasonably well with the field data collected by Doran (1999) and R.W. Beck (2002). Similarly, the model

predictions agreed well with model predictions by Bachus *et al.* (2002) using the finite-difference model VS2DI (Hsieh *et al.* 2000).

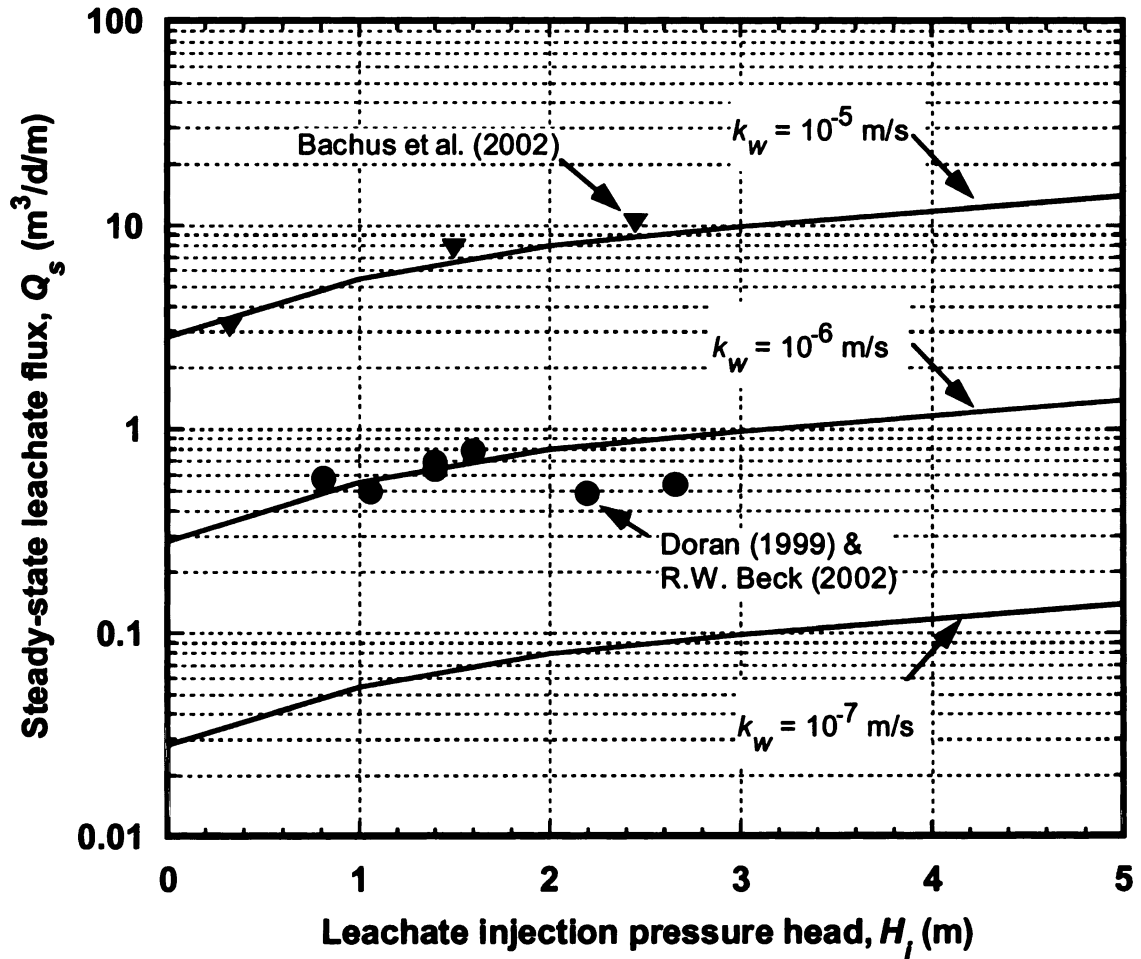


Figure 1-13: Simulated leachate flux at steady-state versus leachate injection pressure head for a horizontal trench for $k_w = 10^{-7}$, 10^{-6} , and 10^{-5} m/s (Haydar and Khire 2005).

SUMMARY AND PRACTICAL IMPLICATIONS

This paper presents a numerical study of key design variables used for design of leachate recirculation system consisting of vertical wells. Even though the range of values we used as input for the parameters we evaluated was based on published field studies, it was not possible to cover the entire possible range for the parameters considered. Hence,

designers are recommended to supplement these results with site-specific modeling or analysis to cover site-specific parameters not exclusively included in this study.

The design of leachate pipe network including the head loss in the pipes, joints, manifolds, and pump has not been considered in this study and needs to be considered separately using Moody (1944) or other appropriate charts. The effect of these parameters was evaluated on the pressure head on the liner and wetted width of the waste at steady-state: (1) liquid injection rate and on/off frequency of leachate dosing; (2) leachate collection system slope and horizontal distance between leachate collection pipes; (3) k_{LCS} , k_{dp} and k_w ; and (4) well diameter, screen height, and distance between the top of the leachate collection system and bottom of the well. The wetted width was defined as the width of the wetted area of waste having degree of saturation $\geq 90\%$ measured along a horizontal line passing through the bottom of the screened height of the well (Figure 1-2). The saturated-unsaturated flow model HYDRUS-2D was used to simulate the hydraulics of leachate recirculation in municipal solid waste landfills. The key findings of this study are as follows.

- The maximum pressure head on the liner due to liquid injection in a vertical well is a function of the liquid injection rate, the hydraulic conductivity of the leachate collection system and waste, slope of the leachate collection system, horizontal distance between leachate collection pipes, and vertical distance between the bottom of the well and top of leachate collection system (Figures 1-3, 1-4, 1-5, and 1-6). However, the effect of k_{LCS} is most significant. For all simulations carried out in this study, when sand having $k_{LCS} = 10^{-4}$ m/s was used to simulate the leachate

collection system, the maximum pressure head on the liner ranged from about 0.3 m to 3 m. However, when pea gravel having $k_{LCS} = 10^{-2}$ m/s was used to simulate the leachate collection system, the maximum pressure head on the liner as result of liquid injection was significantly less than 0.3 m. Thus, pea gravel or materials having hydraulic conductivity $\geq 10^{-2}$ m/s are preferable for constructing leachate collection system where liquid injection is planned. However, when geocomposite drainage layers are used, an equivalent minimum transmissivity needs to be estimated using the methodology presented by Giroud *et al.* (2000a). Additional liquid head due to the impingement of percolation must be added to estimate the total maximum liquid pressure head on the liner.

- Wetted width of waste is primarily a function of liquid injection rate, the hydraulic conductivity of waste, and on/off frequency used for liquid injection (Figures 1-7 and 1-12). For a given hydraulic conductivity of waste, a greater wetted width can be achieved by increasing the liquid injection rate and/or increasing the on to off duration ratio of liquid injection. However, increase in leachate injection rate requires an increase in the injection pressure (Figure 1-8) which needs to be carefully evaluated to make sure that the factor of safety against slope stability of the landfill cell is not jeopardized.
- Well diameter, height of the screened portion of the well, and depth of the well have no impact on the wetted width (Figures 1-10 and 1-11). The hydraulic conductivity of the drainage pack also has no influence on the wetted width as long as $k_{dp} > k_w$.

- For a given liquid injection rate, the liquid injection pressure increases as the hydraulic conductivity of the waste decreases. Hence, site-specific slope stability analysis is necessary to estimate the maximum allowable injection pressures for a target rate of liquid injection.
- The shape of the wetted area presented in Figure 1-3 and the wetted widths presented in Figure 1-7 can be used to design the optimum spacing among wells to achieve uniform wetting of waste.
- The wetted widths and average liquid injection pressures presented in Figures 1-7 and 1-8 depend heavily on k_w . Because it is relatively difficult to measure representative values of field k_w , designers need to assume a range of possible values for k_w and incorporate redundancy in the design. It is also recommended that selective wells are instrumented with water content and pressure sensors to allow monitoring of the wetted widths and use the site-specific data during future design.

Although not explored in this study, designers are recommended to consider these factors when designing a leachate recirculation system: (1) potential decrease in the shear strength of MSW due to liquid injection affecting the slope stability of the landfill; (2) adequate buffer distance to minimize the potential of leachate breakouts from the landfill side slopes; and (3) effect on the efficiency of gas collection system. The designers should also consider the effect of hydraulic properties of daily cover (see details in McCreanor 1998), potential for clogging of the well, and the effect of waste settlement on the long-term performance of the system.

PAPER NO. 2: INSTRUMENTED LARGE SCALE SUBSURFACE LIQUID INJECTION MODEL FOR LANDFILLS

ABSTRACT

A large-scale physical model of a landfill (85 cm long x 30 cm wide x 55 cm high) was constructed and instrumented to simulate a liquid recirculation system consisting of a permeable blanket. The blanket in the landfill model was 50 cm long x 30 cm wide x 2 cm thick and was made up of pea gravel. Uniform fine and coarse sands were used in separate experiments to simulate the underlying waste. The blanket and the waste material below the blanket were instrumented with pressure transducers and water content sensors to monitor the migration of injected water in the blanket and in the underlying soils. This manuscript presents the design of the model and the data collected from the model during experiments where water was injected at flow rates ranging from 20 to 150 cm³/s. The responses of the pressure transducers embedded in the blanket in the model mimicked the responses of the pressure sensors embedded in the instrumented field-scale (55 m long x 9 m wide x 0.15 m thick) permeable blanket made up of crushed recycled glass used for recirculation of leachate. The extent and advance of wetting front of the injected water and the pressure heads in the blanket were influenced by the hydraulic properties of the underlying sand and on the injection rates. The data collected from the model can be used to verify numerical models that are commonly used to design various liquid injection systems and to study hydraulics of bioreactor landfills.

INTRODUCTION

Bioreactor landfills are designed and operated to accelerate the decomposition of organic constituents of municipal solid waste (MSW) and to decrease the time to achieve waste stabilization in the process by purposeful control of biological processes. The most common form of bioreactor landfill operation is moisture addition through the recirculation of leachate (or injection of other liquids) as a means to control and enhance moisture levels within the landfill and creating an environment conducive to rapid degradation of waste. The goal of bioreactor landfill operation is to enhance the bacteria proliferation to increase the rate of degradation of the organic waste fraction and consequently increase the production of biogas resulting from the degradation of organic matter in the landfill and potentially stabilize the waste in the process. A bioreactor landfill is differentiated from a conventional landfill by controlling biological and chemical processes occurring within the landfill primarily through moisture addition. Hence, there is a need to better understand the hydraulics of landfills and to verify the numerical models that are commonly used to design subsurface injection systems (Haydar and Khire 2005; Haydar and Khire 2007; and Khire and Mukherjee 2007).

Leachate recirculation or liquid injection can be performed using multiple techniques, both surface and subsurface. The surface methods consist of spraying leachate over the landfill surface area or constructing leachate pond. The conventional subsurface application techniques are: (1) vertical wells; (2) horizontal trenches; and (3) permeable blankets. Haydar and Khire (2005), Haydar and Khire (2007) and Khire and Mukherjee (2007) have presented design guidelines for horizontal trenches, permeable blankets and vertical wells, respectively, through numerical studies.

OBJECTIVES

Haydar and Khire (2004, 2005, and 2007) and Khire and Mukherjee (2007) have developed guidelines based on numerical modeling for design of subsurface liquid injection systems including the permeable blankets. However, it has not been possible to verify the modeling results because it is not possible to achieve steady-state flow conditions in the field due to relatively large scale of the landfill. For transient scenarios, which are common in the field, often the sensor spacing and frequency of readings is not adequate for the highly heterogeneous waste. Hence, controlled field testing is almost impossible to verify numerical models. Hence, in this project, a large-scale laboratory scale physical model of landfill was developed to conduct controlled lab tests to simulate hydraulics of liquid injection consisting of a permeable blanket. The lab model has sensors embedded in the sand underlying the blanket to understand the hydraulics of liquid flow due to subsurface injection.

The key objective of the study presented in this paper is to describe the design of a laboratory scale landfill model that simulates the field-scale blanket. The effect of hydraulic conductivity of the underlying waste, liquid injection rate, and the average degree of saturation of waste on the hydraulic pressure heads in the blanket is studied. The influence of hydraulic conductivity and injection rate on the extent and advance of wetting front of the injected water and degree of saturation of underlying waste is also explored. The data collected from this physical scale-model will be used to verify numerical models (HYDRUS and Vadose/W) which are commonly used for modeling liquid flow in landfills. The validation of numerical models is beyond the scope for this paper.

Field-Scale Testing of Permeable Blankets

Haydar and Khire (2006) tested the concept of leachate recirculation using a field-scale instrumented permeable blanket. They studied the feasibility of using an automated geotechnical sensing system consisting of water content, temperature and pressure sensors to monitor the migration of recirculated leachate in permeable blankets. Three permeable blankets made up of crushed recycled glass (15 cm thick), shredded tires (60 cm thick), and a geocomposite drainage layer (0.5 cm thick), each of which is about 60 m long by 10 m wide, were installed at a landfill located in Jackson, Michigan in Summer 2003. A 75-mm-diameter, 9.5-m-long perforated leachate injection pipe was installed at the center of each blankets to inject leachate (Khire and Haydar 2005; Haydar and Khire 2006).

Haydar and Khire (2006) have reported the responses of the thermistor and pressure transducer sensors embedded in the glass blanket at 0.5, 4.5, and 14 m distances from the leachate injection pipe. There were a number of intermittent leachate injection events typically of duration of 140 min since July 2003. Figure 2-1 shows the responses of the pressure transducers for three such chronological injection events with the injection rate being reported per meter length of the injection pipe. All pressure transducers detected the migration of leachate by measuring a gradual increase in the pressure head in response to the leachate injection event. The responses of the pressure and temperature sensors were synchronized with respect to the liquid injection events. The pressure heads increased or decreased consistent with the rate of injected flow as shown in Figure 2-1. The increase in the pressure head was earliest and greatest for the sensors located closest to the injection pipe and decreased subsequently with distances away from the injection pipe.

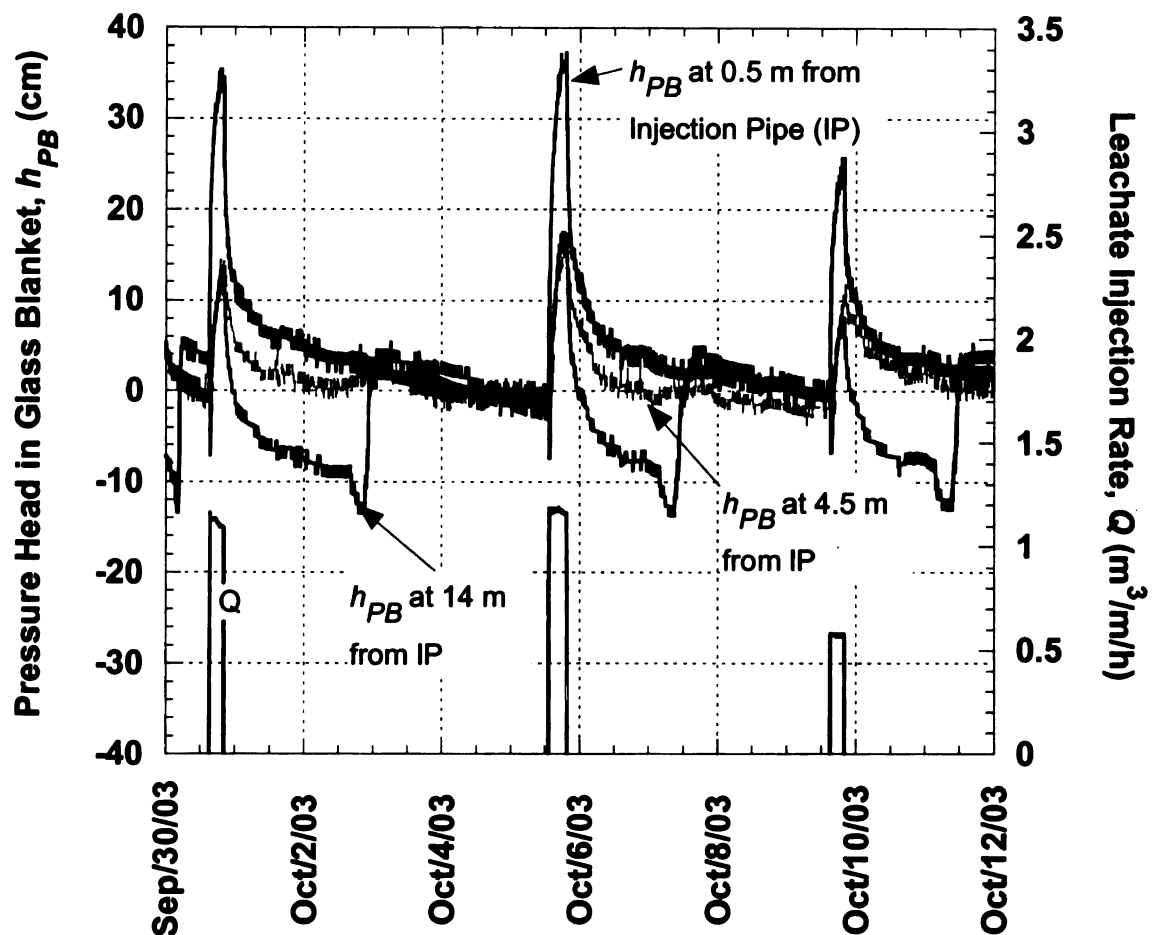


Figure 2-1: Responses of pressure transducers embedded in a field-scale blanket in Michigan showing increase or decrease in pressure heads.

The pressure transducers indicated an immediate but gradual decrease in the leachate pressure head when the leachate injection stopped. When the leachate drained out of the blanket by drainage into the underlying waste and the blanket de-saturated, the pressure head became negative in the blanket for a short duration followed by bouncing back close to zero as shown in Figure 2-1.

MATERIALS AND METHODS

Model Dimensions

Figure 2-2 presents a schematic of the landfill model fabricated to simulate a horizontal permeable blanket recirculation system. Figure 2-3 shows the photo of the instrumented landfill setup. The transparent plexi-glass box for housing the landfill model was designed by simulating the landfill model in saturated/unsaturated numerical model HYDRUS-2D (Simunek *et al.* 1999). The preliminary numerical modeling was conducted to evaluate the sensitivity of pressure heads generated in the blanket and underlying waste to the hydraulic properties of the system for various magnitudes of rates of liquid injection, duration of injection, and frequency of liquid dosing, and initial conditions for steady-state as well as transient conditions. The blanket position was fixed at 17 cm from the top based on the maximum pressure in the blanket simulated by the numerical model. The physical dimensions of the sensors and the number of sensors installed in the model also played a major role in deciding the dimensions of the model. Sands that had conductivities ranging from 10^{-2} to 10^{-3} cm/s were used to simulate the waste below the blanket. Numerical modeling indicated that the chosen hydraulic properties of the sands would generate pressure heads that are within the dimensions of the model and the pressure heads are large enough for measurement using sensors with an accuracy that exceeded 99%. The pumps to inject water were selected based on designed injected flow rates for each of the sands used to simulate waste.

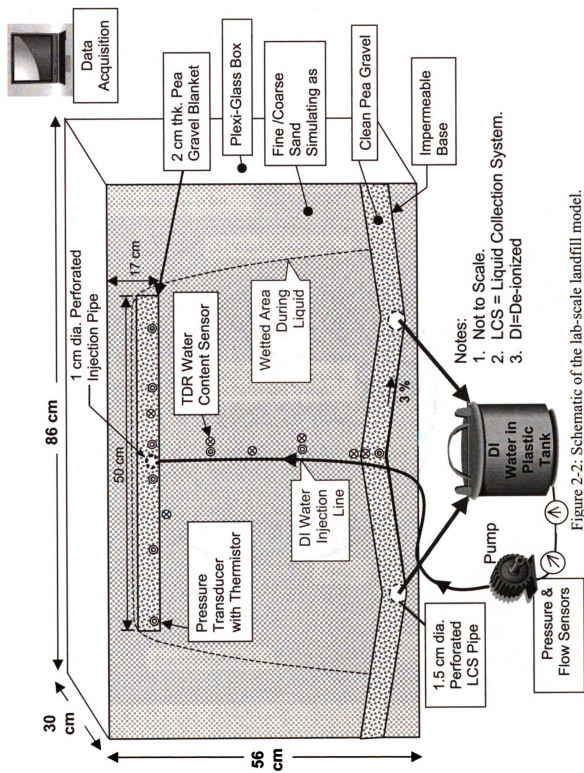


Figure 2-2: Schematic of the lab-scale landfill model.

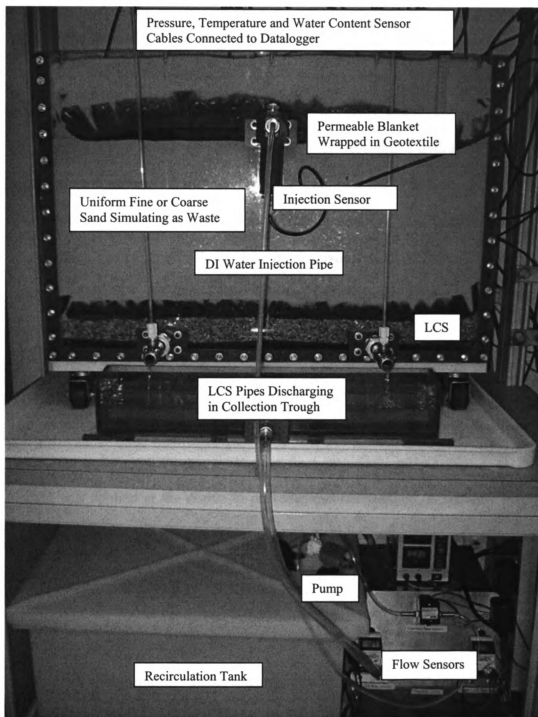


Figure 2-3: Photo of the setup of the instrumented laboratory scale landfill model.

Waste Representation

One of the key objectives of developing the physical model is to verify numerical models. Hence, accurate hydraulic characterization of the system is required. Actual or surrogate waste was not used because MSW is highly heterogeneous and anisotropic (Haydar and Khire 2004). The measurement of representative hydraulic properties (both saturated and unsaturated) of waste is challenging because of its heterogeneity. Hence, in order to allow better hydraulic characterization, relatively homogeneous and isotropic sands which are commercially sold in large quantities as “standard” sands were used below the blanket to simulate waste. Selection of these standard sands would allow other researchers to use these sands for any future related studies.

Fabrication

The acrylic panels of the model were screwed together with 2-mm-thick silicone rubber membrane in-between the panels to provide a watertight box (Figure 2-2). A silicone sealant was applied at the seams to prevent potential leakage. A separate acrylic panel was used to make the bottom of the model representing the leachate collection system (LCS) having a slope of 3%. The perforated seepage pipes within the LCS had at least 10 times higher flow capacity than the flows injected in the model to maintain the pressure head in the LCS within its thickness of 4 cm. Different soils were used to simulate these components of the landfill: waste, leachate collection system, and permeable blanket.

Sensors in Landfill Model

Figure 2-4 shows a photo of the following sensors used in the landfill model: (1) pressure

transducer with built-in thermistor; (2) water content sensor; and (3) flow sensor. The sensor specifications are listed in Table 2-1. All sensors were connected to a datalogger to continuously monitor and log data. The datalogger was programmed to take readings at frequencies ranging from 5 s to 30 min depending upon the experiment.

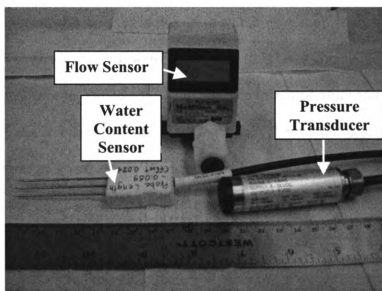


Figure 2-4: Sensors used in the landfill model

Table 2-1: Specifications of the sensors used in the landfill model

Measurement	Dimensions	Range	Accuracy	Output
Pressure and Temperature	Length: 8.5 cm Diameter: 1.2 cm	0-92 cm of water column	$\pm 1\%$	0-5 VDC for pressure and digital modbus-capable interface to read temperature and pressure
Volumetric Water Content	Total Length: 9.7 cm	-	-	Apparent dielectric constant
Flow Rate	Length: 7.5 cm Width: 4 cm	8 - 165 $\frac{\text{cm}^3}{\text{s}}$	$\pm 1\%$	0-5 VDC

Pressure Transducer

The pressure transducer provided temperature compensated analog output proportional to the water pressure. The sensor was made up of corrosion resistant high grade stainless steel. It consisted of a pressure-sensitive diaphragm attached to a vibrating wire. The deflection of the diaphragm due to water pressure caused changes in wire tension. The transducer then utilized the changes in the frequency of the vibrating wire to sense pressure. A thermistor was embedded within the pressure transducer to record temperature. Two measurements were made: the first was the measurement of the temperature of the probe to compensate for changes in its temperature and second was the measurement of the frequency of the vibrating wire. The vented sensors used in this project had a vent tube of 2 mm diameter that connected the chamber behind the diaphragm to the atmosphere. Due to the vent tube, barometric pressure was compensated.

The major historical limitations with the vibrating wire pressure transducers are errors caused by zero drift and corrosion of the vibrating wire (Dunnicliff 1988). In recognition of the concern for zero drift, the accuracy of all sensors was periodically checked while running the experiments. The galvanic corrosion was minimized by not grounding the shield wire connected to the housing of the sensor. The sensors have a dry hermetically sealed cavity around the vibrating wire, thereby minimizing corrosion problems.

Water Content Sensors

TDR-based water content sensors were chosen among the various promising commercial

techniques of measuring the volumetric water content due to its fast response in tracking infiltration fronts (Imhoff *et al.* 2007). The mini-TDR water content sensor consisted of three pointed 0.15 cm diameter stainless steel rods mounted into an encapsulated plastic head. The probe rod length was 6 cm and spacing between the probe rods was 0.6 cm. The water content sensors were connected to the datalogger via an electro-magnetic pulse generator and a coaxial multiplexer. Topp *et al.* (1980) empirically derived calibration equation was used to convert the dielectric constant values to volumetric water content. equation (Equation 2-1):

$$\theta = -5.20 \times 10^{-2} + 2.92 \times 10^{-2} D_a - 5.5 \times 10^{-4} D_a^2 + 4.3 \times 10^{-6} D_a^3 \quad (2-1)$$

where D_a is the apparent dielectric constant of soil and was measured by the TDR sensors.

Flow Sensor

The flow sensor was capable of measuring flow rates ranging from 8 to 165 cm³/s. A 3 1/2 digit non-backlit LCD flow rate display was integrated into the sensor unit and was programmed to read the flow rates in the specified range. The flow sensor incorporated a pelton-type turbine wheel having diameter and thickness equal to 1.6 cm and 0.075 cm, respectively to measure the flow rate of water. The rotational speed of the turbine wheel increased proportionally to the volumetric flow rate. The micro-turbine wheel had alternating white and black sections evenly spaced on one side of the wheel. An infrared beam was reflected off each white section as the wheel rotates and was directed to a

phototransistor which detected each reflected beam and converted it into pulses. Pulse rate increased as the wheel spun faster. Pulses were not generated when the wheel stopped under no flow conditions. Consequently, zero drift was not possible and zero adjustments were never required. The sensors provided analog DC voltage output proportional to the flow rate and the flow rate in engineering units was shown on the integrated display.

Laboratory Testing and Calibration

Calibration of Pressure Transducers and Flow Sensor

Before installing the sensors in the landfill model, all sensors were tested for accuracy and were calibrated. The pressure transducers were calibrated in the laboratory by applying known pressures and measuring the response. In order to evaluate the accuracy of their measurements, the pressure transducers were placed in a container in the position they would be eventually embedded in the LCS, sand, and the blanket in the landfill model. All transducers were placed vertically with the tip facing upward except in the LCS where the transducers were placed in a horizontal position. The pressure transducers were tested by adding de-ionized (DI) water at depths ranging from 15 to 35 cm in a container. A linear relationship between the depth of water and recorded pressure head readings was observed. The accuracy of the pressure transducer was within ± 0.5 cm.

A linear relationship was observed between the flow rates recorded by the flow sensor and the flow calculated from the levels measured by the pressure transducer. The accuracy of the flow sensor was within $\pm 0.5\%$.

Calibration of TDR Water Content Sensor

The TDR water content sensors were fully inserted vertically in a container filled with dry sand and then water was gradually added in known steps until the sand got saturated. The volumetric water content was calculated using Topp's (Topp *et al.* 1980) empirically derived calibration Equation 1-1. For both sands, a linear relationship between the volumetric water content calculated from known addition of water and the volumetric water content measured by the TDR water content sensors was observed.

Signal Drift in Pressure Transducers

Periodically, water was ponded in the landfill model and maintained at a fixed level for few hours to measure and correct for signal drift for the pressure sensors. At the end of the experiments, when the setup was dismantled, the calibration of the sensors was re-checked and corrected, if needed. The zero was found to have drifted approximately 0.3 to 0.6 cm.

Pump

The maximum flow that a pump needed to deliver in the landfill model was based on the hydraulic conductivity of the sand underlying the blanket and the injection rate. A miniature gear pump was used for relatively low injection flow rates ($8 \text{ cm}^3/\text{s} - 42 \text{ cm}^3/\text{s}$) when the finer sand was used and a brushless magnetic drive pump was used for higher injection flow rates ($75 \text{ cm}^3/\text{s} - 300 \text{ cm}^3/\text{s}$) when the coarser sand was used. Both pumps were operated with a variable power DC power supply to obtain variable injection flow rates. These pumps were chosen because of their ability to deliver “pulseless” flows

because the rate of flow had to be constant to achieve consistent results. A quartz based digital timer was used to operate the pump in on/off mode. The timer could be programmed for various durations of on/off injection cycles.

Materials

Table 2-2 shows the grain size and hydraulic characteristics of the soils used in the landfill model. The blanket and the LCS were made up of pea gravel. The waste was represented by uniform OK110 sand (fine sand) and in another experiment using uniformly graded Ottawa sand (coarse sand). The Ottawa sand was ASTM graded sand conforming to ASTM C778.

Table 2-2: Grain size distribution and hydraulic properties of soils used in the landfill model

Soil type	Simulated landfill unit	Grain size distribution				Saturated and unsaturated hydraulic properties				
		D ₅₀ (mm)	C _u	C _c	ρ_d (g/cm ³)	K_s (cm/s)	θ_s	θ_r	α (1/cm)	n
Fine Sand (OK 110)	Waste	0.11	1.34	1.06	1.55	1.8×10^{-3} to 6.4×10^{-3}	0.42	0.03	0.01 to 0.02	6.5
Coarse sand (Ottawa)	Waste	0.35	2.04	1.4	1.76	0.07 to 0.09	0.4	0.03	0.023 to 0.09	4.5
Pea Gravel	Blanket and LCS	2.84	1.68	0.96	1.55	2	0.43	0.01	0.45	3.3

Notes: LCS- Leachate Collection System

Specific gravity of all soils $G_s = 2.65$

θ_s = saturated volumetric water content [dimensionless];

θ_r = residual volumetric water content [dimensionless]; and

α [1/L] and n are van Genuchten's fitting parameters (van Genuchten 1980)

Saturated Hydraulic Conductivity

The saturated hydraulic conductivities (K_s) of the fine sand, coarse sand, and pea gravel were measured in the laboratory using a rigid wall permeameter (ASTM D 2434-68) using a Mariotte bottle. In addition, the saturated hydraulic conductivity of the fine sand was also measured in a flexible wall permeameter using falling head method (ASTM D 5084-03). The saturated hydraulic conductivities of the soils presented in Table 2-2 are average values obtained from triplicate tests. The saturated hydraulic conductivity of the fine sand ($\sim 10^{-3}$ cm/s) lies in the range of K_s values of MSW published by Hughes *et al.* (1971), Fungaroli and Steiner (1979), Korfiatis *et al.* (1984), Oweis *et al.* (1990), Chen and Chynoweth (1995) and Jang *et al.* (2002).

Soil Water Characteristics Curves

The relationship between volumetric water content and matric suction of fine sand, coarse sand, and pea gravel was obtained through a hanging column experimental setup comprised of Buchner funnel with porous ceramic plate (ASTM D 6836-02). Drying as well as wetting soil water characteristics curves (SWCC) were generated. Because of limitations associated with the height of the laboratory room to achieve the residual water content using the hanging column method, tempe cell method (ASTM D 6836 – 02) was used for determining the residual water content for the fine sand. The experiments for determining the SWCCs for all soils were repeated twice. The soil water characteristic curves are described in terms of the van Genuchten (1980) fitting equation. The fitting parameters are tabulated in Table 2-2.

Fabrication of Instrumented Landfill Model

Leachate Collection System

Figure 2-2 shows a schematic of the landfill model. A 4-cm thick LCS made up of washed pea gravel was constructed at the bottom of the plexi-glass tank. The dry density of the pea gravel was about 1.55 g/cm^3 . In the LCS, two 45-cm long PVC seepage pipes having 1.5-cm diameter were placed at 45 cm apart. Each of the pipes was perforated with 200 equally spaced perforations having diameter equal to 2 mm. The seepage pipes discharged freely into the atmosphere to simulate typical field conditions where the LCS riser pipes are vented. In the middle of the LCS, between the two LCS pipes, a water content sensor and a pressure transducer were placed.

The seepage pipes and the tip of the pressure sensor were wrapped in a woven geomesh having 2 mm opening size to minimize clogging. Piezometers consisting of 6 mm diameter glass tubes were inserted in the projected portion of the LCS seepage pipes outside the box to observe the pressure heads generated during the experiments. The LCS and the overlaying sand were separated by a non-woven geo-textile having thickness of about 2 mm (ASTM D 5199), mass per unit area of 270 g/m^2 , and a hydraulic conductivity of 0.3 cm/s (ASTM D 4491). A water content sensor was placed within 1 cm of geotextile to monitor the water content near the interface.

Sand Layer Simulating Waste

About 38-cm thick dry sand (OK110 and Ottawa Sands, in separate experiments) having 1.6 g/cm^3 in-situ density and porosity of about 0.42 was placed below the blanket. In the

sand layer, two pressure sensors were embedded in vertically upright position at 10-cm intervals. Before placing the sensors in the sand, in the setup with the fine sand, the sensing tips of these pressure sensors were wrapped in a non-woven geotextile and the space above the diaphragm within the sensor was filled with DI water to remove air. In the setup with the coarse sand, the pressure sensors in the sand were wrapped in a woven geotextile because the sand particles were relatively large. The woven geotextile had a thickness of about 0.6 mm (ASTM D 5199), mass per unit area of 190 g/m^2 , and a hydraulic conductivity of 0.5 cm/s (ASTM D 4491). A water content sensor was placed near the sensing tip of the pressure sensor in the sand.

Permeable Blanket

The permeable blanket for the recirculation system was made up of the same pea gravel used for the LCS. The blanket was about 50 cm long and 30 cm wide. The thickness of the blanket was 2-cm. The permeable blanket was wrapped in the non-woven geotextile to separate the blanket from the surrounding sand. Installation of the blanket was done using the following steps: (1) embedded six pressure transducers in the sand at designated locations in vertically upward position; (2) placed the geotextile with holes punched at the sensor locations such that the tips of the sensors were in the blanket; (3) embedded a 30-cm long perforated (two rows of holes having diameter equal to 1.6 mm, 10 holes per row) PVC pipe of 1 cm diameter at the center of the blanket in the direction parallel to the width of the blanket where water was injected under a positive pressure (Figure 2-2); (4) placed washed pea gravel layer of 2-cm thickness and of 1.55 g/cm^3 in-situ density on the geotextile; (5) inserted two water content sensors on either side of the injection pipe;

and (6) wrapped the blanket with the geotextile followed by placement of the sand on top of the blanket. In the setup with coarse sand simulating as waste, a water content sensor and a pressure transducer were placed outside the blanket on either sides and at the same level as the sensors embedded in the blanket. The hydraulic conductivity of the pea gravel used for the LCS and the blanket was 2 cm/s.

The end of the injection pipe inside the blanket was capped and the other end was connected to a pressure transducer to measure the injection pressure and a flow sensor to measure the injection flow rate. The flow sensor was connected to a pump to deliver water from a storage tank into the blanket. A pressure transducer was also placed in the storage tank to monitor the change in head of water in the tank to monitor if and when a steady-state is reached. A closed loop recirculation system was formed wherein the injected water after flowing through the blanket, sand, and discharging freely in the atmosphere from the seepage pipes got collected in the storage tank which was injected back into the blanket.

Falling Head Tests

Falling head tests were performed on the landfill model to measure the saturated hydraulic conductivity of the whole system. This allowed capturing the effect of scale, sensors, and sensor cables on the vertical hydraulic conductivity of the model and thus providing the “in-situ” conductivity. The saturated hydraulic conductivity of the system was greater than measured using a 10-cm-diameter sample in a conventional rigid wall permeameter. For the fine sand, the measured saturated hydraulic conductivity of the landfill model ranged from 1.8×10^{-3} to 6.4×10^{-3} cm/s and for the coarse sand (Ottawa

sand) it ranged from 7×10^{-2} to 9×10^{-2} cm/s (Table 2-2).

RESULTS AND DISCUSSION

The effect of the following parameters was evaluated on the hydraulic pressure head in the blanket (h_m), the degree of saturation (S) of the underlying soil, and the wetted width of the blanket: (1) hydraulic conductivity of the sand simulating the waste (k_w); and (2) liquid injection rate (Q).

Effect of Hydraulic Conductivity of Underlying Soil on Pressure Head

Deionized (DI) water was pumped into the blanket through the injection pipe at injection rates ranging from 20 to 150 cm³/s. The hydraulic conductivity of the permeable blanket was 2 to 3 orders higher than the underlying sand. As the water injected in the blanket traveled through the blanket, the hydraulic pressure heads in the blanket (h_m) increased. The pressures in the blanket increased rapidly at the beginning of the infiltration event and approached a steady-state value within a few minutes to hours depending upon if the sand was coarse or fine, respectively. For a fixed injection rate (Q), the h_m values were greater for the fine sand which has about one order magnitude lower hydraulic conductivity compared to the coarse sand (Table 2-2). For example, the average h_m was 11 cm for $Q = 21$ cm³/s in fine sand (Figure 2-5) whereas in the coarse sand, the sensors in the blanket did not register any pressure head for $Q = 21$ cm³/s. With the coarse sand, pressure heads in the blanket developed in the blanket only when the injection rate

exceeded $80 \text{ cm}^3/\text{s}$. Thus, the pressure heads, h_m developed in the blanket and the injection rate, Q are a function of hydraulic conductivity of waste underlying the blanket, k_w .

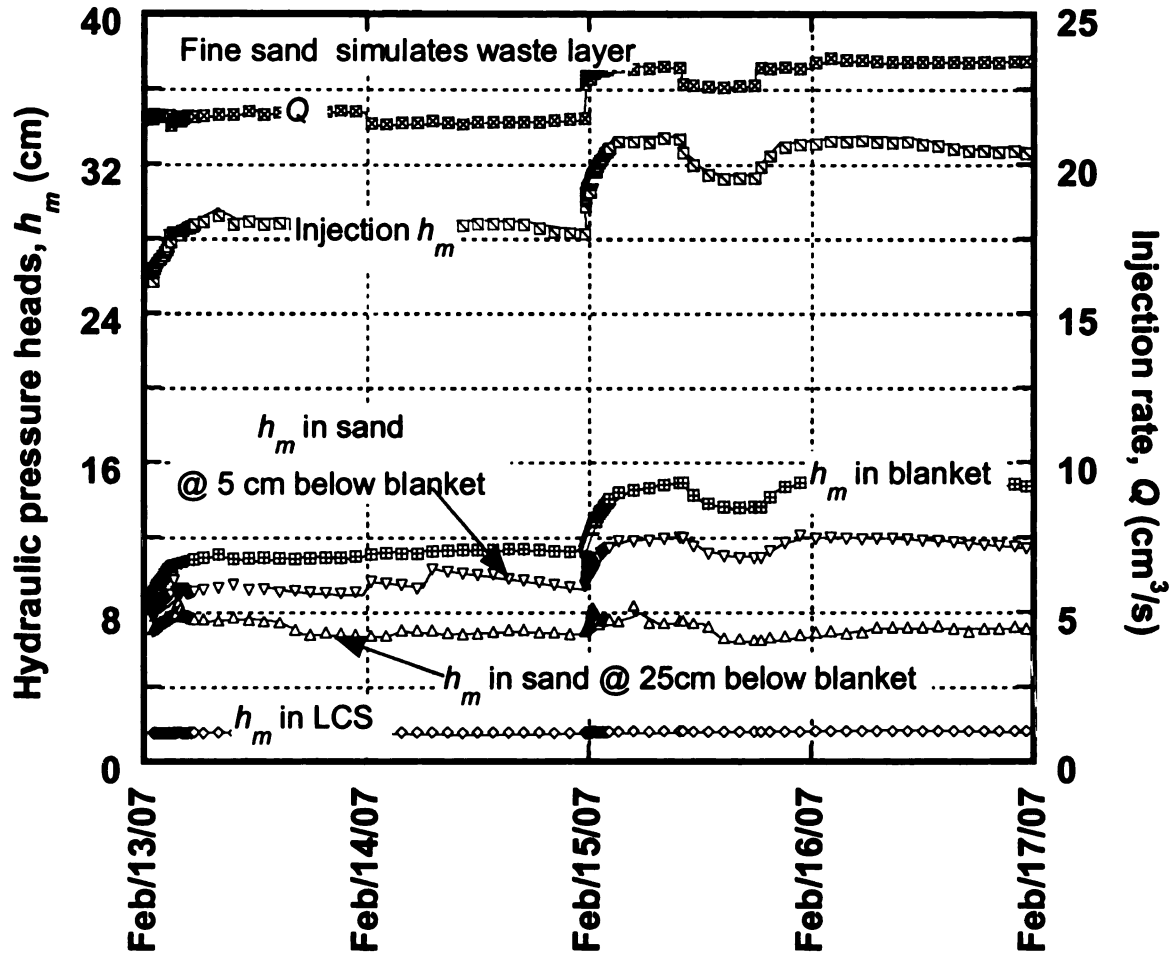


Figure 2-5: Pressure heads in injection pipe, blanket, LCS and in fine sand simulating waste.

The pressure heads decrease with increase in hydraulic conductivity. In order to maintain the pressure heads in the blanket within the physical boundaries of the model (Figure 2-2), the liquid injection experiments were carried out for the fine sand and the coarse sand

at flow rates ranging from 10 to 20 cm³/s and 85 to 150 cm³/s, respectively.

Effect of Injection Rate on Pressure Head

Figure 2-5 shows the variations in the liquid pressure heads in the blanket, sand, and the LCS as the rate of injection was varied. The pressure heads changed even with the slightest variation in the rate of flow. The pressure heads in the blanket increased with the increase in the rate of liquid injection and this finding is similar to the data from the field-scale blanket (Figure 2-1). The pressure heads were maximum in the blanket and decreased downwards till they were almost zero in the LCS.

The maximum pressure head in the blanket, h_m did not exceed the injection pressure. This is in agreement with the findings of Haydar and Khire (2007). For $Q = 23$ cm³/s, the injection pressure was about 33 cm in the fine sand, whereas it was about 7 cm in the coarse sand. The injection pressure was more for fine sand which has lower hydraulic conductivity. This finding is consistent with the findings of Khire and Mukherjee 2007; Haydar and Khire 2007.

Figure 2-6 show the pressure heads h_m in the blanket when DI water was injected at a constant rate of 150 cm³/s in the setup with coarse sand.

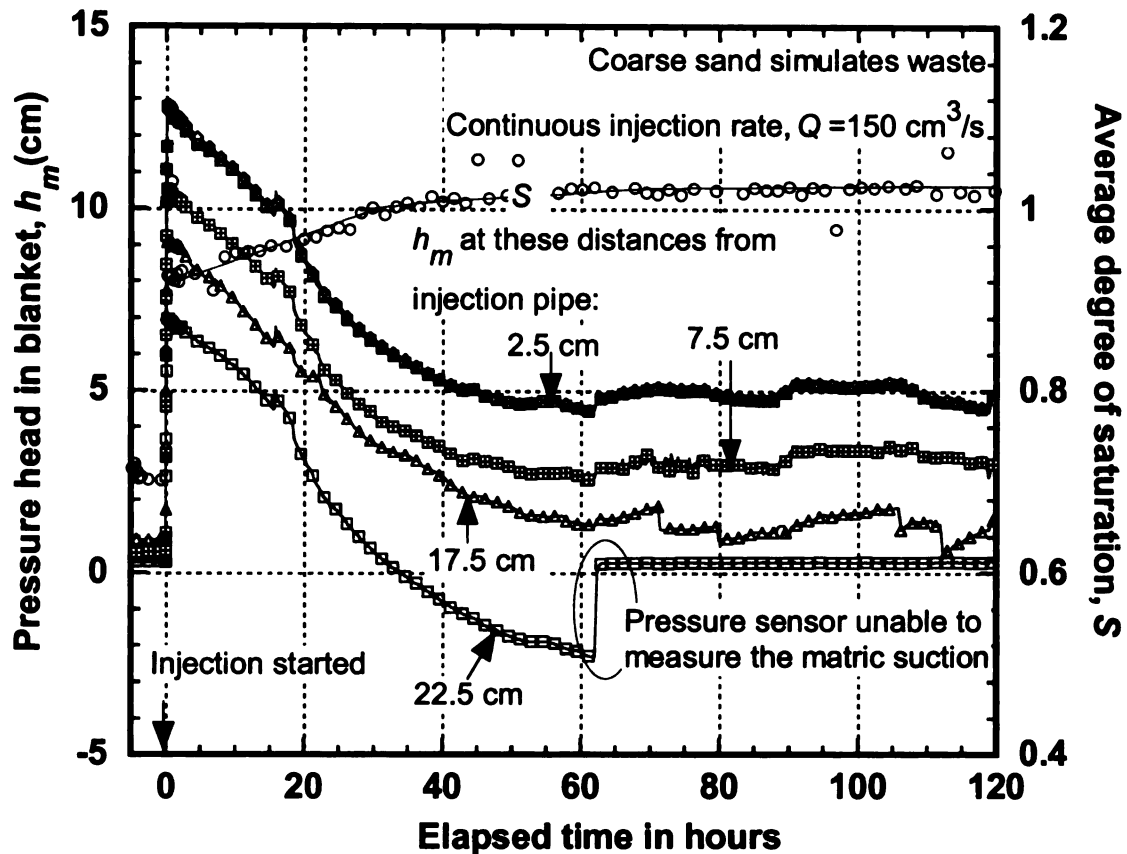


Figure 2-6: Decrease in pressure heads in blanket with increase in average degree of saturation.

The increase in the pressure head was earliest and greatest for the sensors located closest to the injection pipe and decreased subsequently with distances away from the injection pipe. This finding is similar to the data from the field-scale blanket (Figure 2-1). When the liquid injection was started, the average degree of saturation of the sand below the blanket was 70% as shown in Figure 2-6. The pressure heads were relatively high in the beginning because the unsaturated hydraulic conductivity of the sand was low. As the degree of saturation of the sand increased due to the continuous injection of water, the pressure heads in the blanket decreased because of increase in the hydraulic conductivity of the underlying sand. In about 60 hours after the injection began, the pressure heads

reached a steady-state. A steady-state was assumed to have reached when the injected flow in the blanket equated the outflow from the LCS and the pressure heads in the blanket did not show upward or downward trend for several hours after the flows became equal. Hence, the pressure heads are directly related to the injection rate and are also dependent on the degree of saturation of the underlying soil. The pressure heads in the blanket decreased as the degree of saturation of the sand increased.

Effect of Hydraulic Conductivity on Degree of Saturation

Figure 2-7 shows the responses of the water content sensors to the injection of water in the fine sand. The water content sensors in the blanket showed increase in water content. The water content sensors embedded in the sand registered increase after the blanket. Thus, the water filled the blanket before substantial quantity of water started infiltrating into the underlying sand.

The hydraulic conductivity of the sand influenced the downward migration of water in the soil. The migration of water in the fine sand was relatively slow compared to the coarse sand. Figure 2-7 shows that it took greater than 350 hours for all water content sensors in the fine sand reaching $S \sim 100\%$. The transient water content profiles for the coarse sand (Figure 2-8) show that the water contents in the coarse sand reached $S \sim 100\%$ after 40 to 85 hours after the injection started. The water content sensors embedded in sand indicated increase in water content sequentially (Figures 2-7 and 2-8), as the saturated wetting front moved downwards.

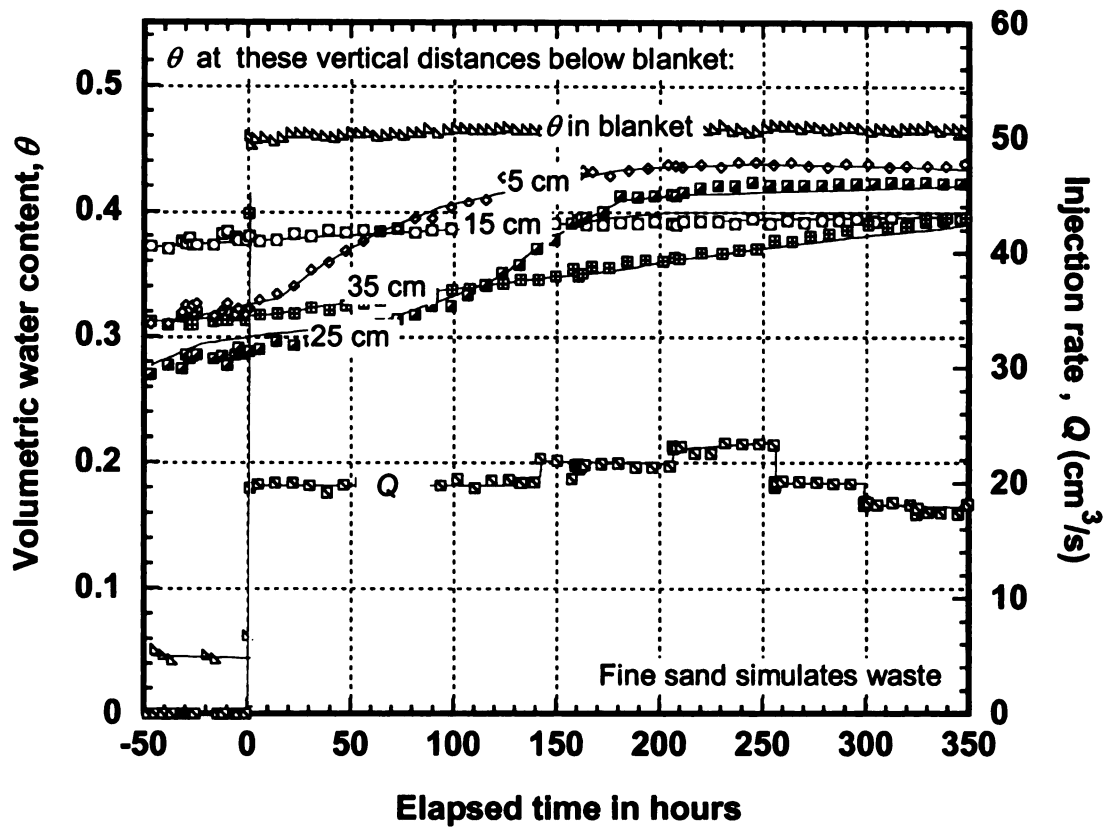


Figure 2-7: Increase in average degree of saturation of underlying fine sand due to continuous injection.

Effect of Injection Rate on Degree of Saturation

Figure 2-8 shows the water content profiles in the coarse sand for two flow rates. The water contents increased in the top down order and the rate of increase in the water content was faster for the higher flow rate (Figure 2-8b). For example, the water content of the soil 15 cm below the blanket reached saturation after 86 hours for $Q = 120 \text{ cm}^3/\text{s}$ (Figure 2-8a), whereas it reached saturation after 43 hours for $Q = 150 \text{ cm}^3/\text{s}$ (Figure 2-7b). Hence, the average degree of saturation of the underlying sand increased faster with

higher flow rates as observed in Figure 2-8.

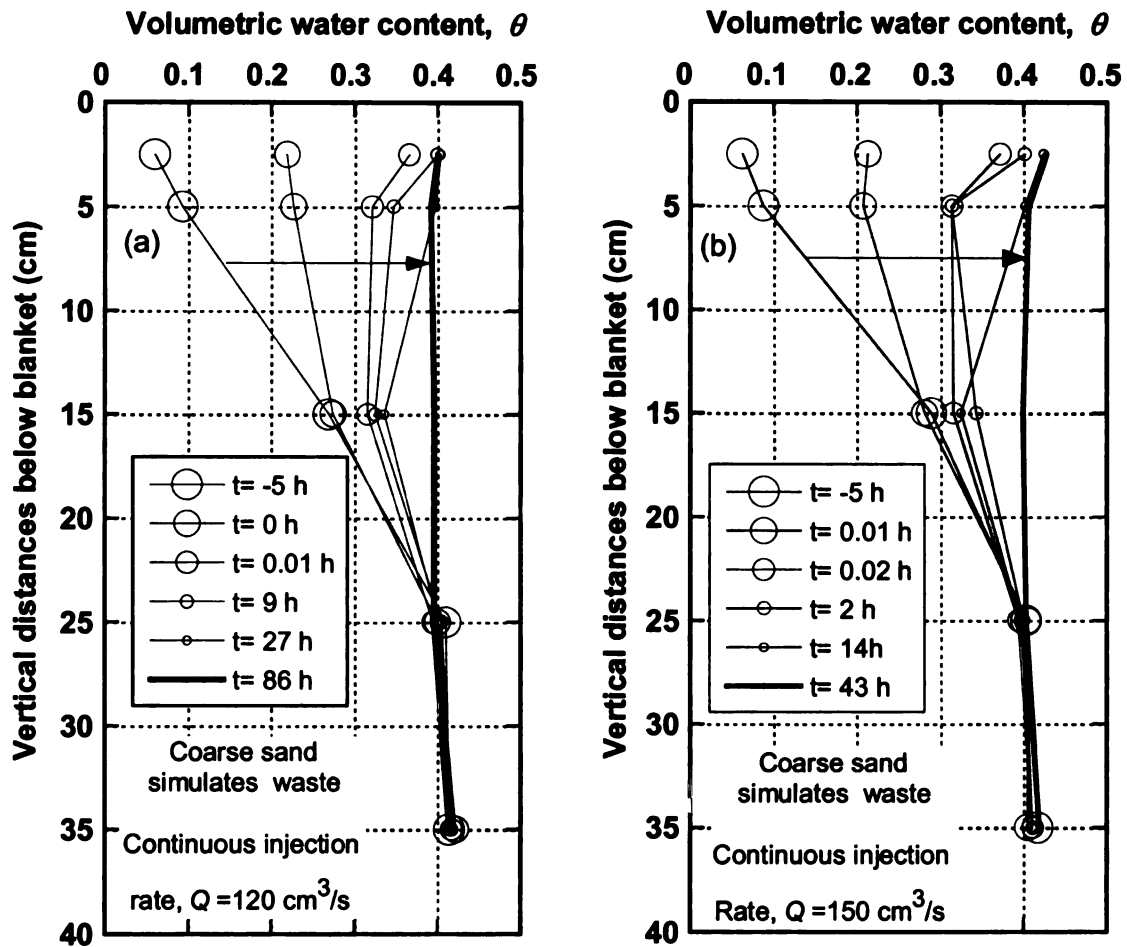


Figure 2-8: Transient water content profiles in coarse sand due to continuous injection at: (a) $120 \text{ cm}^3/\text{s}$; and (b) $150 \text{ cm}^3/\text{s}$.

Effect of Hydraulic Conductivity and Injection Rate on Wetted Width

Figure 2-9 shows the pressure heads in the blanket when DI water was injected at rates varying from $85 \text{ cm}^3/\text{s}$ to $150 \text{ cm}^3/\text{s}$ when the coarse sand was used. The objective of this experiment was to measure the extent of the wetted width of the blanket indicated by the

responses of the pressure sensors in the blanket as a function of injection rate. The wetted width is an important design parameter when permeable blankets are used for leachate recirculation (Khire and Haydar 2007; Haydar and Khire 2007). The injection at a flow rate was continued until the pressure heads in the blanket (h_m) reached a steady-state. For $Q=85 \text{ cm}^3/\text{s}$ as well as $90 \text{ cm}^3/\text{s}$, only the sensors within 7.5 cm from the injection pipe responded to the injection event. This indicated that the wetted width was less than 7.5 cm on either side of the blanket.

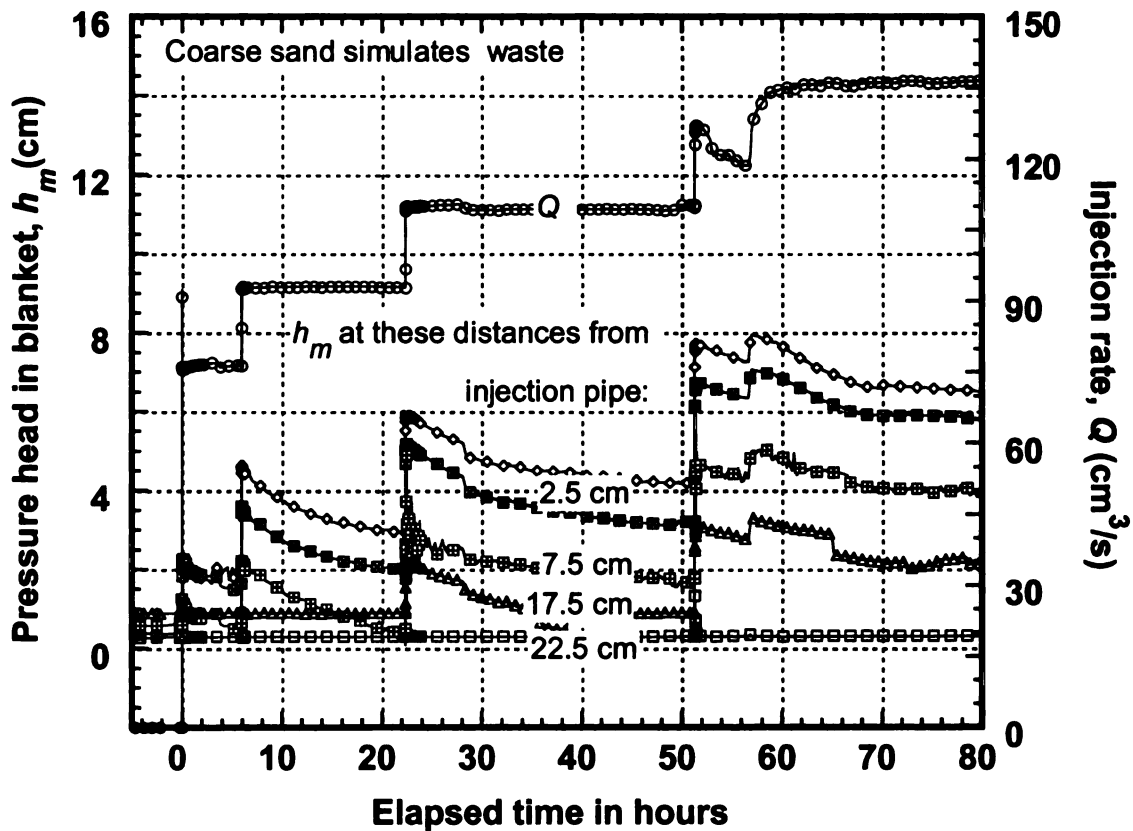


Figure 2-9: Wetted width at various injection rates in coarse sand.

For $Q=120 \text{ cm}^3/\text{s}$, the sensor located at 7.5 cm indicated increase in pressure head and the extent of wetted width increased further when the sensor located at 17.5 cm

responded for $Q=150 \text{ cm}^3/\text{s}$. Depending upon the magnitude of the rate of injection, some pressure sensors showed increase in h_m initially. As the degree of saturation of the underlying sand increased and hydraulic conductivity of the underlying sand increased, a steady-state approached and the wetted width decreased as indicated by drop in the pressure head to almost zero (Figure 2-9). This indicates that the wetted width of permeable blankets that are in continuous operation in the field would decrease if the degree of saturation of the underlying waste increases.

The wetted width increased with increase in injection rate. The injection pressure increases as the injection rate increases as shown in Figure 2-5. Thus, when injection pressure increases, it results in a greater wetted width due to greater hydraulic gradient in the blanket. This finding is consistent with the finding for vertical wells presented by Khire and Mukherjee (2007), McCreanor (1998) and for horizontal trenches and permeable blankets presented by Haydar and Khire (2005) and Haydar and Khire (2007). For a fixed flow rate, the wetted width of the blanket was greater with fine sand compared to the coarse sand due to lower hydraulic conductivity of the fine sand. This finding is consistent with the findings of Khire and Mukherjee (2007) and Haydar and Khire (2007) in numerical studies.

Hence the extent of wetting front can be determined from the responses of the pressure sensors located at designed positions in the blanket (Haydar and Khire 2006). The extent of wetting front depends on the hydraulic properties of the porous media and on the injection rate.

In Figure 2-6, when the injection was carried out at a constant rate of $Q= 150 \text{ cm}^3/\text{s}$

with initial degree of saturation of the underlying sand equal to 70%, the initial h_m at the sensor located 2.5 cm from the injection pipe was about 13 cm. Figure 2-9 shows that with increase in average degree of saturation due to preceding injection events, the initial h_{PB} observed for the same sensor located 2.5 cm from the injection pipe at the same injection rate of $Q = 150 \text{ cm}^3/\text{s}$ was about 8 cm. This confirms that h_{PB} decreases with increase in the degree of saturation of the underlying sand.

On/Off Dosing

Leachate is not continuously injected in landfills, rather it is injected in on/off dosing cycles. This may be to prevent buildup of excessive liquid pressure head on the liner, minimize leachate seep outs, and to minimize the occurrence of slope stability failures due to increase in leachate pressures. Daily leachate production at the landfill and available leachate management options influence the volume and duration of the on/off dosing cycles. Figure 2-1 shows the leachate recirculation at the landfill in Michigan where leachate has been injected in on/off dosing cycles since 2003. We simulated liquid injection in on/off dosing cycles in the landfill model for 3 min on/ 10 sec off. Figure 2-10 and Figure 2-11 shows the pressure heads in the blanket. The pressure heads in the blanket increased during the injection and dropped rapidly after the injection was stopped. This behavior is similar to observed in the field-scale blanket (Figure 2-1).

The sensors in the field showed negative pressures in the blanket after the injection was stopped (Figure 2-1). The lab model also showed suction in the blanket when the injection was stopped and the injected water drained from the blanket similar to the

response observed in the field. Additional experiments were carried out at other on/off dosing frequencies and other flow rates. The steady-state pressure heads in the blanket are a function of the on/off duration ratio and the rate of injection. However, when water was injected in on/off modes, the pressure heads in the blanket at steady-state for a fixed flow rate during the “on” period were higher than those at steady-state when water was injected continuously. The key reason is that the average degree of saturation of the sand is lower when water is allowed to drain during the off period and hence the infiltration capacity is reduced due to lower unsaturated hydraulic conductivity. The pressure heads increase to maintain the flow rate.

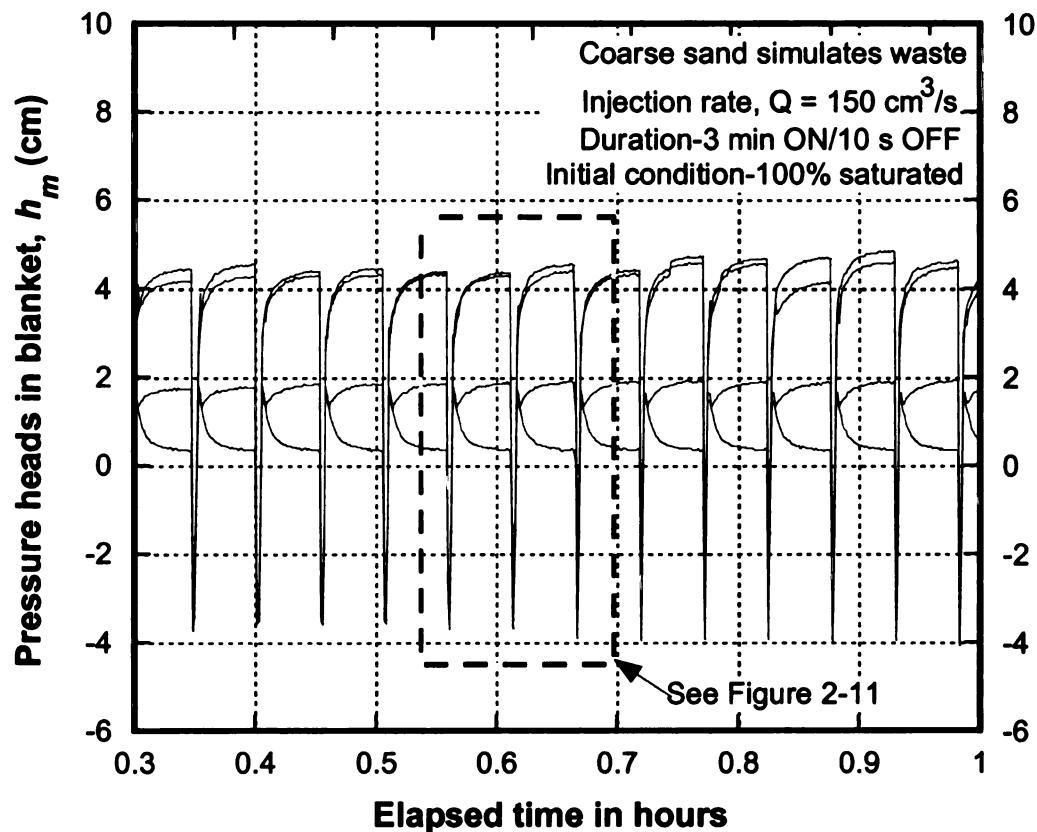


Figure 2-10: Simulation of on/off dosing cycles in the landfill model for a larger time interval.

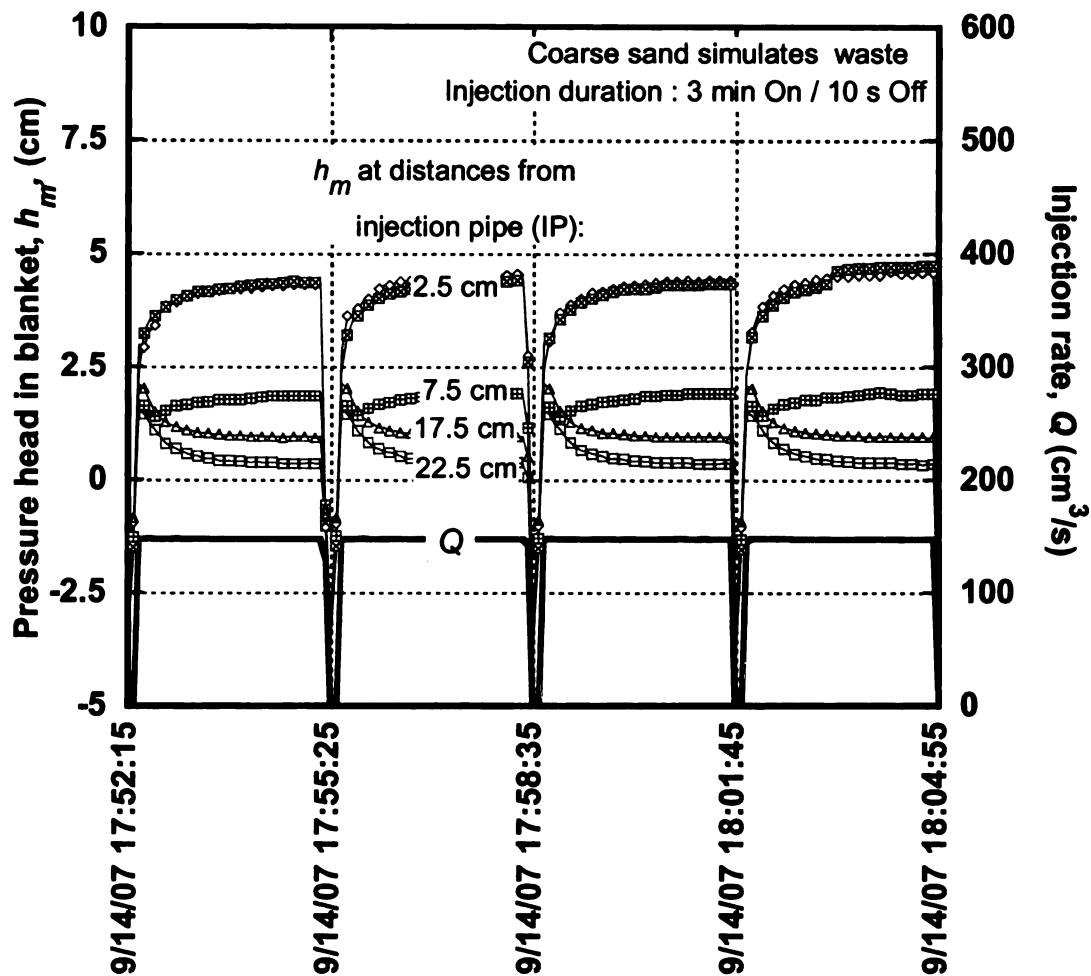


Figure 2-11: Snap shot of few on/off dosing cycles showing the pressure distribution in various sensors in the blanket.

SUMMARY AND PRACTICAL IMPLICATIONS

In the large-scale lab model of a landfill, hydraulic pressure heads in a permeable blanket due to liquid injection were measured using an automated sensing system consisting of pressure sensors. The degree of saturation of sand underlying the blanket below the blanket was measured using water content sensors. The key findings of this study are as follows:

- The landfill model was able to mimic the responses from a field-scale instrumented permeable blanket. Similar to the field responses of pressure sensors, the increase in the pressure head recorded by the blanket sensors in the lab-scale landfill model was earliest and greatest for the sensors located closest to the injection pipe and decreased subsequently with distances away from the injection pipe. Similarly, the pressure heads increased with the increase in the rate of injection and the sensors experienced suction as water drained from the blanket. The landfill model was able to simulate steady-state and transient conditions.
- The pressure heads in the blanket are a function of the rate of injection in the blanket and hydraulic conductivity of the underlying material. For a given liquid injection rate, the liquid injection pressure increases as the hydraulic conductivity of the waste decreases. In the field, for a fixed injection rate if the pressure heads in the blanket increase in course of time, it can be attributed partly to decrease in the hydraulic conductivity of the waste over time. This finding implies the need to monitor flow and pressure heads when liquid is injected in landfills.
- The advance of wetting front in the blanket as well as below the blanket depends on the hydraulic properties of the underlying material and on the flow rates.
- The wetted width of the blanket is a function of liquid injection rate and the hydraulic conductivity of the underlying soil. For a given injection rate, the wetted width is more for a lower hydraulic conductivity of the underlying soil (or waste). For a given hydraulic conductivity, a greater wetted width can be achieved by increasing the liquid injection. For continuous injection, the wetted width decreases as the degree of saturation of the system increases. If the rate of injection and

duration of on/off cycle is increased, the degree of saturation of the underlying waste would increase. However, when dosing is carried out in on/off cycles, it would be impossible to saturate relatively thick mass of waste because it would require relatively large volume of leachate or liquid injection needs to be carried for considerably long period of time.

PAPER NO. 3: NUMERICAL MODELING OF SUBSURFACE INJECTION IN AN INSTRUMENTED LANDFILL MODEL

ABSTRACT

A large-scale physical model of a landfill (85 cm long x 30 cm wide x 55 cm high) with permeable blanket as liquid recirculation system was developed in order to test the predictive capabilities of numerical models commonly used in numerical studies pertaining to subsurface liquid injection in bioreactor landfills. A 50 cm long x 30 cm wide x 2 cm thick horizontal permeable blanket made up of pea gravel was built in the landfill model for subsurface liquid injection. Homogeneous and isotropic fine and coarse sands were tested below the blanket in separate experiments in the setup. The blanket and the sandy soil below the blanket were instrumented with embedded sensors consisting of pressure transducers with built-in thermistors and time domain reflectometry (TDR)-based water content sensors connected to a datalogger, to monitor the migration of injected liquid in the blanket and in the underlying sand. Liquid injections in the blanket were carried out at varying rates either continuously or in on/off mode using magnetic drive or gear pump. The injected flow was monitored by flow sensor. Saturated/unsaturated finite element models HYDRUS-2D and Vadose/W were used to confirm the pressure heads and water contents measured in the physical model. The numerical models were able to simulate the pressure heads and water contents relatively accurately when a steady-state was reached. However, the models were not able to simulate the pressure heads and gradual increase in water contents before the steady-state was reached. This study implied that entrapped air bubbles have significant influence on hydraulic pressure heads which commonly used unsaturated flow models do not consider.

INTRODUCTION

Bioreactor landfills are designed and operated to accelerate the decomposition of organic constituents of municipal solid waste (MSW) by recirculating leachate (or injecting other liquids) as a means to enhance moisture levels within the landfill and creating an environment conducive to rapid degradation of organic waste fraction. The time to achieve waste stabilization is decreased through these purposeful controls of biological processes.

Leachate recirculation or liquid injection can be performed using multiple techniques, both surface and subsurface. The surface methods consist of spraying leachate over the landfill surface area or constructing leachate pond. The conventional subsurface application techniques are: (1) vertical wells; (2) horizontal trenches; and (3) permeable blankets. The design guidelines available for the leachate recirculation systems are based on numerical studies. Haydar and Khire (2005), Haydar and Khire (2007) and Khire and Mukherjee (2007) have presented design guidelines for horizontal trenches, permeable blankets and vertical wells, respectively, through numerical studies.

The numerical models used in the studies for leachate recirculation helped to predict and evaluate different scenarios without the effort and expense of physical experimentation. However, these mathematical models are idealized representations of physical processes driven by assumptions and available input data and hence the models' predictive capabilities must be confirmed by comparing the modeled results with controlled lab/field testing. However, it has not been possible to verify the modeling results for leachate recirculation application because it is not possible to achieve steady-state flow conditions in the field due to the scale of the system. For transient scenarios,

which are common in the field, often the sensor spacing and frequency of readings is not adequate for the highly heterogeneous waste. Hence, controlled field testing in landfills is almost impossible to verify numerical models which make it essential to confirm the predictive capabilities of the numerical models that are commonly used to design subsurface injection systems.

A lab-scale physical model of landfill was developed to conduct controlled lab tests to simulate hydraulics of liquid injection consisting of an instrumented permeable blanket. The lab model has sensors embedded in the sand underlying the blanket to characterize the hydraulics of liquid flow due to subsurface injection. The key objective of the study presented in this paper is to confirm numerical models through demonstration of agreement between observed and predicted pressure heads in the blanket and the water contents of the underlying soil due to subsurface liquid injection. This paper presents the design of the landfill model, data collected from the model, and numerical modeling results obtained from finite-element models - HYDRUS-2D and Vadose/W.

PHYSICAL MODEL

Figure 3-1 presents a schematic of the landfill model fabricated to simulate a horizontal permeable blanket. All acrylic panels of the model were screwed together with rubber seals in-between the panels to provide a watertight box to contain the soils subjected to injection of water. A silicone sealant was applied at the seams to prevent potential leakage. A separate acrylic panel was used to make the bottom of the leachate collection system (LCS) raised to a fixed slope of 3%.

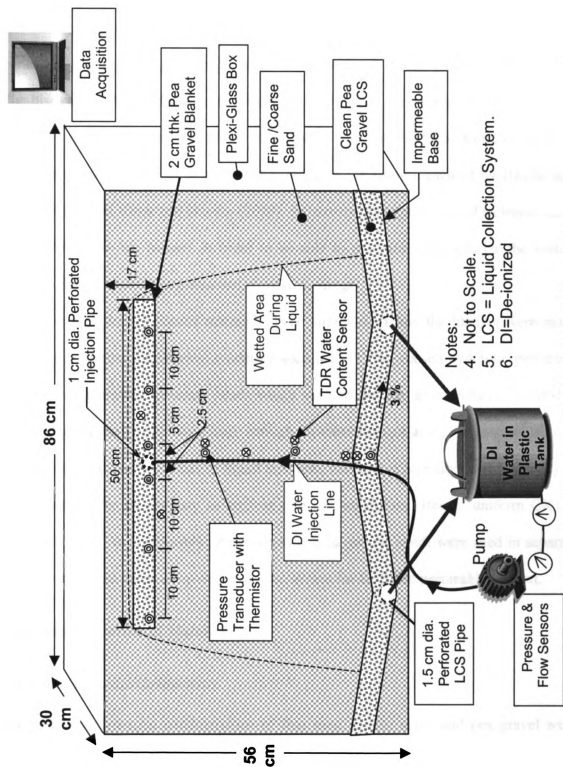


Figure 3-1: Schematic of the lab-scale landfill model.

Landfill Components

Various soils were used to simulate these components of the landfill model: leachate collection system (LCS), permeable blanket, and porous material underlying the blanket. The blanket and the LCS were made up of pea gravel. Pea gravel was chosen as the LCS drainage material because it results in lower liquid heads in the LCS (Khire *et al.* 2006) and it was also considered as a blanket material in the study presented by Haydar and Khire (2007) and Khire and Haydar (2003). Relatively homogeneous and isotropic sands were used below the blanket in order to be able to accurately characterize the system components to confirm the numerical models' findings.

The selection of porous materials to be simulated below the blanket were made based on preliminary numerical modeling such that: (1) the chosen hydraulic properties of the sands generated pressure heads which were within the dimensions of the model; and (2) the pressure heads were large enough for measurement using the pressure sensors for various magnitudes of rates of liquid injection, duration of injection, and frequency of liquid dosing, for steady-state as well as transient conditions. Hence, uniform OK110 sand (fine sand) and uniformly graded Ottawa sand (coarse sand) were used in separate experiments in the same setup with the same design for LCS and permeable blanket.

Hydraulic Properties of Materials

Saturated Hydraulic Conductivity

The saturated hydraulic conductivities of fine sand, coarse sand, and pea gravel were measured in the laboratory using a rigid wall permeameter (ASTM D 2434-68) using the Mariotte bottle (constant head test). Alternatively, the saturated hydraulic conductivity of

the fine sand was also measured in a flexible wall permeameter using falling head method (ASTM D 5084-03). The saturated hydraulic conductivities of all the soils presented in Table 3-1 are average values obtained from triplicate tests.

Soil-Water Characteristic Curves

The relationship between volumetric water content and matric suction of fine sand, coarse sand, and pea gravel was obtained through a hanging column experimental setup comprised of Buchner funnel with porous ceramic plate (ASTM D 6836-02). Drying as well as wetting soil-water characteristics curves (SWCC) were generated. The experiments for determining the SWCC for all soils were repeated twice. The soil-water characteristic curves are described in terms of the van Genuchten (1980) fitting equation. The fitting parameters are tabulated in Table 3-1. Soil-water characteristics curves for fine and coarse sand are shown in Figures 3-2a and 3-2b.

Table 3-1: Saturated and unsaturated hydraulic properties of soils used in the landfill model.

Soil type	Location	Saturated and unsaturated hydraulic properties				
		K_s (cm/s)	θ_s	θ_r	α (1/cm)	n
Fine Sand	Below and above blanket	1.8 to 6.4×10^{-3}	0.42	0.03	0.01 to 0.02	6.5
Coarse sand	Below and above blanket	0.05 to 0.09	0.4	0.03	0.023 to 0.09	4.5
Pea Gravel	Blanket and LCS	2	0.43	0.01	0.45	3.0

Note: LCS = Leachate Collection System

θ_s = saturated volumetric water content [dimensionless];

θ_r = residual volumetric water content [dimensionless]; and

α [1/L] and n are van Genuchten's fitting parameters (van Genuchten 1980)

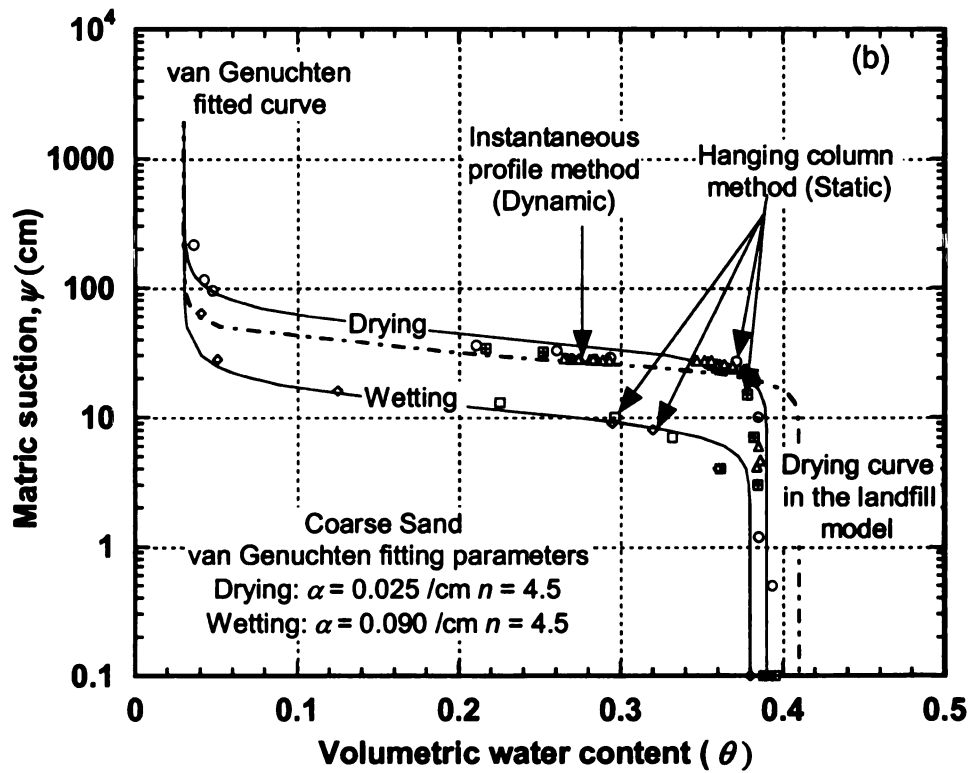
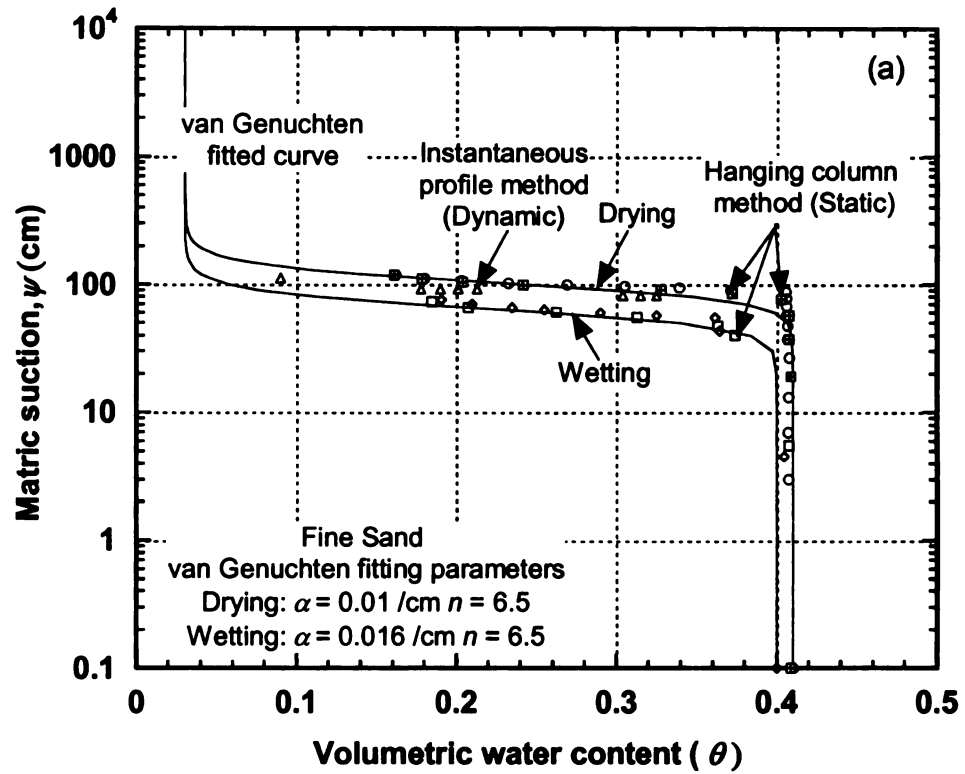


Figure 3-2: Soil-water characteristics curves for fine sand (a); and coarse sand (b).

Figure 3-2b shows that, during the wetting path, a different path for the relationship between the matric suction head and the degree of saturation was obtained. The maximum degree of saturation achieved during wetting was less than the full saturation although the matric suction head had dropped to zero. The degree of saturation with trapped air is equivalent to the difference between full saturation and maximum saturation achieved at zero suction head.

The SWCC for the in-situ coarse sand in the physical model was also obtained. The pressure head is the negative of elevation above the water table for hydrostatic equilibrium. Considering the capillary barrier at the interface of sand and LCS, formed after water drained under gravity at the end of injection experiments as the water table, the soil water retention curve was obtained by associating water contents measured by the sensors in the sand with the negative of elevation above water table. The in-situ desorption SWCC was observed to correlate with the drying curve obtained from hanging column method and instantaneous profile method for unsaturated hydraulic conductivity experiments as shown in Figure 3-2b. Similar drying curve for fine sand could not be obtained since fine sand did not drain easily under gravity like the coarse sand.

Unsaturated Hydraulic Conductivity

Unsaturated hydraulic conductivities for fine and coarse sand were determined in the laboratory using the instantaneous profile method via evaporation. The tests were conducted in a 20 cm diameter and 20 cm high PVC cylinder. The sample was instrumented with four sets of each of TDR-based water content sensors and heat dissipation matric potential sensors which were equally spaced along the center of the soil column (vertical spacing = 2 cm) to reduce radial boundary effects during testing.

The water content sensors and the heat dissipation matric potential sensors were placed at the same elevation so that the suction and water content data could be directly correlated. The permeameter was placed in the laboratory where isothermal conditions prevailed due to which temperature gradients could be reduced. The soil profile was saturated through the bottom of the sample and was allowed to de-saturate only through the top by evaporation processes by plugging the port at the bottom. A continuous supply of air from a fan was applied across the top of the permeameter to increase the rate of evaporation from the surface (Meerdink *et al.* 1996).

The measured water contents and matric suction at different depths correlated with the desorption soil-water characteristics curve obtained from hanging column experiments as shown in Figure 3-2. The rigorous instantaneous profile method was numerically simulated in HYDRUS-2D. The simulated water content and suction as a function of time were compared with the measured water content and suction data from the nested sensors at different depths.

The numerical model was created using axisymmetrical radial option in HYDRUS-2D. The problem domain was divided into fine rectangular grids with closer spacing of nodes near the soil surface. The nodal spacing near the surface was important because the effect was related to the movement of the drying front through the soil profile and development of potentially very high suction heads (and gradients) near the soil surface. A correct conceptualization of the problem was established involving boundary conditions and initial conditions. The top boundary was simulated as atmospheric boundary to account for the movement of drying front through the soil profile due to evaporation. All other boundaries were simulated as no-flux boundaries. Potential

evapotranspiration was calculated using Thornthwaite (1948) water balance method. The locations of the nest of sensors were simulated as observation nodes.

HYDRUS-2D model uses the van Genuchten-Mualem (Mualem 1976) function to predict the unsaturated hydraulic conductivities using the van Genuchten fitting parameters and the saturated hydraulic conductivities. The van Genuchten fitting parameters were adjusted such that the predicted decrease in water content and suction with time at the observation nodes fitted the experimentally measured data from the sensors in an optimal manner. The fitting parameters from this experiment were found close to those determined from the hanging column experiments.

Instrumentation and Calibration

The following sensors were used in the landfill model: (1) pressure transducers with built-in thermistors; (2) water content sensors; and (3) flow sensors. All sensors were connected to a datalogger to continuously monitor and log the data. The water content sensors were connected to the datalogger via an electro-magnetic pulse generator and a coaxial multiplexer. The datalogger was programmed to take readings at frequencies 5 s to 30 min.

Pressure Transducer

The length and diameter of pressure transducer were 8.5 cm and 1.2 cm, respectively. The pressure transducer provided temperature compensated analog 0-5 VDC output proportional to the water pressure experienced by it. The sensitivity of the sensor was $\pm 1\%$ and have a measurement range of 0 to 92 cm of water head. Since the sensors were vented, barometric pressure was not recorded by the diaphragm. In recognition of the

concern for zero drift and offsets, the accuracy of all sensors was checked from time to time by ponding water and checking the measured static heads during the course of experiments.

The pressure transducers were calibrated by applying known pressures and measuring the response. In order to evaluate the accuracy of their measurements, the pressure transducers were placed in a container in the position they were eventually embedded in the LCS, sand and the blanket in the landfill model. The pressure transducers were tested by adding de-ionized (DI) water at depths ranging from 15 to 35 cm. A linear relationship between the depth of water in the container and the pressure head readings recorded by the pressure transducers was observed. The accuracy of the pressure transducer was within ± 0.5 cm. Periodically, water was ponded in the landfill model and maintained at a fixed level for few hours to measure signal drift for the pressure sensors. At the end of the experiments, when the setup was dismantled, the calibration of the sensors was re-checked and corrected, if needed. The zero was found to have drifted approximately by 0.3 to 0.6 cm.

TDR Water Content Sensor

The mini-TDR water content sensor consisted of three pointed 0.15 cm diameter stainless steel rods mounted into an encapsulated plastic head. The probe rod length was 6 cm and spacing between the probe rods was 0.6 cm. Topp's (Topp *et al.* 1980) empirically derived calibration equation was used to convert the dielectric constant values to volumetric water content.

The TDR water content sensors were fully inserted vertically in a container filled with dry sand and then water was gradually added in known steps until the sand got

saturated. For both sands, a linear relationship between the volumetric water content calculated from known addition of water and the volumetric water content measured by the TDR water content sensors was observed.

Flow Sensor

The flow sensor was capable of measuring flow rates ranging from 8 to 165 cm³/s. The flow sensor incorporated a pelton-type turbine wheel having diameter and thickness equal to 1.6 cm and 0.075 cm, respectively to measure the flow rate of water. The rotational speed of the turbine wheel increased proportionally to the volumetric flow rate generating electric pulses. The sensors provided analog DC voltage output proportional to the flow rate and the flow rate in engineering units was shown on the integrated LCD display.

A linear relationship was observed between the flow rates recorded by the flow sensor and the flow calculated from the levels measured by the pressure transducer. The accuracy of the flow sensor was within $\pm 0.5\%$.

Pump

The maximum flow that a pump needed to deliver in the landfill model was based on these factors: (1) hydraulic conductivity of sand underlying the blanket; and (2) injection rate. A miniature gear pump was used for relatively low injection flow rates (8 cm³/s – 42 cm³/s) when fine sand was used and a brushless magnetic drive pump was used for higher injection flow rates (75 cm³/s – 300 cm³/s) when coarse sand was used. Both pumps were operated with a variable power DC power supply to obtain variable injection flow rates. These pumps were chosen because of their ability to deliver “pulseless” flows

because the rate of flow had to be constant to achieve consistent results. A quartz based digital timer was used to operate the pump in on/off mode which could be programmed for various durations of on/off injection cycles.

Fabrication of Instrumented Model Landfill

Figure 3-1 shows the schematic of the landfill model and the location of sensors. A 4-cm thick LCS made up of pea gravel was constructed at the bottom slope of the plexi glass tank. Two 1.5-cm diameter perforated pipes discharging freely into the atmosphere were placed 45 cm apart in the LCS pea gravel layer. The perforated seepage pipes for LCS had at least 10 times higher flow capacity than the flows injected in the model to maintain the pressure head in the LCS within its thickness of 4 cm. A geotextile was placed between the LCS and the sand to prevent clogging of the LCS.

About 40-cm thick dry sand having dry density equal to 1.6 g/cm^3 and porosity of about 0.42 was placed below the blanket. In the sand layer, two pressure transducers were embedded in vertically upright position at 10-cm intervals. A TDR water content sensor was placed in the sand immediately next to the sensing tip of the pressure sensor.

The permeable blanket for the recirculation system was made up of the same pea gravel used in LCS. The blanket was about 50 cm long and 30 cm wide. The thickness of the blanket was 2.0 cm. The perforated injection pipe of 1 cm diameter was embedded at the center of the blanket in the direction parallel to the width of the blanket where water was injected under a positive pressure. Total six pressure transducers in vertically upward position were embedded in the sand at designated locations such that the tip of the sensor was within the blanket. The injection pipe, the tip of the pressure transducers and the LCS pipes were wrapped with a mesh to prevent clogging of gravel particles in them. The

blanket was wrapped with a geotextile to separate the permeable material from the surrounding sand to prevent clogging of the blanket.

The end of the injection pipe inside the blanket was capped and the other end was connected consecutively to a pressure transducer to measure the injection pressure and a flow sensor to measure the injection flow rate. A closed loop recirculation system was formed wherein the injected water after flowing through the soil and discharging freely in the atmosphere from the seepage pipes (LCS) got collected in the storage tank which was again injected back into the blanket as shown in Figure 3-1. A pressure transducer was also placed in the storage tank to monitor the change in head of water in the tank to monitor if and when a steady-state is reached.

Falling Head Tests

Falling head tests were performed on the landfill model to measure the saturated hydraulic conductivity of the whole system. This allowed measuring the effect of scale, presence of sensors, and sensor cables on the vertical hydraulic conductivity of the model and thus providing the “in-situ” conductivity. At the end of each liquid injection experiment, falling head tests were conducted to measure the in-situ saturated hydraulic conductivity of the whole system due to the current injection of water. For the fine sand, the measured saturated hydraulic conductivity of the landfill model ranged from 1.8×10^{-3} to 6.4×10^{-3} cm/s and for the coarse sand it ranged from 5×10^{-2} to 9×10^{-2} cm/s (Table 3-1).

The maximum value for saturated hydraulic conductivity of 0.09 cm/s for coarse sand was obtained by constant head test after saturating the entire sand in the model. In this experiment, the whole model was continuously saturated for a period of 15 days by

pumping water at a very high rate from the top surface of the overlying sand. In doing so the air was compressed and/or dissolved in the water under pressure. Additional water content sensors with longer probe rods were inserted outside the blanket which confirmed gradual increase in saturation of the sand.

NUMERICAL MODEL

HYDRUS-2D and Vadose /W

HYDRUS-2D and Vadose/W were the opted numerical models to mathematically simulate the hydraulics of the landfill model. Both models numerically solve modified forms of Richards' equation (1931) for saturated/unsaturated water flow and have an option of using van Genuchten (van Genuchten 1980) function for soil-water characteristic curves and van Genuchten-Mualem (Mualem 1976) model for predicting the unsaturated hydraulic conductivity function. Assuming homogeneous and isotropic soil properties, the governing partial differential equation for water flow is the 2-D form of Richards' equation which is as follows (Equation 2-1):

$$\frac{\partial \theta}{\partial t} = -\frac{\partial}{\partial x}\left[k(\psi)\frac{\partial \psi}{\partial x}\right] - \frac{\partial}{\partial z}\left[k(\psi)\frac{\partial \psi}{\partial z}\right] + \frac{\partial k(\psi)}{\partial z} - S_w \quad (2-1)$$

where θ = volumetric water content [dimensionless]; ψ = matric suction head [L]; k = hydraulic conductivity of the porous material which is strongly dependant on the matric suction or water content [L/T]; z = vertical dimension [L]; S_w = volume of water removed per unit time per unit volume of soil by plant water uptake or evaporation (sink term) [1/T]; and t = time [T]. HYDRUS-2D and Vadose/W uses the Galerkin finite-element method to solve the governing equation of flow.

HYDRUS-2D and Vadose/W can simulate water and heat in unsaturated, partially saturated, or fully saturated porous media. Both the programs are capable of simulating steady-state and transient conditions. HYDRUS-2D has been used for saturated/unsaturated liquid and solute transport through porous media in several studies (Haydar and Khire 2007; Khire and Mukherjee 2007; Haydar and Khire 2005; Haydar and Khire 2004; Scanlon *et al.* 2002; Henry *et al.* 2002; Rassam *et al.* 2002; Pang *et al.* 2000).

Input Parameters for HYDRUS-2D

Mesh Discretization

Figure 3-3 shows the mesh sizes generated in HYDRUS-2D. An unstructured mesh was automatically generated to discretize the flow domain into triangles. The minimum size of the finite-elements used for discretization of the problem domain, the time step, and the error tolerances for pressure head and water content were selected such that cumulative water balance error did not exceed 0.1%.

In order to achieve such a low mass balance error, the problem domain was divided in to approximately 13,000 nos. fine triangular finite elements. The dimensions of the finite elements grid were smaller around the injection pipe, where the hydraulic gradient was higher. An error tolerance of 0.1% for the volumetric water content and 0.01 cm for the matric suction head were assigned in the input. A minimum time step of 10^{-10} s and a maximum time step of 0.1 s were used.

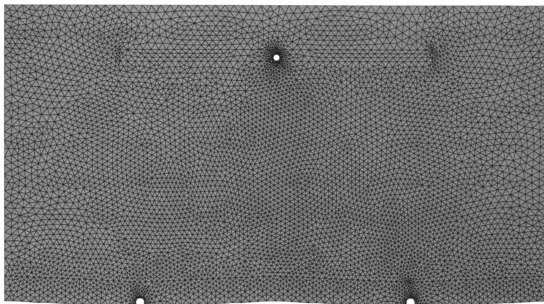


Figure 3-3: Typical mesh used for modeling in HYDRUS-2D.

Material Properties

The saturated and unsaturated properties tabulated in Table 3-1 were input as material properties for all landfill components. Because water entered the soil, the retention parameters for wetting were considered. Effect of hysteresis was also explored. Hysteresis had no effect on the simulated results. Only isothermal water flow was considered in the study.

Initial and Boundary Conditions

The initial conditions input to the numerical model were consistent with those measured in the physical model before the injection was started. The initial condition was entered in the form of volumetric water content, measured by the water content sensors at various depths in the sand before injection started.

Specifying conditions to the boundaries is a key component of numerical analysis. All external boundaries were simulated as zero-flux boundaries which indicate that no water flows into or out of the domain through this boundary. Leachate collection pipes embedded in the leachate collection system were simulated as seepage face boundaries. A seepage face boundary allows flow only when the boundary is saturated. This boundary condition is conservative for predicting liquid pressure head in LCS because no flow is allowed across the boundary when LCS is unsaturated. However, the flow actually occurred under saturated as well as unsaturated conditions. The pore pressure head is equal to zero along the saturated part of the seepage face through which water seeps out from the saturated part of the domain. The seepage face is a dynamic drainage boundary condition that changes according to the flow conditions during the simulation.

The perforated injection pipe was simulated as a constant flux boundary for steady-state problems and variable flux boundary for transient problems. In variable flux boundary for on/off conditions, the flux was input as a time series. For each record in the time series in variable flux boundary, the input flux was effective during the period between the time of the previous record and the current one. The pipe became a zero flux boundary during the “off” period of the pump. The input flux was calculated by dividing the injected flow rate per cm length of the injection pipe by the circumference of the pipe.

Other Input Parameters

The locations of sensors were input as observation nodes in order to obtain simulated pressure heads and water contents. The effect of temperature was ignored due to isothermal conditions prevailing in the laboratory.

Input Parameters in Vadose/W

Mesh Discretization

Figure 3-4 shows the mesh sizes generated in Vadose/W. The problem domain was divided into a structured mesh in the form of 4,250 quadrilateral elements. The time stepping was adjusted to discretize the time domain into a series of incremental time steps. The minimum and maximum time steps were set to 0.0001 and 1 second, respectively. The spacing between the nodes located near the flux and seepage boundaries were relatively small to ensure as little numerical error as possible due to the assigned boundary conditions.

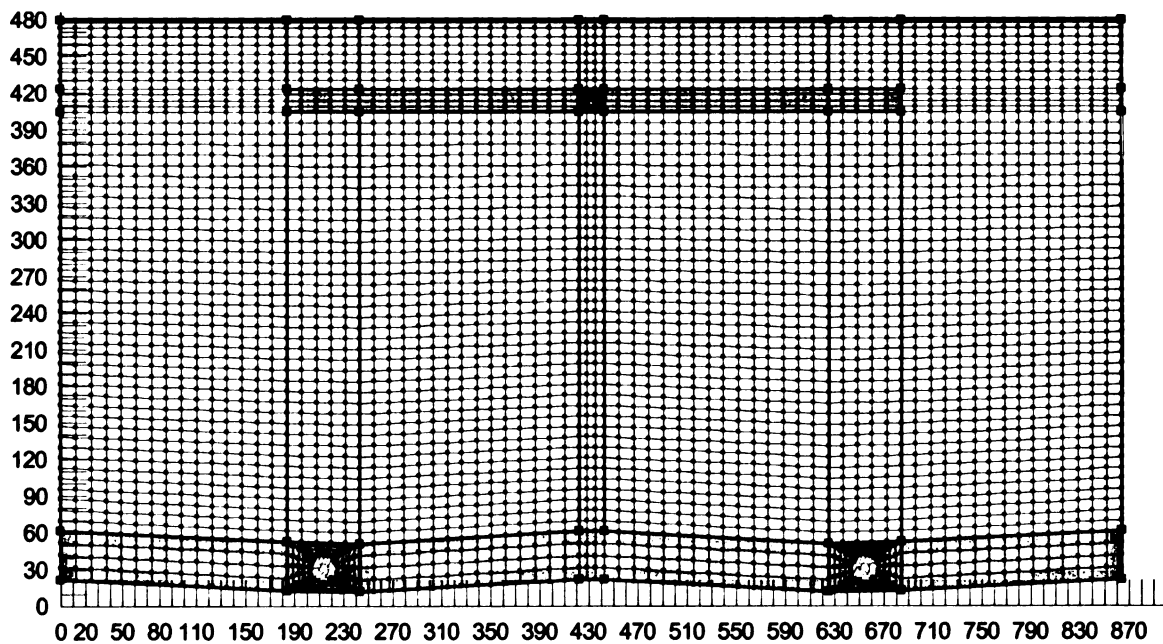


Figure 3-4: Typical mesh used for modeling in Vadose/W.

Material Properties

Apart from the saturated and unsaturated properties listed in Table 3-1, the coefficient of compressibility (m_v) was also input in the hydraulic function. Because water can be released by compressing the soil skeleton and reducing the size of voids, the coefficient of volume compressibility m_v is input to adequately represent the slope of the water content function in the positive pore-water pressure region. The m_v for pea gravel and the sand were assumed as 1×10^{-5} 1/kPa as per the Vadose/W User's manual (Geo-Slope 2004). A sensitivity analysis was carried out by varying the order of magnitudes of m_v but it had no effect on the results.

Because temperature and moisture gradients influence vapor and liquid flow in unsaturated soils, Vadose/W couples heat and mass flows, for which two thermal functions are required by the program for each material type, i.e. volumetric specific heat and thermal conductivity functions. The ability of the soil to transfer heat is described by its volumetric heat capacity and thermal conductivity. The thermal conductivity of soil is dependent on its water content, because of differences in thermal conductivity of air and water, and hence is a function of the soil water characteristic curve. Typical values of soil mineral mass specific heat capacity of $0.71 \text{ kJ/kg}^\circ\text{C}$ and soil mineral thermal conductivity of $216 \text{ kJ/day m}^\circ\text{C}$ for the materials used in this study were derived from the Vadose/W User's manual (Geo-Slope 2004) based on soil mineralogy. The thermal conductivity functions and volumetric heat capacity for each material were estimated using the built-in Vadose/W estimation tool.

Initial and Boundary Conditions

In order to obtain initial head conditions, steady-state analyses were conducted by specifying matric suctions corresponding to in-situ water contents and an initial temperature equal to room temperature of 20°C above the base of the model. The subsequent file generated was used as the initial condition file for the transient analysis.

The total injected flow rate was applied as total nodal flux equally distributed at the nodes of the circular boundary representing the injection pipe. For the input of total flux, the thickness of elements was specified. For on/off conditions, the nodal flux as a function of time was input in cyclic mode in hydraulic boundary condition. All external boundaries were simulated as zero-flux boundaries and the leachate collection pipes were simulated as seepage face boundaries.

RESULTS

Continuous Injection in Coarse Sand

Pressure Heads in Blanket

Figures 3-5 and 3-6 show the measured pressure heads, (h_m) and simulated pressure heads, (h_s) when de-ionized (DI) water was injected at a constant rate, $Q = 150 \text{ cm}^3/\text{s}$ in the setup with coarse sand. The injection event was simulated in both HYDRUS-2D and Vadose/W. Figure 3-5 shows HYDRUS-2D simulated pressure heads h_s in the blanket and Figure 3-6 shows Vadose/W simulated pressure heads h_s in the blanket.

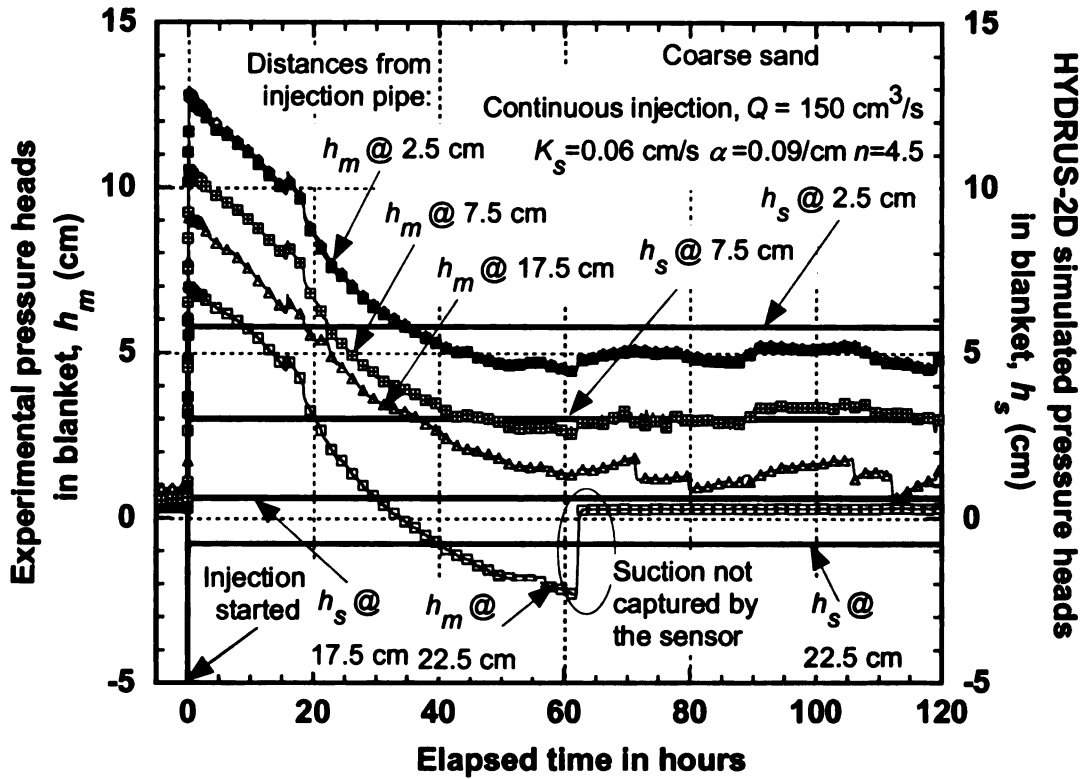


Figure 3-5: Measured and HYDRUS-2D predicted pressure heads in the blanket due to continuous injection with coarse sand underlying the blanket.

Figures 3-5 and 3-6 show that because the hydraulic conductivity of the permeable blanket is two orders of magnitude greater than the underlying sand, the water traveled across the blanket relatively faster compared to its infiltration into the underlying sand. As the injected water traveled through the blanket, the hydraulic pressure heads (henceforth referred to as pressure heads) in the blanket increased. All pressure transducers in the blanket indicated an increase in the pressure head in response to the liquid injection event which was also confirmed from numerical simulations. The measured pressure heads were relatively high in the beginning which decreased as the average degree of saturation and the hydraulic conductivity of the sand increased due to

continuous injection of water. In about 60 hours after the injection began, the pressure heads reached a steady-state when the average degree of saturation of underlying sand reached 100%. The steady-state was assumed to have reached when the average degree of saturation of the underlying sand in the landfill model reached 100% and the pressure heads in the blanket did not show upward or downward trend for several hours. While the inflow rate was measured using a flow sensor, outflow rate could not be measured in the setup. It was measured indirectly from the water level in the water tank measured by a piezometer.

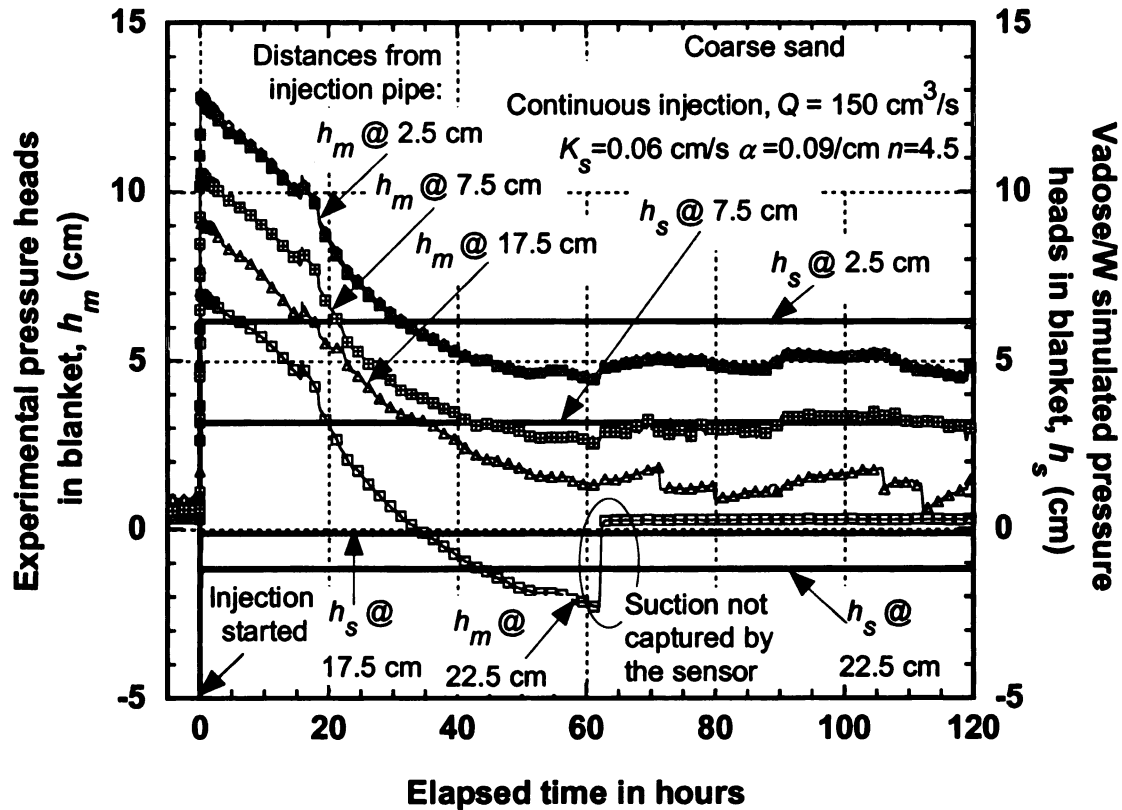


Figure 3-6: Measured and Vadoso/W predicted pressure heads in the blanket due to continuous injection with coarse sand underlying the blanket.

The increase in the pressure head was earliest and greatest for the sensors located closest to the injection pipe and decreased subsequently with distances away from the injection pipe which was confirmed from numerical simulations. The simulated pressure heads in the blanket were relatively close to the measured pressure heads at steady-state. However, the numerical models were unable to simulate the initial high pressure heads in the blanket. The simulated pressure heads reached steady-state immediately whereas it took many hours (>60 hrs) for the heads to reach steady-state in the physical model.

Because both numerical models, HYDRUS-2D and Vadose/W, produced similar results, results from only one of the models will be presented in subsequent sections.

Water Content of Sand

Figure 3-7 shows the measured increase in water content, (θ_m) and simulated increase in water content, (θ_s) at various depths in the sand due to continuous injection, $Q = 150 \text{ cm}^3/\text{s}$ in the setup with coarse sand. In the physical model, the water content sensors embedded in the sand indicated sequential increase in water content, as the saturated wetting front moved. The time when the pressure heads reached steady-state (Figure 3-5 and Figure 3-6) the water contents in the sand reached saturation (Figure 3-7). A capillary barrier existed at the interface of the LCS and the sand before the injection started, which was indicated by the water content sensors reading saturation at locations 35 cm and 25 cm below the blanket closer to the LCS.

The modeling results from Vadose/W and HYDRUS-2D (not shown here) showed that the underlying sand reached saturation within 2.5 min after injection started whereas

measured water contents increased gradually and reached saturation after 60 h (Figure 3-7).

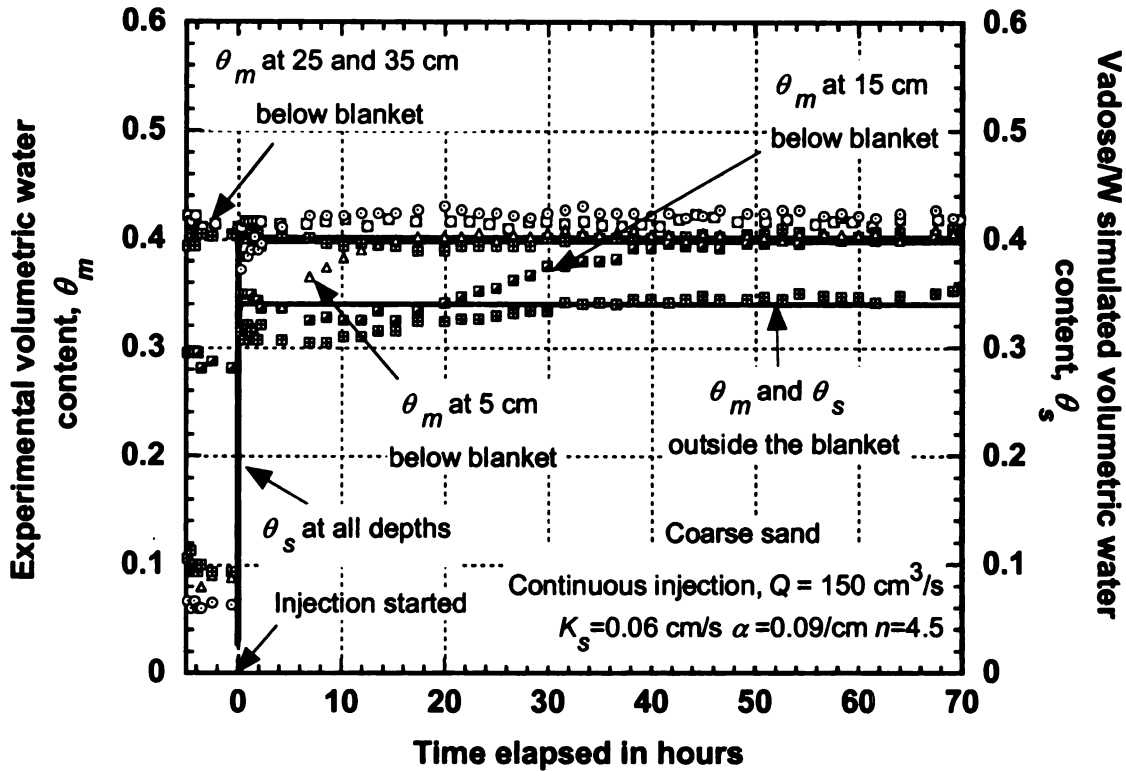


Figure 3-7: Measured and Vadose/W simulated water content at different depths within the coarse sand below the blanket due to continuous injection.

Observed versus Simulated Results

The simulated and observed pressure heads in the blanket and water contents in the sand due to injection were relatively close at steady-state. However, the initial high heads and the gradual increase in water content were not captured by HYDRUS-2D and Vadose/W. Both models produced similar results. Entrapped air in the sand during the experiment

and single phase approach by the models contributed to the discrepancies between the observed and simulated results before the steady-state was reached.

Air Compression in the Physical Model

Downward infiltration into an initially unsaturated soil generally occurs under the combined influence of suction and gravity gradients. During the early stages of infiltration, when the wetting front was near the surface, the matric potential gradients dominated over the gravitational force. When the injected water infiltrated the sand from the saturated blanket in the landfill model, the fine pores began to fill rapidly at first, because the smaller pore space produce an environment in which there is a greater capillary force. Unsaturated flow is actually a special case of multiphase flow through porous media, with two phases, air and water, coexisting in the pore channels. When water moved through the soil pores, if an equal volume of air was displaced without viscous resistance, the air pressure in the pores does not build up. Hence, infiltration is a process of two phase immiscible displacement.

The saturated region at the interface of gravel and sand caused due to capillary break, created a water-bounded profile having small air permeability in that region. The lateral escape of soil air was also restricted due to the boundaries of the model. Hence, the pore air could escape to the atmosphere so long there were passages created in the sand with various connected large pore spaces upwards to the open surface of the sand. Encapsulated air or non-continuous air bubbles isolated from atmosphere were formed in the wet sand due to advance of water through preferred pores or pore sequences on some occasions resulting in sealing by water of all paths through which gaseous air would need to escape for the complete wetting of another pore or group of pores. Occluded air

bubbles commonly occur in unsaturated soils having a degree of saturation greater than 90% (Fredlund and Rahardjo 1993). The entrapped air content typically ranges from 0 to 20% of the bulk soil volume (Fayer and Hillel, 1986).

The build up in air pressure due to restriction of air flow in presence of a shallow water table, or by lateral obstructions have been observed, both in field (Dixon and Linden 1972) and in laboratory columns (Free and Palmer 1940; Wilson and Luthin 1963; Vachaud *et al.* 1974; Touma and Vauclin 1986; Grismer *et al.* 1994; Wang *et al.* 1997). Investigations on air encapsulation and entrapment were done by Wang *et al.* (1997), Seymour (2000) and Wangemann (2000).

Effect of Entrapped Air Bubbles

The pressure in an entrapped air bubble can be related to matric potential by Equation 3-2:

$$p_b - \frac{2T_s}{r} = p_w = p_a + \psi \quad (3-2)$$

where p_b = pressure in air bubble; p_w = pore-water pressure; and p_a = pore-air pressure; r = radius of air bubble; ψ = matric potential and T_s = surface tension of liquid.

The air bubbles are under pressure greater than atmospheric and greater than the surrounding water as observed from Equation 3-2. Substituting $T_s = 0.072$ N/m at 20° C in Equation 3-2 and assuming the tiniest air bubble to be 0.02 cm same as the pore size, the pressure head in a bubble which exceeds that in the surrounding water can be up to 7 cm.

Encapsulated air has been shown to affect saturated hydraulic conductivity (Christiansen 1944; Gupta and Swartzendruber 1964; Seymour 2000) at or near saturation (Sakaguchi *et al.* 2005). Since the saturated hydraulic conductivity is a key parameter in many unsaturated hydraulic conductivity models, the presence of entrapped air may affect not only the saturated hydraulic conductivity itself, but also the entire unsaturated hydraulic conductivity function due to the fact that entrapped air clogs the largest water conducting pores (Sakaguchi *et al.* 2005). Hence initial pore water pressure heads recorded by the pressure sensors were high due to the entrapped air bubbles and their effect on hydraulic conductivity. The initial high pressure heads decreased due to increase in hydraulic conductivity of sand and hydraulic conductivity is known to increase when entrapped air is removed (Christiansen 1944).

The rate at which the water content gradually increased at different depths indicated the rate at which air from the bubbles was going into solution or escaping. With downward flow of water, the air dissolved gradually by the water passing through the soil and successive soil layers became freed of air from top downward. The air bubbles were removed due to the following possibilities:

- (i) the bubbles may have moved by buoyancy or the motion of water to an interface with external air where they exploded (Peck 1969);
- (ii) the pore necks isolating bubbles may have drained;
- (iii) air solubility in water increases with increasing pressure. Henry's Law states that:

The solubility of a gas in a liquid is directly proportional to the pressure of that gas above the surface of the solution. Hence, the air molecules from air bubbles were dissolved into water to relieve the pressure; and/or

(iv) under constant temperature conditions, the density of air is a function of air pressure.

Since all the experiments were carried out in temperature controlled laboratory, an increase in pressure in air bubbles will develop a pressure difference between dissolved air and air in bubble. This pressure difference became the driving potential for air in the bubbles to diffuse into water following Fick's law.

Hence, considering temperature and atmospheric pressure to be constant in the laboratory, the rate of air bubble dissipation is dependent on the amount of air present in the soil, diffusion coefficient of air in soil water, hydraulic conductivity of soil, the rate of water flow, the capacity of water to absorb additional air and the dissolved air content of the flowing water. However, some entrapped air bubbles remained in soil which could not be removed. Total saturation is ensured only when the air phase in soil is evacuated or replaced with readily soluble carbon dioxide or if the entire model was subjected to vacuum. This was not possible in the model.

Single Phase Approach

Most of the unsaturated/saturated numerical models like HYDRUS-2D and Vadose/W are designed to model only the single phase flow of water. In the unsaturated (one-phase) flow theory, the two physical effects which both tend to reduce infiltration are neglected, namely, the viscous resistance to airflow and the air compression ahead of the wetting front (Phuc and Morel Seytoux, 1971). The flow equations describing the flow of water in unsaturated soil are usually written with the implicit assumption that the air phase is continuous, is in equilibrium with the atmospheric pressure, can move freely between atmosphere and the unfilled pores of the soil and does not impact the infiltration of water

into soil. It is also assumed that the density and viscosity of air is negligible in comparison to water.

Many researchers have considered the general problem of infiltration as a two-phase flow problem, including air as the second phase in the two phase flow approach and solving air phase partial differential equation (Phuc and Morel Seytoux 1971; Touma and Vauclin 1986; Wang *et al.* 1997; Hammecker *et al.* 2003; Lugomela 2007). Vachaud *et al.* (1973) has shown that if the pore air phase was made continuous with atmosphere by allowing lateral escape of air, the classical one-phase flow approach (Richard's equation) was correct in describing the flow process. Hence, the numerical models used here were unable to estimate the initial increase in the pressure heads measured in the blanket.

Supporting Experiments

Additional experiments and numerical simulations aimed to prove the presence of entrapped air were carried out. Ways to measure soil air pressure are known (Fluhler *et al.*, 1986) and are helpful in evaluating air entrapment and its effects on transient flow of soil water. However, no attempt had been made in this study to actually measure the soil air pressure.

1) Air Injection

Figures 3-8a and 3-8b compare the pressure heads in blanket after air was injected and in normal conditions in the coarse sand. Figures 3-9a and 3-9b compare the pressure heads in sand after air was injected within the coarse sand and in normal conditions.

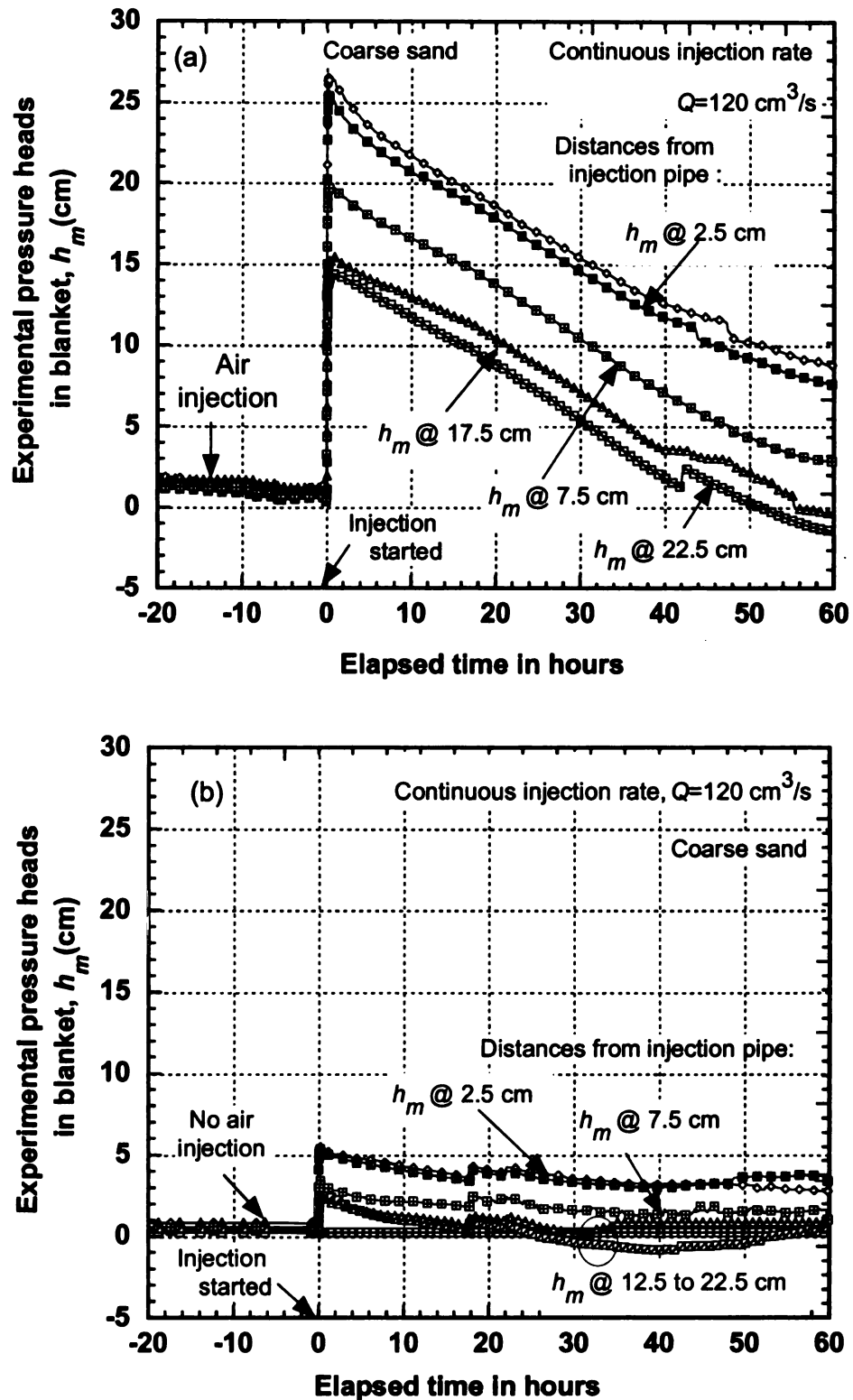


Figure 3-8: Measured pressure heads in the blanket with coarse sand underlying the blanket: (a) with pre air injection; and (b) without pre air injection.

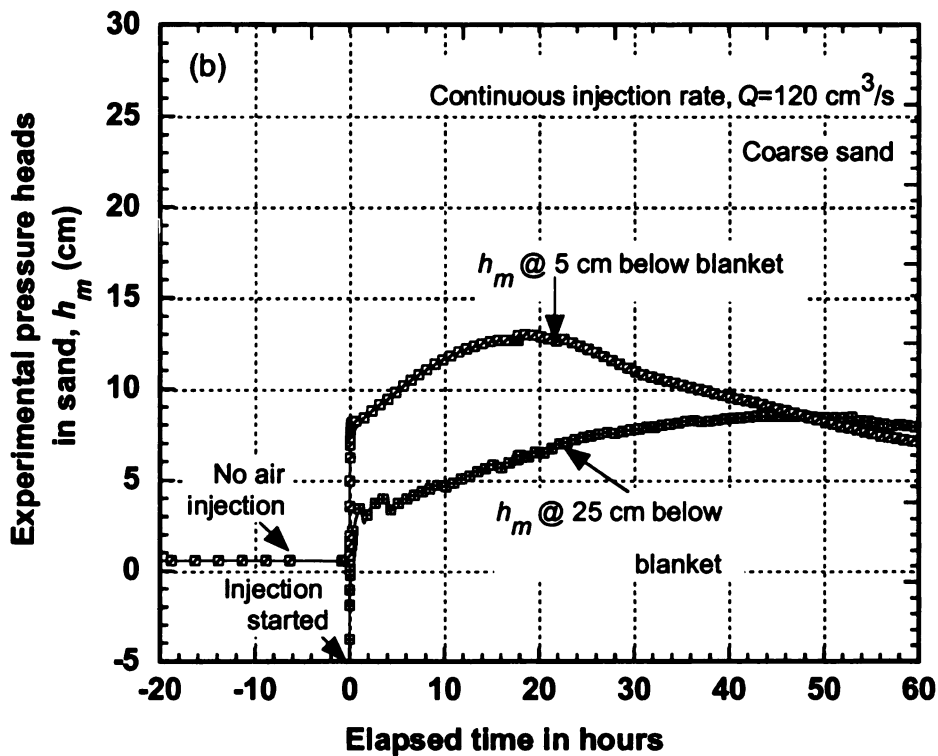
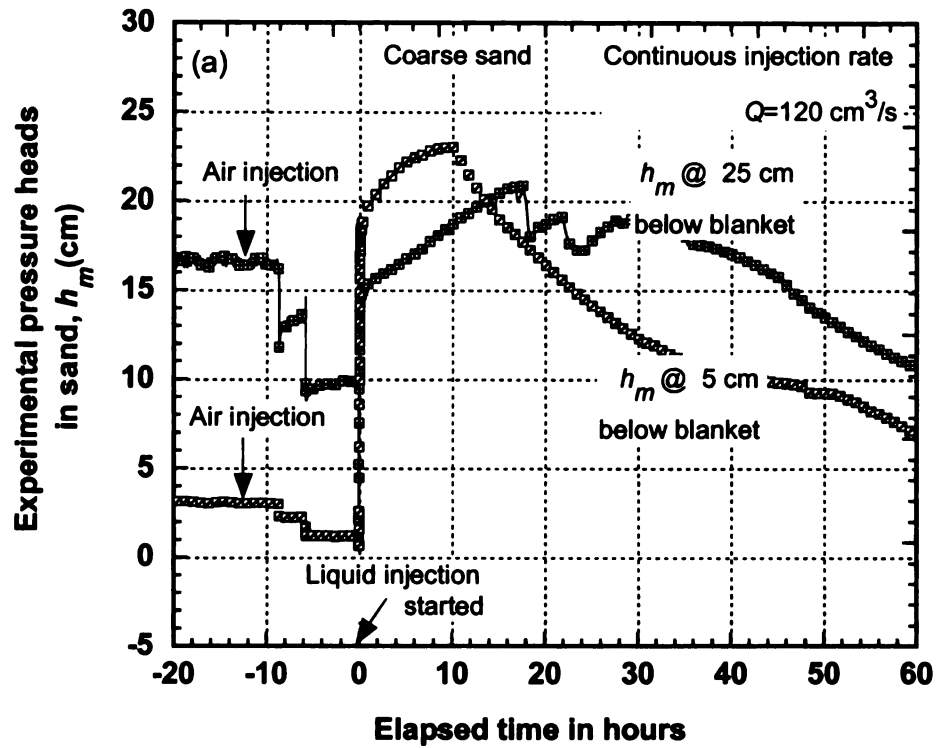


Figure 3-9: Measured pressure heads in the coarse sand underlying the blanket: (a) with pre air injection; and (b) without pre air injection.

Air was injected continuously for 40 h through one of the bottom seepage pipes in the physical model at a pressure head of 35 cm of water keeping the other seepage pipe closed. The air injection was stopped before water was injected in the model thus trapping the air in the deeper regions of the sand. The air content was thus quite high in the sand compared to normal conditions.

When water was injected at $Q = 150 \text{ cm}^3/\text{s}$, the pressure heads in the blanket raised relatively high creating overflowing artesian conditions and hence had to be stopped immediately. The pressure heads were more than 30 cm as compared to 13 cm for normal conditions. After water drained out and the injection of air was resumed for about 24 hours, the water was again injected, but now at a lower rate, $Q = 120 \text{ cm}^3/\text{s}$. The pressure head closest to the injection pipe was 27 cm (Figure 3-7a) as compared to 5.5 cm for normal conditions with no air trapped inside as shown in Figure 3-7b. The pressure heads in sand after air injection, were also higher than under normal conditions. This indicates that initial higher air content in the sand and its scope of venting caused reduction in hydraulic conductivity leading to high pressure heads.

2) Upward Flow Test

An upward flow test was conducted in the model so that air could be displaced easily with the upward moving water front. The sand was completely dried before this experiment. Water was injected in the upward direction through one of the seepage pipes, keeping the other blocked. The injection rate was chosen in such a way that boiling of sand did not occur. Figures 3-10 and 3-11 show the measured and simulated water contents and pressure heads respectively, in the sand due to upward injection.

The upward flow test was numerically modeled in HYDRUS-2D where the boundary conditions for the inlet and outlet were interchanged keeping everything else the same. In this model, the seepage pipe was assigned variable flux boundary and the injection pipe as seepage face boundary. The seepage pipe was assigned variable flux boundary because the injection rate varied from $100 \text{ cm}^3/\text{s}$ to $85 \text{ cm}^3/\text{s}$ over the period of 15 min duration of the experiment. The injection rate could not be maintained constant in this experiment because pumping head increased during the experiment as water filled the sand creating back pressure.

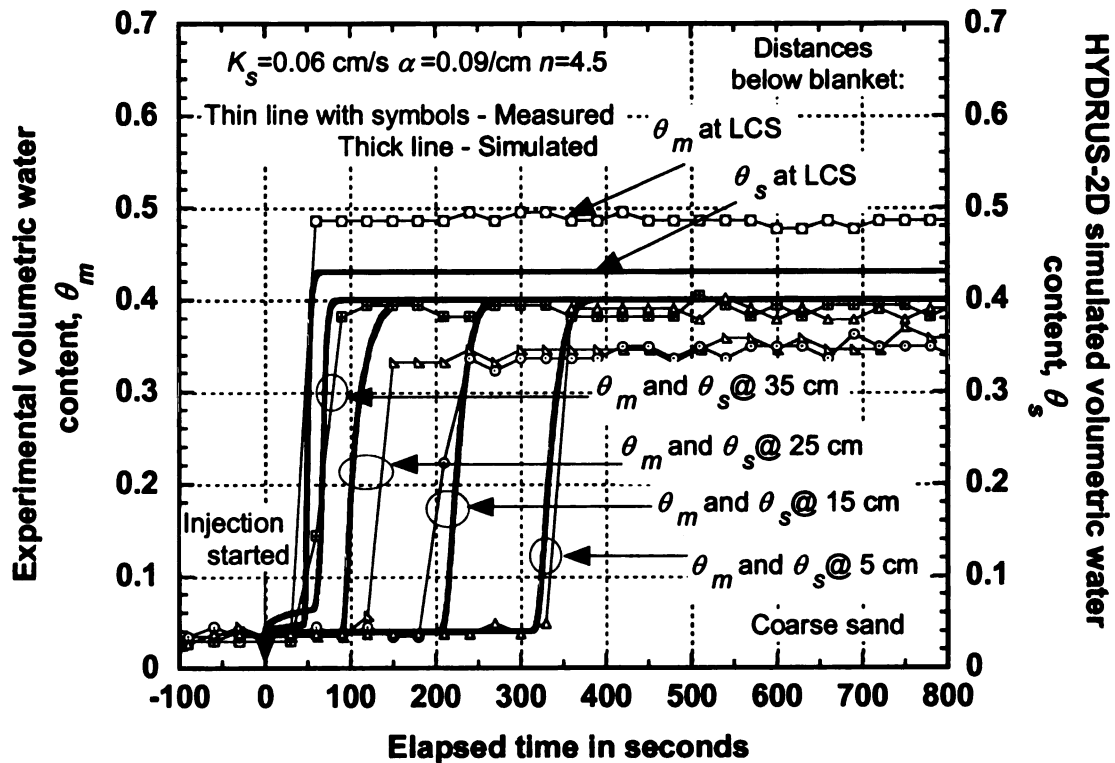


Figure 3-10: Measured and simulated rise in water content in coarse sand due to an average upward injection rate of $95 \text{ cm}^3/\text{s}$.

Figure 3-10 shows the measured and simulated responses of the water content sensors in the sand sequentially, as the water front moved upwards. The rate of increase in simulated water contents with time was almost the same as that for the measured values. The measured water contents at some depths were less than saturation because of entrapped air. Small pockets of entrapped air were observed in dotted form throughout the depth of the sand as the water front moved upwards.

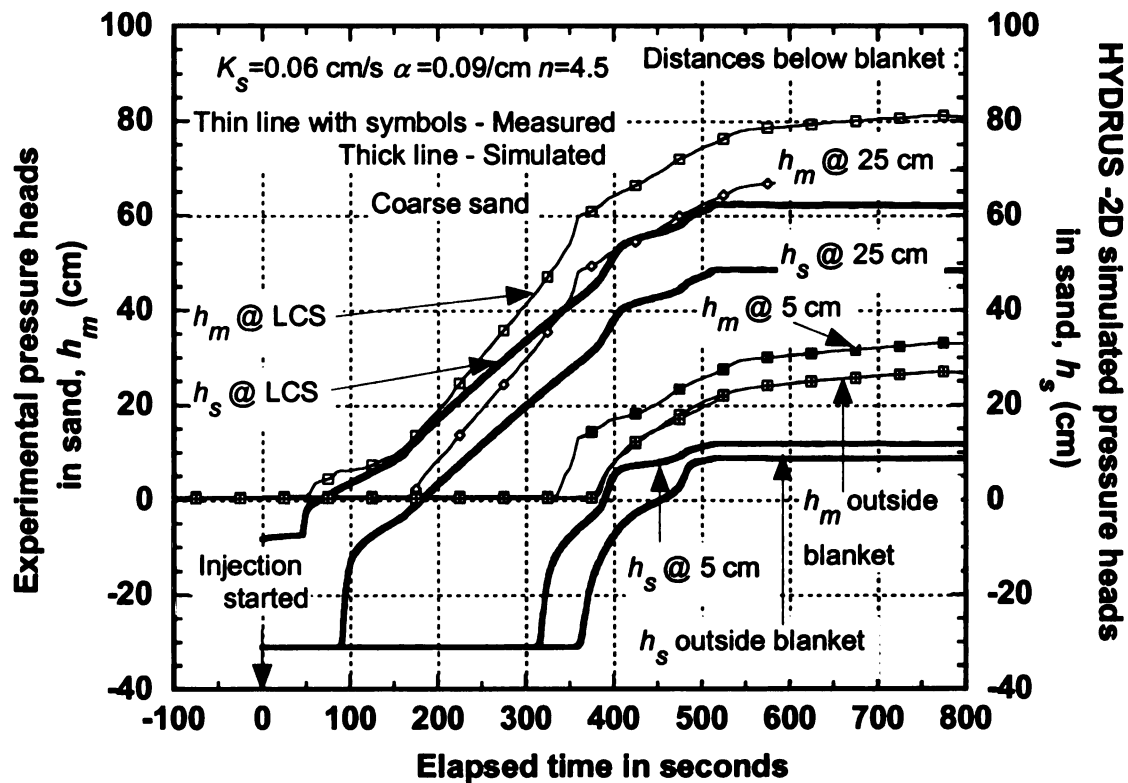


Figure 3-11: Measured and simulated pressure heads in coarse sand due to an average upward injection rate of $95 \text{ cm}^3/\text{s}$.

Figure 3-11 shows the measured and simulated responses of the pressure head sensors in the sand. The rate of increase in simulated pressure heads was also similar to that of the measured pressure heads. The measured pressure heads were higher probably

because of trapped air. Hence, upward flow through the soil provides no assurance that air will be eliminated which is in accordance with Christiansen (1944).

3) Hydrostatic Pressure Heads

Several static ponding events were carried out during which ponded water was maintained at a fixed level on the surface of the sand for few hours. The ponding events were carried out not only to measure signal drift for the pressure sensors but also to check entrapped air within the sand by comparing the hydrostatic pressure heads. With fine sand which took a substantial amount of time to get saturated, the ponding events were carried out at various degrees of saturation.

Figure 3-12a shows the comparison of measured and estimated hydrostatic pressure heads at different depths within the fine sand at different degrees of saturation of the sand. Except in the blanket and the LCS, the pressure heads were high at 5 cm and 25 cm below the blanket when the average degree of saturation of the sand was low. It was observed that with increase in saturation and increase in hydraulic conductivity which occurred over time with removal of air bubbles, the measured pressure heads moved closer to the hydrostatic pressures (1:1 line). This shows that the presence of entrapped air can buoy up the liquid pressure heads. Figure 3-12a also shows that the measured pressure heads in the blanket and the LCS during the static ponding experiments were equal to the hydrostatic pressure heads.

Similarly, Figure 3-12b shows the comparison of measured and estimated hydrostatic pressure heads at different depths within the coarse sand. The same phenomenon as discussed above was observed. The difference between the measured and hydrostatic pressure is believed to be the pressure head contributed by entrapped air.

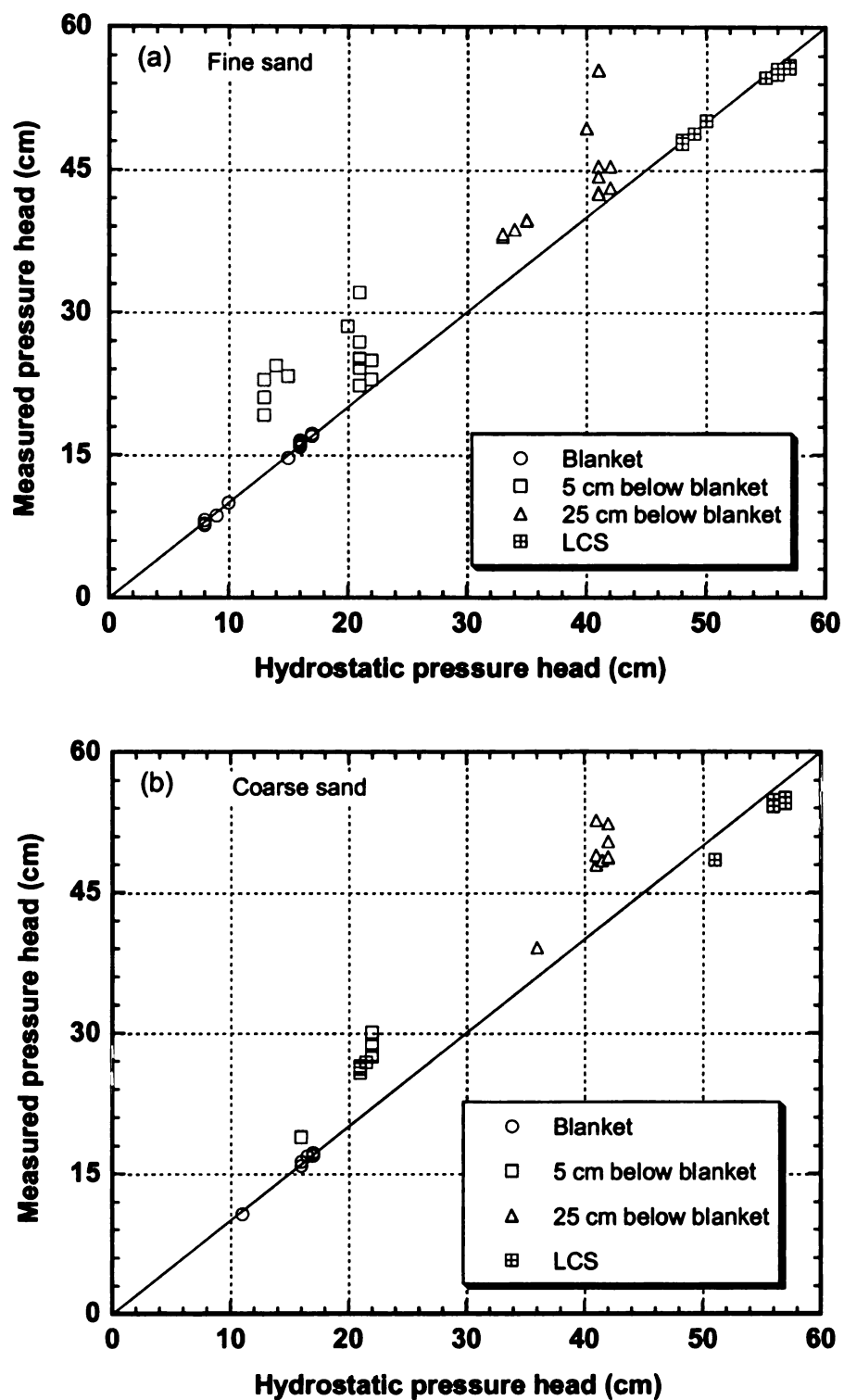


Figure 3-12: Measured and estimated hydrostatic pressure heads from ponding events for: fine sand (a); and coarse sand (b).

4) Bucket Experiment

A simple experiment was conducted to prove how the presence of entrapped air can lead to higher than hydrostatic pressure in the system. A bucket was half filled with oven dried coarse sand and two pressure transducers were embedded in the sand. One of the sensors was buried at a depth of 10.5 cm below the surface and the other one at a depth of 3 cm below the surface. Water was slowly added from the top till it ponded to a depth of about 3 cm on the sand surface. Such addition of water from top is similar to when water is injected in the blanket in the model (Figure 3-1). Figure 3-13 shows the hydrostatic pressure heads measured by the sensors. The arrows shown on the right side in Figure 3-13 indicate the actual hydrostatic pressure heads at the location of the buried sensors. Due to the entrapped air in the sand, the pressure heads measured by the sensors were higher than the true hydrostatic pressure head.

After letting the water to stand in the closed bucket for about 20 hours, vacuum was applied through the lid of the bucket. Figure 3-13 shows that during the 20-hr standing period, the pressure heads measured by the sensor did not change. However, as soon as vacuum was applied, the entrapped air nearer to the surface was removed which was indicated by the sensor located nearer to the surface measuring ponded water depth. With the applied vacuum, the entrapped air in the deeper regions could not be completely removed and hence the pressure head measured by the sensor was still slightly higher than the true hydrostatic pressure head as shown in Figure 3-13. The vacuum could not be increased any further due to the limitations of the wall strength of the bucket.

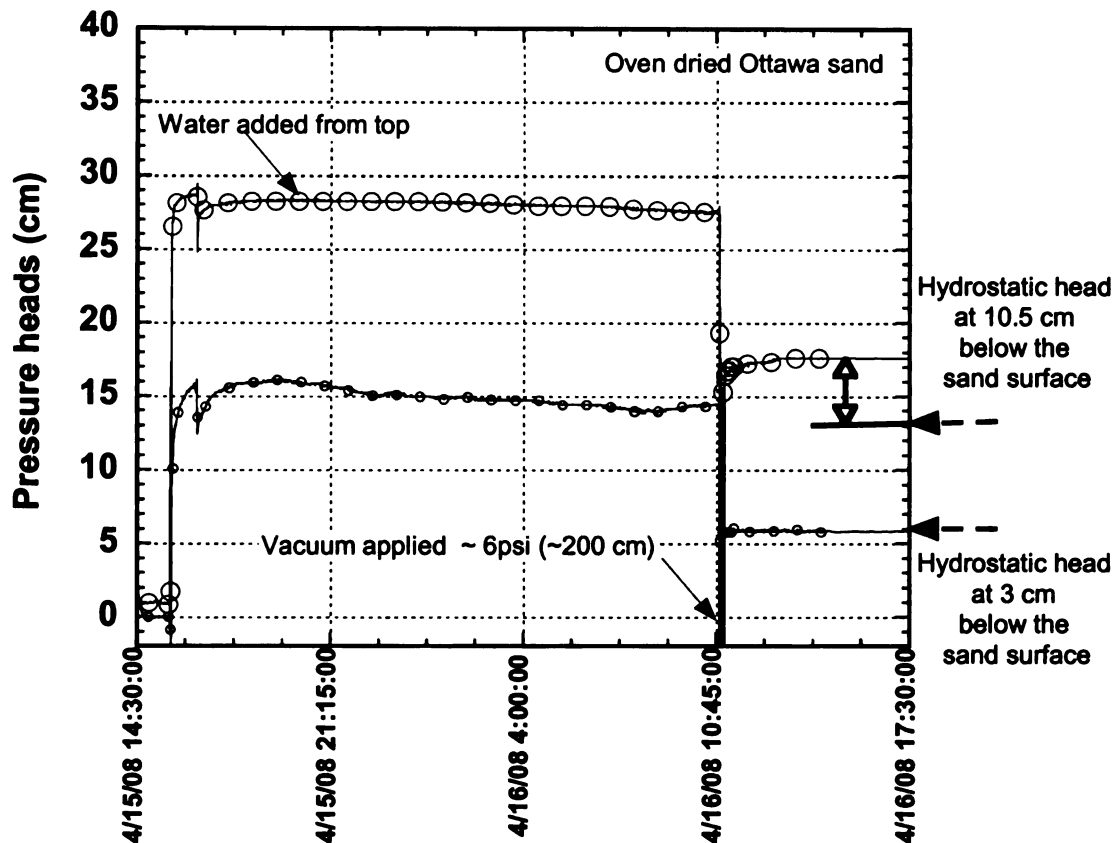


Figure 3-13: Measured hydrostatic pressure heads in coarse sand.

Thus, all experiments that were carried out confirmed the presence of entrapped air.

Continuous Injection in Coarse Sand

Pressure Heads in Sand

The presence of entrapped air is also evident from the responses of the sensors embedded in the sand. Figure 3-14 shows the pressure heads in the sand at two locations due to continuous injection at $150 \text{ cm}^3/\text{s}$. Figure 3-14 shows that the pressure head at 5 cm below the blanket gradually reached its maximum of 18 cm. Wilson and Luthin (1963) reported a similar gradual rise in air pressure head to about 80 cm within a 4.5 cm diameter and 31 cm long soil column containing a barrier of reduced air permeability.

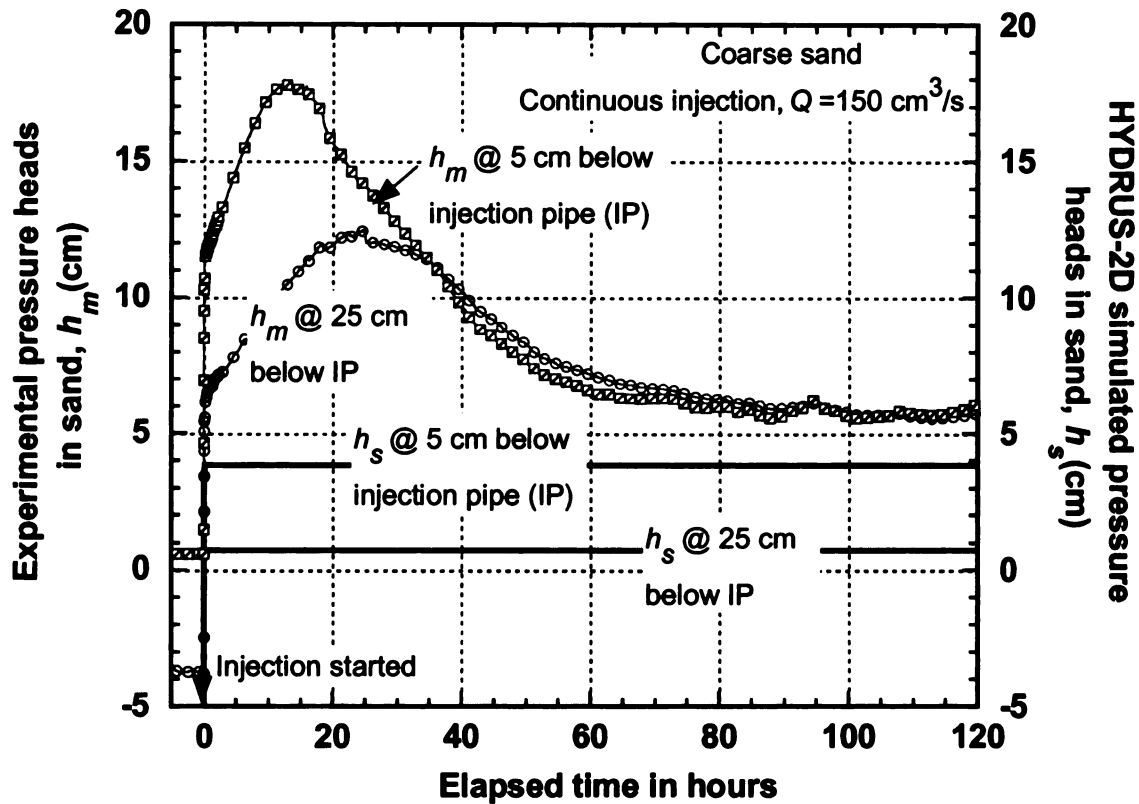


Figure 3-14: Measured and simulated pressure heads at different depths within coarse sand underlying the blanket.

The pressure head in sand at 5 cm below the blanket was higher than the blanket pressure heads before steady-state was reached. Since the sand is homogeneous and hydraulic conductivity was expected to be constant everywhere, the pressure heads in the sand could be calculated by considering a linear drop in the hydraulic heads. The calculated pressure heads were less than the measured pressure heads. The difference in the measured and calculated pressure heads is believed to be the air pressure head.

In the beginning of infiltration process, the suction gradients dominated over the gravitational gradient as water moved through the capillary pores entrapping air in the

process and hence contributing to pore air pressure heads. As the water penetrated deeper and wetted part of sand profile lengthened, the suction gradient eventually became negligible leaving the constant gravitational gradient in effect as the only force moving water downward. Hence, in Figure 3-14 it is observed that water moved under unit gradient from $t = 60$ h onwards.

Figure 3-14 shows that the simulated pressure heads did not match with the measured pressure heads at steady-state. Full saturation was not practically possible except under vacuum. Hence the sand contained residual air content which contributed to the difference between the measured and simulated pressure heads. Additionally, it can be thought that some of the entrapped air bubbles potentially migrated to the space above the diaphragm of the pressure sensor embedded in sand along with water. The relatively small bubbles got dissolved in the water till a point when the water became saturated with air after which any bubble could not dissolve. There is also a possibility that a bubble would remain trapped within the space above the diaphragm which contributed to measured high pressure heads.

Continuous Injection in Fine Sand

Figure 3-15 shows the experimentally measured and HYDRUS-2D simulated pressure heads in the blanket when DI water was injected at rates of 21 and 23 cm³/s in the setup with fine sand. The average degree of saturation during this time was nearing 100% (not shown here). Once the underlying sand was saturated, the numerical models could accurately simulate the pressure heads in the blanket for the specified injected flows.

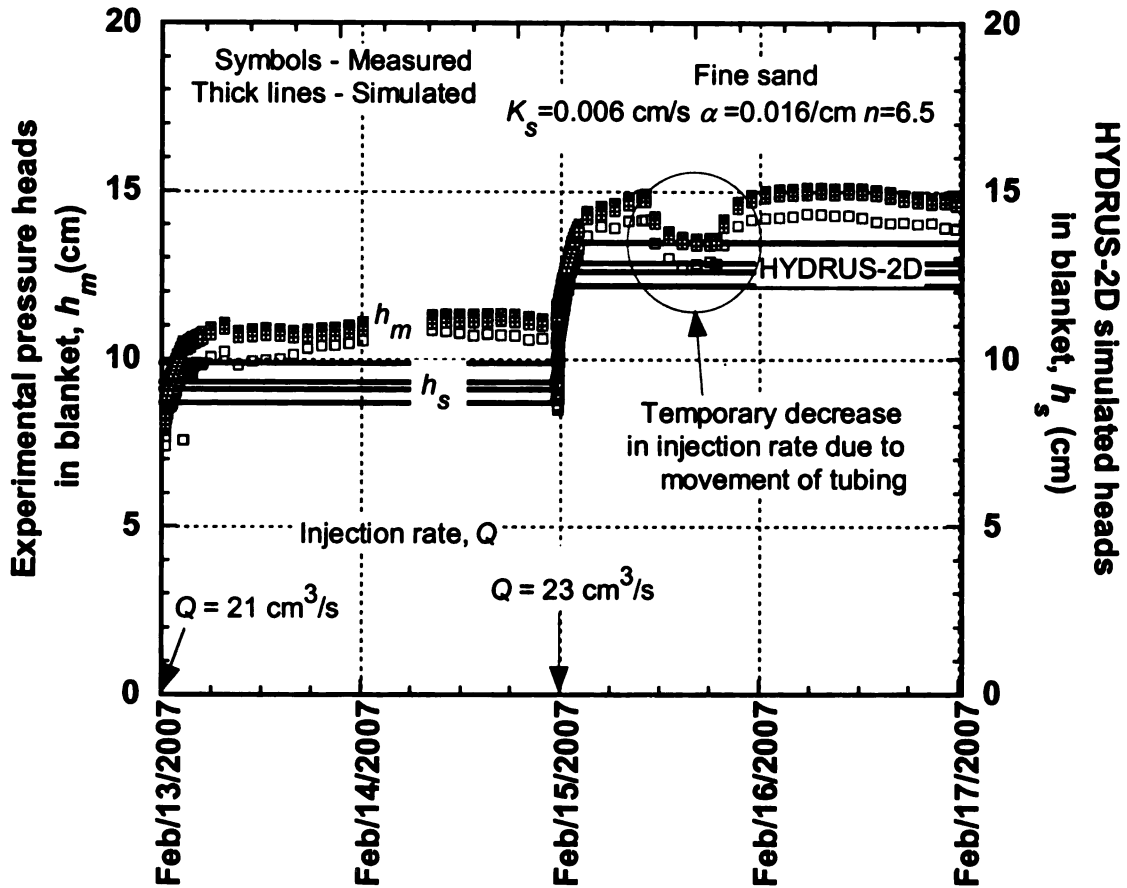


Figure 3-15: Simulated and measured pressure heads in blanket with fine sand underlying the blanket for different injection rates.

Figure 3-16 shows the experimentally measured and HYDRUS-2D simulated pressure heads in the fine sand when DI water was injected at rates of 21 and 23 cm³/s in the setup with fine sand. The simulated and measured pressure heads at 5 cm below the blanket matched. The simulated pressure head at 25 cm below the blanket indicated suction head (unsaturated). Although the water content at that location had reached saturation, the simulation results indicated that the matric suction did not reach zero.

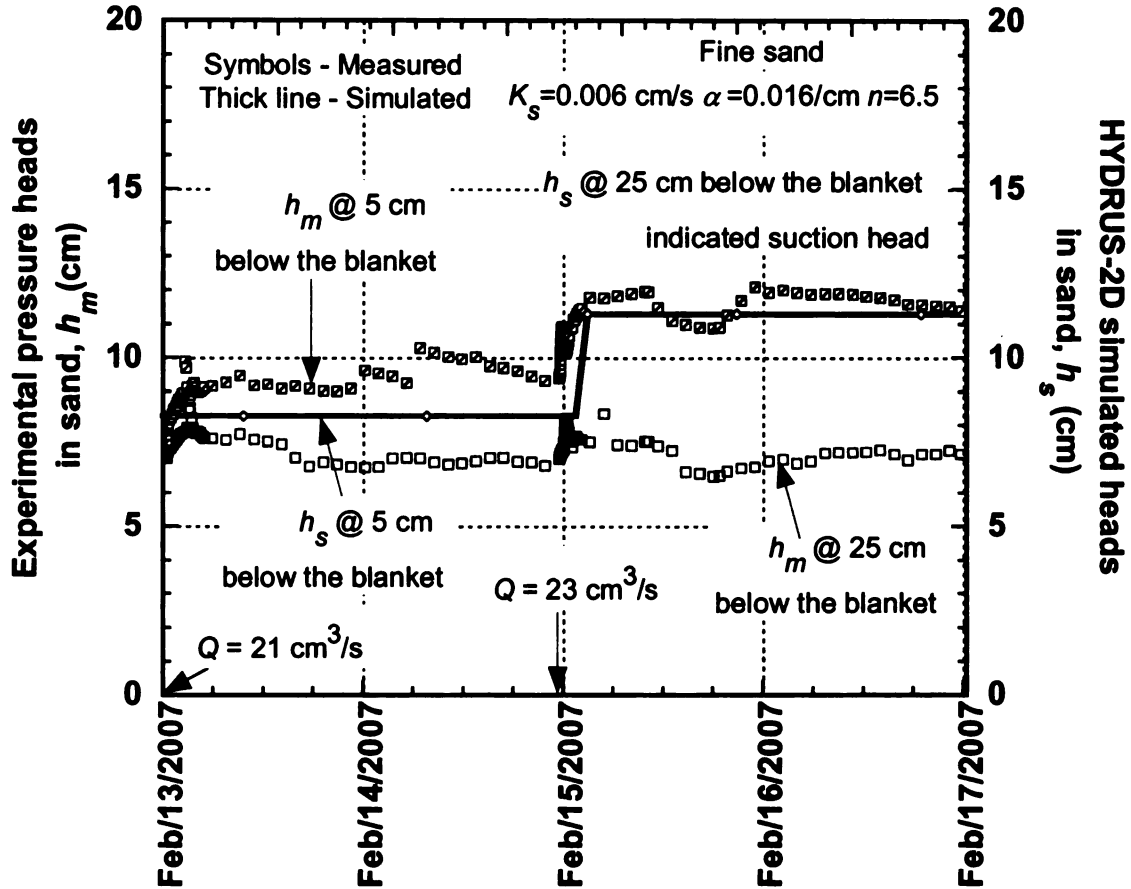


Figure 3-16: Simulated and measured pressure heads in fine sand underlying the blanket for different injection rates.

Figure 3-17 shows the average pressure heads h_{av} in the blanket when DI water was injected at various rates when the degree of saturation of sand had reached 100%. Both HYDRUS-2D and Vadose/W predicted the pressure heads in the blanket accurately. This plot also illustrated that the flow is directly proportional to the heads in the blanket at saturation.

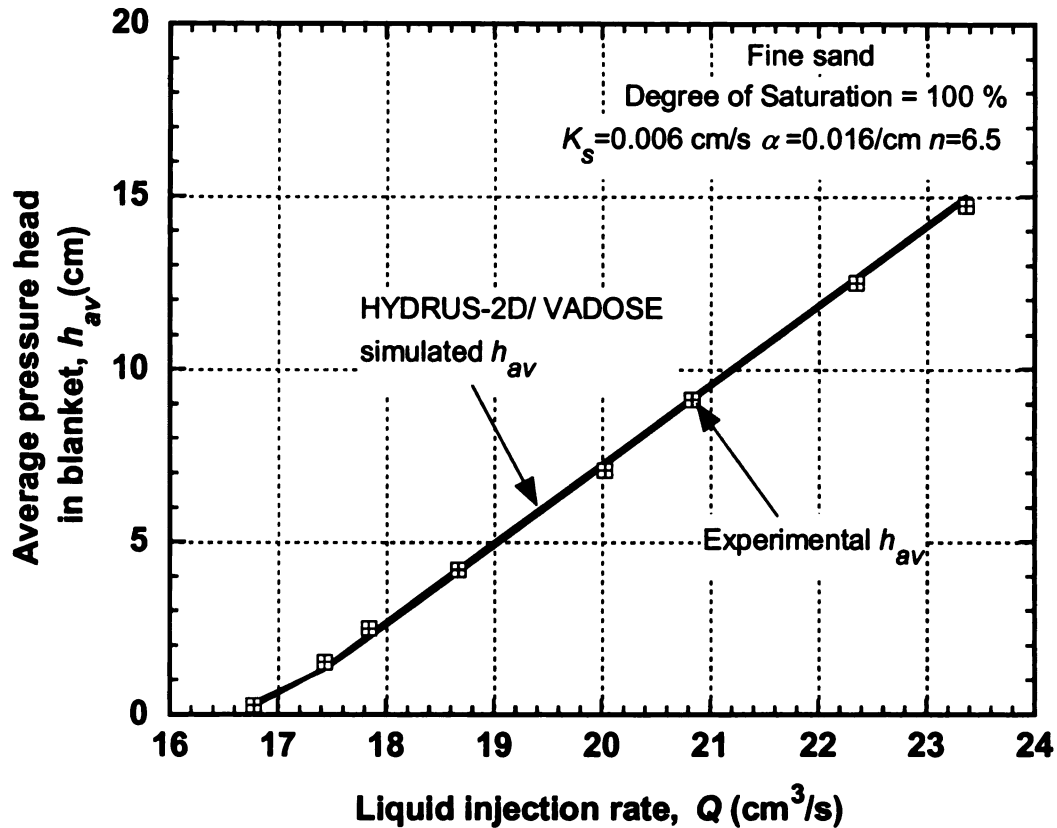


Figure 3-17: Measured and numerically simulated average pressure heads in the blanket due to various rates of injection with fine sand underlying the blanket.

On and Off Dosing in Coarse Sand

Figure 3-18 shows the measured and Vadose/W simulated peak pressure heads in the blanket when DI water was injected at a rate of 150 cm³/s for a dosing frequency of 3 min on and 10 s off with coarse sand underlying the blanket. The “off” period of 10 sec was selected based on maximum rate of drop in water contents registered by the water content sensors when water drained from the sand under gravity. Similar to the continuous injections described earlier, the pressure heads were higher in the beginning which then gradually decreased as shown in Figure 3-18a.

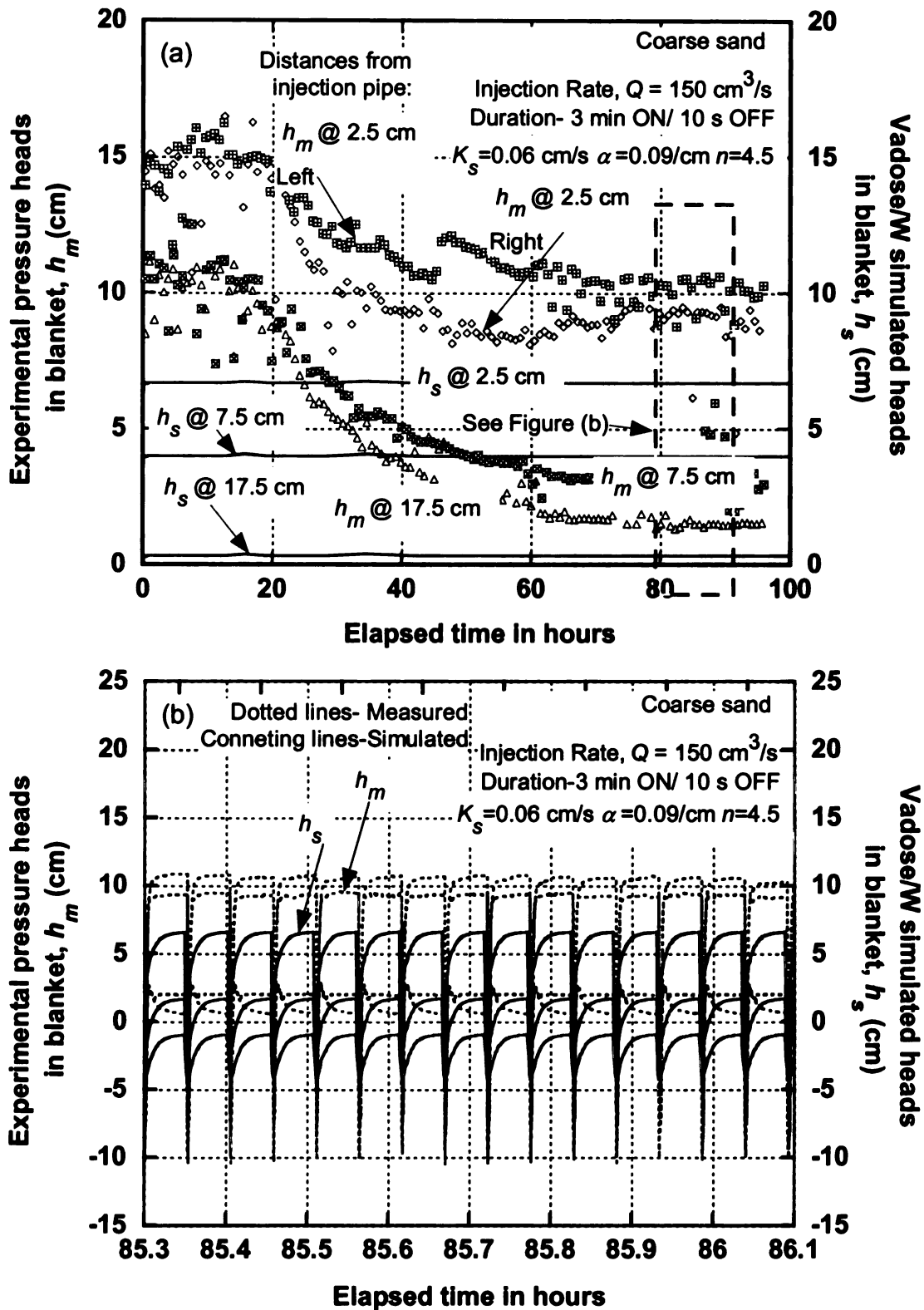


Figure 3-18: Measured and simulated: (a) peak pressure heads; and (b) snap shot of few cycles showing the pressure distribution in blanket due to on/off dosing cycles.

The pressure heads in the blanket increased during the injection period and dropped rapidly after the injection was stopped which is shown in Figure 3-18b. The numerical models were unable to simulate the initial high pressure heads but unlike the continuous injections scenario the measured and simulated pressure heads did not match at steady-state conditions either. Hysteresis option was evaluated in the numerical model but it had no effect on the pressure heads.

Repeated wetting–drying cycles lead to entrapment of air in the pores of the soil. During the drainage period between successive wettings, the largest pores de-watered first and the smaller pores within the matrix did not have sufficient time or gradient to de-water. In the subsequent wetting period, the water filled up recently dewatered larger pore spaces. Because smaller pores and passages around the larger pores have not dewatered, discontinuous air bubbles were trapped in the larger pores. The immobilized trapped air bubbles during on/off injection frequency did not have enough time to dissolve in mass of flowing water similar to that in continuous injection. Hence, the trapped air persisted during subsequent cycles of wetting and draining, suggesting an effect that lasted through several dosing cycles. Air entrapment reduces saturated hydraulic conductivity (Seymour 2000; Sakaguchi *et al.* 2005) and results in positive air pressure. Hence, the pressure heads were high and did not equate with the steady-state values obtained from continuous injection as shown in Figure 3-19.

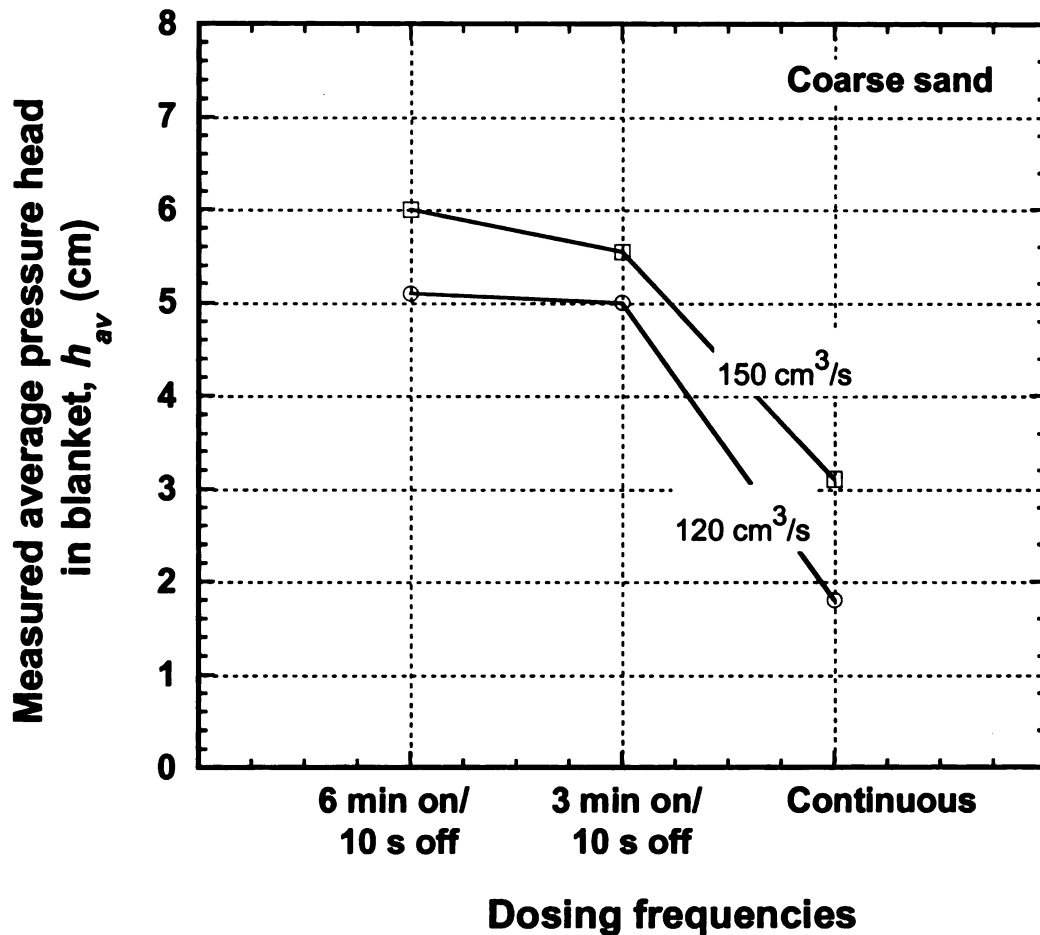


Figure 3-19: Average pressure heads in the blanket for different dosing frequencies.

The presence of entrapped air was the reason for the differences between pressure heads obtained from on/off and continuous injection was confirmed when injection was started with initial condition - 100% saturated. In this experiment, the entire model was continuously saturated for a period of 15 days by pumping water at a very high rate from the top surface of the overlying sand. Figure 3-20 shows the measured and Vadose/W simulated pressure heads in the blanket when DI water was injected at a rate of 150 cm³/s for a dosing frequency of 3 min on/10 s off with 100% saturated coarse sand underlying

the blanket. The measured and simulated pressure heads matched much closer in the absence of substantial air pressure.

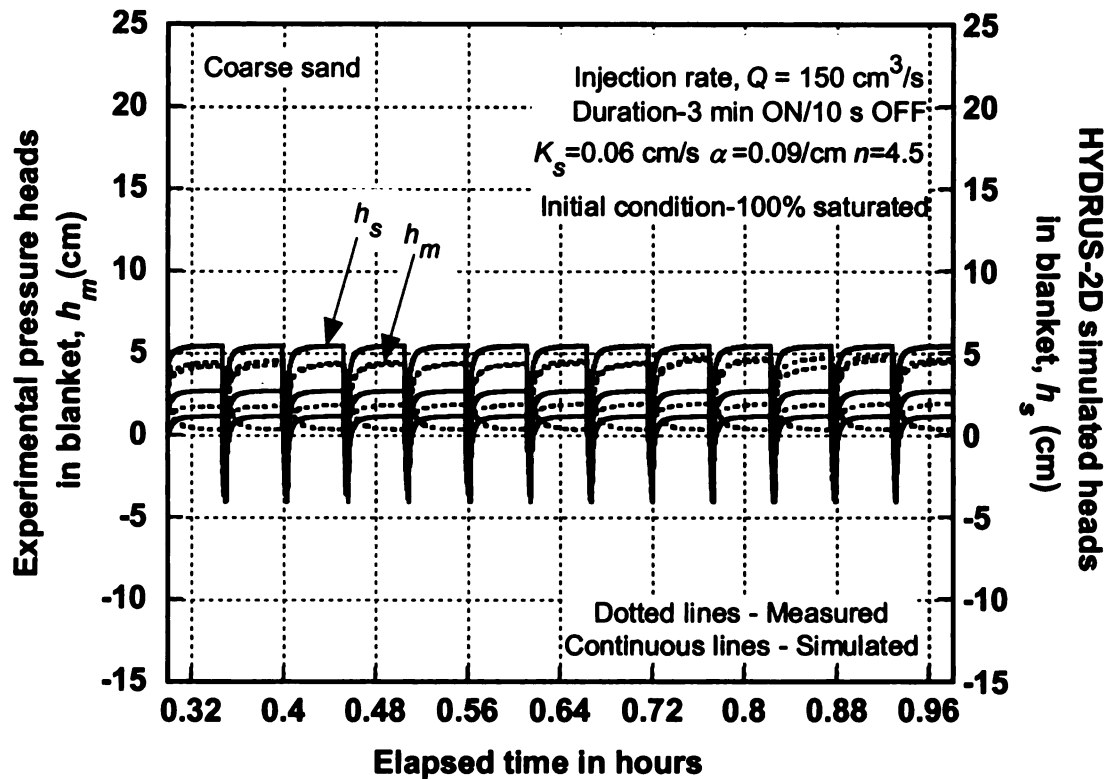


Figure 3-20: Measured and simulated pressure heads with snap shot of few cycles showing the pressure distribution in blanket due to on/off dosing cycles with 100% saturation as initial condition.

Figure 3-21 shows the measured and simulated pressure heads in the sand for the same injection event. The measured pressure heads indicated unit gradient. The simulated pressure head at 5 cm below the blanket matched with the measured pressure head at that location. However, there was a difference in the pressure heads at 25 cm below the blanket.

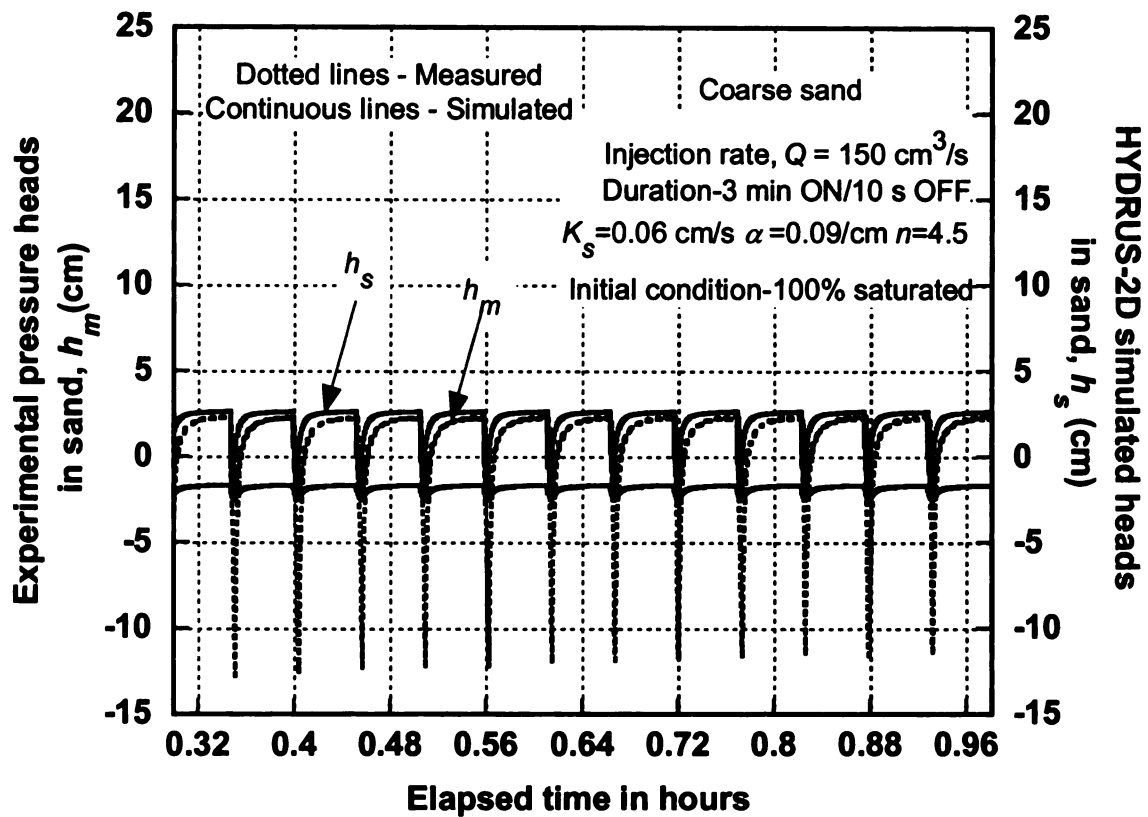


Figure 3-21: Measured and simulated pressure heads with snap shot of few cycles showing the pressure distribution in sand due to on/off dosing cycles with 100% saturation as initial condition.

Hence, the numerical models were able to accurately predict the pressure heads when entrapped air was absent. The on/off injection could not be simulated in the setup with fine sand since it did not drain easily like the coarse sand.

PRACTICAL IMPLICATIONS

Landfill gas is produced during the decomposition of the organic portion of waste which takes place immediately after waste disposal in the presence of entrapped atmospheric air. The gas pressure and composition vary during the active life of the landfill. The maximum rate of gas generation is at lower depth and in phase 2. The gas pressure

increases with depth (Nastev *et al.* 2001). The pressure gradients lead to gas advection, as well as concentration gradients that lead to gas diffusion. Following the path of least resistance, gas migrates either vertically to the atmosphere or laterally beyond landfill boundaries in surrounding geological formations. In bioreactor landfills, higher gas pressures restrict the downward migration of leachate and/or low conductivity daily cover layers create isolated saturated regions. Entrapment of gas occurs within these localized leachate regions where liquid phase is continuous due to liquid injection.

Figure 3-22 shows the pressure head data from the instrumented field blanket in McGill landfill in Michigan (Haydar and Khire 2006). For the same injection rate in January 2004 and March 2004 the pressure heads in the blanket were found to be higher in March 2004. With time, gas production increased within the wide wetted domain underneath the instrumented blanket. At fixed vertical stress (as indicated by load sensor), pressure due to entrapped gas within the wetted area caused hydraulic conductivity of waste to decrease (Powrie *et al.* 2008) and hence subsequently increase the pressure heads within the blanket.

Hence, sensors embedded in blanket/waste are liable to be affected by gas pressures. In doing so, the sensors would not measure the actual pore water pressure.

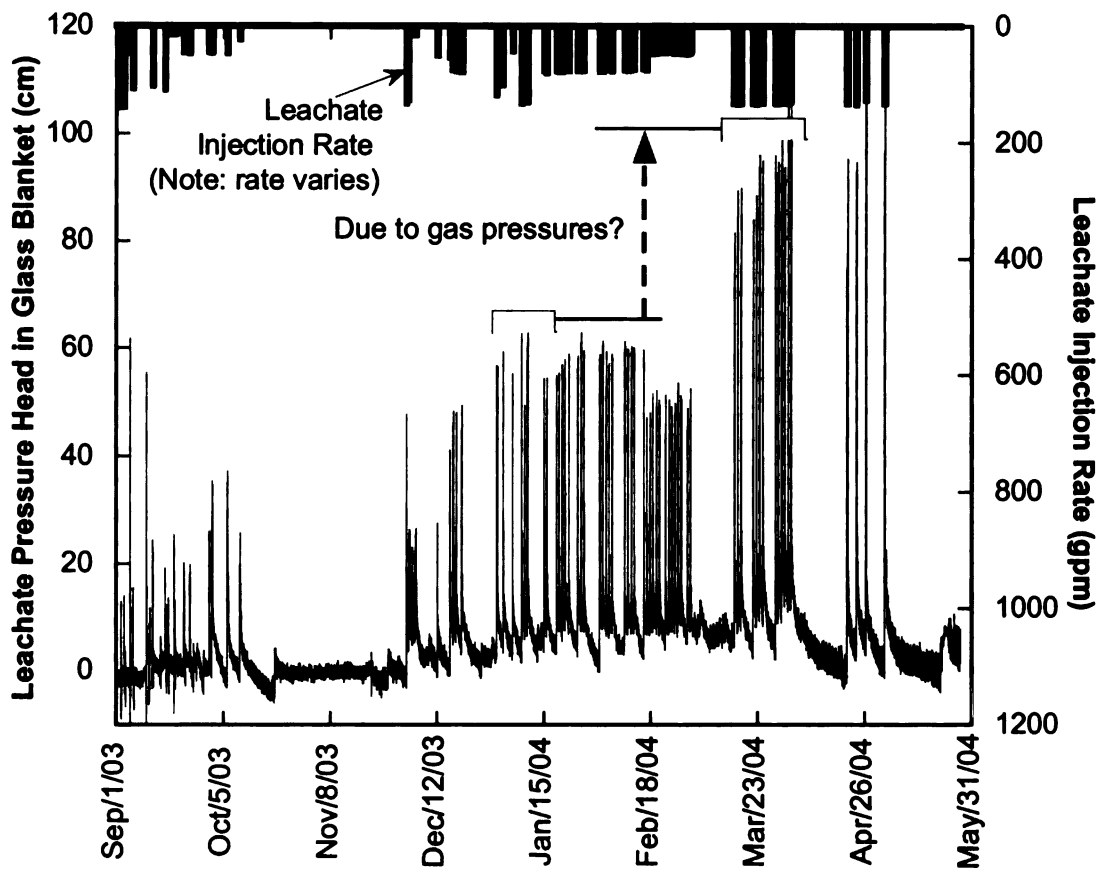


Figure 3-22: Measured pressure heads in the field-scale blanket in Michigan Landfill.

SUMMARY AND CONCLUSIONS

The key objective of this paper was to test the predictive capabilities of numerical models on the basis of comparison between results of simulations and experimental observations. Experiments were carried out in a laboratory scale instrumented landfill model. Pressure heads in a blanket due to liquid injection were measured using an automated sensing

system consisting of pressure sensors. The degree of saturation of the sand underlying the blanket was measured using water content sensors. HYDRUS-2D and Vadose/W were used to numerically simulate the flow processes observed in the landfill model. The key conclusions of this study are as follows:

- Numerical models cannot be verified and validated. Some data agree with predictions and some do not. Thus, models are representations, useful for guiding further study but not susceptible to proof (Oreskes *et al.* 1994).
- Unsaturated/saturated numerical models HYDRUS-2D and Vadose/W are conceptually similar although the algorithms are slightly different. The predictions of both models were identical.
- The pressure heads in the blanket and the soil water content distributions predicted by HYDRUS-2D and Vadose/W, agreed reasonably with the measured data when the entrapped air was minimal at steady-state.
- Occurrence of air bubble entrapment is common occurrence in wetted soils. Two processes enhanced air entrapment in the physical model: (1) movement of air out of filling micropores into conducting macropores; and (2) an interruption in water injection due to on/off dosing cycles resulting in partial drainage of the macropores and the entry of air with more water following to trap the air.
- Upward flow of water in soil is no assurance of air elimination.
- Discrepancies between observed and predicted responses of the system are the manifestations of errors incorporated in the mathematical model. For example, the numerical models solve Richard's equation which assumes air phase to have no pressure. However, in reality, the presence of entrapped air influenced the kinetics

of infiltration. Consequently, for the experimental situations dealing with an immiscible two-phase flow problem, one of which is compressible, the effect of soil air phase cannot be neglected. This is the reason the numerical models were not able to simulate the measured initial high pressure heads and the gradual increase in average degree of saturation of the sand.

- The simulated and measured pressure heads matched in the absence of pore air pressure.
- It can be concluded that in bioreactor landfills, the generation of landfill gas and design and operation of gas extraction or gas venting systems will have a significant impact on the pressure heads in the liquid injection system components (e.g. trench, well, blanket). At high saturation levels at the bottom of the landfill, the air permeability of the waste is lower (Stoltz and Gourc 2008) and hence there is likelihood of entrapment of gas within the wetting front. The presence of discrete entrapped gas bubbles can cause the pressure heads to rise in waste. The sensors used for instrumenting field-scale blankets or trenches would not measure the actual pore water pressure because the gas pressures would interfere with the pore water pressures.
- Multiphase flow approach should be adopted for simulating liquid flow in bioreactor landfills with gas pressures taken into account in the flow equations.

PAPER NO. 4: INSTRUMENTED PERMEABLE BLANKETS FOR ESTIMATION OF SUBSURFACE HYDRAULIC CONDUCTIVITY

ABSTRACT

An instrumented lab-scale physical model of a landfill with permeable blanket as liquid recirculation system was developed to test the hypothesis that vertical hydraulic conductivity of a porous medium underlying the blanket can be estimated using hydraulic pressure and flow data from the blanket. The model was approximately 85 cm long x 30 cm wide x 55 cm high. A 50 cm long x 30 cm wide x 2 cm thick horizontal permeable blanket made up of pea gravel having saturated hydraulic conductivity of about 2 cm/s was built in the landfill model for subsurface liquid injection. Fine and coarse sands were used as homogeneous and isotropic porous media below the blanket in separate experiments in the same setup. The blanket and the sandy soil below the blanket were instrumented with sensors consisting of pressure transducers with built-in thermistors and time domain reflectometry (TDR)-based water content sensors connected to a datalogger, to monitor the migration of injected liquid in the blanket and in the sand. Liquid injection in the blanket was carried out at varying rates either continuously or in on/off mode using a magnetic drive pump or a gear pump. The injected flow was monitored by flow sensor. A new method called Analysis of Conductivity in Real-time using Embedded Sensors (ACRES) was developed to estimate the hydraulic conductivity of the underlying sand using the flow and pressure data from the sensors embedded in the blanket. In addition, the hydraulic conductivity of the underlying sand was estimated through inverse modeling using the saturated/unsaturated finite element model Vadose/W. Falling head

tests and tracer tests were carried out independently to verify the estimated hydraulic conductivity values. Finally, field-scale simulations were carried out and ACRES method was applied to the simulated pressure heads to develop a design framework to apply this method in the field.

INTRODUCTION

Bioreactor landfills are designed and operated to accelerate the decomposition of organic constituents of municipal solid waste (MSW) and to decrease the time to achieve waste stabilization in the process by purposeful control of biological processes. The goal of bioreactor landfill operation is to enhance the bacteria proliferation through the recirculation of leachate (or injection of other liquids) to maximize the rate of degradation of the organic waste fraction and consequently increase the production of biogas resulting from biodegradation of organic matter in the landfill and stabilize the waste in the process.

Leachate recirculation or liquid injection can be performed using multiple techniques, both surface and subsurface. The surface methods consist of spraying leachate over the landfill surface area or constructing leachate pond. The conventional subsurface application techniques are: (1) vertical wells; (2) horizontal trenches; and (3) permeable blankets. The design procedures for subsurface leachate recirculation system (LRS) are outlined by McCreanor and Reinhart (1996), Haydar and Khire (2005), Haydar and Khire (2007) and Khire and Mukherjee (2007). Important inputs which are required to design these LRSs include the injection rate, associated injection pressure and hydraulic conductivity of waste. Hydraulic conductivity of landfilled waste is the key design and operational parameter for bioreactor landfills because it has a significant

impact on leachate migration through waste (Demetracopoulos and Korfiatis 1983; McCreanor 1998).

Proper assessment of the field-scale hydraulic characteristics of the landfilled waste is important in:

1. Modeling leachate migration through waste (McCreanor 1998; Bou-Zeid and El-Fadel 2004);
2. Design of liquid injection system to achieve uniform and optimal wetting of the waste (Khire and Mukherjee 2007);
3. Design of an effective leachate collection system including the sizing of pump and leachate collection pipes;
4. Estimating the water balance of landfills to estimate the leachate generation rates and potential storage capacity of the waste. Water balance predictions are sensitive to hydraulic conductivity (Demetrocopoulos *et al.* 1986). A slight change in the magnitude of the hydraulic conductivity results in a relatively large change in the predicted leachate production rate or maximum head on the landfill liner (Khire *et al.* 1997; Giroud *et al.* 2000);
5. U.S. EPA's Hydrologic Evaluation of Landfill Performance (HELP) model that is most commonly used for modeling the water or leachate balance of a landfill requires hydraulic conductivity of waste as an input (Khire *et al.* 1997);
6. Estimating the maximum leachate pressure head on the liner and potential impacts related to uncontrolled migration of leachate on ground water quality (Oweis *et al.* 1990). The U.S. landfill regulations (Subtitle D) require that the maximum leachate head on the liner must not exceed 300 mm. It is only possible to

accurately estimate the leachate head on the liner only if we know the representative hydraulic conductivity and also monitor the changes in the hydraulic conductivity as the waste undergoes physical, chemical and biological changes; and

7. Analyzing failure related to slope stability, shallow slope liner stability, steep slope liner stability, leachate and gas wells integrity (Dixon and Jones 2005).

ESTIMATION OF HYDRAULIC CONDUCTIVITY OF WASTE

Many researchers have measured the hydraulic conductivities of landfilled waste from laboratory or field tests. The methods, the sample sizes, and the hydraulic conductivity values obtained are summarized in Table 4-1. The data presented in Table 4-1 is also better illustrated in Figure 4-1.

Table 4-1: Previous studies reporting various methods used for estimating hydraulic conductivity of waste.

Source	Method	Sample size	Hydraulic conductivity (cm/s)
Laboratory-Scale Methods:			
Fungaroli and Steiner (1979)	Constant head test	Lysimeter, 3.96 m high x 1.83 m x 1.83 m	10^{-4} to 10^{-2}
Korfiatis <i>et al.</i> (1984)	Constant head test	56 cm diameter and 183 cm high	8×10^{-3} to 1.3×10^{-2}
Noble and Arnold (1991)	Constant head test	4.7 cm diameter and 40.7 cm high	8.4×10^{-5} to 6.6×10^{-4}
Bleiker <i>et al.</i> (1993)	Falling head test	6.3 cm diameter and 1.9 cm high	1×10^{-8} to 3×10^{-7}
Beaven and Powrie (1995)	Constant head tests at a given applied vertical stress	2 m diameter and 2.5 m high	3.7×10^{-6} to 1.5×10^{-2}
Chen and Chynoweth (1995)	Constant head tests compacted to different densities	38.1 cm outer diameter and 122 cm long	4.7×10^{-5} to 9.6×10^{-2}
Landva <i>et al.</i> (1998)	Constant head tests for vertical permeability	44.7 cm diameter and 54 cm high	2×10^{-6} to 2×10^{-3}
Landva <i>et al.</i> (1998)	Constant head tests for horizontal permeability	76 cm diameter and 45 cm high	4×10^{-5} to 1×10^{-3}
Jang <i>et al.</i> (2002)	Constant head tests at different degree of compaction	72 mm diameter and 120 mm high	2.91×10^{-4} to 2.95×10^{-3}
Olivier and Gourc (2007)	Raising/falling head tests	1 m x 0.98 m x 1 m rectangular box	5×10^{-6} to 5×10^{-5}
Zhan <i>et al.</i> (2008)	Constant head tests	100 mm diameter and 200 mm high	4.81×10^{-2} to 3.56×10^{-4}
Hossain <i>et al.</i> (2008)	Constant head tests	15.24 cm diameter and 24 cm high	1.3×10^{-2} to 8.8×10^{-2}
Reddy <i>et al.</i> (2008)	Rigid-wall permeameter	Not reported	0.17×10^{-2} to 3.04×10^{-2}

Table 4-1: Continued

Source	Method	Sample size	Hydraulic conductivity (cm/s)
Field-Scale Methods:			
Hughes <i>et al.</i> (1971)	Slug tests/pumping tests	-	2.9×10^{-9} to 2.7×10^{-3}
Ettala (1987)	Pumping tests	-	5.9×10^{-3} to 0.25
Oweis <i>et al.</i> (1990)	Pumping tests/test pit/falling head test	-	1×10^{-3} to 1.5×10^{-4}
Shank (1993)	Slug tests in the existing gas vents	-	6.7×10^{-5} to 9.8×10^{-4}
Townsend <i>et al.</i> (1995)	Surface infiltration pond	-	3×10^{-6} to 4×10^{-6}
Landva <i>et al.</i> (1998)	Infiltration pits	-	10^{-3} to 3.9×10^{-2}
Jang (2000)	Pumping tests/Slug tests	-	2.2×10^{-3} to 3.3×10^{-3}
Jain <i>et al.</i> (2006)	Borehole permeameter test	-	5.4×10^{-6} to 6.1×10^{-5}
Schroeder <i>et al.</i> (1994)	HELP Default value		10^{-3}

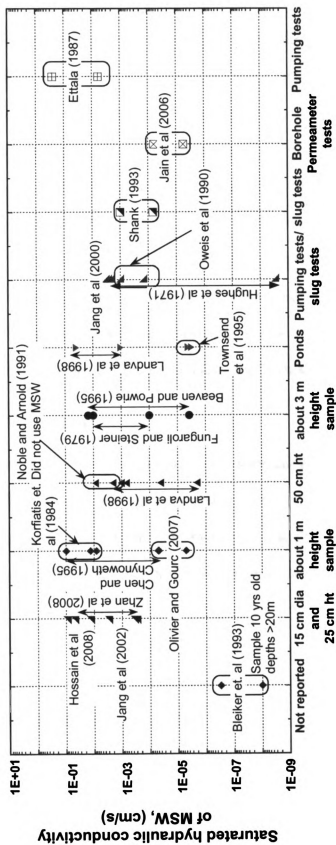


Figure 4-1: Hydraulic conductivity values for waste as estimated by various researchers.

Figure 4-1 shows that smaller specimens obtained through point measurements tend to produce a narrow range of values of hydraulic conductivity of waste. Larger specimens like the one used by Beaven and Powrie (1995) and field tests, on the other hand, produce a wider range of hydraulic conductivity values. This is because the conventional lab-scale methods for measuring hydraulic conductivity of waste using small permeameters are not appropriate for evaluating the spatial and temporal variation of the hydraulic properties of waste because the size of the sample is often insufficient to represent the mean degree of heterogeneity, fissures, and stratifications which are typical in waste. Small specimens do not adequately represent the network of pores controlling the field-scale hydraulic conductivity and hence erroneous conclusions can be drawn if these specimens are used to estimate the field-scale hydraulic conductivity (Benson *et al.*, 1997).

Reported Field Studies

Because the current study is related to field-scale estimation of hydraulic conductivity, reported field experiments are reviewed in detail. Townsend *et al.* (1995) applied Zaslavsky's method to estimate the hydraulic conductivity of waste at the Alachua County Southwest Landfill (ACSWL) for vertical flow from infiltration pond through horizontal strata of various hydraulic conductivities. Landva *et al.* (1998) constructed flow nets to evaluate the hydraulic conductivity of waste from the test pits in landfills at Canada. Ettala (1987) conducted pumping tests in Lahti and Hollola landfills in Finland and applied Jacob's method to estimate the hydraulic conductivity. Oweis *et al.* (1990) conducted pumping tests at an unlined MSW landfill in New Jersey and used Theis method to calculate the hydraulic conductivity of waste by estimating a saturated waste thickness from site geometry and field data. Shank (1993) conducted slug tests in flooded

gas wells at an unlined MSW landfill in Florida and used Bouwer and Rice method to estimate the hydraulic conductivity of waste. Jang (2000) conducted pumping and slug tests in Kimpo landfill in Korea and employed all the above methods to estimate the hydraulic conductivity of waste. Jain *et al.* (2006) employed the borehole permeameter technique in a MSW landfill in Florida to estimate the hydraulic conductivity of waste.

The application of standard aquifer pumping tests employed by Ettala (1987), Oweis *et al.* (1990) and Shank (1993) for estimating the saturated hydraulic conductivity of landfills may be limited due to these reasons: (1) sufficient water may not exist in the wells to represent conditions of saturated aquifer; and (2) wells may penetrate zones of perched water which may form due to low permeability cover soils. The infiltration ponds used by Townsend *et al.* (1995) and Landva *et al.* (1998) required the tests to be carried out in dry weather conditions to minimize interference from rain and storm water. The borehole permeameter test employed by Jain *et al.* (2006) was based on the assumption that the gas phase would offer no resistance to the leachate flow. In reality, the gas phase impacts the liquid flow.

Analysis of Conductivity in Real-time using Embedded Sensors (ACRES)

Haydar and Khire (2006, 2007) developed the permeable blanket leachate recirculation system as an alternative to the conventional leachate recirculation methods. Haydar and Khire (2006) instrumented field-scale permeable blankets to demonstrate the hydraulic performance of permeable blankets for bioreactor landfills. They studied the feasibility of using an automated geotechnical sensing system consisting of water content, temperature and pressure sensors to monitor the migration of recirculated leachate in permeable blankets.

An inert permeable blanket, if instrumented, can be used as a platform to estimate the field-scale vertical hydraulic conductivity of waste in real-time which may eliminate the need to place sensors in waste. Due to high transmissivity of the blanket, the sensors embedded in the blanket measure regional or average conditions within the landfill which may be more representative of the overall average condition. Hence, the use of an instrumented permeable blanket was explored to measure the in-situ vertical hydraulic conductivity of waste. In order to use the instrumented permeable blanket as a source for estimation of hydraulic conductivity, the hypothesis was tested in the laboratory.

OBJECTIVES

The objective of this study was to develop a method for estimation of in-situ vertical hydraulic conductivity of subsurface soils or potentially waste underlying an instrumented blanket on a continuous and real-time basis by analyzing pressures and flow data obtained from sensors embedded in the blanket. A laboratory-scale physical model of landfill was developed to conduct controlled lab tests in order to independently verify the proposed method. The lab model had sensors embedded in the sand underlying the blanket which helped to understand the hydraulics of liquid flow due to subsurface injection. The objectives of the study presented in this paper are as follows:

- test a new analytical method (ACRES) for estimation of vertical hydraulic conductivity of a porous material underlying an instrumented blanket;
- carry out numerical modeling of the test using Vadose/W;
- verify independently the estimated hydraulic conductivities using falling head tests on the model and tracer tests; and

- develop design parameters to apply the ACRES method in the field.

MATERIALS AND METHODS

Figure 4-2 presents a schematic of the landfill model fabricated to simulate a horizontal permeable blanket. All acrylic panels of the model were screwed together with rubber seals in-between the panels to provide a watertight box to contain the soils subjected to injection of water. A silicone sealant was applied at the seams to prevent potential leakage. A separate acrylic panel was used to make the bottom of the leachate collection system (LCS) raised to a fixed slope of 3%.

Landfill Components

Various soils were used to simulate these components of the landfill model: leachate collection system (LCS), permeable blanket, and porous material underlying the blanket. The blanket and the LCS were made up of pea gravel. Pea gravel was chosen as the LCS drainage material because it results in lower liquid heads in the LCS (Khire *et al.* 2006) and it was also considered as a blanket material in the study presented by Haydar and Khire (2007) and Khire and Haydar (2003). Relatively homogeneous and isotropic sands were used below the blanket in order to be able to accurately characterize the system components to confirm the numerical models' findings.

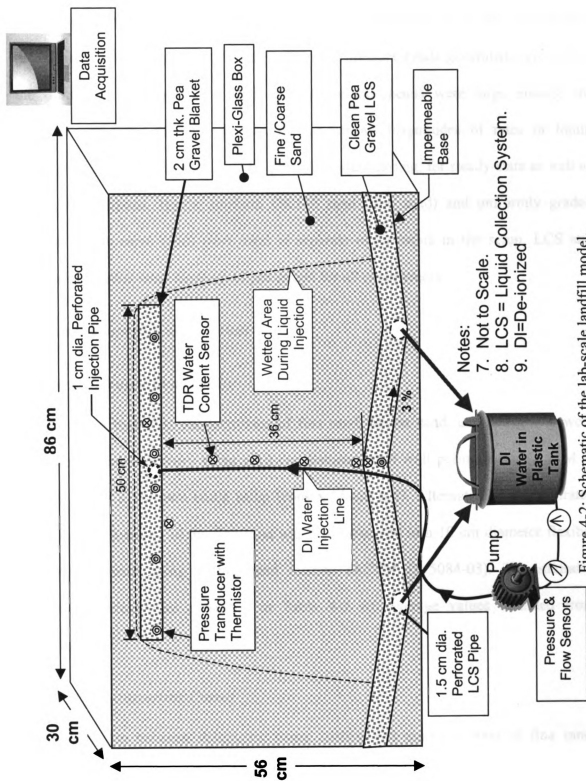


Figure 4-2: Schematic of the lab-scale landfill model.

The sands placed below the blanket were selected based on the results of numerical modeling which indicated that: (1) the maximum pressure heads generated were within the dimensions of the model; and (2) the pressure heads were large enough for measurement using the pressure sensors for various magnitudes of rates of liquid injection, duration of injection, and frequency of liquid dosing, for steady-state as well as transient conditions. Hence, uniform OK110 sand (fine sand) and uniformly graded Ottawa sand (coarse sand) were used in separate experiments in the setup. LCS and permeable blanket were made up of pea gravel for all experiments.

Hydraulic Properties of Materials

Saturated Hydraulic Conductivity

The saturated hydraulic conductivities of fine sand, coarse sand, and pea gravel were measured in the laboratory using a 10 cm diameter rigid wall permeameter (ASTM D 2434-68) with a Mariotte bottle setup (constant head test). Alternatively, the saturated hydraulic conductivity of the fine sand was also measured in a 10 cm diameter flexible wall permeameter using falling head method (ASTM D 5084-03). The saturated hydraulic conductivities presented in Table 4-2 are average values obtained from triplicate tests.

Soil-Water Characteristic Curves

The relationship between volumetric water content and matric suction of fine sand, coarse sand, and pea gravel was obtained from a hanging column experimental setup. It consisted of a Buchner funnel with porous ceramic plate (ASTM D 6836-02). Drying as

well as wetting soil-water characteristics curves (SWCC) were generated. Replicate experiments were carried out for determining the SWCCs of all soils.

The soil water characteristic curves are described in terms of the van Genuchten (van Genuchten 1980) fitting equation (Equation 4-1) as well as Fredlund and Xing (Fredlund and Xing 1994) fitting equation (Equation 4-2):

$$\theta = \theta_r + \frac{\theta_s - \theta_r}{\left(1 + |\alpha\psi|^n\right)^m} \quad (4-1)$$

where ψ = matric suction head [L]; θ = volumetric water content [dimensionless]; θ_s = saturated volumetric water content [dimensionless]; θ_r = residual volumetric water content [dimensionless]; and α [1/L], n , and m ($m = 1 - n^{-1}$) are the van Genuchten fitting parameters.

$$\frac{\theta}{\theta_s} = C_\psi \left[\frac{1}{\ln(2.71828 + |\psi / \alpha|^n)^m} \right] \quad (4-2)$$

where C_ψ = correction function; and a , n , and m are the Fredlund Xing fitting parameters which are determined as follows:

$$a = \psi_i; \quad m = 3.67 \ln(\theta_s / \theta_i); \quad n = (1.31^{m+1})(3.72s\psi_i) / m\theta_s \quad (4-3)$$

where ψ_i = suction corresponding to the water content occurring at the inflection point of the curve, and s = the slope of the line tangent to the function that passes through the inflection point. The a , n , and m values were determined using a fitting algorithm and

applying it to measured data points in Vadose/W. The fitting parameters are tabulated in Table 4-2.

Table 4-2: Saturated and unsaturated hydraulic properties of soils used in the landfill model.

Soil Type	Location	Saturated hydraulic conductivity, K_s (cm/s)	Unsaturated hydraulic properties						
			van Genuchten fitting parameters				Fredlund-Xing fitting parameters		
			θ_s	θ_r	α (1/cm)	n	a (kPa)	n	m
Fine Sand	Below and above blanket	1.8 to 6.4×10^{-3}	0.42	0.03	0.01 to 0.02	6.5	5.5 to 9.25	24 to 30	0.36 to 0.47
Coarse sand	Below and above blanket	0.05 to 0.09	0.4	0.03	0.023 to 0.090	4.5	1.5 to 3	3 to 7.5	1 to 2.5
Pea Gravel	Blanket and LCS	2	0.43	0.01	0.35 to 0.45	3	0.35 to 0.55	1.9 to 2.7	1.8 to 5

Notes: LCS = Leachate Collection System

θ_s = saturated volumetric water content [dimensionless];

θ_r = residual volumetric water content [dimensionless]; and

α [1/L] and n are van Genuchten's fitting parameters (van Genuchten 1980)

a, n and m are Fredlund-Xing's fitting parameters (Fredlund and Xing 1994)

Instrumentation and Calibration

The following sensors were used in the landfill model: (1) pressure transducers with built-in thermistors; (2) water content sensors; and (3) flow sensors. All sensors were connected to Campbell scientific CR1000 datalogger to continuously monitor and log data. The water content sensors were connected to the datalogger via an electro-magnetic

pulse generator and a coaxial multiplexer. The datalogger was programmed to take readings at frequencies ranging from 5 s to 30 min.

Pressure Transducer

The length and diameter of pressure transducer were 8.5 cm and 1.2 cm, respectively. The pressure transducer provided temperature compensated analog 0-5 VDC output proportional to the water pressure experienced by it. The sensitivity of the sensor was $\pm 1\%$ and have a measurement range of 0 to 92 cm of water head. Since the sensors were vented, barometric pressure was not recorded by the diaphragm. In recognition of the concern for zero drift and offsets, the accuracy of all sensors was checked from time to time by ponding water and checking the measured static heads during the course of experiments.

The pressure transducers were calibrated by applying known pressures and measuring the response. In order to evaluate the accuracy of their measurements, the pressure transducers were placed in a container in the position they were eventually embedded in the LCS, sand and the blanket in the landfill model. The pressure transducers were tested by adding de-ionized (DI) water at depths ranging from 15 to 35 cm. A linear relationship between the depth of water in the container and the pressure head readings recorded by the pressure transducers was observed. The accuracy of the pressure transducer was within ± 0.5 cm. Periodically, water was ponded in the landfill model and maintained at a fixed level for few hours to measure signal drift for the pressure sensors. At the end of the experiments, when the setup was dismantled, the calibration of the sensors was re-checked and corrected, if needed. The zero was found to have drifted approximately by 0.3 to 0.6 cm.

TDR Water Content Sensor

The mini-TDR water content sensor consisted of three pointed 0.15 cm diameter stainless steel rods mounted into an encapsulated plastic head. The probe rod length was 6 cm and spacing between the probe rods was 0.6 cm. Topp's (Topp *et al.* 1980) empirically derived calibration equation was used to convert the dielectric constant values to volumetric water content.

The TDR water content sensors were fully inserted vertically in a container filled with dry sand and then water was gradually added in known steps until the sand got saturated. For both sands, a linear relationship between the volumetric water content calculated from known addition of water and the volumetric water content measured by the TDR water content sensors was observed.

Flow Sensor

The flow sensor was capable of measuring flow rates ranging from 8 to 165 cm³/s. The flow sensor incorporated a pelton-type turbine wheel having diameter and thickness equal to 1.6 cm and 0.075 cm, respectively to measure the flow rate of water. The rotational speed of the turbine wheel increased proportionally to the volumetric flow rate generating electric pulses. The sensors provided analog DC voltage output proportional to the flow rate and the flow rate in engineering units was shown on the integrated LCD display.

A linear relationship was observed between the flow rates recorded by the flow sensor and the flow calculated from the levels measured by the pressure transducer. The accuracy of the flow sensor was within $\pm 0.5\%$.

Pump

The maximum flow and the pressure head that a pump needed to deliver in the landfill model was based on these factors: (1) hydraulic conductivity of sand underlying the blanket; and (2) injection rate. A miniature gear pump was used for relatively low injection flow rates ($8 \text{ cm}^3/\text{s} - 42 \text{ cm}^3/\text{s}$) when fine sand was used and a brushless magnetic drive pump was used for higher injection flow rates ($75 \text{ cm}^3/\text{s} - 300 \text{ cm}^3/\text{s}$) when coarse sand was used. Both pumps were operated with a variable power DC power supply to obtain variable injection flow rates. These pumps were chosen because of their ability to deliver “pulseless” flows because the rate of flow had to be constant to achieve consistent results. A quartz based digital timer was used to operate the pump in on/off mode which could be programmed for various durations of on/off injection cycles.

Fabrication of Model Landfill

Figure 4-2 shows a schematic of the landfill model and the location of sensors. A 4-cm thick LCS made up of pea gravel was placed at the bottom of the plexi glass tank. Two 1.5-cm diameter perforated pipes discharging freely into the atmosphere were placed 45 cm apart in the LCS pea gravel layer. The perforated seepage pipes for LCS had at least 10 times higher flow capacity than the flows injected in the model to maintain the pressure head in the LCS within its thickness of 4 cm. A geotextile was placed between the LCS and the sand to prevent clogging of the LCS.

About 40-cm thick dry sand both coarse and fine sand having dry density equal to 1.6 g/cm^3 and porosity of about 0.42 was placed below the blanket. In the sand layer, two pressure transducers were embedded in vertically upright position at 10-cm intervals. A

water content sensor was placed in the sand immediately next to the sensing tip of the pressure sensors.

The permeable blanket for the liquid recirculation system was also made up of the pea gravel used in LCS. The blanket was about 50 cm long and 30 cm wide. The average thickness of the blanket was 2.0 cm. The perforated injection pipe having 1 cm diameter was embedded at the center of the blanket in the direction parallel to the width of the blanket where water was injected under a positive pressure. Total six pressure transducers were embedded in the sand in vertically upward position at designated locations such that the tip of the sensor was within the blanket. The injection pipe, the tip of the pressure transducers and the LCS pipes were wrapped with a polymer mesh to prevent migration of sand or gravel particles. The blanket was wrapped with a non-woven geotextile to separate the permeable material from the surrounding sand to prevent clogging of the blanket.

The end of the injection pipe inside the blanket was capped and the other end was connected consecutively to a pressure transducer to measure the injection pressure and a flow sensor to measure the injection flow rate. A closed loop recirculation system was formed wherein the injected water after flowing through the soil and discharging freely in the atmosphere from the seepage pipes was collected in the storage tank from where it was injected back into the blanket system as shown in Figure 4-2. A pressure transducer was also placed in the storage tank to monitor the change in head of water in the tank to monitor if and when a steady-state is reached. Minimal change in tank level signified inflow and outflow to be almost the same.

Falling Head Tests

Falling head tests were performed on the landfill model before injection through the blanket to measure the saturated hydraulic conductivity of the whole system. This allowed capturing the effect of model scale, sensors, and sensor cables on the vertical hydraulic conductivity of the model and thus providing the “in-situ” conductivity before the injection experiments began. Falling head tests were also conducted at the end of experiments to estimate the hydraulic conductivity of sand achieved at the end of that injection events. For the fine sand, the measured saturated hydraulic conductivity of the landfill model ranged from 1.8×10^{-3} to 6.4×10^{-3} cm/s and for the coarse sand it ranged from 5×10^{-2} to 9×10^{-2} cm/s (Table 4-1).

The maximum value for saturated hydraulic conductivity of 0.09 cm/s for coarse sand was obtained after saturating the entire sand in the model. In this experiment, the model was continuously saturated for a period of 15 days by pumping water at a relatively high rate from the top surface of the overlying sand. In doing so, entrapped air was presumably compressed or dissolved in the recirculated water. Additional water content sensors with long probes were inserted outside the blanket which showed gradual increase in saturation. The 100% saturation of the sand was assumed when all water content sensors recorded water content corresponding to saturation.

Vadose/W 2007 Numerical Model

Vadose/W was used to numerically simulate the hydraulics of the landfill model as well as to simulate field-scale blanket. Vadose/W numerically solves the Richards' equation (1931) for saturated/unsaturated water flow and has an option of using van Genuchten

(van Genuchten 1980) function for soil-water characteristic curves and van Genuchten-Mualem (Mualem 1976) model for predicting the unsaturated hydraulic conductivity function. For a homogeneous and isotropic soil, the governing partial differential equation for water flow is 2-D form of Richards' equation which is presented in Equation 4-4:

$$\frac{\partial \theta}{\partial t} = -\frac{\partial}{\partial x}\left[k(\psi)\frac{\partial \psi}{\partial x}\right] - \frac{\partial}{\partial z}\left[k(\psi)\frac{\partial \psi}{\partial z}\right] + \frac{\partial k(\psi)}{\partial z} - S_w \quad (4-4)$$

where θ = volumetric water content [dimensionless]; ψ = matric suction head [L]; k = hydraulic conductivity of the porous material which is strongly dependant on the matric suction or water content [L/T]; z = vertical dimension [L]; S_w = volume of water removed per unit time per unit volume of soil by plant water uptake or evaporation (sink term) [1/T]; and t = time [T]. Vadose/W uses the Galerkin finite-element method to solve the governing equation of flow. Vadose/W can simulate water and heat in unsaturated, partially saturated, or fully saturated porous media and is capable of performing steady-state and transient conditions.

Input Parameters for Numerical Model

Mesh Discretization

The problem domain was divided into a structured mesh in the form of 4 noded 4,250 quadrilateral elements. The time stepping was adjusted to discretize the time domain into a series of incremental time steps. The minimum and maximum time steps were set at 0.0001 and 1 second, respectively. The spacing between the nodes located near the flux and seepage boundaries were relatively small to ensure as little numerical error as possible due to the assigned boundary conditions.

Material Properties

The saturated and unsaturated properties described by van Genuchten fitting parameters (Table 4-1) were input to the model. The coefficient of compressibility (m_v) was input in the hydraulic function. Because water can also be released by compressing the soil skeleton and reducing the size of voids, the coefficient of volume compressibility m_v is input to adequately represent the slope of the water content function in the positive pore-water pressure region. The m_v for pea gravel and the sand were equal to $1\text{e-}5$ 1/kPa as per Vadose/W User's manual (Geo-Slope 2004). A sensitivity analysis was carried out by varying the order of magnitudes of m_v but it had no effect on the results.

Temperature and moisture gradients influence vapor and liquid flow in unsaturated soils, Vadose/W couples heat and mass flows, for which two thermal functions are required by the program for each material type, i.e. volumetric specific heat and thermal conductivity functions. The ability of the soil to transfer heat is described by its volumetric heat capacity and thermal conductivity. The thermal conductivity of soil is dependent on its water content, because of differences in thermal conductivity of air and water, and hence is a function of the soil water characteristic curve. Typical values of soil mineral mass specific heat capacity of $0.71 \text{ kJ/kg}^\circ\text{C}$ and soil mineral thermal conductivity of $216 \text{ kJ/day m}^\circ\text{C}$ for the materials used in this study were derived from the Vadose/W User's manual (Geo-Slope 2004) based on soil mineralogy. The thermal conductivity functions and volumetric heat capacity for each material were estimated using the built-in Vadose/W estimation tool.

Initial and Boundary Conditions

In order to obtain initial head conditions, steady-state analyses were conducted by specifying matric suctions corresponding to in-situ water contents and an initial temperature equal to room temperature of 20°C above the base of the model. The subsequent file generated was used as the initial condition file for the transient analysis.

The total injected flow rate was applied as total nodal flux equally distributed at the nodes of the circular boundary representing the injection pipe. For the input of total flux, the thickness of elements was specified. For on/off conditions, the nodal flux as a function of time was input in cyclic mode in hydraulic boundary condition. All external boundaries were simulated as zero-flux boundaries and the leachate collection pipes were simulated as seepage face boundaries.

Input Parameters for Field-scale Simulations

Conceptual Model

The conceptual model developed by Haydar and Khire (2007) for numerical simulation of permeable blankets was adapted in this study (Figure 4-3). The conceptual model consisted of a 15-cm-thick, 60-m-wide permeable blanket and a leachate collection system (LCS). The 0.1-m-diameter perforated injection pipe ran perpendicular to the plane of the paper through the center of the blanket. The vertical distance between the blanket and the top of the LCS was 15 m. Distance from the top of the blanket to the upper zero flux boundary was assumed equal to 5 m to contain all injected leachate and to prevent possible artesian conditions for the simulated leachate injection rates. The LCS consisted of two 0.15-m-diameter perforated pipes embedded in a 0.3-m-thick gravel

layer at a horizontal spacing equal to 60 m. The slope of the LCS was assumed equal to 3.5%. The hydraulic conductivity of the LCS drainage material was assumed equal to 10^{-2} m/s. The chosen LCS design parameters resulted in less than 0.3-m-leachate pressure head on the lining system for all simulations presented in this study.

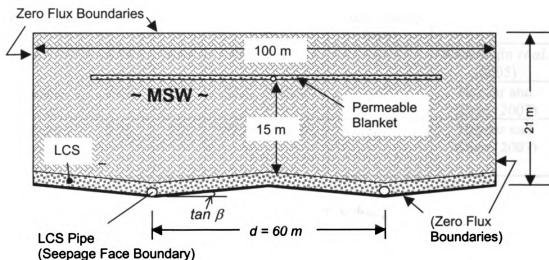


Figure 4-3: Conceptual model for field-scale simulations (adapted from Haydar and Khire 2007).

Material Properties and Assumptions

The simulated saturated hydraulic conductivity of MSW, k_w , was assumed equal to 10^{-5} m/s. This value was selected from typical values published by Hughes *et al.* (1971), Fungaroli and Steiner (1979), Korfiatis *et al.* (1984), Oweis *et al.* (1990), and Bleiker *et al.* (1993) shown in Table 4-1. The saturated and unsaturated hydraulic properties of the

simulated waste, blanket material, and LCS gravel layer input to Vadose/W are presented in Table 4-3.

Table 4-3: Saturated and unsaturated hydraulic properties used in field-scale simulations.

Landfill Unit	θ_r	θ_s	α (1/m)	n	Saturated hydraulic conductivity (m/s)	Source
Waste	0.14	0.58	15	1.6	10^{-5}	Kazimoglu <i>et al.</i> (2005)
Permeable Blanket	0.01	0.3	57.4	2.44	10^{-2}	Haydar and Khire (2007)
Leachate Collection System	0.01	0.3	57.4	2.44	10^{-2}	Haydar and Khire (2007)

Notes: θ_s = saturated volumetric water content [dimensionless];

θ_r = residual volumetric water content [dimensionless]; and

α [1/L] and n are van Genuchten's fitting parameters (van Genuchten 1980)

Leachate was simulated as pure water. The effect of gas flow, temperature and biochemical reactions occurring within a landfill was ignored. The option transient-isothermal was chosen for the simulations in Vadose/W. Leachate flow as a result of percolation from the cap or waste above the model domain was assumed zero. This assumption is reasonable since subsurface hydraulics of injected leachate was simulated in this study. The waste was assumed to be homogeneous and isotropic.

Mesh Discretization

The problem domain was divided into a structured mesh in the form of 4 noded quadrilateral and triangular elements. The time stepping was adjusted to discretize the time domain into a series of incremental time steps. The spacing between the nodes located near the flux and seepage boundaries were relatively small to ensure as little numerical error as possible due to the assigned boundary conditions. The minimum size of the finite-elements used for discretization of the problem domain, the time step, and the error tolerances for pressure head and water content were selected such that cumulative water balance error did not exceed 10 %.

Initial and Boundary Conditions

The initial condition of MSW was entered in the form of initial water table at 1 m below the bottom of the problem domain with maximum negative pressure head of 0.1 m which yielded initial saturation of 75%. The initial total head at each node was computed proportionally to the vertical distance between the node and the defined water table.

All external boundaries were simulated as zero flux boundaries. The perforated pipe used for leachate injection was simulated as a node to which nodal flux was assigned as constant for continuous injection or as a function of time in cyclic mode for on/off injection. The input flux was calculated by dividing the injected flow rate per 10 m length of the injection pipe. The simulated leachate injection rates (Q) ranged from 300 to 700 m^3/d . These rates were selected based on leachate injection rates used in the field for the blanket at McGill landfill in Jackson (Khire and Haydar 2005). During the period from September 2003 to April 2004, about 3,200 m^3 of leachate was injected in the glass

blanket corresponding to approximately 90 leachate recirculation events at leachate injection rates ranging from 250 to 850 m³/d.

Leachate collection pipes embedded in the LCS were simulated as seepage face boundaries. The seepage face is a dynamic drainage boundary condition that changes according to the flow conditions during the simulation. The pore pressure head is equal to zero along the saturated part of the seepage face through which water seeps out from the saturated part of the domain.

RESULTS

A method called Analysis of Conductivity in Real-time using Embedded Sensors (ACRES) was developed to estimate the hydraulic conductivity of the underlying sand in the landfill model using pressure and flow data collected from the instrumented blanket. The hydraulic conductivity was also estimated using inverse numerical simulation. The estimated hydraulic conductivities were confirmed from falling head tests and tracer test conducted on the landfill model.

ACRES

Approach

In this method, an analytical model based on Darcy's law was developed to estimate hydraulic conductivity of the underlying sand. Darcy's law is commonly applicable to the 1-D flow of water in a saturated soil but it is also applied for the flow of water through unsaturated soils as long as the soil water storage does not change (Darcy-Buckingham Equation). In unsaturated soils, water flows only through the pore spaces filled with

water. Thus, the measured hydraulic conductivity would be lower in the absence of complete saturation of the soil sample. Hence the proposed equation would give an estimate of the hydraulic conductivity for an average degree of saturation that exists at steady-state.

In the landfill model, Darcy's law is applied when the water content measured by the water content sensors reached constant values for a certain injection rate. Based on Darcy's law, the vertical hydraulic conductivity of the soil located between the blanket and the LCS (Figure 4-2) for a given average degree of saturation can be estimated using Equation 4-5:

$$K_{ACRES} = \frac{Q \times D}{W_w \times L \times \Delta H} \quad (4-5)$$

where K_{ACRES} = average vertical hydraulic conductivity of porous material between the blanket and LCS;

Q = Rate of injection at steady-state;

D = vertical depth of porous material between the blanket and LCS;

L = Length of the blanket parallel to the length of the injection pipe;

W_w = Wetted width of the blanket; and

ΔH = difference in total heads (elevation and pressure) between the blanket and LCS.

Assuming the datum passes through LCS, the total head in blanket can be estimated by adding its elevation head to the average pressure head in the blanket. The elevation head is actually the thickness of the sand, D , between the blanket and the LCS. The pressure head in blanket is actually assumed equal to the arithmetic mean of pressure

heads, h_m , recorded by all pressure transducers embedded in the blanket. The elevation head is zero in the LCS and the pressure head can be ignored in LCS when LCS pipes freely drain into atmosphere. Hence, Equation 4-5 can be re-written in simplified form,

$$K_{ACRES} = \frac{Q \times D}{W_w \times L \times (D + h_{av})} \quad (4-6)$$

where h_{av} = arithmetic mean of pressure heads, h_m , recorded by all pressure transducers embedded in the blanket.

During the experiment, injection rate Q is fixed. The wetted width W_w of the blanket and the pressure heads, developed in the blanket were estimated from the responses of the sensors embedded in the blanket. The wetted width dictates the lateral extent of infiltration of injected liquid through the underlying soil which can be determined from the responses of pressure sensors at designed locations in the blanket. The wetted width can be accurately estimated if the blanket contains adequate number of pressure sensors.

Application to the Data from Landfill Model

1. Coarse sand

Figure 4-4 shows the measured pressure heads, h_m , in the blanket when DI water was injected at a constant rate, $Q = 150 \text{ cm}^3/\text{s}$ in the setup with coarse sand. Before the liquid injection in the blanket was started, the average degree of saturation, S of the sand

below the blanket was 70% which increased to 90% within 40 hours after the start of injection as shown in Figure 4-4.

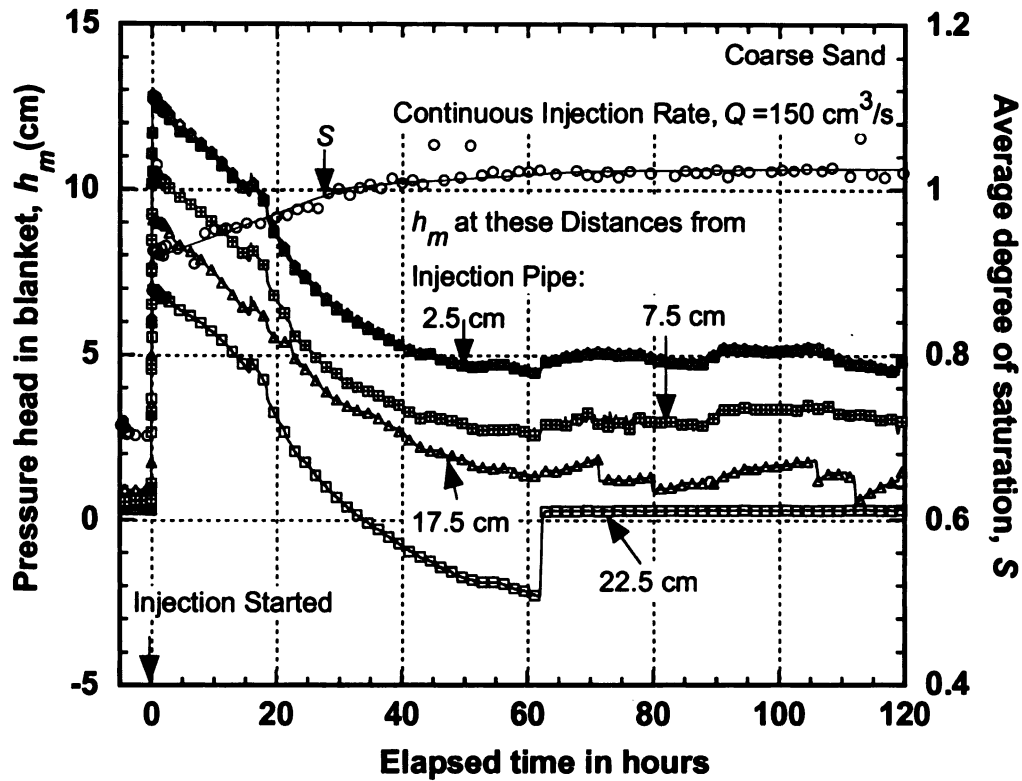


Figure 4-4: Measured pressure heads in blanket showing decrease in pressure heads with increase in average degree of saturation of underlying sand.

The pressure heads were relatively high in the beginning because entrapped air or non-continuous air bubbles isolated from atmosphere were formed due to the advance of water through preferred pores or pore sequences resulting in trapping the gaseous air. The trapped air bubbles were under pressure greater than atmosphere. Hence initial pore water pressure heads recorded by the pressure sensors were high due to the entrapped air bubbles and their effect on hydraulic conductivity. The initial high pressure heads decreased due to increase in hydraulic conductivity of sand and hydraulic conductivity is

known to increase when entrapped air is removed (Christiansen 1944). In about 60 hours after the injection began, the pressure heads reached a steady-state. A steady-state was assumed to have reached when the pressure heads in the blanket did not show upward or downward trend for several hours.

Some pressure sensors showed increase in h_m initially. As the average degree of saturation, S , of the underlying sand increased and hydraulic conductivity of the underlying sand increased, the wetted width decreased as indicated by drop in the pressure heads to almost zero for some sensors (Figure 4-4).

Because the wetted width varied during the period of injection, K_{ACRES} was calculated using various values of W_w . In the beginning, when all sensors responded, the total length of the blanket of 50 cm was considered as W_w . When a steady-state was attained, the extent of wetted width was revised to 35 cm because the pressure sensors located beyond 17.5 cm from the injection pipe did not respond to the injection rate of $Q=150 \text{ cm}^3/\text{s}$ (Figure 4-4).

Similarly, the hydraulic conductivity of the underlying sand was estimated at various degrees of saturation for on/off injection rates. For a certain average degree of saturation, the maximum pressure head, h_m in the blanket attained just before the pump turned “off” was considered in the estimation of h_{av} in Equation 4-6.

2. Fine sand

In the setup with fine sand below the blanket, DI water was continuously injected for specific periods at rates varying from 15 – 25 cm³/s. Because migration of water in the fine sand was relatively slow compared to the coarse sand, it took greater than 350 hours for all water content sensors in the fine sand to reach 100% degree of saturation. There was always ponded water during these injection events. Hence, the hydraulic conductivity of the underlying sand was estimated applying ACRES method at various degrees of saturation considering the total length of the model domain of 86 cm as W_w .

Comparison with Falling Head Conductivities

Because K_{ACRES} was estimated using Equation 4-6 for various rates of injection for fine and coarse sands at various degrees of saturation, a hydraulic conductivity function could be obtained as shown in Figure 4-5. Because falling head tests were also done to independently verify the hydraulic conductivity estimated with ACRES method at various degrees of saturation, it was important to compare the hydraulic conductivity values for the in-situ sand. The unsaturated hydraulic conductivities were estimated using the van Genuchten-Mualem prediction model (Mualem, 1976) presented in Equation 4-7:

$$\frac{K_{FH}}{K_s} = \frac{\left\{ 1 - (\alpha\psi)^{n-1} \left[1 + (\alpha\psi)^n \right]^{-m} \right\}^2}{\left[1 + (\alpha\psi)^n \right]^{m/2}} \quad (4-7)$$

where ψ = matric suction head [L]; K_{FH} = hydraulic conductivity of sand which is strongly dependant on the matric suction or water content [L/T]; K_s is saturated hydraulic

conductivity [L/T] obtained from falling head tests; and α , n , m ($m = 1 - n^{-1}$) are the fitting parameters obtained from the soil-water characteristic curves as shown in Table 4-2. The maximum saturated hydraulic conductivity of 0.09 cm/s which was obtained from the falling head tests shown in Table 4-2 was used as K_s .

The average hydraulic conductivity function from falling head tests K_{FH} was compared with K_{ACRES} at the same degree of saturation. The ratios between the two hydraulic conductivities for various rates of injection for fine and coarse sands are tabulated in Table 4-4. Figure 4-5 shows the comparison between K_{ACRES} and K_{FH} . The K_{ACRES} estimated is in the ball parks of predicted K_{FH} .

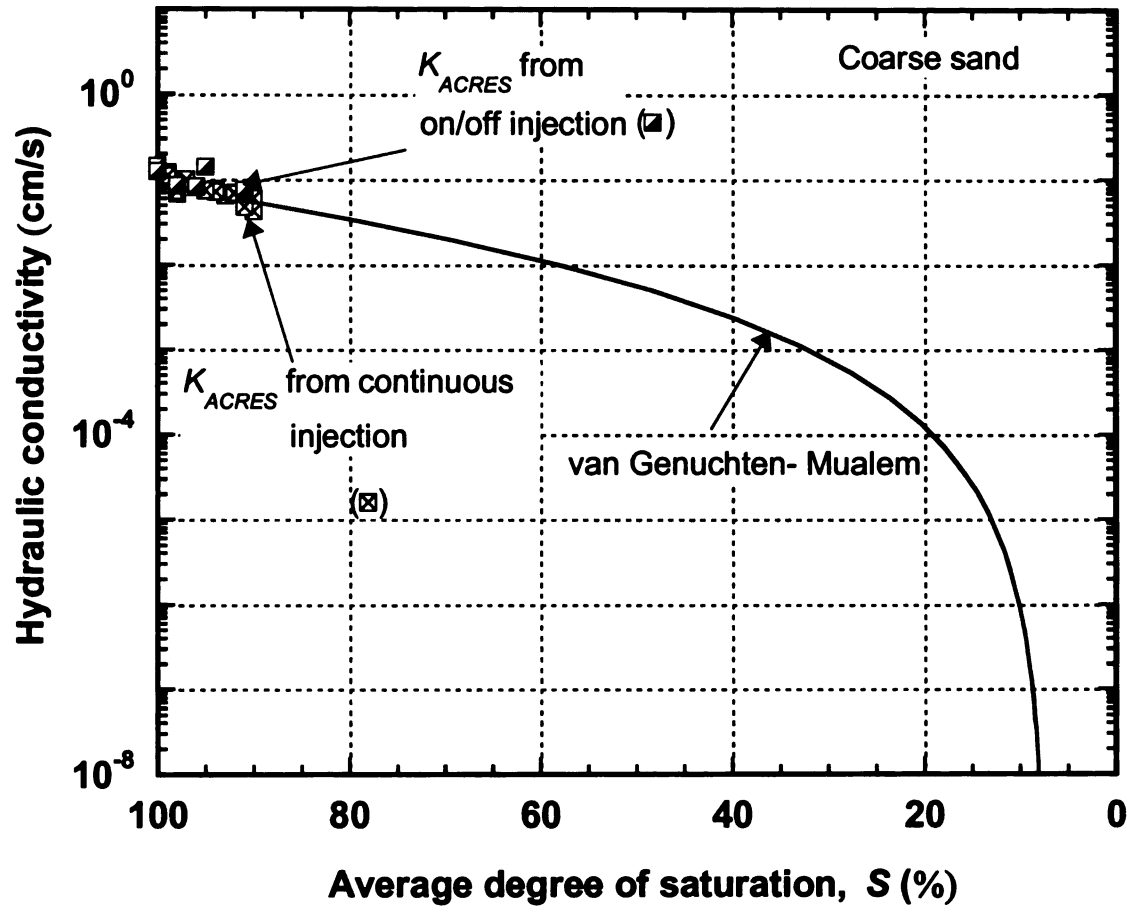


Figure 4-5: Estimation of hydraulic conductivity function using ACRES method from continuous and on/off injection experiments for coarse sand.

Table 4-4: Comparison between the hydraulic conductivities estimated through ACRES and falling head tests.

Experiment	Injection rate, Q_3 (cm ³ /s)	Average pressure heads in blanket, h_{av} (cm)	Wetted width, W_w (cm)	Degree of saturation, S (%)	K_{ACRES}/K_{FH}			
					Coarse sand		Fine sand	
					Continuous	On/Off	Continuous	On/Off
Continuous Injection	18	5.3	86	76	-	-	2.6	-
	20	9.6	86	82	-	-	2	-
	20	8.6	86	92	-	-	1.3	-
	20	6.7	86	98	-	-	1.1	-
	23	13.6	86	100	-	-	1	-
Continuous Injection	120	3	50	91	1.2	-	-	-
	120	2.3	25	95	2	-	-	-
	120	1.8	25	100	1.6	-	-	-
3 min on/ 10 s off	92	6.8	50	91	-	0.86	-	-
	92	6.23	25	97	-	1.29	-	-
3 min on/ 10 s off	120	9.5	50	90	-	1.13	-	-
	120	7.5	50	93	-	1.02	-	-
	120	5	50	98	-	0.83	-	-

Table 4-4: Continued

Experiment	Injection rate, Q (cm ³ /s)	Average pressure heads in blanket, h_{av} (cm)	Wetted width, W_w (cm)	Degree of saturation, S (%)	K_{ACRES}/K_{FH}			
					Coarse sand		Fine sand	
					Continuous	On/Off	Continuous	On/Off
6 min on/ 10 s off	120	8.5	50	92	-	1.13	-	-
	120	7.65	50	94	-	1.06	-	-
	120	6.3	50	95	-	1.06	-	-
	120	5.1	50	98	-	0.91	-	-
Continuous Injection	150	10	50	91	1.3	-	-	-
	150	8	50	96	1.1	-	-	-
	150	5.3	50	98	1	-	-	-
	150	3.1	35	100	1.3	-	-	-
3 min on/ 10 s off	150	11.78	86	90	-	0.78	-	-
	150	8.91	50	94	-	1.15	-	-
	150	7	50	96	-	1.11	-	-
	150	5.55	35	99	-	1.33	-	-
3 min on/ 10 s off	150	3.48	35	100	-	1.34	-	-

Table 4-4: Continued

Experiment	Injection rate, Q (cm^3/s)	Average pressure heads in blanket, h_{av} (cm)	Wetted width, W_w (cm)	Degree of saturation, S (%)	K_{ACRES}/K_{FH}			
					Coarse sand		Fine sand	
					Continuous	On/Off	Continuous	On/Off
6 min on/ 10 s off	150	13	86	91	-	0.82	-	-
	150	8	50	98	-	0.89	-	-
	150	6	35	99	-	1.21	-	-

The ratio of K_{ACRES}/K_{FH} for coarse sand is illustrated in Figure 4-6 as a function of dosing frequency for the coarse sand. It is observed that K_{ACRES}/K_{FH} for injections carried out in on/off dosing cycles varied from 0.75 to 1.4 and for continuous injection the ratio varied from 1 to 2.

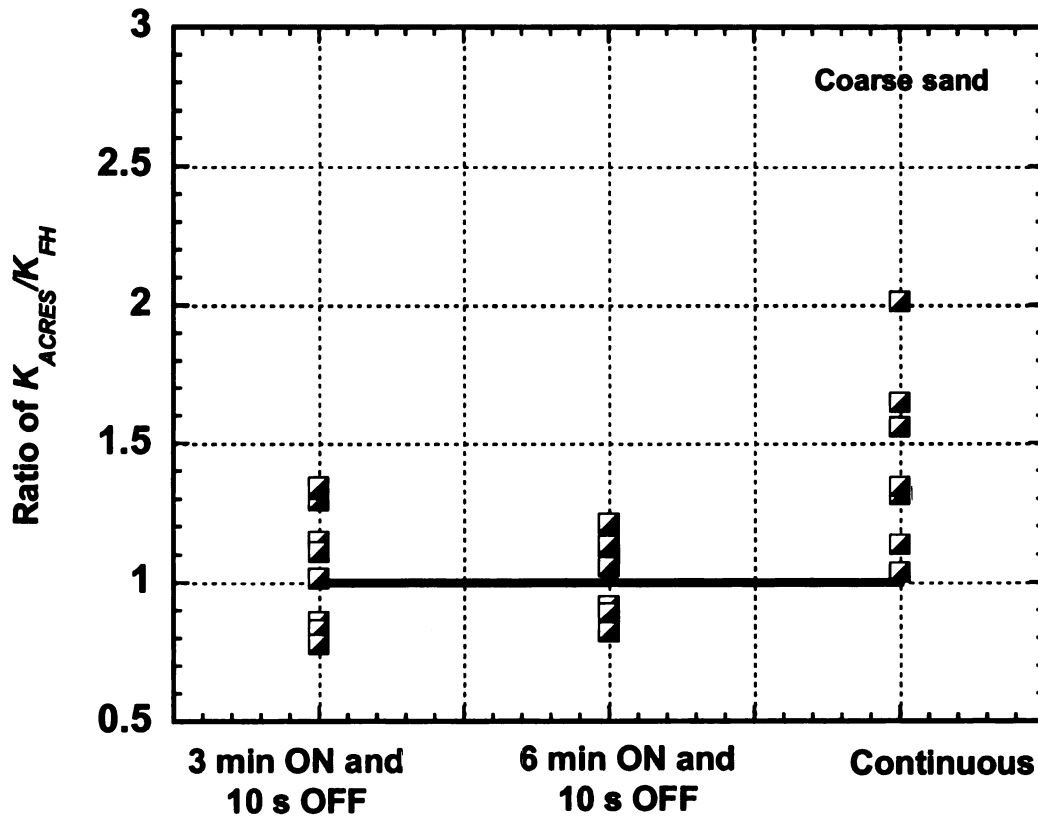


Figure 4-6: Ratio of K_{ACRES}/K_{FH} for various dosing frequencies for coarse sand.

Inverse Numerical Modeling

The injection events in the landfill model were numerically modeled in Vadose/W. Vadose/W requires the input of saturated and unsaturated properties of the blanket, underlying and overlying soil to simulate the pressures within the blanket. Hence, once the hydraulic properties of the blanket, which included hydraulic conductivity, porosity,

and soil water retention curve, were known, the inverse modeling approach required trying a range of saturated hydraulic conductivities of the underlying soil as an input to Vadose/W until a best match between the simulated and measured pressure heads was obtained at steady-state. The unsaturated hydraulic properties using van Genuchten parameters (Table 4-2) were input to the numerical model. For a given injection rate and initial conditions prevailing in the model, the only unknown parameter was the saturated hydraulic conductivity, K_w of the sand. K_w was adjusted such that the pressure heads measured by the pressure sensors embedded in the blanket in the landfill model at steady-state matched with the simulated pressure heads at the observation nodes in the numerical model. The reasons behind the discrepancies in the simulated and measured pressure heads in the beginning are discussed in detail in the Paper no. 3 of this dissertation. The K_w obtained from this inverse modeling was confirmed from the falling head tests which were conducted after the end of the injection experiments. The K_w agreed reasonably well with falling head values as shown in Figures 4-7 and 4-8. Figure 4-8 shows the measured and simulated pressure heads in the blanket at 2.5 cm and 7.5 cm distance from the injection pipe for a 6 min on/ 10 s off injection event at $Q = 150 \text{ cm}^3/\text{s}$.

Different unsaturated properties were also input and it was observed the retention properties are irrelevant at steady-state. This finding is consistent with the findings of Haydar and Khire (2007).

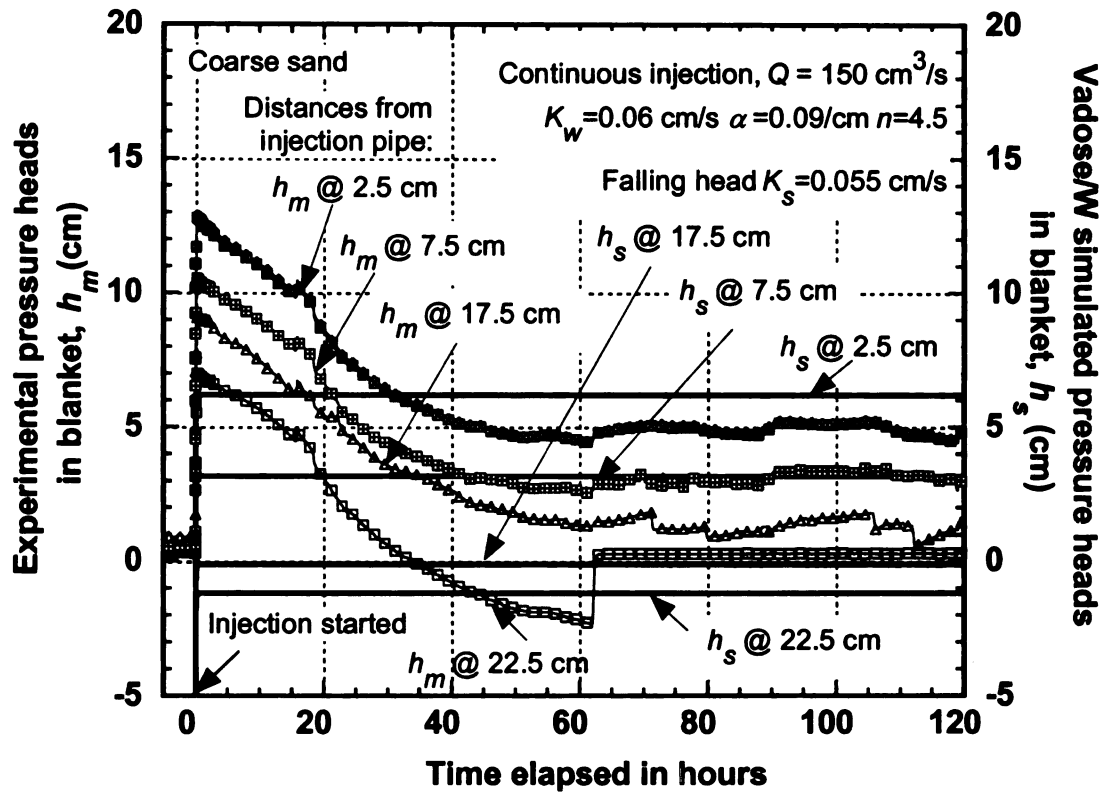


Figure 4-7: Estimation of hydraulic conductivity of underlying sand using inverse numerical simulation for continuous injection.

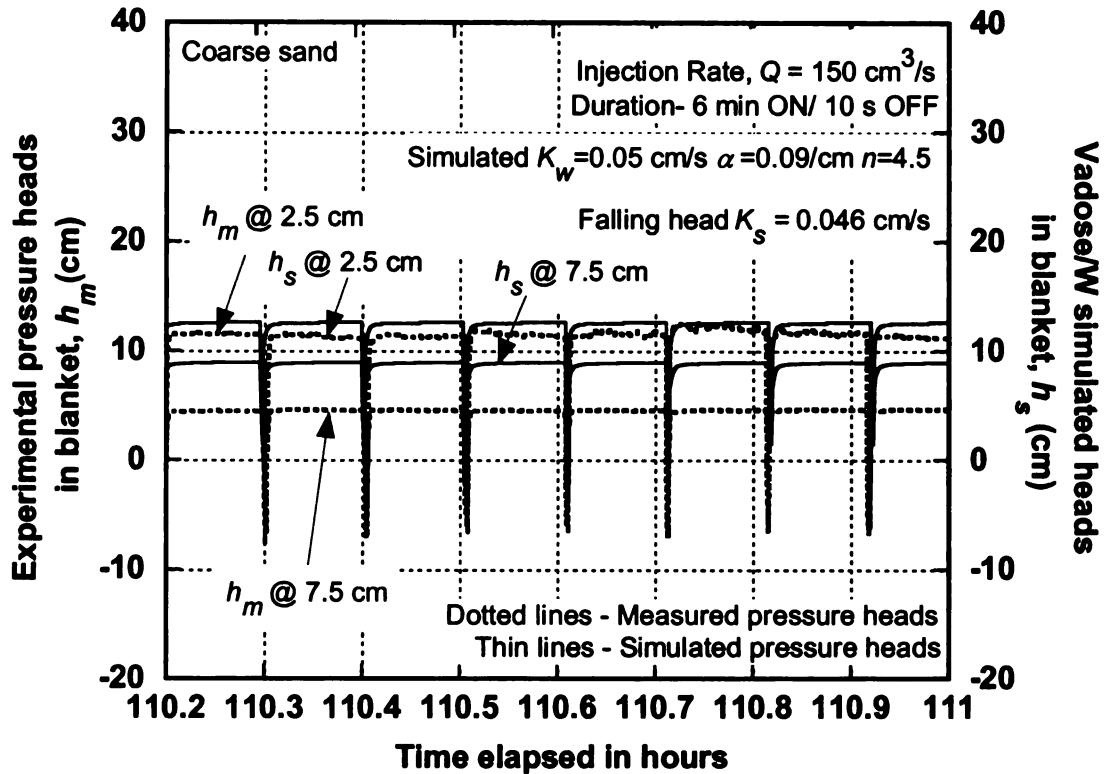


Figure 4-8: Estimation of hydraulic conductivity of underlying sand through inverse numerical simulation for 6 min on and 10 s off injection duration.

Tracer Test

Rosqvist & Bendz (1999) have used tracers in large-scale lab studies on waste. In this study, a tracer test was conducted in the fine sand to estimate the saturated hydraulic conductivity of the underlying soil. Before injecting the tracer test, the water was injected continuously into the blanket at a rate equal to $20 \text{ cm}^3/\text{s}$ for a considerable amount of time to obtain steady-state conditions (i.e. the inflow and outflow rates were equal and the readings from the pressure transducers in the blanket were steady). A non-reactive tracer, potassium chloride (KCl) dissolved in DI water to achieve 0.005 N solution was chosen for the tracer test. The tracer concentration in the system prior to the introduction

of the tracer was zero. The tracer was pumped from a 0.08 m³ capacity tank, where KCl had been dissolved, into the steady-state flow regime in the permeable blanket. Water samples for potassium chloride concentration analysis were collected from the LCS pipes. After the tracer was injected, samples were collected: (1) every 2 min till the estimated time of arrival of the front; and (2) every 5 min after the tracer pulse injection was stopped and DI water was pumped. The KCl concentration was measured with the help of an electrical conductivity meter. The tracer concentration in the system was expressed as a relative concentration, defined as C/C_0 , where C is the concentration in the discharge and C_0 is the original concentration in the injection pipe.

If it is assumed that the tracer moved through the soil with no mechanical dispersion or molecular diffusion, the tracer front will pass through as a slug. But in reality, mechanical dispersion and molecular diffusion occur and the breakthrough curve spreads out causing the tracer to appear in the outflow before the arrival of water traveling with average linear velocity. The measured breakthrough curve is shown in Figure 4-9. The arrival time for the tracer was about 34 min. The saturated hydraulic conductivity of the soil was calculated from advective seepage velocity using Equation 4-8:

$$K_{Tracer} = \frac{v_s \times n_e}{i} = \frac{D \times n_e}{t \times i} \quad (4-8)$$

where K_{Tracer} = average hydraulic conductivity of the porous medium between the blanket and LCS;

v_s = advective seepage velocity;

D = vertical depth of soil between the blanket and LCS;

t = breakthrough time;

n_e = effective porosity; and

i = hydraulic gradient.

The saturated hydraulic conductivity of the soil estimated from tracer test $K_{Tracer} = 0.0074$ cm/s agreed with the values from falling head test carried on the sand as shown in the Figure 4-9.

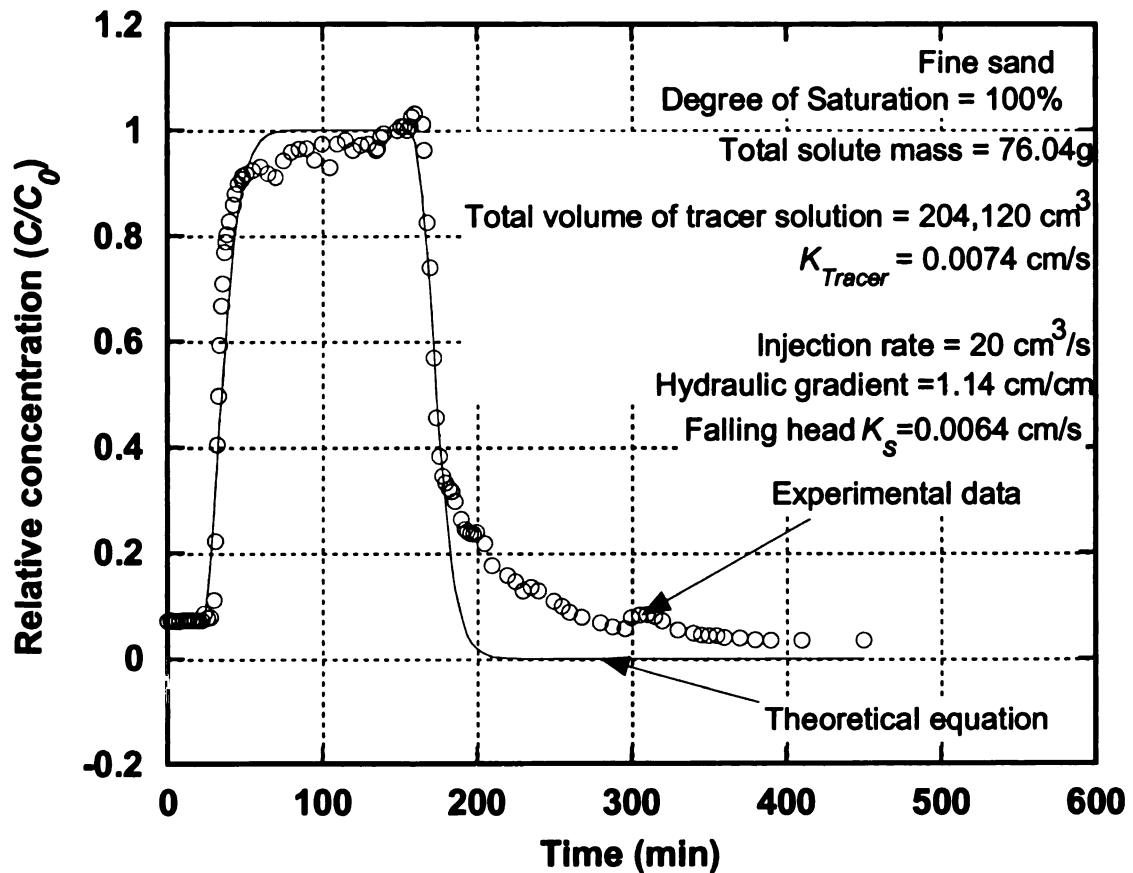


Figure 4-9: Breakthrough curve of tracer in fine sand.

The 1-D advection dispersion theoretical equation was fitted to the tracer pulse by performing the method of least squares as shown in Figure 4-9. The best fit dispersivity of the soil after optimization in MATLAB was determined to be 1.3 cm and the porosity as 0.42. The porosity found out from this optimization was in agreement with the porosity calculated from the dry density of the sand under the blanket. The relatively small value of dispersivity suggested that there was less mixing of the solute front as it advanced. The migration of water through the soil was mainly dominated by advection. Hence, hydraulic conductivity of the sand using advective flow of solute is relatively close to the value estimated using the falling head test.

Performance of ACRES Method

Figure 4-10 shows the hydraulic conductivity of fine sand measured using various methods. The hydraulic conductivities estimated using ACRES method were relatively close to the falling head tests. Figure 4-10 shows that with a significant increase in saturation from 60-100%, the hydraulic conductivity did increase in both falling head tests and in the ACRES method. However, the increases were relatively small.

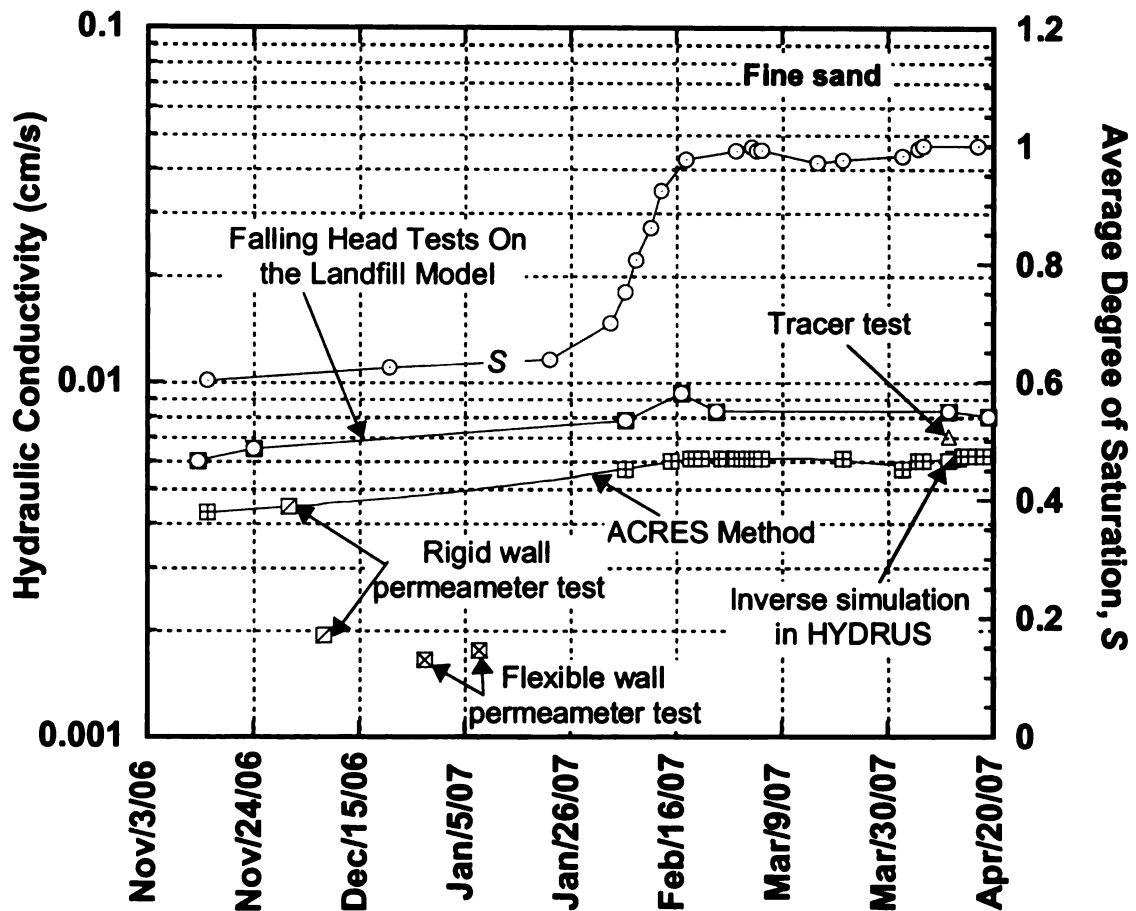


Figure 4-10: Correlation of the hydraulic conductivity values obtained from ACRES method, falling head tests, inverse numerical modeling, tracer tests and constant head permeameter tests.

In order to provide an explanation for the hydraulic conductivity values not increasing as rapidly as expected for increase in saturation, the hydraulic conductivity function using both Van Genuchten-Mualem and Fredlund *et al.* (1994) were compared. The Fredlund *et al.* method is generally more accurate for sandy soils (Fredlund *et al.* 1994). The Fredlund *et al.* (1994) method consists of developing the unsaturated hydraulic conductivity function by integrating along the entire curve of the volumetric water content function. Since the volumetric water content was curve-fit using Fredlund – Xing model in Vadose/W, the hydraulic conductivity function could also be predicted

over the entire suction range in Vadose/W. If the two models for hydraulic conductivity prediction function estimated from SWCC of sand are compared as shown in Figure 4-11, it is observed that the Fredlund-Xing model shows very little change in hydraulic conductivities as average degree of saturation increases from 60% to 100%. This explains the reason why the hydraulic conductivity values did not increase as rapidly when the degree of saturation increased from 60-100%.

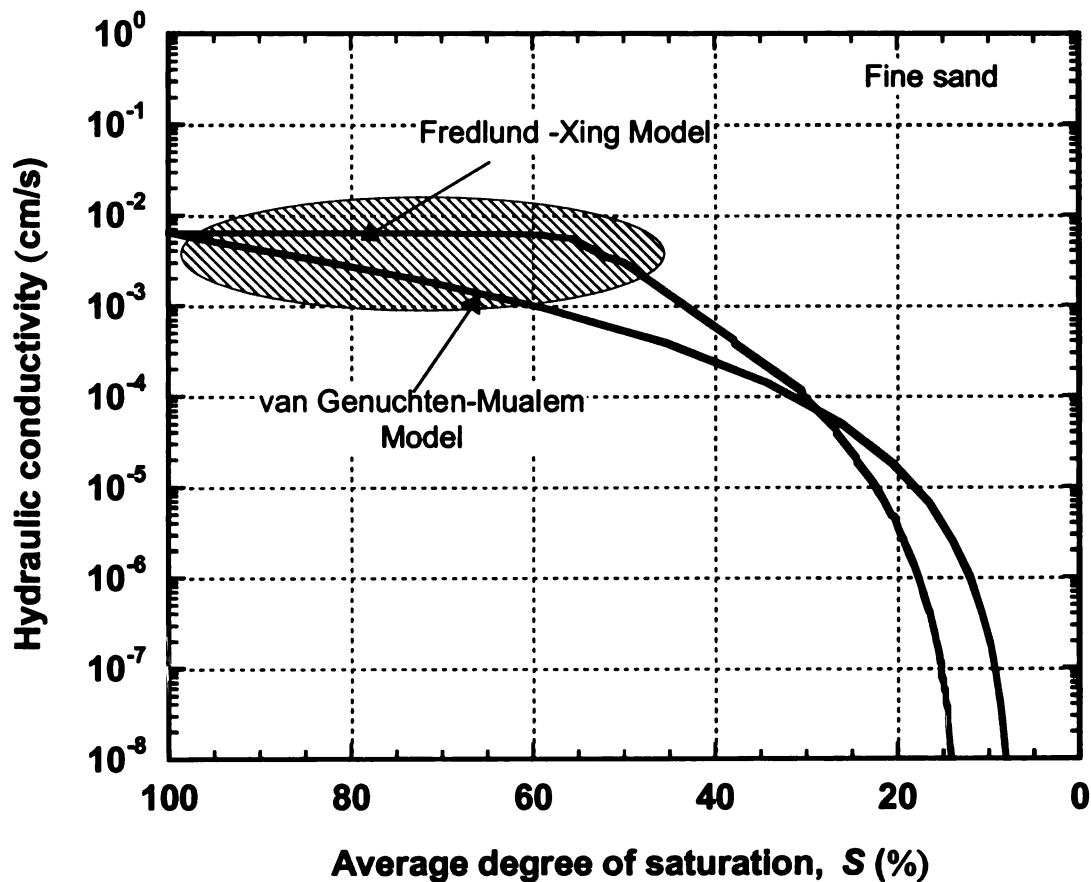


Figure 4-11: Hydraulic conductivity functions obtained from two models.

The hydraulic conductivities estimated from inverse numerical modeling and tracer test were close to those estimated from ACRES method. The sand when packed loosely in rigid walled permeameter, in a similar manner as it was done in the landfill

model. It yielded hydraulic conductivity that was same as that obtained from ACRES method as shown in Figure 4-10. On the other hand, when the sand was packed densely in the permeameter, which was done by compacting with a porcelain hammer, yielded lower hydraulic conductivities. This is because hydraulic conductivity decreases with density increases.

The hydraulic conductivities obtained from flexible walled permeameter were lower, almost in the same range as values obtained from densely packed sand in the rigid wall permeameter. Possible reason contributing to the lower values was that when sand sample was prepared in the flexible walled permeameter, vacuum was applied to hold the sample which most likely led to the densification of the sand.

Table 4-4 and Figure 4-10 shows that the hydraulic conductivities from ACRES method were relatively close to those estimated from falling head tests, constant head tests, inverse numerical modeling and tracer tests. Hence, the new approach of estimating hydraulic conductivity of underlying porous material presented in this study is appropriate.

Numerical Simulation of Field Application of ACRES Method

Simulations representing field-scale conditions were carried out and ACRES method was applied to the simulated pressure heads to develop a design framework to apply this method in the field to estimate field-scale hydraulic conductivities of waste. All field simulations were conducted in Vadose/W using the following parameters as input: (1) blanket width = 60 m; (2) blanket depth = 0.15 m; (3) initial degree of saturation of waste, $S = 75\%$; (4) vertical spacing between the blanket and LCS (D) = 15 m; (5)

saturated and unsaturated hydraulic properties of blanket, LCS and waste are those presented in Table 4-3.

Figure 4-12 presents the simulated wetted width W_w and average pressure head h_{av} in the 60-m-wide blanket for continuous injection rates varying from 300 m³/d to 700 m³/d. The wetted width W_w and average pressure head h_{av} increased with injection rates.

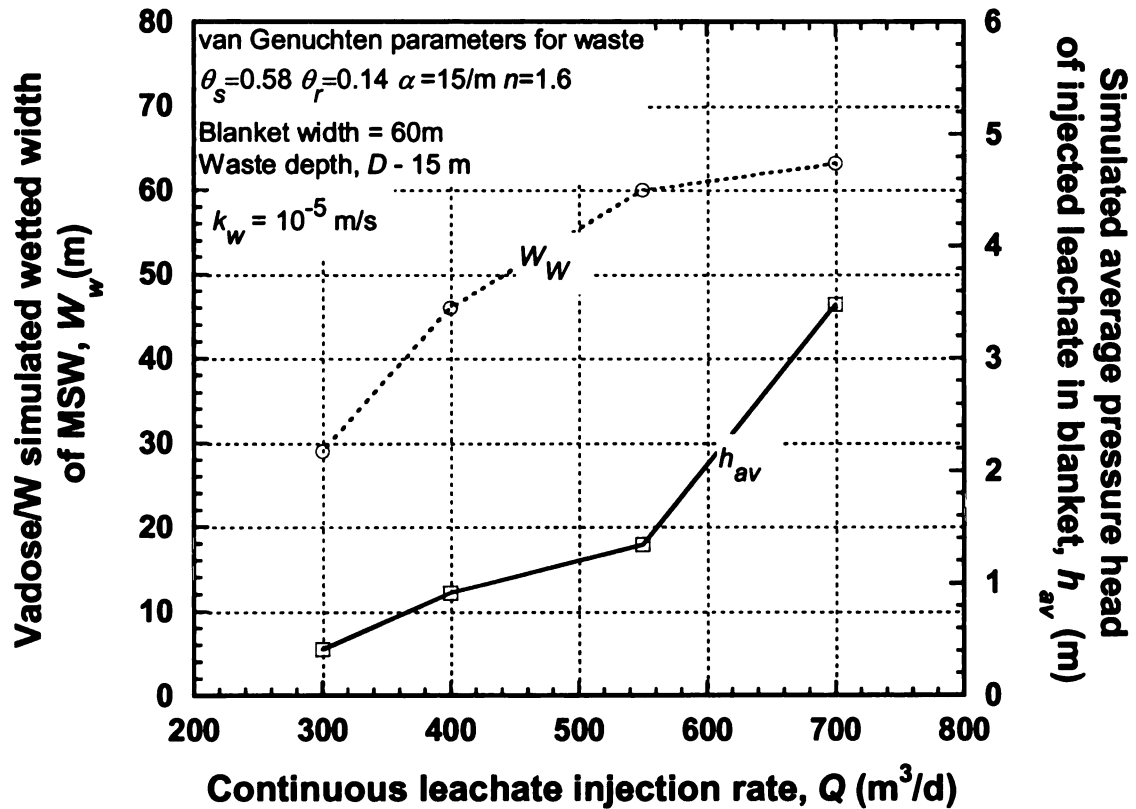


Figure 4-12: Simulated wetted width and average pressure heads of injected leachate in field-scale blanket for various continuous leachate injection rates.

Figure 4-12 shows that the simulated average pressure head (h_{av}) was 0.4 m throughout the leachate injection period for $Q = 300$ m³/d. This result is consistent with

the modeling results from Haydar and Khire (2007). The authors had used unsaturated properties of underlying material same as that of loam and used the numerical model HYDRUS-2D to simulate the flow of injected leachate using permeable blankets in bioreactor landfills. However, in this study soil water retention curves for MSW measured by Kazimoglu *et al.* (2005) were used. This shows that the unsaturated properties of underlying material are not critical for long term injection simulations, which is consistent with the findings of Haydar and Khire (2007). In addition, the results presented in Paper no. 3 show that HYDRUS and Vadose/W models yield the same results.

Once the injected leachate reached the 30-m-distance on either side of the blanket and saturated the entire blanket, h_{av} increased as the storage capacity of the blanket was exceeded. Figure 4-12 shows that simulated h_{av} was about 3.5 m for $Q = 700 \text{ m}^3/\text{d}$ compared to about 0.4 m for $Q = 300 \text{ m}^3/\text{d}$. The wetted width increased with increase in injection rates.

For a given injection rate Q and depth of waste (D), the hydraulic conductivity K_{ACRES} was estimated using Equation 4-6 with simulated values of W_w and h_{av} . The estimated hydraulic conductivities matched exactly with input waste hydraulic conductivity k_w of 10^{-5} m/s when the wetted width at steady-state was considered. The hydraulic conductivities were underestimated when the total blanket width was considered instead of the actual wetted width. This shows that if appropriate number of pressure sensors are placed in the blanket, the wetted width W_w can be defined relatively

accurately and that would lead to an accurate estimation of the field-scale hydraulic conductivity.

In order to reduce: (1) pore water pressure increase in the waste; (2) leachate breakouts; and (3) liquid pressure heads on the liner resulting in possible slope instabilities, leachate is not continuously injected in landfills. Instead, leachate is injected in on/off dosing cycles. The dosing volume and frequency for leachate injection may vary depending on the daily leachate generation volume and the operational needs of the landfill.

The effect of dosing frequencies for injection rates, $Q = 400 \text{ m}^3/\text{d}$, $Q = 550 \text{ m}^3/\text{d}$ and $Q = 700 \text{ m}^3/\text{d}$ on W_w , h_{av} and hence on K_{ACRES} was evaluated by simulating leachate injection for 2 hours on/22 hours off, 4 hours on/20 hours off, and 8 hours on/16 hours off. Figure 4-13 presents the effect of various dosing frequencies on h_{av} for $k_w = 10^{-5} \text{ m/s}$ and when the initial degree of saturation, S of the waste was 75%. The pressure heads, h_{av} reported in Figure 4-13 were those obtained when the system reached a dynamic equilibrium, a quasi steady-state. The magnitude of h_{av} was a function of the on to off duration ratio. Greater the on to off duration ratio, greater was the magnitude of h_{av} . The wetted width W_w was also a function of the ratio of on to off leachate injection duration. The wetted width of waste was greater for a dosing cycle where the on to off duration ratio was greater.

Because h_{av} , W_w and the outflow increased with increase in on to off duration ratio, the ratio of K_{ACRES}/k_w also increased approaching constant value. For $Q = 400$

m^3/d , the ratio of K_{ACRES}/k_w was 0.24 for 2 hours on/22 hours off which increased to 0.83 for 8 hours on/16 hours off. For $Q = 550 \text{ m}^3/\text{d}$, the ratio of K_{ACRES}/k_w was 0.41 for 2 hours on/22 hours off which increased to 0.96 for 8 hours on/16 hours off. For $Q = 700 \text{ m}^3/\text{d}$, the ratio of K_{ACRES}/k_w was close to 1 and did not differ significantly with the injection frequencies. The wetted width W_w for $Q = 700 \text{ m}^3/\text{d}$ was greater than the blanket width for all the dosing frequencies. However, for estimation of K_{ACRES} , the W_w was assumed equal to the blanket width because it would be difficult to estimate the wetted width in the waste in absence of instrumentation in the waste. Figure 4-13 shows that, in order to estimate k_w accurately, either leachate needs to be injected continuously to achieve steady-state or injected at the highest possible injection rate and highest on to off dosing ratio.

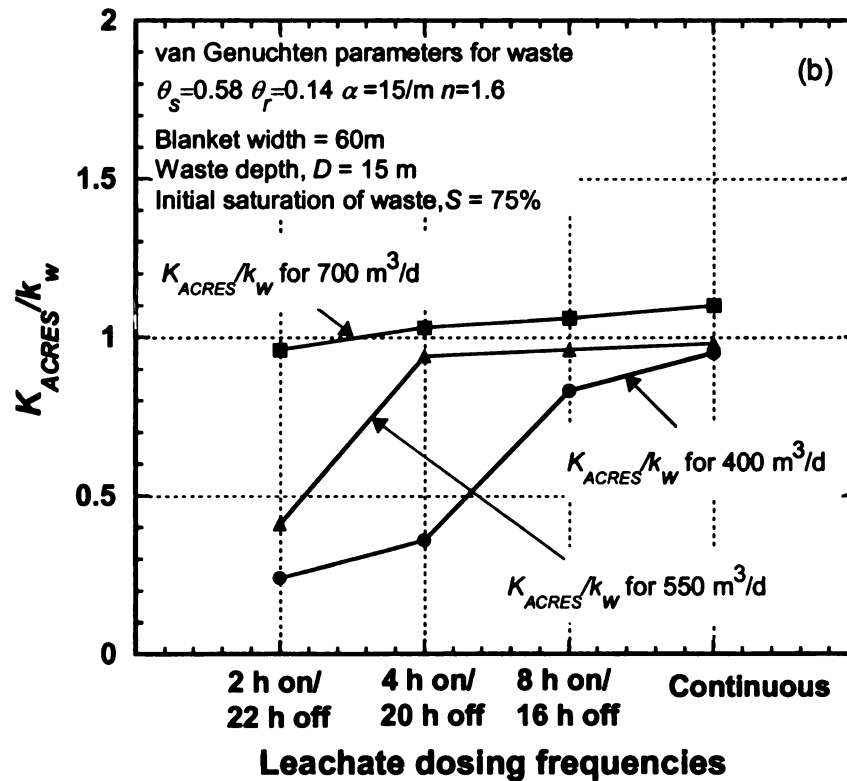
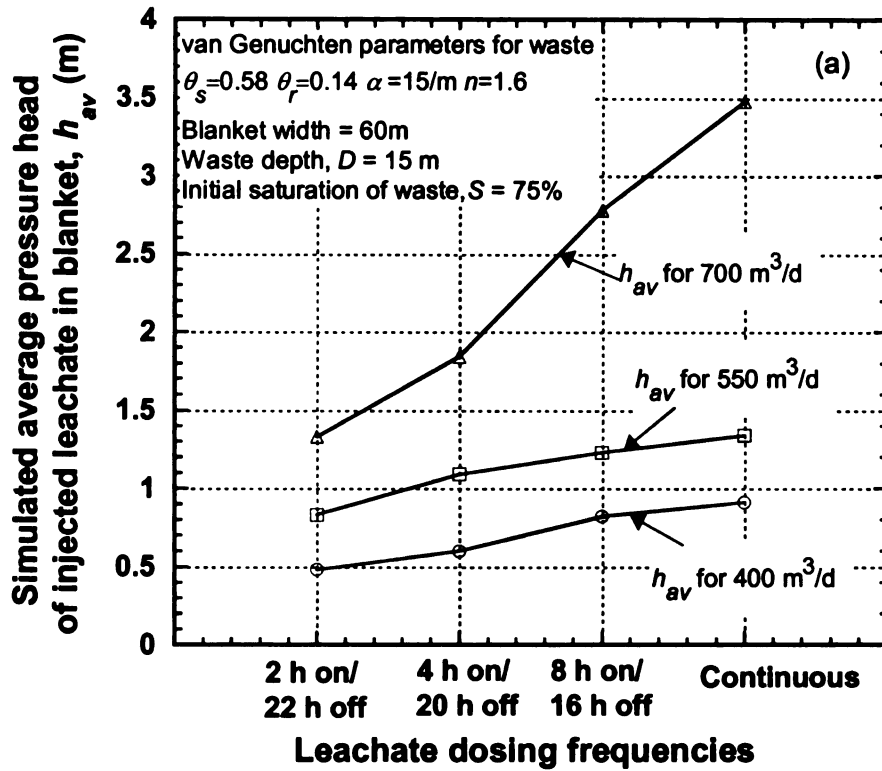


Figure 4-13: For different injection rates and dosing frequencies: simulated average pressure heads in the blanket (a); the ratio of K_{ACRES}/k_w (b).

In order to better understand the variation of the ratio of K_{ACRES}/k_w for different injection rates and dosing frequencies, it is important to know the degree saturation of the waste. Figure 4-14 shows the water content profiles along the depth of the waste below the blanket due to injection rates $Q = 400 \text{ m}^3/\text{d}$ and $Q = 550 \text{ m}^3/\text{d}$ and injection frequencies of 2 hours on/22 hours off, 4 hours on/20 hours off, and 8 hours on/16 hours off.

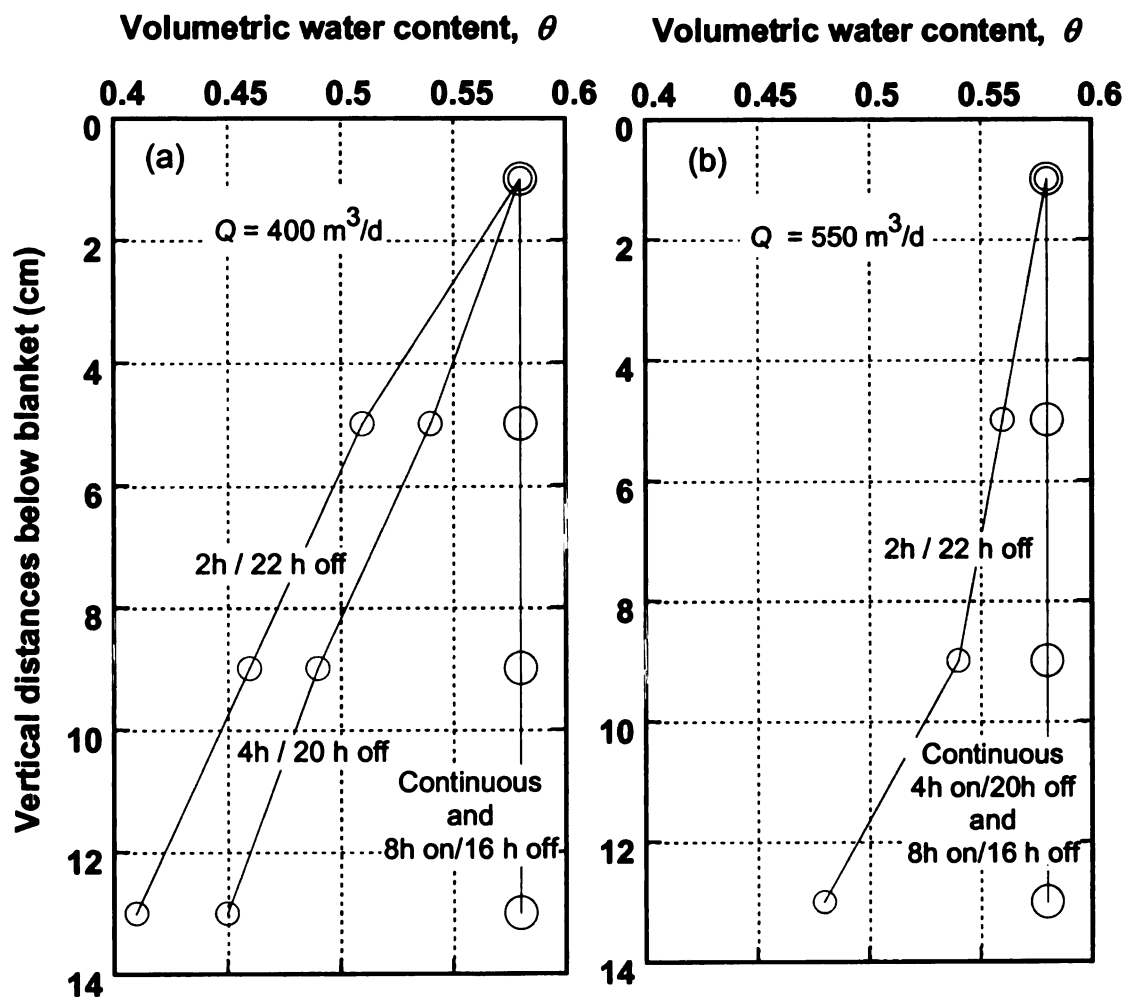


Figure 4-14: Transient water content profiles in waste due to injection rates at: (a) $400 \text{ m}^3/\text{d}$; and (b) $550 \text{ m}^3/\text{d}$.

Figure 4-14 shows that for lower injection rate and lower injection duration, the waste was unsaturated in the deeper region of the waste vertically below the blanket which resulted in lower values of K_{ACRES}/k_w as observed in Figure 4-13. As injection rate or injection duration were increased, due to greater amount of liquid being injected resulted in a greater depth of waste getting saturated leading to an increase in the ratio of K_{ACRES}/k_w closer to unity.

Irrespective of the initial degrees of saturation of the waste, the maximum h_{av} and W_w remained unchanged after a few days (long-term) of leachate dosing for a given value of Q and dosing frequency. It took progressively longer time to reach the maximum W_w for lower values of initial average degree of saturation. Figure 4-15 shows that the system reached equilibrium in a shorter time when the initial saturation was 75% compared to when the initial saturation was 40%. This finding is consistent with results presented by Haydar and Khire (2007).

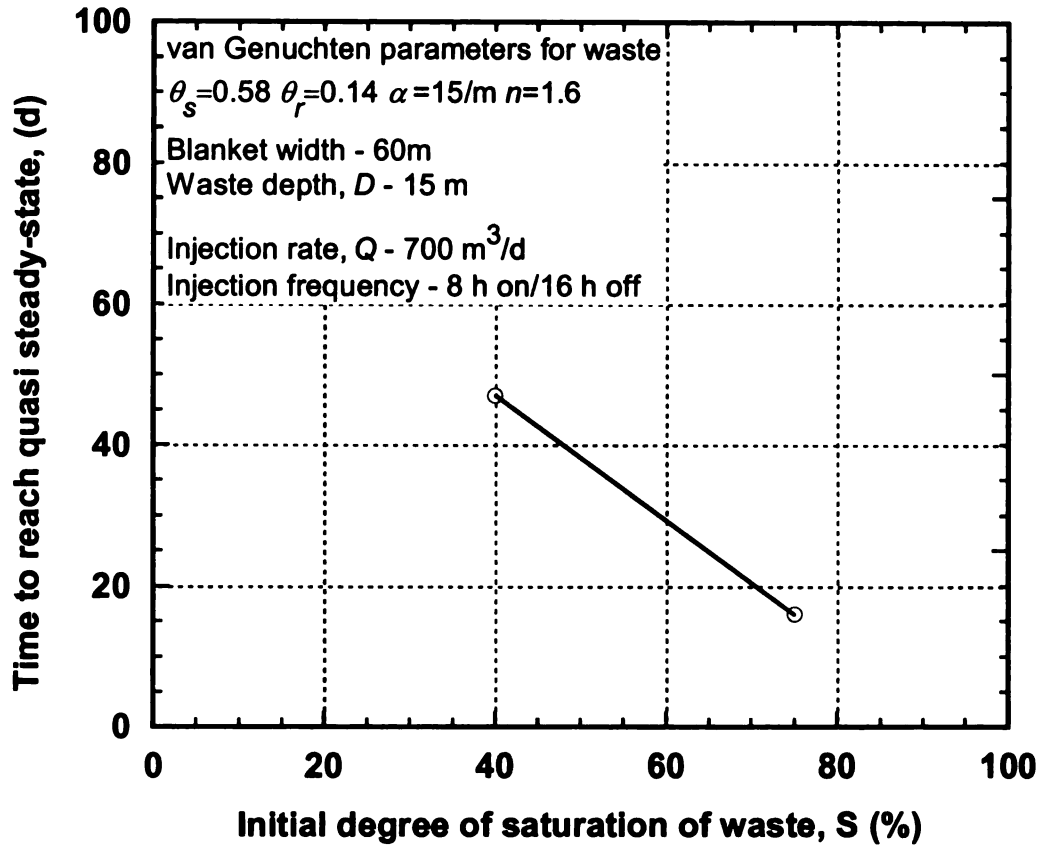


Figure 4-15: Simulated time to reach quasi steady-state as a function of the initial degree of saturation of waste (S).

Effect of Anisotropy Ratio

The deposition and compaction of waste and construction of operational components such as gas wells and daily and intermediate soil covers, lead to anisotropy and layered heterogeneity within a landfill. The horizontal hydraulic conductivity of landfilled waste has been reported to be greater than the vertical hydraulic conductivity (Powrie and Beaven 1999). The effect of anisotropy on the ratio of K_{ACRES}/k_w was evaluated by simulating continuous injection rate at $Q = 400 \text{ m}^3/\text{d}$ for various ratios of anisotropy. The vertical hydraulic conductivity K_y was kept fixed at 0.001 cm/s and the horizontal

hydraulic conductivity K_x was varied according to the anisotropy ratio K_y/K_x . Figure 4-16 shows that the anisotropy ratio has no effect on K_{ACRES}/k_w and on the average pressure heads in the blanket. This is because a blanket acts as an engineered heterogeneity and reduces the effect of spatial variation of waste properties when wetting the waste resulting in a relatively uniform distribution of leachate vertically in the landfill. The wetting is essentially governed by the hydraulic conductivity in the vertical direction even if the horizontal hydraulic conductivity is greater and hence the anisotropy ratio was found to have no effect on K_{ACRES}/k_w and on the average pressure heads in the blanket.

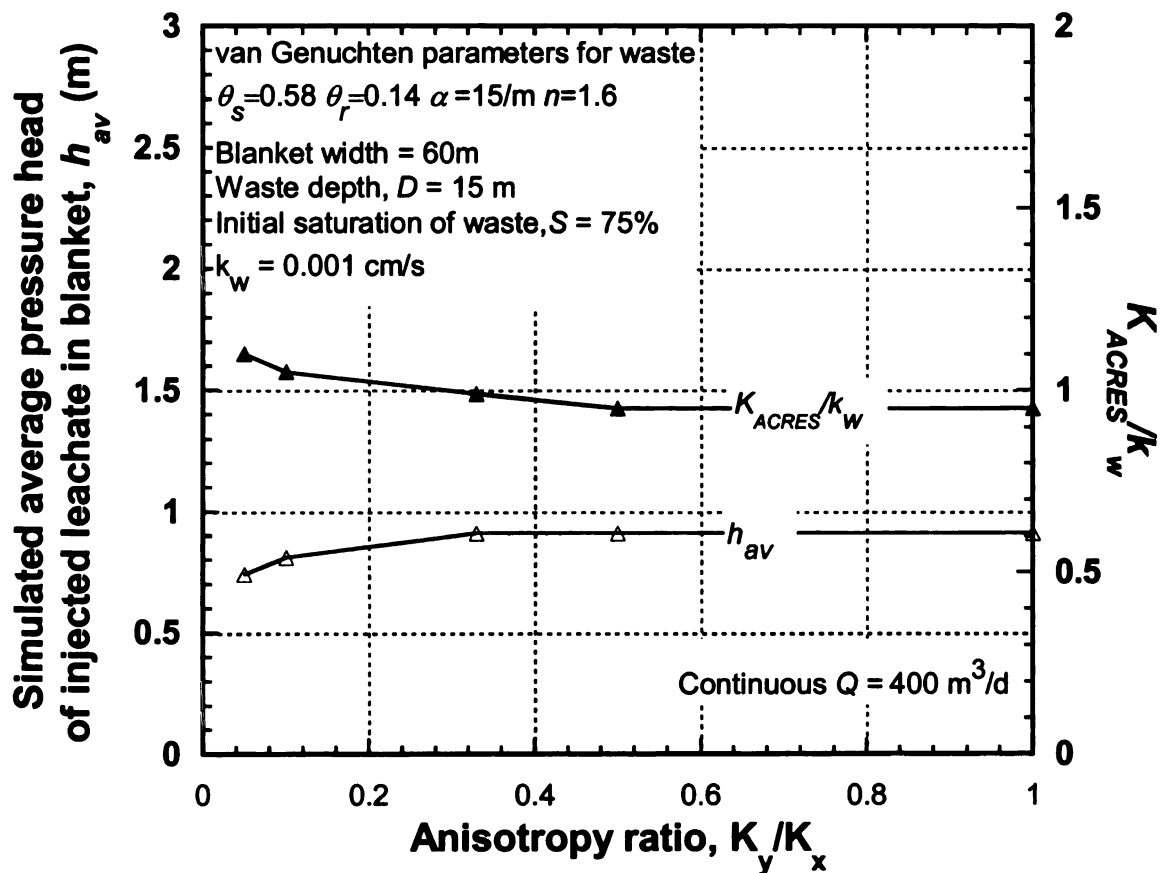


Figure 4-16: Effect of anisotropy ratio on the ratio of K_{ACRES}/k_w .

Effect of Unsaturated Properties of Waste

The effect of unsaturated properties of the waste on K_{ACRES}/k_w was explored. Figure 4-17 shows the soil water characteristics curves for waste reported by Kazimoglu *et. al* (2005) and Benson and Wang (1998). These unsaturated properties were used separately in the simulations to compare the average pressure heads developed in the blanket and the wetted widths due to various injection dosing frequencies.

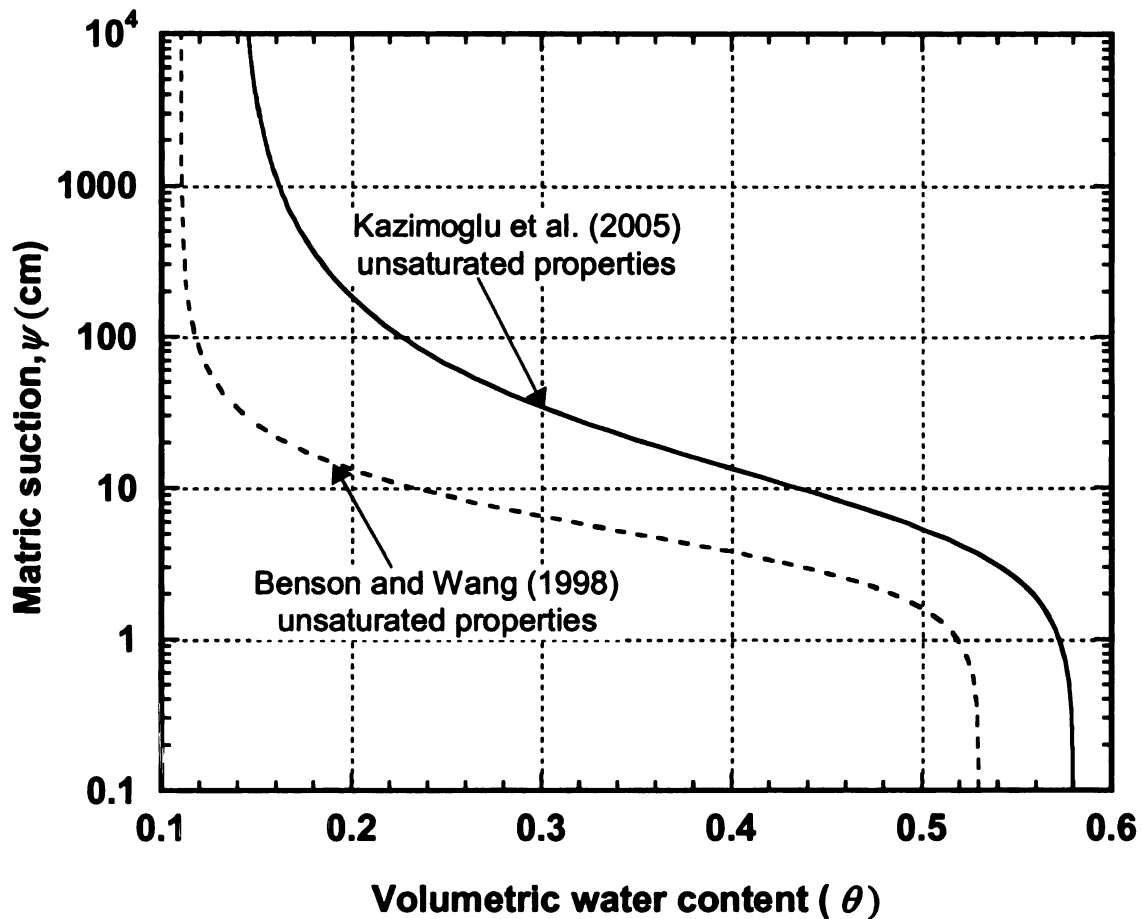


Figure 4-17: Soil water characteristics of waste.

Figure 4-18 shows the effect of unsaturated properties on the average pressure heads developed in the blanket and henceforth on the ratio of K_{ACRES}/k_w due to dosing

frequencies of 2 hours on/22 hours off, 4 hours on/20 hours off and 8 hours on/16 hours off.

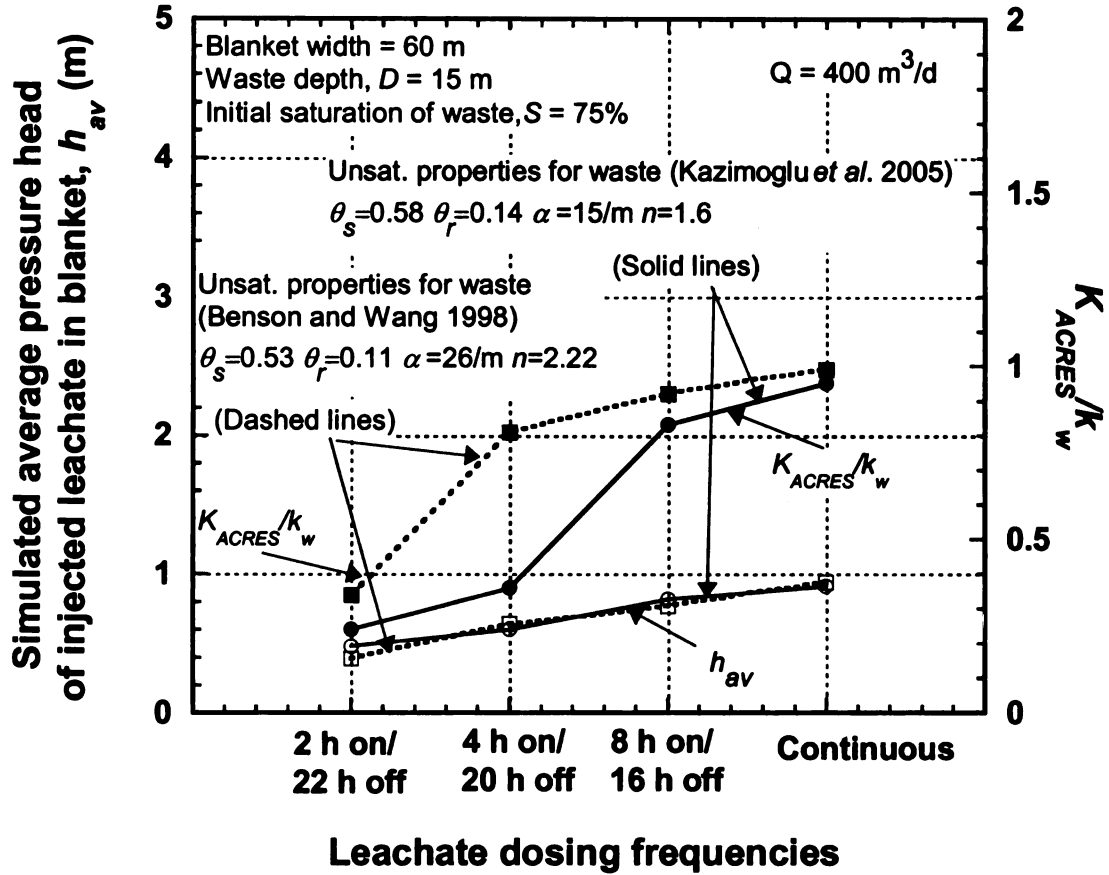


Figure 4-18: Effect of unsaturated properties of waste on the ratio of K_{ACRES}/k_w .

The unsaturated properties were observed to have negligible effect on the average pressure heads in the blanket. The ratio of K_{ACRES}/k_w for the two sets of unsaturated properties increased gradually with the increase in injection duration but they were different at lower on to off ratios of dosing. This was because although the average pressure heads are same for the two sets of unsaturated properties, the wetted widths W_w were different at the same dosing frequency. Hence, the unsaturated properties influence

the estimation of k_w at lower on to off ratios of dosing. The unsaturated properties have no effect on the pressure heads for continuous injection which is consistent with the findings of Haydar and Khire (2007).

LIMITATIONS

The method for estimating vertical hydraulic conductivity described in this study worked well in the laboratory. However, its feasibility for usage as a field method needs to be explored in the challenging environment of landfills by carrying out field-scale research in real world landfills. The limitations associated with this method are presented as follows:

1. A limitation of this method is that it is dependent on sensors working properly in the corrosive environment of landfills.
2. A limitation of Darcy's law relates to the scale of the flow system. On a landscape scale where the waste is heterogeneous and may include domains of both laminar and turbulent flows in varying directions and tortuosities, Darcy's law may not be applicable. However, the prevailing approach for modeling water flow processes in solid waste media relies on the assumption of a homogeneous porous media (e.g. Straub and Lynch 1982; Schroeder *et al.* 1984 in HELP model; Korfiatis *et al.* 1984). The conventional standard aquifer pump tests, borehole permeameter tests, Zaslavsky's method used in reported field studies also assumed waste to be homogeneous and isotropic porous medium. The numerical studies on design of subsurface LRS are also based on the assumption of homogeneous and isotropic porous medium (Haydar and Khire 2007; Khire and Mukherjee 2007). Hence

applicability of ACRES method may be reasonable when overall performance of the system is modeled or analyzed.

3. MSW consists of a heterogeneous mix of materials, particle sizes, and moisture contents. Although compaction partially opens, flattens, and orients the objects in the horizontal direction, large pore spaces still exist which act as interceptors of horizontal and vertical flow channels. Due to the presence of relatively large size particles and particle size variation in MSW, flow channels form in interconnected macropores and lead to the rapid discharge of large leachate volumes. With continued infiltration, channeled discharge continues, but a fraction of infiltration either enters directly or slowly redistributes from the channels into the dense matrix sections of waste through head and capillary pressure differences. Research efforts have developed preliminary information on preferential flow paths in MSW (Zeiss and Major 1992; Zeiss and Uguccioni 1994; Zeiss and Uguccioni 1997). This preferential flow and leachate channeling will have a profound effect on the leachate pressure heads in the blanket and hence on the conductivity estimations.
4. In the landfill model, the pore air pressure due to entrapped air bubbles had a significant effect on the pressure heads. Similarly, the gas produced due to biodegradation in real landfills would be expected to influence the measured pressure heads and hence will impact the hydraulic conductivity estimates.

Hence, all the limitations listed above warrant further research to be carried out for the applicability of this method in real landfills.

SUMMARY AND CONCLUSIONS

The key objective of this study was to estimate hydraulic conductivity of underlying sand using pressure head and flow data from an instrumented permeable blanket in a lab-scale landfill model. Experiments were carried out in a laboratory scale instrumented landfill model. Pressure heads in the blanket due to liquid injection were measured using an automated sensing system consisting of pressure sensors. The degree of saturation of the sand underlying the blanket was measured using water content sensors. The key conclusions of this study are as follows:

- The hydraulic conductivity of the sand underlying the blanket can be estimated by using an analytical approach based on Darcy's law using these parameters: (1) length of blanket; (2) injection rate; (3) depth of waste between the blanket and LCS; (4) liquid pressure heads developed in blanket; and (5) achieved wetted width due to injection.
- The hydraulic conductivity of porous material underlying the blanket can also be estimated through inverse numerical modeling. Except the hydraulic conductivity of waste, other parameters either need to be known (e.g., rate, duration, and frequency of liquid injection) or can be measured in the lab (e.g., hydraulic properties of materials used for blanket). The hydraulic conductivity can be estimated by inverse numerical simulation by matching the measured pressure heads in the blanket.
- The hydraulic conductivities estimated using the ACRES method were relatively close to independently determined conductivities from falling head tests and tracer tests.

- The hydraulic conductivity estimated using the ACRES method is potentially applicable to field scale application where leachate is pumped continuous or in on/off cycles. When leachate is injected in on/off dosing cycles, W_w and h_{av} are directly proportional to the on to off duration ratio and the magnitude of the liquid flux during the on period.
- The hydraulic conductivity estimated using the ACRES method for lower injection rate and lower injection duration was lower than the saturated hydraulic conductivity. This is because the waste was unsaturated in the deeper region of the waste vertically below the blanket. With increase in injection rate or with injection duration, due to the greater amount of liquid being injected, resulted in a greater thickness of waste being saturated leading to the value of K_{ACRES} closer to directly measured saturated hydraulic conductivity.
- Waste anisotropy has no effect on the ACRES estimated hydraulic conductivity.
- The unsaturated properties influence ACRES estimated hydraulic conductivity at lower on to off ratios of dosing. The unsaturated properties of soil underlying the blanket have no effect on the hydraulic conductivity estimations as long as the rate of injection and frequency of dosing are relatively high.
- Further research is needed for potential usage of the ACRES method as a new field scale method for bioreactor landfills.

PAPER NO. 5: INSTRUMENTED PERMEABLE BLANKET FOR ESTIMATION OF HYDRAULIC CONDUCTIVITY OF HETEROGENEOUS SUBSURFACE

ABSTRACT

An instrumented lab-scale physical model of a landfill with permeable blanket as liquid recirculation system was developed to test the Analysis of Conductivity in Real-time using Embedded Sensors (ACRES) method with a heterogeneous porous medium underlying the blanket. The model was approximately 85 cm long x 30 cm wide x 55 cm high. A 2-cm-thick horizontal permeable blanket made up of pea gravel having saturated hydraulic conductivity of about 2 cm/s was built in the landfill model for subsurface liquid injection. The soil below the blanket was simulated as structured heterogeneous matrix consisting of block shaped regions comprised of fine, coarse and driller sands. The blanket and the sandy soils below the blanket were instrumented with embedded sensors consisting of pressure transducers and time domain reflectometry (TDR)-based water content sensors connected to a datalogger, to monitor the migration of injected liquid in the blanket and in the sands. Liquid injections in the blanket were carried out at varying rates either continuously or in on/off mode using a magnetic drive pump. The injected flow rate was monitored by flow sensor. The key objective of this paper was to study the effect of heterogeneity on the hydraulics of subsurface flow in landfills and compare it with homogeneous sand. The finite element model HYDRUS-2D was used to predict the measured pressure heads and increase in water content in the sands and the blanket due to liquid injection. The vertical hydraulic conductivity of the underlying sand was estimated using ACRES and was independently verified by carrying out falling head tests on the model and analytical equations for stratified soils. Finally, field-scale simulations were

carried out and ACRES method was applied to the simulated pressure heads to develop a design framework to apply this method in the field considering a large scale structured heterogeneous waste domain with different configurations of placements of daily cover soil layers.

INTRODUCTION

Leachate recirculation or liquid injection in bioreactor landfills can be performed using multiple techniques, both surface and subsurface. The surface methods consist of spraying leachate over the landfill surface area or constructing leachate pond. The conventional subsurface application techniques are: (1) vertical wells; (2) horizontal trenches; and (3) permeable blankets. The subsurface systems are advantageous than surface systems as liquids can be added at higher flow rates and can be operated at higher pressure. The liquid injection pressures depend heavily on hydraulic conductivity of waste (Khire and Mukherjee 2007). Hence hydraulic conductivity is the key design and operational parameter for liquid recirculation systems.

Waste materials in landfills differ widely in type, composition, consistency and state of biochemical decay. Typical examples for different waste materials are municipal waste, excavated soil, construction material debris, sludges etc. showing large variations in type and properties of its constituents. Hence, the properties of landfill waste such as moisture content, and porosity distribution are randomly distributed over the entire landfill. The deposition and compaction of waste and construction elements like gas wells and daily and intermediate soil covers, leads to anisotropy and layered heterogeneity within a landfill. This results in significant heterogeneity and anisotropy in the hydraulic properties of the landfilled municipal solid waste. For example, Ettala (1987) from field

studies reported variation in hydraulic conductivity in different parts of the same landfill. Thus, spatial variations in hydraulic conductivity are abundant in a typical municipal solid waste landfill.

The spatial variation of hydraulic conductivity in landfill causes non-uniform wetting of MSW due to leachate recirculation (McCreanor and Reinhart 2000; Haydar and Khire 2004). Among the subsurface leachate recirculation systems, the permeable blankets owing to its relatively high transmissivity essentially distribute the injected leachate relatively uniformly and fast within the blanket resulting in a relatively uniform impingement of leachate within the waste and hence reduces the effect of spatial variation of waste properties when wetting the waste (Haydar 2005).

Analysis of Conductivity in Real-time using Embedded Sensors (ACRES)

Haydar and Khire (2006, 2007) had developed the permeable blanket leachate recirculation system as an alternative to the conventional leachate recirculation methods. Haydar and Khire (2006) instrumented field-scale permeable blankets to demonstrate the hydraulic performance of permeable blankets for bioreactor landfills. They studied the feasibility of using an automated geotechnical sensing system consisting of water content, temperature and pressure sensors to monitor the migration of recirculated leachate in permeable blankets.

The inert permeable blanket if instrumented can be used as a platform to estimate the field-scale vertical hydraulic conductivity of waste in real-time which may eliminate the need to place sensors in waste. Due to relatively high transmissivity of the blanket, the sensors embedded in the blanket measure regional or average conditions within the landfill which are more representative of the overall average condition. Hence, the use of

an instrumented permeable blanket was explored to measure the in-situ vertical hydraulic conductivity of waste. In order to use the instrumented permeable blanket as a source for estimation of hydraulic conductivity, the hypothesis was tested in the laboratory.

OBJECTIVES

The key objective of this study was to develop a method for estimation of in-situ vertical hydraulic conductivity of subsurface heterogeneous soils or waste in a landfill underlying an instrumented blanket by analyzing data obtained from sensors embedded in the blanket. A laboratory-scale physical model of MSW landfill was developed to conduct controlled lab tests in order to independently verify the proposed method. The structured heterogeneous sand comprised of homogeneous blocks of fine sand (OK 110 silica sand), coarse sand (Ottawa sand) and driller sand. The lab model had sensors embedded in each block of sand underlying the blanket.

Materials and Methods

Figure 5-1 presents a schematic of the fabricated landfill model. All acrylic panels of the model were screwed together with rubber seals in-between the panels to provide a watertight box to contain the soils subjected to injection of water. A silicone sealant was applied at the seams to prevent potential leakage. A separate acrylic panel was used to make the bottom of the leachate collection system (LCS) raised to a fixed slope of 3%.

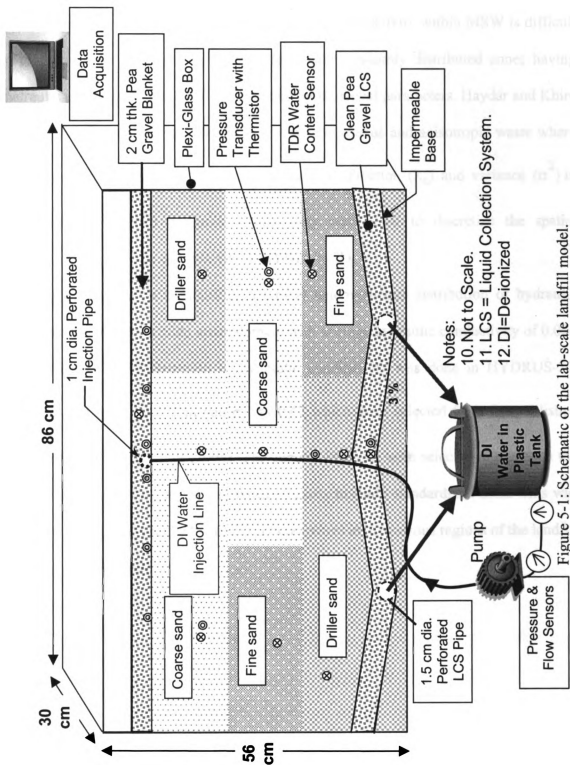


Figure 5-1: Schematic of the lab-scale landfill model.

Representation of Heterogeneity

The exact nature of random variations in hydraulic conductivity within MSW is difficult to predict but landfills can be assumed to contain randomly distributed zones having hydraulic properties that can be characterized by statistical parameters. Haydar and Khire (2004) carried out numerical simulations of heterogeneous and anisotropic waste where correlation lengths in the lateral (λ_x) and vertical direction (λ_z) and variance (σ^2) in lognormally distributed hydraulic conductivity were used to discretize the spatial distribution of hydraulic conductivity in HYDRUS-2D.

Figure 5-2 shows contours of a typical heterogeneous distribution of hydraulic conductivities in a 50 m wide waste domain with average hydraulic conductivity of 0.001 cm/s. The spatial discretization of hydraulic conductivity was done in HYDRUS-2D using λ_x as 2 m, λ_z as 0.5 m and σ^2 as 0.42 which were selected from the published studies of Haydar and Khire (2004). The contour intervals were selected to represent the hydraulic conductivities of various types of geotechnically standardized soils. This was done in order to compare the hydraulic conductivities in the various regions of the landfill with the classified soils.

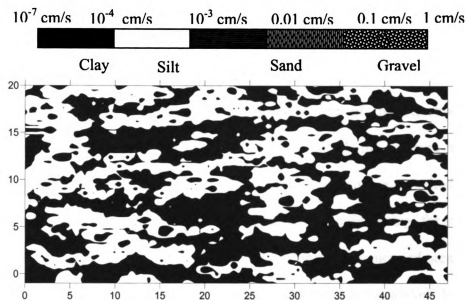


Figure 5-2: Typical spatial distribution of hydraulic conductivities with stochastic parameters: $\lambda_x = 2$ m, $\lambda_z = 0.5$ m and $\sigma^2 = 0.42$.

Because the key objective was to study the effect of heterogeneity on the pressure heads in the blanket due to liquid injection, any such realization created with stochastic parameters as shown in Figure 5-2 to represent a heterogeneous porous medium in the landfill model, would create much difficulty in understanding the hydraulic processes and in applying deterministic mathematical equations to such heterogeneous systems. Therefore, an alternative approach in the form of structured heterogeneity to characterize a heterogeneous porous medium was sought.

In order to allow better hydraulic characterization, relatively homogeneous and isotropic sands which differed in hydraulic conductivities by orders of magnitude were used to simulate a “structured heterogeneous” material. The configuration for structured heterogeneous porous media as shown in Figure 5-1 was made based on preliminary numerical modeling considering these factors: (1) continuous layer of fine soil was avoided because it produced relatively high pressure heads in the blanket which exceeded

the dimensions of the model; (2) the chosen configuration of the sands generated pressure heads which were within the dimensions of the model; (3) the flow rate to be injected in the chosen configuration of the sands was same as one of the injection rates in homogeneous sand so that the results could be compared; (4) the pressure heads were large enough for measurement using the pressure sensors for various magnitudes of rates of liquid injection, duration of injection, and frequency of liquid dosing, for steady-state as well as transient conditions; and (5) the chosen configuration generated pressure heads which were different on either side of the injection pipe due to random locations of blocks of sand with different hydraulic conductivities.

Materials

Table 5-1 shows the hydraulic characteristics of the soils used in the landfill model. The blanket and the LCS were made up of pea gravel. Pea gravel was chosen as LCS drainage material because it results in relatively low liquid heads in LCS (Khire and Mukherjee 2007) and it was also considered as a blanket material in the studies of Haydar and Khire (2007) and Khire and Haydar (2003). The heterogeneous sand was composed of blocks of three kinds of homogeneous sands - uniform OK110 sand (fine sand), uniformly graded Ottawa sand (coarse sand) and driller sand. The Ottawa sand was ASTM graded sand conforming to ASTM C778. The driller sand was quartz sand pack typically used for monitoring wells, water wells, underdrains etc. The average particle size (D50) for the three sands were 0.011 cm, 0.035 cm and 0.06 cm respectively.

Table 5-1: Saturated and unsaturated hydraulic properties of soils used in the landfill model.

Soil Type	Simulated unit	Saturated hydraulic conductivity, K_s (cm/s)	Unsaturated hydraulic properties represented by van Genuchten fitting parameters			
			θ_s	θ_r	α (1/cm)	n
Fine sand	Block in structured heterogeneity	0.0064	0.42	0.03	0.02	6.5
Coarse sand	Block in structured heterogeneity	0.06	0.4	0.03	0.090	4.5
Driller sand	Block in structured heterogeneity	0.55	0.45	0.2	0.15	7.5
Pea Gravel	Blanket and LCS	2	0.43	0.01	0.45	3

Note: LCS- Leachate Collection System

θ_s = saturated volumetric water content [dimensionless];

θ_r = residual volumetric water content [dimensionless]; and

α [1/L] and n are van Genuchten's fitting parameters (van Genuchten 1980)

Saturated Hydraulic Conductivity

The saturated hydraulic conductivities of fine and coarse sand presented in Table 5-1 were obtained from the falling head tests carried out in the landfill model when these sands were packed separately as homogeneous sands in previous experiments. The reported saturated hydraulic conductivity for driller sand was the average value obtained from triplicate tests using a rigid wall permeameter (ASTM D 2434-68) using Mariotte bottle in a constant head test.

Soil-Water Characteristic Curves

The relationship between volumetric water content and matric suction of fine sand, coarse sand, driller sand and pea gravel was obtained through a hanging column experimental setup comprised of Buchner funnel with porous ceramic plate (ASTM D 6836-02). The experiments for determining the SWCCs for all soils were repeated twice. The drying soil water characteristic curves of all the soils were described in terms of the van Genuchten (van Genuchten 1980) fitting equation and are illustrated in Figure 5-3. The fitting parameters are tabulated in Table 5-1.

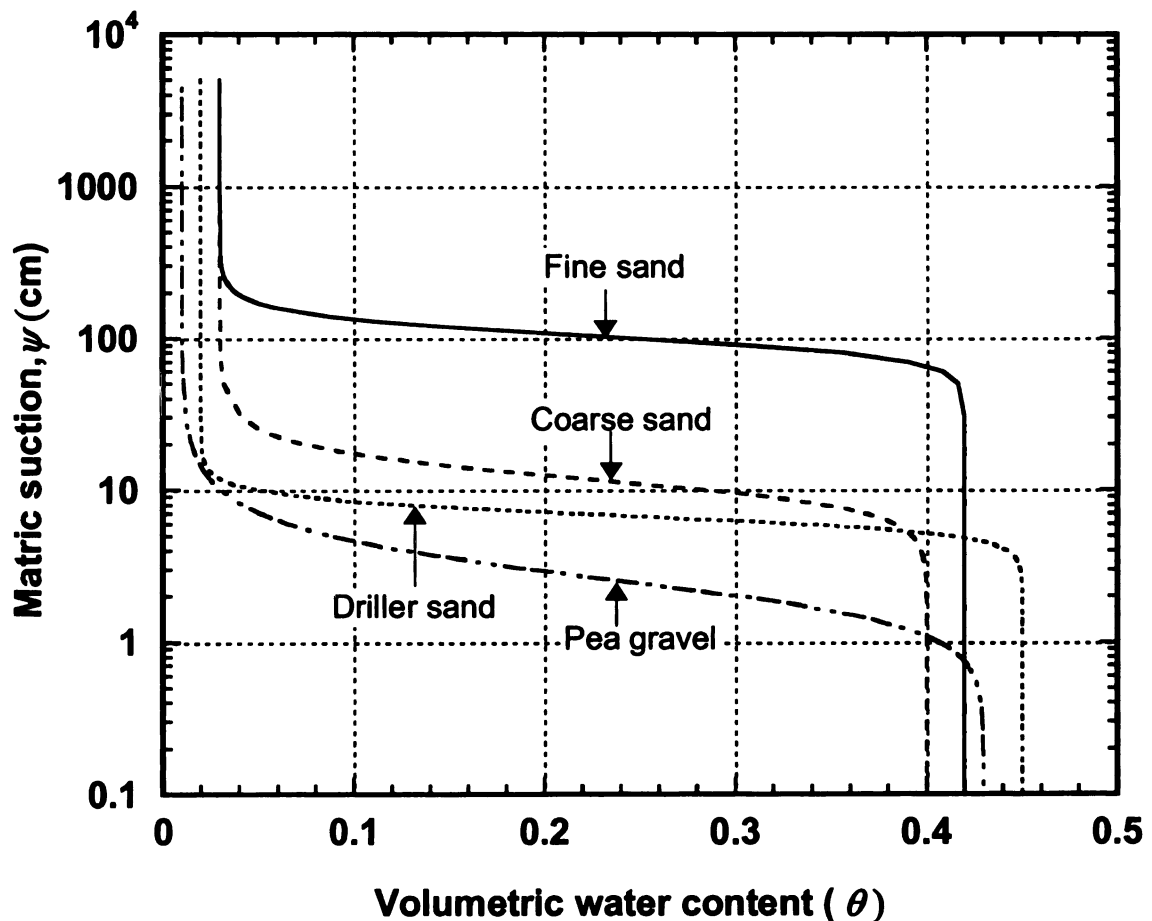


Figure 5-3: Soil-water characteristics curves for all the soils in the landfill model.

Instrumentation and Calibration

The following sensors were used in the landfill model: (1) pressure transducers with built-in thermistors; (2) water content sensors; and (3) flow sensors. All sensors were connected to a datalogger to continuously monitor and log the data. The water content sensors were connected to the datalogger via an electro-magnetic pulse generator and a coaxial multiplexer. The datalogger was programmed to take readings at frequencies 5 s to 30 min.

Pressure Transducer

The length and diameter of pressure transducer were 8.5 cm and 1.2 cm, respectively. The pressure transducer provided temperature compensated analog 0-5 VDC output proportional to the water pressure experienced by it. The sensitivity of the sensor was $\pm 1\%$ and have a measurement range of 0 to 92 cm of water head. Since the sensors were vented, barometric pressure was not recorded by the diaphragm. In recognition of the concern for zero drift and offsets, the accuracy of all sensors was checked from time to time by ponding water and checking the measured static heads during the course of experiments.

The pressure transducers were calibrated by applying known pressures and measuring the response. In order to evaluate the accuracy of their measurements, the pressure transducers were placed in a container in the position they were eventually embedded in the LCS, sand and the blanket in the landfill model. The pressure transducers were tested by adding de-ionized (DI) water at depths ranging from 15 to 35 cm. A linear relationship between the depth of water in the container and the pressure

head readings recorded by the pressure transducers was observed. The accuracy of the pressure transducer was within ± 0.5 cm. Periodically, water was ponded in the landfill model and maintained at a fixed level for few hours to measure signal drift for the pressure sensors. At the end of the experiments, when the setup was dismantled, the calibration of the sensors was re-checked and corrected, if needed. The zero was found to have drifted approximately by 0.3 to 0.6 cm.

TDR Water Content Sensor

The mini-TDR water content sensor consisted of three pointed 0.15 cm diameter stainless steel rods mounted into an encapsulated plastic head. The probe rod length was 6 cm and spacing between the probe rods was 0.6 cm. Topp's (Topp *et al.* 1980) empirically derived calibration equation was used to convert the dielectric constant values to volumetric water content.

The TDR water content sensors were fully inserted vertically in a container filled with dry sand and then water was gradually added in known steps until the sand got saturated. For both sands, a linear relationship between the volumetric water content calculated from known addition of water and the volumetric water content measured by the TDR water content sensors was observed.

Flow Sensor

The flow sensor was capable of measuring flow rates ranging from 8 to 165 cm³/s. The flow sensor incorporated a pelton-type turbine wheel having diameter and thickness equal to 1.6 cm and 0.075 cm, respectively to measure the flow rate of water. The rotational speed of the turbine wheel increased proportionally to the volumetric flow rate generating

electric pulses. The sensors provided analog DC voltage output proportional to the flow rate and the flow rate in engineering units was shown on the integrated LCD display.

A linear relationship was observed between the flow rates recorded by the flow sensor and the flow calculated from the levels measured by the pressure transducer. The accuracy of the flow sensor was within $\pm 0.5\%$.

Fabrication of Instrumented Model Landfill

LCS

Figure 5-1 shows a schematic of the landfill model and the location of sensors. A 4-cm thick LCS made up of pea gravel was constructed at the bottom slope of the plexi glass tank. Two 1.5-cm diameter perforated pipes discharging freely into the atmosphere were placed 45 cm apart in the LCS pea gravel layer. The perforated seepage pipes for LCS had at least 10 times higher flow capacity than the flows injected in the model to maintain the pressure head in the LCS within its thickness of 4 cm. A geotextile was placed between the LCS and sand to prevent clogging of the LCS.

Heterogeneous Subsurface Soils

Figure 5-4 shows a photo of the structured heterogeneous soil. Three types of sand (OK110, Ottawa and driller sand) of different dry densities, γ_d , comprising structured heterogeneous porous medium were placed in the form of equal sized grid blocks having dimensions equal to 30 cm long x 13 cm high x 30 cm wide as shown in Figure 5-5. Sand blocks are designated as: the sand type followed by its row number and then by its column number in accordance to its position in the grid as shown in Figure 5-5. The

blocks were constructed by placing a stiff geomembrane as a vertical separator between the blocks at the designated location. Dry sand was loosely poured on either side of the geomembrane forming blocks after which the geomembrane was slid out. Each block of sand was instrumented in the middle with either a water content sensor or in combination with a pressure transducer. The blocks were separated by an insect mesh at the bottom interface in order to prevent mixing of sands.

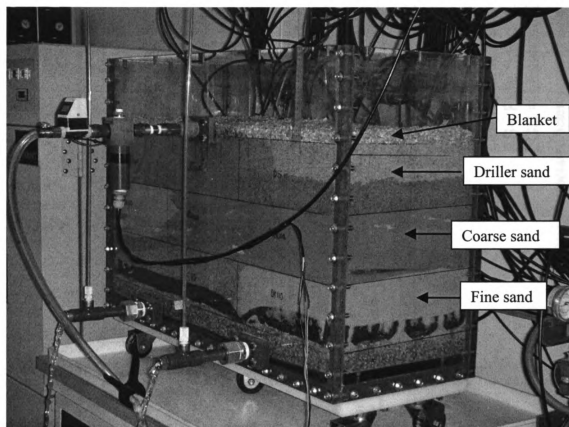


Figure 5-4: Photo of the structured heterogeneous soil below the blanket.

Blanket			
CS31 $\gamma_d = 1.61 \text{ g/cm}^3$ $K_s = 0.06 \text{ cm/s}$ 13 cm	CS32 $\gamma_d = 1.61 \text{ g/cm}^3$ $K_s = 0.06 \text{ cm/s}$	DS33 $\gamma_d = 1.49 \text{ g/cm}^3$ $K_s = 0.55 \text{ cm/s}$	
FS21 $\gamma_d = 1.47 \text{ g/cm}^3$ $K_s = 0.006 \text{ cm/s}$ 13 cm	CS22 $\gamma_d = 1.62 \text{ g/cm}^3$ $K_s = 0.06 \text{ cm/s}$ 30 cm	CS23 $\gamma_d = 1.62 \text{ g/cm}^3$ $K_s = 0.06 \text{ cm/s}$ 30 cm	
DS11 $\gamma_d = 1.51 \text{ g/cm}^3$ $K_s = 0.55 \text{ cm/s}$ 13 cm	DS12 $\gamma_d = 1.51 \text{ g/cm}^3$ $K_s = 0.55 \text{ cm/s}$ LCS	FS13 $\gamma_d = 1.45 \text{ g/cm}^3$ $K_s = 0.006 \text{ cm/s}$	

Notes:
CS = Coarse Sand
DS = Driller Sand
FS = Fine Sand
LCS = Leachate Collection System

Figure 5-5: Schematic of structured heterogeneous sand.

Blanket

The permeable blanket for the recirculation system was made up of the same pea gravel used in the LCS. The blanket extended along the entire length and width of the model. The thickness of the blanket was 2.0 cm. The perforated injection pipe of 1 cm diameter was embedded at the center of the blanket in the direction parallel to the width of the blanket where water was injected under a positive pressure. Total six pressure transducers in vertically upward position were embedded in the sand at designated locations such that the tip of the sensor was within the blanket. The injection pipe, the tip of the pressure transducers and the LCS pipes were wrapped with a mesh to prevent clogging of gravel particles in them.

The end of the injection pipe inside the blanket was capped and the other end was connected consecutively to a pressure transducer to measure injection pressure and a flow sensor to measure injection flow rate. A closed loop recirculation system was formed wherein the injected water after flowing through the soil and discharging freely in the atmosphere from the seepage pipes get collected in the storage tank which was again injected back to the system as shown in Figure 5-1. A brushless magnetic drive pump operated with a variable power DC power supply was used for injection of liquid in the blanket. A quartz based digital timer was used to operate the pump in on/off mode which could be programmed for various durations of on/off injection cycles.

Falling Head Tests

Falling head tests were performed on the landfill model to measure the saturated hydraulic conductivity of the whole system. This allowed capturing the effect of scale,

sensors, and sensor cables on the vertical hydraulic conductivity of the model and thus providing the “in-situ” conductivity. The measured saturated hydraulic conductivity of the landfill model was 0.06 cm/s which was same as that of the coarse sand. The water percolated mainly through the coarse sand blocks and went around the saturated fine sand blocks with least hydraulic conductivity. Because driller sand has relatively high hydraulic conductivity, it transmitted the most water through them. Hence, the hydraulic conductivity of the whole system was close to the coarse sand.

NUMERICAL MODELS

HYDRUS-2D and Vadose /W

HYDRUS-2D and Vadose/W were the opted numerical models to mathematically simulate the real physical process in the landfill model and in field-scale simulations respectively. Both the programs numerically solve the Richards’ equation (1931) for saturated/unsaturated water flow and have an option of using van Genuchten (van Genuchten 1980) function for soil-water characteristic curves and van Genuchten-Mualem (Mualem 1976) model for predicting the unsaturated hydraulic conductivity function. Both the models were conceptually similar and predictions were found to be almost similar although the algorithms might be significantly different. The governing partial differential equation for water flow is the 2-D form of Richards’ equation which is as follows:

$$\frac{\partial \theta}{\partial t} = -\frac{\partial}{\partial x}\left[k(\psi)\frac{\partial \psi}{\partial x}\right] - \frac{\partial}{\partial z}\left[k(\psi)\frac{\partial \psi}{\partial z}\right] + \frac{\partial k(\psi)}{\partial z} - S_w \quad (5-1)$$

where θ = volumetric water content [dimensionless]; ψ = matric suction head [L]; k = hydraulic conductivity of the porous material which is strongly dependant on the matric suction or water content [L/T]; z = vertical dimension [L]; S_w = volume of water removed per unit time per unit volume of soil by plant water uptake or evaporation (sink term) [1/T]; and t = time [T]. HYDRUS-2D and Vadose/W uses the Galerkin finite-element method to solve the governing equation of flow.

HYDRUS-2D and Vadose/W can simulate water and heat in unsaturated, partially saturated, or fully saturated porous media. Both the programs are capable of performing steady-state and transient conditions. HYDRUS-2D has been used for saturated/unsaturated liquid and solute transport through porous media in several studies (Haydar and Khire 2007; Khire and Mukherjee 2007; Haydar and Khire 2005; Khire and Haydar 2004; Scanlon *et al.* 2002; Henry *et al.* 2002; Rassam *et al.* 2002; Pang *et al.* 2000).

HYDRUS-2D Input

Mesh Discretization and Material Properties

An unstructured mesh was automatically generated to discretize the flow domain into triangles. The minimum size of finite-elements used for discretization of the problem domain, the time step, and the error tolerances for pressure head and water content were selected such that cumulative water balance error did not exceed 0.1%. In order to achieve such a low mass balance error, the problem domain was divided into 20000 nos. fine triangular finite elements. The dimensions of the finite elements grid were smaller around the injection pipe, where the hydraulic gradient was higher. An error tolerance of

0.1% for the volumetric water content and 0.01 cm for the matric suction were used. A minimum time step of 10^{-10} s and a maximum time step of 0.1 s were used.

The saturated and unsaturated properties tabulated in Table 5-1 were input as material properties for all landfill components. The effect of temperature was ignored due to isothermal conditions prevailing in the laboratory.

Initial and Boundary Conditions

The initial conditions input to the numerical model were consistent with those measured in the physical model before the injection was begun. The initial condition was entered in the form of volumetric water content, measured by the water content sensors at different regions in the heterogeneous sand before injection started.

All external boundaries were simulated as zero-flux boundaries which indicate that no water flows into or out of the domain through this boundary. Leachate collection pipes embedded in the LCS were simulated as seepage face boundaries. A seepage face boundary allows flow only when the boundary is saturated. This boundary condition is conservative for predicting liquid pressure head in LCS because no flow is allowed across the boundary when LCS is unsaturated. However, the flow actually occurred under saturated as well as unsaturated conditions. The pore pressure head is equal to zero along the saturated part of the seepage face through which water seeps out from the saturated part of the domain. The seepage face is a dynamic drainage boundary condition that changes according to the flow conditions during the simulation.

The perforated injection pipe was simulated as a constant flux boundary for steady-state problems and variable flux for transient problems. In variable flux boundary for on/off conditions, the flux was input as a time series. For each record in the time series in

variable flux boundary, the input flux was effective during the period between the time of the previous record and the current one. The pipe became a zero flux boundary during the “off” period of the pump. The input flux was calculated by dividing the injected flow rate per cm length of the injection pipe by the circumference of the pipe.

Other Input Parameters

The locations of sensors were input as observation nodes in order to obtain simulated pressure heads and water contents at those locations.

Input Parameters in Vadose/W for Field-scale Simulations

Conceptual Model for Field Scenario

The conceptual model which was developed by Haydar and Khire (2007) for numerical simulation of permeable blankets was used in this study which is shown in Figure 5-6. The conceptual model consisted of a 15-cm-thick, 60-m-wide permeable blanket and a leachate collection system (LCS). The 0.1-m-diameter perforated injection pipe ran perpendicular to the plane of the paper through the center of the blanket. The vertical distance between the blanket and the top of the LCS was 15 m. Distance from the top of the blanket to the upper zero flux boundary was assumed equal to 5 m to contain all injected leachate and to prevent possible artesian conditions for the simulated leachate injection rates. The LCS consisted of two 0.15-m-diameter perforated pipes embedded in a 0.3-m-thick gravel layer at a horizontal spacing equal to 60 m. The slope of the LCS was assumed equal to 3.5%. The hydraulic conductivity of the LCS drainage material was assumed equal to 10^{-2} m/s. The chosen LCS design parameters resulted in less than

0.3-m-leachate pressure head on the lining system for all simulations presented in this study.

The impact of daily cover materials on the estimation of vertical hydraulic conductivity using ACRES method was assessed using the permeable blanket recirculating leachate continuously and intermittently at 2 h on/22 h off and 8 h on/16 h off at an injection rate of $400 \text{ m}^3/\text{d}$. The 0.15-m-thick cover soil was assumed to have a hydraulic conductivity same as that of silt. The layers of daily cover were modeled as continuous and breached with 2 m gaps. Figures 5-7 and 5-8 shows the different configurations of placement of daily cover soil layers within the waste. The cover soil layers were placed at every 3-5 m intervals of waste height.

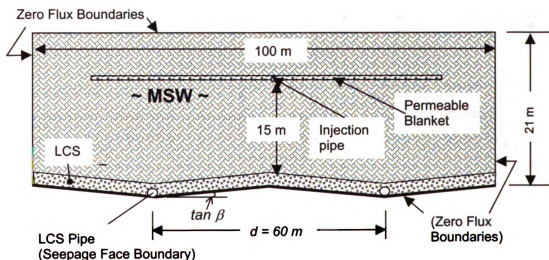


Figure 5-6: Conceptual model for field-scale simulations showing waste with no daily cover soil layers (adapted from Haydar and Khire 2007).

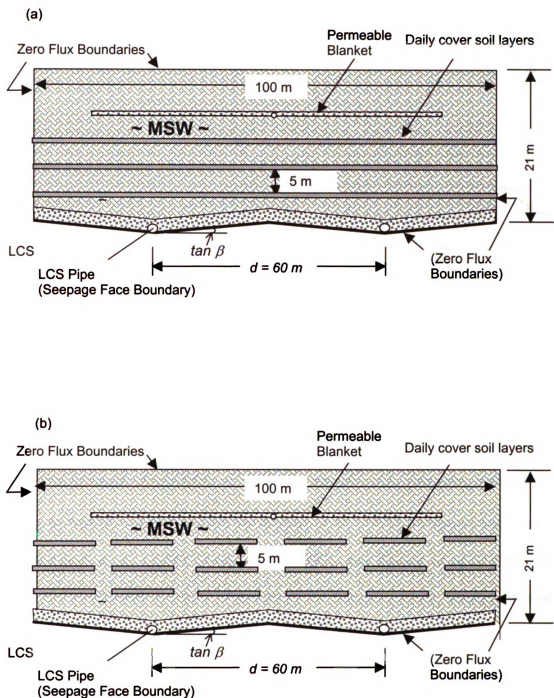


Figure 5-7: Conceptual model for field-scale simulations showing waste with (a) continuous daily cover soil layers; (b) breached daily cover soil layers.

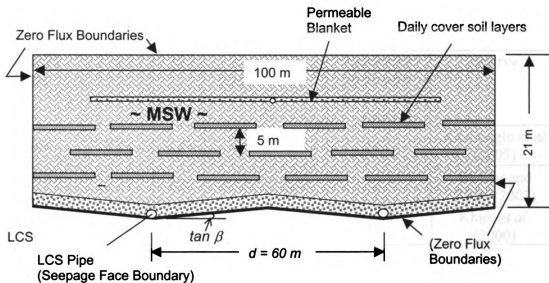


Figure 5-8: Conceptual model for field-scale simulations showing waste with staggered breached cover soil layers.

Material Properties and Assumptions

The saturated hydraulic conductivity of MSW, k_w , was 10^{-5} m/s. This value was selected according to typical values published by Hughes *et al.* (1971), Fungaroli and Steiner (1979), Korfiatis *et al.* (1984), Oweis *et al.* (1990), and Bleiker *et al.* (1993). The saturated and unsaturated hydraulic properties of the simulated waste, blanket material, and LCS gravel layer input to Vadose/W are presented in Table 5-2.

Table 5-2: Saturated and unsaturated hydraulic properties for field-scale simulations.

Landfill Unit	θ_r	θ_s	α (1/m)	n	Saturated hydraulic conductivity (m/s)	Source
Waste	0.14	0.58	15	1.6	10^{-5}	Kazimoglu <i>et al</i> (2005)
Permeable Blanket	0.01	0.3	57.4	2.44	10^{-2}	Haydar and Khire (2007)
Daily cover soil layers	0.02	0.35	1.2	1.125	10^{-7}	Khire <i>et al.</i> (2000)
Leachate Collection System	0.01	0.3	57.4	2.44	10^{-2}	Haydar and Khire (2007)

Note: θ_s = saturated volumetric water content [dimensionless];
 θ_r = residual volumetric water content [dimensionless]; and
 α [1/L] and n are van Genuchten's fitting parameters (van Genuchten 1980)

Apart from the saturated and unsaturated properties tabulated in Table 5-2 which were input as material properties, the coefficient of compressibility (m_v) was also input. Because water can be released by compressing the soil skeleton and reducing the size of voids, the coefficient of volume compressibility m_v is input to adequately represent the slope of the water content function in the positive pore-water pressure region. The m_v for pea gravel and the waste were assumed as $1 \text{ e-}5 \text{ 1/kPa}$ as per the Vadose/W User's manual (Geo-Slope 2004).

Leachate was simulated as pure water. The effect of gas flow, temperature and biochemical reactions occurring within a landfill was ignored. The option transient-isothermal was chosen for the simulations in Vadose/W. Leachate flow as a result of percolation from the cap or waste above the model domain was assumed zero. This

assumption is reasonable since subsurface hydraulics of injected leachate was simulated in this study. The waste was assumed to be homogeneous and isotropic.

Mesh Discretization

The problem domain was divided into a structured mesh in the form of 4-noded quadrilateral and triangular elements. The time stepping was adjusted to discretize the time domain into a series of incremental time steps. The spacing between the nodes located near the flux and seepage boundaries were relatively small to ensure as little numerical error as possible due to the assigned boundary conditions. The minimum size of the finite-elements used for discretization of the problem domain, the time step, and the error tolerances for pressure head and water content were selected such that cumulative water balance error did not exceed 10 %.

Initial and Boundary Conditions

The initial condition of MSW was entered in the form of initial water table at 1 m below the bottom of the problem domain with maximum negative pressure head of 0.1 m which yielded initial saturation of 75%. The initial total head at each node was computed proportionally to the vertical distance between the node and the defined water table by Vadose/W.

All external boundaries were simulated as zero flux boundaries. The perforated pipe used for leachate injection was simulated as a node to which nodal flux was assigned as constant for continuous injection or as a function of time in cyclic mode for on/off injection. The input flux was calculated by dividing the injected flow rate per 10 m length of the injection pipe. The injection rate was selected from a range of 250 to 850 m³/d

based on leachate injection rates used in the field for the blanket at McGill landfill in Jackson (Khire and Haydar 2005).

Leachate collection pipes embedded in the LCS were simulated as seepage face boundaries.

RESULTS AND DISCUSSION

Pressure Heads in Blanket Due to Continuous Injection

Homogeneous and Isotropic Sand

Figure 5-9 shows the measured pressure heads (h_m) and HYDRUS-2D simulated pressure heads (h_s) in the blanket when DI water was injected at a constant rate, $Q = 120 \text{ cm}^3/\text{s}$ in the homogeneous setup with coarse sand.

Before the liquid injection in the blanket was started, the average degree of saturation, S , of the sand below the blanket was 70% as shown in Figure 5-10. The hydraulic conductivity of blanket being greater than the underlying sand, the water traveled through the blanket relatively faster compared to infiltrating into the underlying sand. As the injected water traveled through the blanket, the hydraulic pressure heads in the blanket increased. The pressure heads were relatively high in the beginning which decreased as injection continued. The increase in the pressure head was earliest and greatest for the sensors located closest to the injection pipe and decreased subsequently due to pressure loss with distances away from the injection pipe.

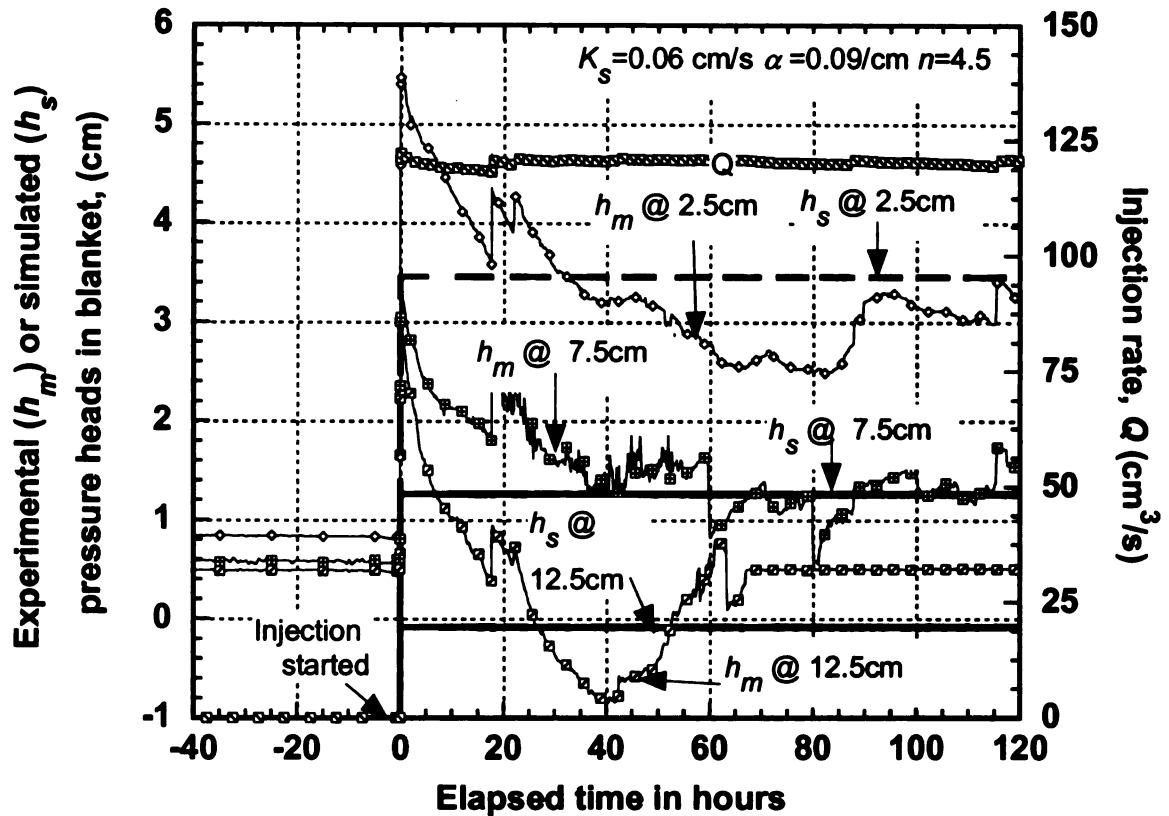


Figure 5-9: Measured and simulated pressure heads in blanket in homogeneous coarse sand.

At same distance from the injection pipe on either side, the pressure heads were same due to homogeneous sand underlying the blanket. The pressure sensor at 12.5 cm from injection pipe had shown increase in pressure heads initially. As the degree of saturation of the underlying sand increased and hydraulic conductivity of the sand increased, the reading of that sensor dropped close to zero as shown in Figure 5-9.

In about 60 hours after the injection began, the pressure heads reached a steady-state when the average degree of saturation of underlying sand reached 100%. The pressure sensors in blanket reaching steady-state were correlated with the water content sensors in sand reaching saturation (see Figure 5-10). A steady-state was assumed to have reached when the pressure heads in the blanket did not show major upward or downward

trend for several hours. The wetted width at steady-state can be considered to be between 15 cm and 25 cm because the pressure sensor at 7.5 cm responded to the injection event and the pressure sensor at 12.5 cm stayed close to zero.

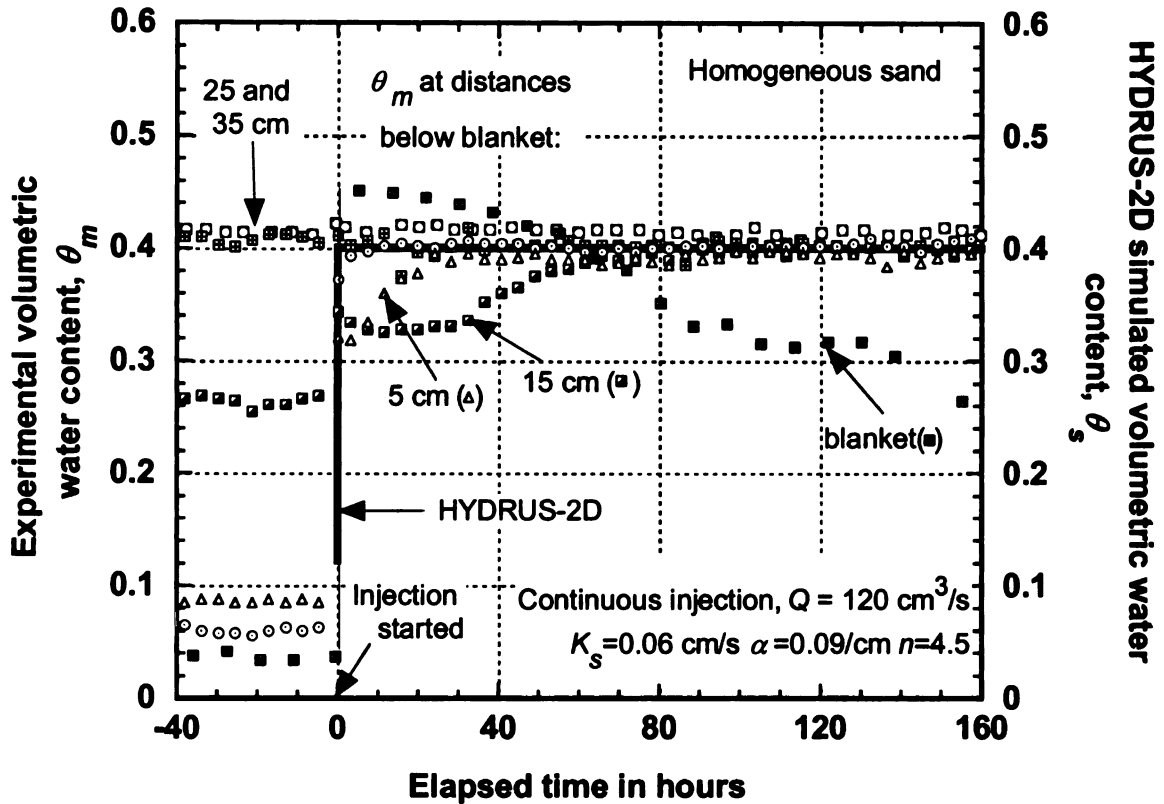


Figure 5-10: Measured and simulated increase in water content of homogeneous sand due to continuous injection.

The simulated and observed pressure heads in the blanket due to injection at steady-state were relatively close. The initial high heads were not captured by HYDRUS-2D. The pressure heads were relatively high in the beginning because entrapped air or non-continuous air bubbles isolated from atmosphere were formed due to the advance of water through preferred pores or pore sequences resulting in trapping the gaseous air. The trapped air bubbles were under pressure greater than atmosphere. Hence initial pore

water pressure heads recorded by the pressure sensors were high due to the entrapped air bubbles and their effect on hydraulic conductivity. The initial high pressure heads decreased due to increase in hydraulic conductivity of sand and hydraulic conductivity is known to increase when entrapped air is removed (Christiansen 1944). In about 60 hours after the injection began, the pressure heads reached a steady-state. A steady-state was assumed to have reached when the pressure heads in the blanket did not show upward or downward trend for several hours.

Most of the numerical models like HYDRUS-2D are designed to model only the single phase flow of water solving Richard's equation, which assumes that the air phase is always at a constant atmospheric pressure and is able to escape freely and does not impact the infiltration of water into soil. Hence, the numerical model did not calculate the initial increase in the water pressure heads measured in the blanket.

Heterogeneous and Isotropic Sand

Figure 5-11 shows the measured pressure heads (h_m) and HYDRUS-2D simulated pressure heads (h_s) in the blanket due to DI water injection at a constant rate, $Q = 120 \text{ cm}^3/\text{s}$ in the structured heterogeneous sand setup. Before liquid was injected in the blanket at $Q = 120 \text{ cm}^3/\text{s}$, water was injected at a constant rate, $Q = 85 \text{ cm}^3/\text{s}$ and the average degree of saturation, S of the sand below the blanket was elevated to 90%.

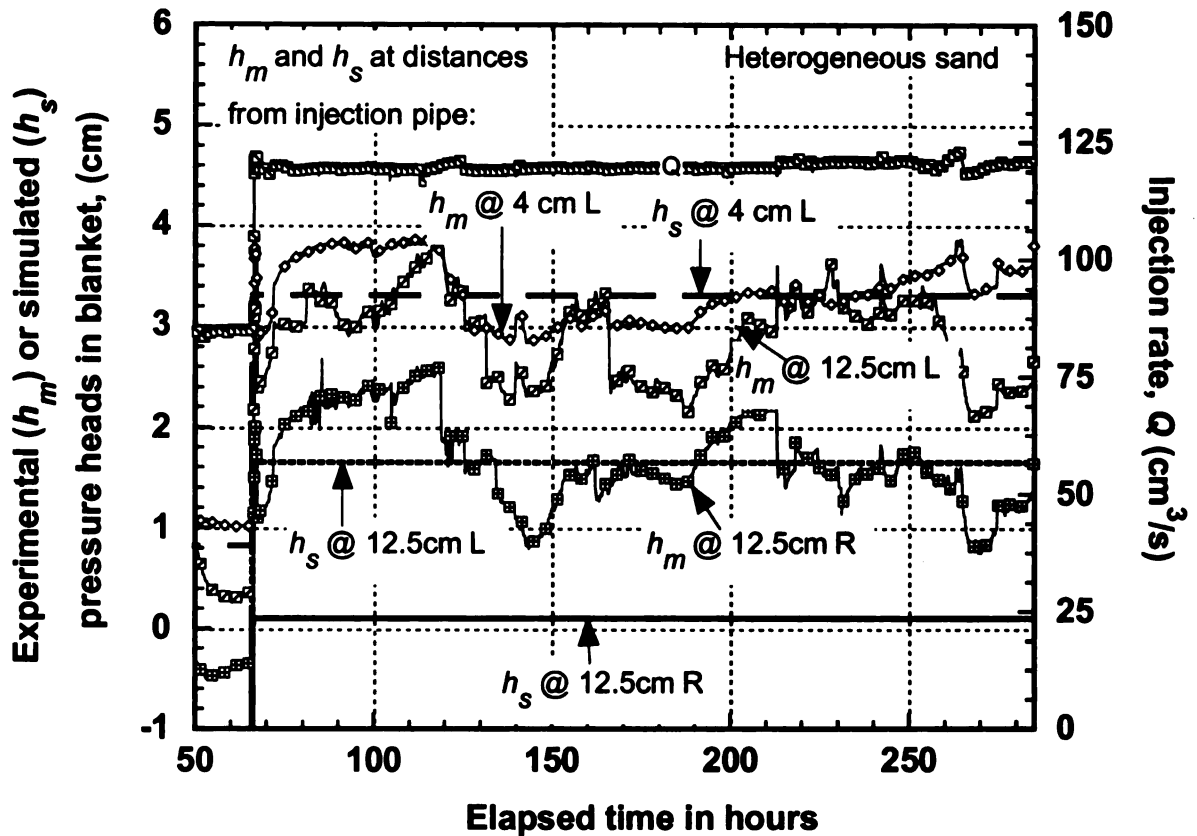


Figure 5-11: Measured and simulated pressure heads in blanket in heterogeneous sand.

Although the injected flow was more or less constant, the pressure heads in the blanket underwent relatively high fluctuations. Similar to the homogeneous setup, the increase in the pressure head was earliest and greatest for the sensors located closest to the injection pipe and decreased subsequently with distances away from the injection pipe. The pressure head closest to the injection pipe was approximately same as that in the homogeneous sand.

Unlike in the homogeneous setup, the pressure heads were not identical at a given distance from the injection pipe on either side. In the homogeneous setup, the pressure sensor at 12.5 cm did not register any increase in pressure heads at steady-state but in the heterogeneous setup, the pressure sensors located at 12.5 cm from the injection pipe

registered increase in pressure heads. The pressure head at 12.5 cm left of the injection pipe was higher than that at 12.5 cm right of the injection pipe in the heterogeneous setup. This was because to the left side of the injection pipe, there was coarse sand block with lower hydraulic conductivity underlain by fine sand with lowest hydraulic conductivity below the blanket and on the right hand side, there was driller sand block with highest hydraulic conductivity underlain by coarse sand below the blanket. The difference in hydraulic conductivities of sand blocks below the blanket on either side generated different pressure heads on either side. The simulated pressure heads were relatively close to the measured pressure heads. The average pressure heads in the blanket in heterogeneous sand were slightly higher than that in homogeneous sand.

Average Degree of Saturation of Sand Due to Continuous Injection

Homogeneous and Isotropic Sand

Figure 5-10 shows the measured water content, (θ_m) and HYDRUS-2D simulated water content, (θ_s) in the underlying homogeneous coarse sand and blanket for constant injection event at $Q = 120 \text{ cm}^3/\text{s}$. The water content sensors in the blanket showed increase in water content first. The water content sensors embedded in the sand registered increase after the blanket. Thus, the injected water filled the blanket before substantial quantity of water started infiltrating into the underlying sand. The water content sensors in the sand were able to detect the gradual progressive changes in the degree of saturation of the underlying sand. The time when the pressure heads reached steady-state as shown in Figure 5-9 synchronized with the water contents in the sand reaching saturation.

Figure 5-10 shows that HYDRUS-2D was not able to simulate the gradual increase in the water contents within the sand. The numerical modeling results indicated that the increase in water content of the underlying sand was immediate as compared to the measured water contents which increased gradually and sequentially from top down. The reasons behind the discrepancies are same as discussed earlier in Paper no. 3.

Heterogeneous and Isotropic Sand

Figures 5-12 show the measured water contents (θ_m) and HYDRUS-2D simulated water contents (θ_s) in the different blocks of heterogeneous sand underlying the blanket. In the preceding experiments (not shown here) when water was first injected in dry sand, the water after leaving the blanket moved vertically downwards through the coarse sand blocks CS32 and CS22 and saturated the fine sand blocks FS13 and FS21 in the process by capillary conduction through small pores. Though not shown in Figures 5-12a and 5-12b, spot measurements for water content in the block FS21 indicated saturation as well. The fine sand blocks once saturated remained in that saturated state and did not drain even when injection of water was stopped owing to its high air entry value (Figure 5-2). Hence, as observed in Figure 5-12a, the water content in FS13 was at saturation before the current experiment was started.

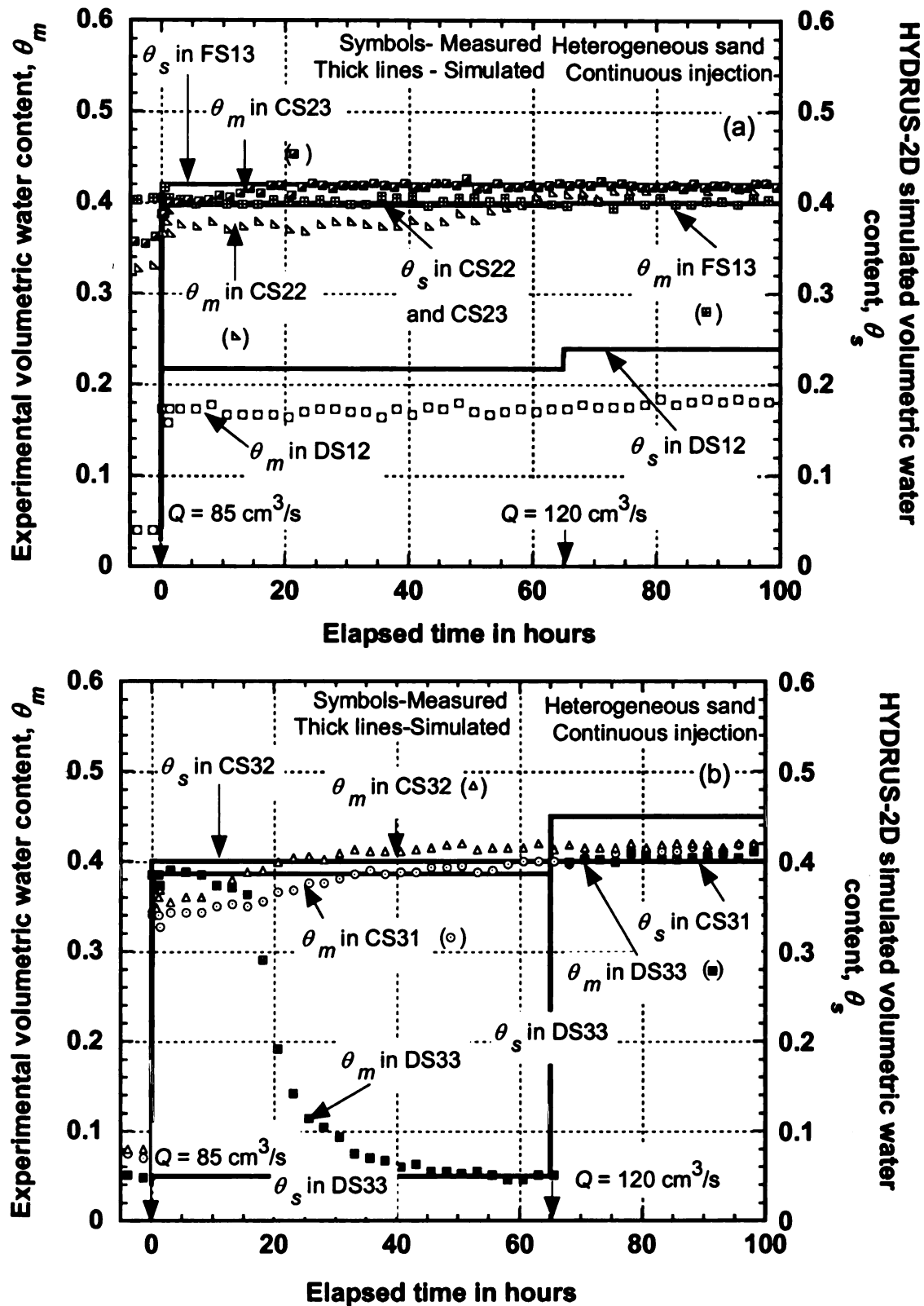


Figure 5-12: Measured and simulated water content in different blocks of heterogeneous sand due to continuous injection.

When water was injected at $Q = 85 \text{ cm}^3/\text{s}$, initially most of the injected water preferentially moved through the DS33 block of highest hydraulic conductivity. The flow of water through DS33 and through capillary conduction from CS22 caused the degree of saturation of CS23 to increase. DS33 drained after a while when CS23 reached saturation since most of the water now moved through CS22 and CS32 saturating the blocks and displacing air in the process. The displaced air escaped through the continuous large pore spaces of DS33 having relatively small air entry suction and hence drained the block. The driller sand block DS12 being highly transmissive never reached saturation even when the injection rate was raised. DS33 reached saturation when water was injected at a higher rate of $Q = 120 \text{ cm}^3/\text{s}$.

Unlike in the homogeneous setup, the increase in water content due to injection was less gradual in the heterogeneous setup. The measured and the simulated water content in various blocks of sand were relatively close. This was because when water moved down in the soil, the air in the soil voids was pushed laterally to give room to the moving water and the lateral escape was aided through the relatively large pores of driller sand block (DS33). The blanket was also not buried under sand. Hence, continuous pathways of air to the atmosphere were created through the large pores of DS33 and blanket. This caused less air entrapment and compression in the model due to the advance of the wetting front in sharp contrast to that in homogeneous setup.

Pressure Heads in Sand Due to Continuous Injection

Homogeneous and Isotropic Sand

Figure 5-13 shows the measured pressure heads (h_m) and HYDRUS-2D simulated pressure heads (h_s) in the sand when DI water was injected at a constant rate, $Q = 120 \text{ cm}^3/\text{s}$ in the homogeneous setup with coarse sand. The pressure head in the sand at 5 cm below the blanket gradually increased to about 13 cm due to pore air pressure.

At the beginning of infiltration process, the suction gradients predominated over the gravitational gradient as water moved through the capillary pores entrapping air in the process and hence contributing to pore air pressure heads. As the water penetrated deeper and wetted part of sand profile lengthened, the suction gradient eventually became negligible leaving the constant gravitational gradient in effect as the only force moving water downward. Hence, we observe in Figure 5-11 that water moved under unit gradient from time equal to 85 h onwards. The measured pressure heads were same at the two locations and water moved under elevation difference due to gravity. However, the simulated pressure heads did not match with the measured pressure heads at steady-state.

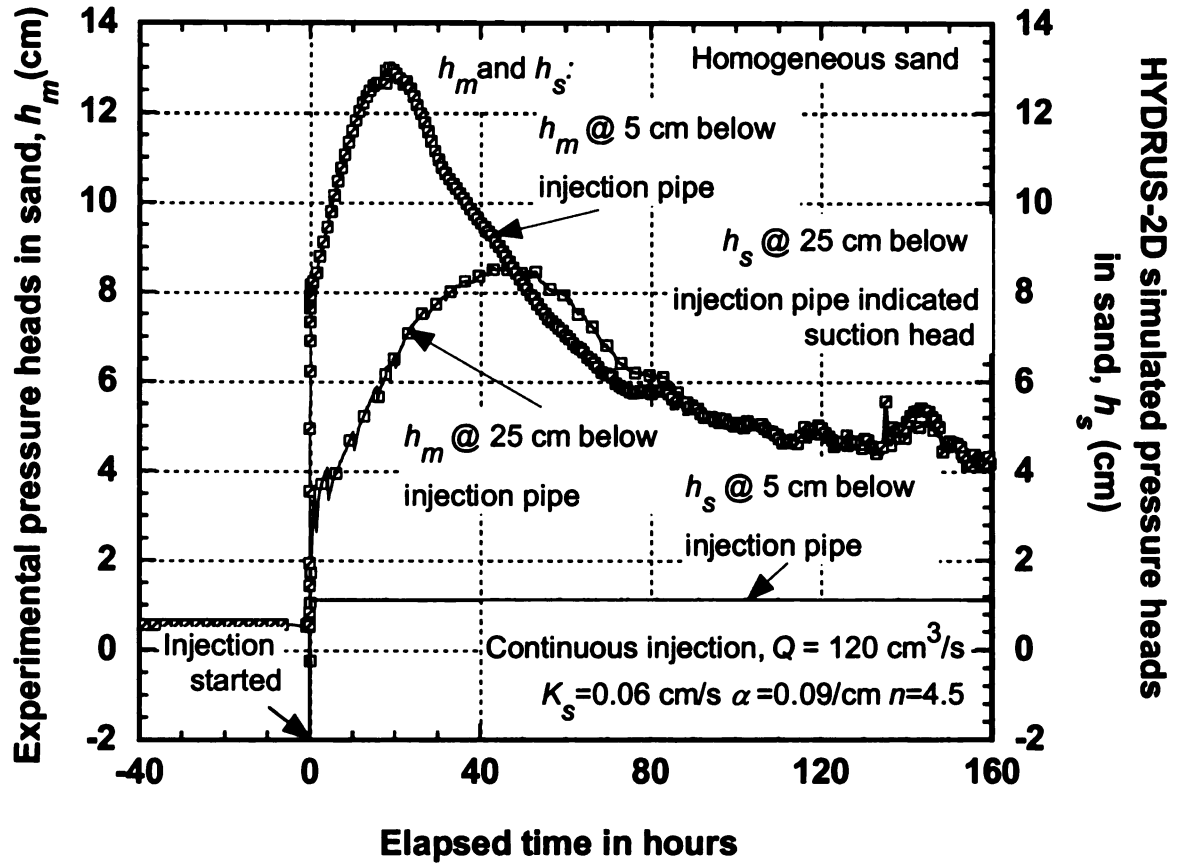


Figure 5-13: Measured and simulated pressure heads within homogeneous sand.

Heterogeneous and Isotropic Sand

Figure 5-14 show the measured pressure heads (h_m) and HYDRUS-2D simulated pressure heads (h_s) in the different blocks of sand when DI water was injected at a constant rate of $120 \text{ cm}^3/\text{s}$ in the heterogeneous sand.

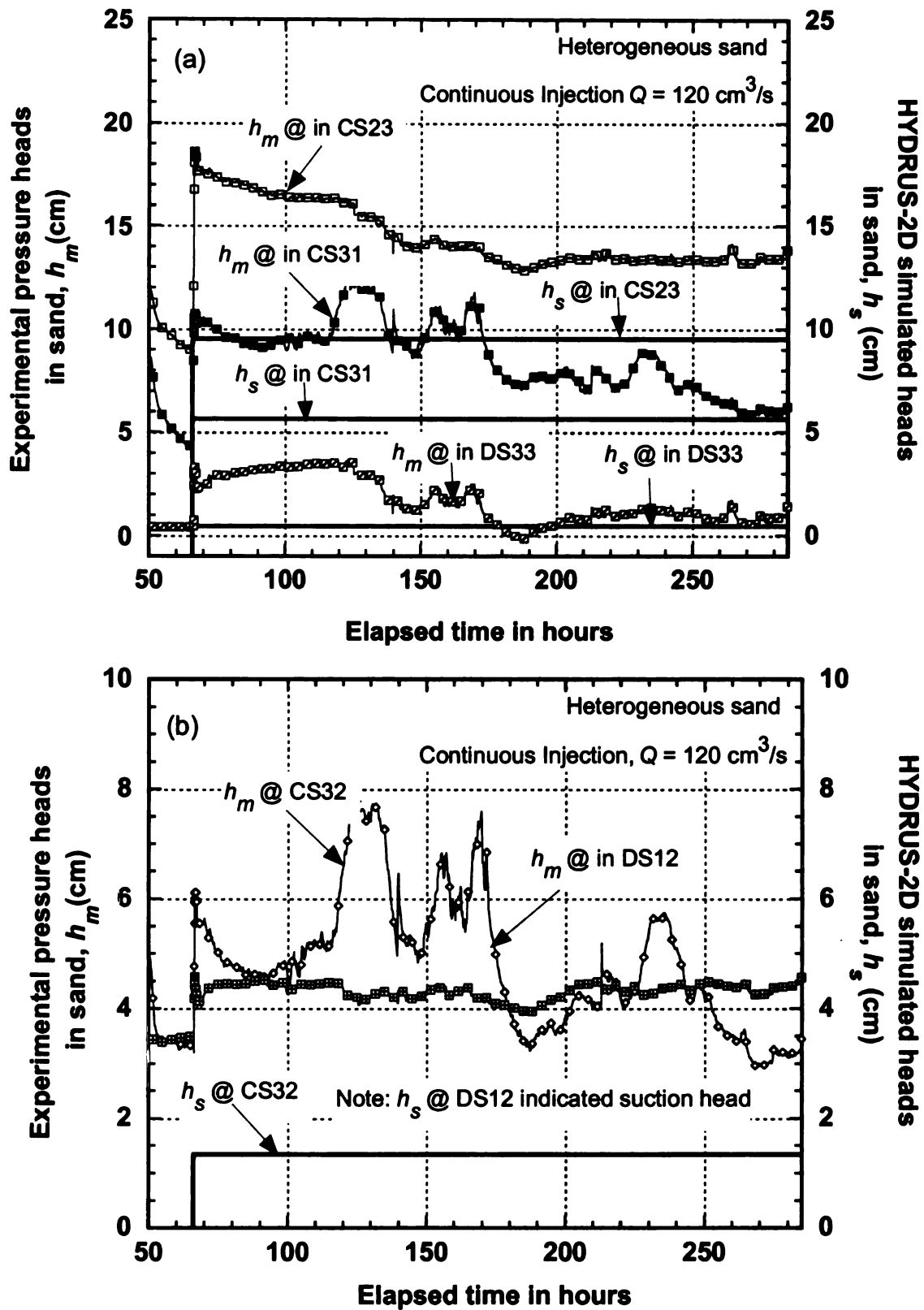


Figure 5-14: Measured and simulated pressure heads in various blocks of heterogeneous sand with different hydraulic conductivities.

Similar to the homogeneous setup, the pressure heads in all the blocks were higher in the beginning. The pressure heads in the coarse sand blocks which were immediately above the fine sand blocks with lowest hydraulic conductivity were higher than the rest. The hydrostatic pressure built up in coarse sand because the presence of fine sand below the coarse sand blocks offered more resistance to flow than the coarse sand. This caused build up in pressure in order to push the water through the fine sand at the same rate as it moved through the coarse sand. Figure 5-14 shows that the measured and simulated pressure heads matched only in DS33 whereas in other blocks they differed.

Pressure Heads in Blanket Due to On and Off Injection

Homogeneous and Isotropic Sand

Figure 5-15a shows the measured peak pressure heads in the blanket when DI water was injected at a rate of $120 \text{ cm}^3/\text{s}$ for a dosing frequency of 6 min on and 10 s off in the homogeneous setup with coarse sand. Peak pressures typically occur just before the pump goes off. Similar to the constant injection rate, the pressure sensors at 12.5 cm to 25 cm from the injection pipe did not respond to the intermittent injection event. Figure 5-13b shows the comparison between the measured pressure head, (h_m) and HYDRUS-2D simulated pressure heads (h_s) in the blanket when a quasi steady-state was reached after a few cycles. The quasi steady-state is defined as a state when the system reaches a dynamic equilibrium and the pressure heads reach a constant value during the injection period in each on/off cycle.

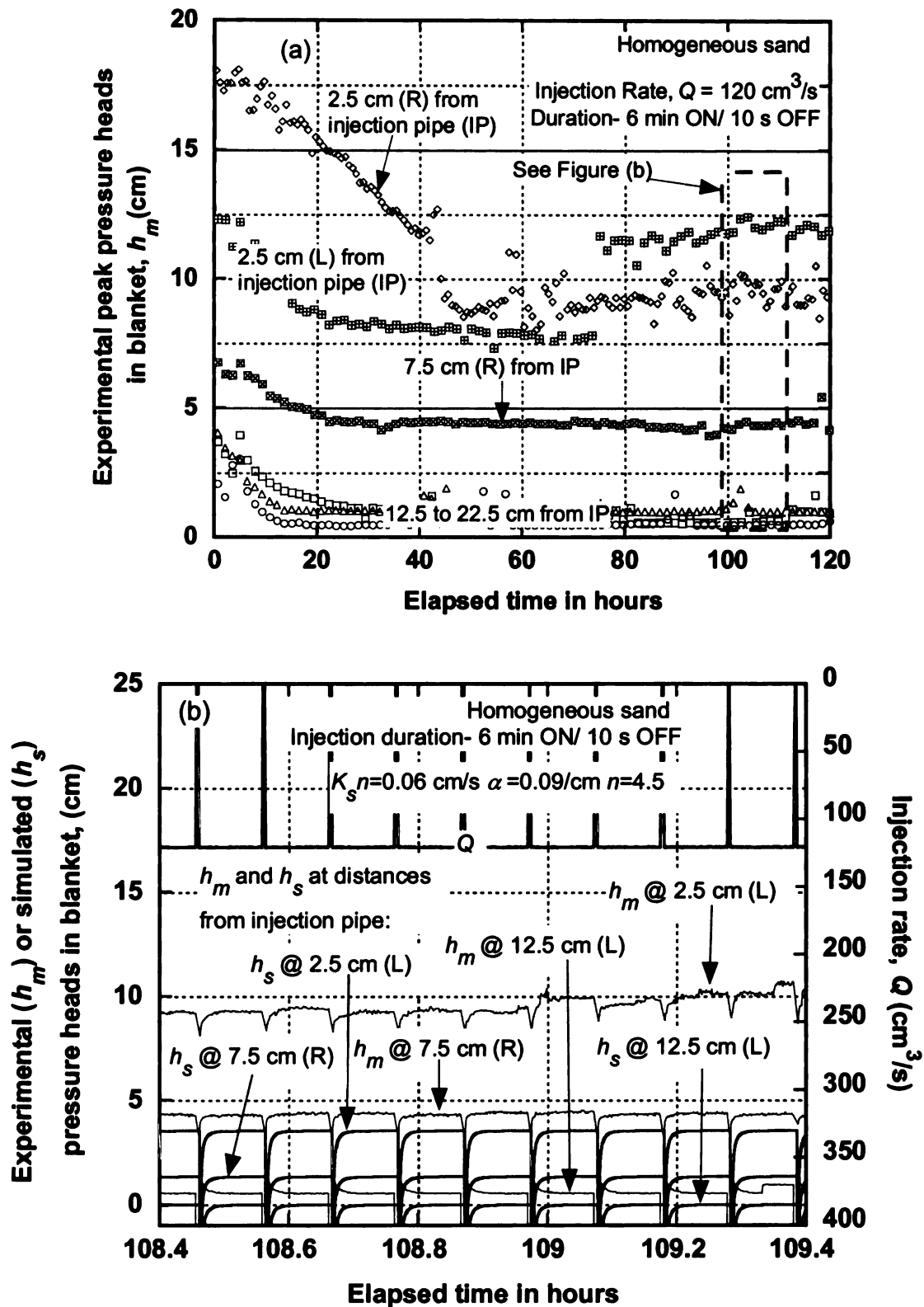


Figure 5-15: Measured and simulated: (a) peak pressure heads; and (b) snapshot of few on/off cycles in blanket for homogeneous sand for 6 min on and 10 s off injection.

Figure 5-15b shows that the simulated and the measured pressure heads did not match at quasi-steady state. Measured pressure heads were greater than simulated values. During the drainage period between successive wettings, the largest pores de-watered first and the smaller pores within the matrix did not have sufficient time to de-water fully. In the subsequent wetting period, the water filled up dewatered larger pore spaces. Because smaller pores and passages around the larger pores have not dewatered, discontinued air bubbles were trapped in the larger pores. The trapped air bubbles during on/off injection frequency did not have enough time to dissolve in water like that in continuous injection. Entrapped air reduces saturated hydraulic conductivity (Christiansen 1944; Gupta and Swartzendruber 1964; Seymour 2000; Sakaguchi *et al.* 2005). Hence, the pressure heads were higher and did not equate with the steady-state values obtained from continued injection event. The single phase approach of numerical model was unable to capture the effect of entrapped air bubbles on the pressure heads.

Heterogeneous and Isotropic Sand

Figure 5-16a shows the measured peak pressure heads in the blanket when DI water was injected at a rate of $120 \text{ cm}^3/\text{s}$ for a dosing frequency of 6 min on/10 s off in the heterogeneous sand. The pressure head at 12.5 cm left (L) from the injection pipe was higher than that at 12.5 cm right (R) from the injection pipe as observed earlier in Figure 5-11.

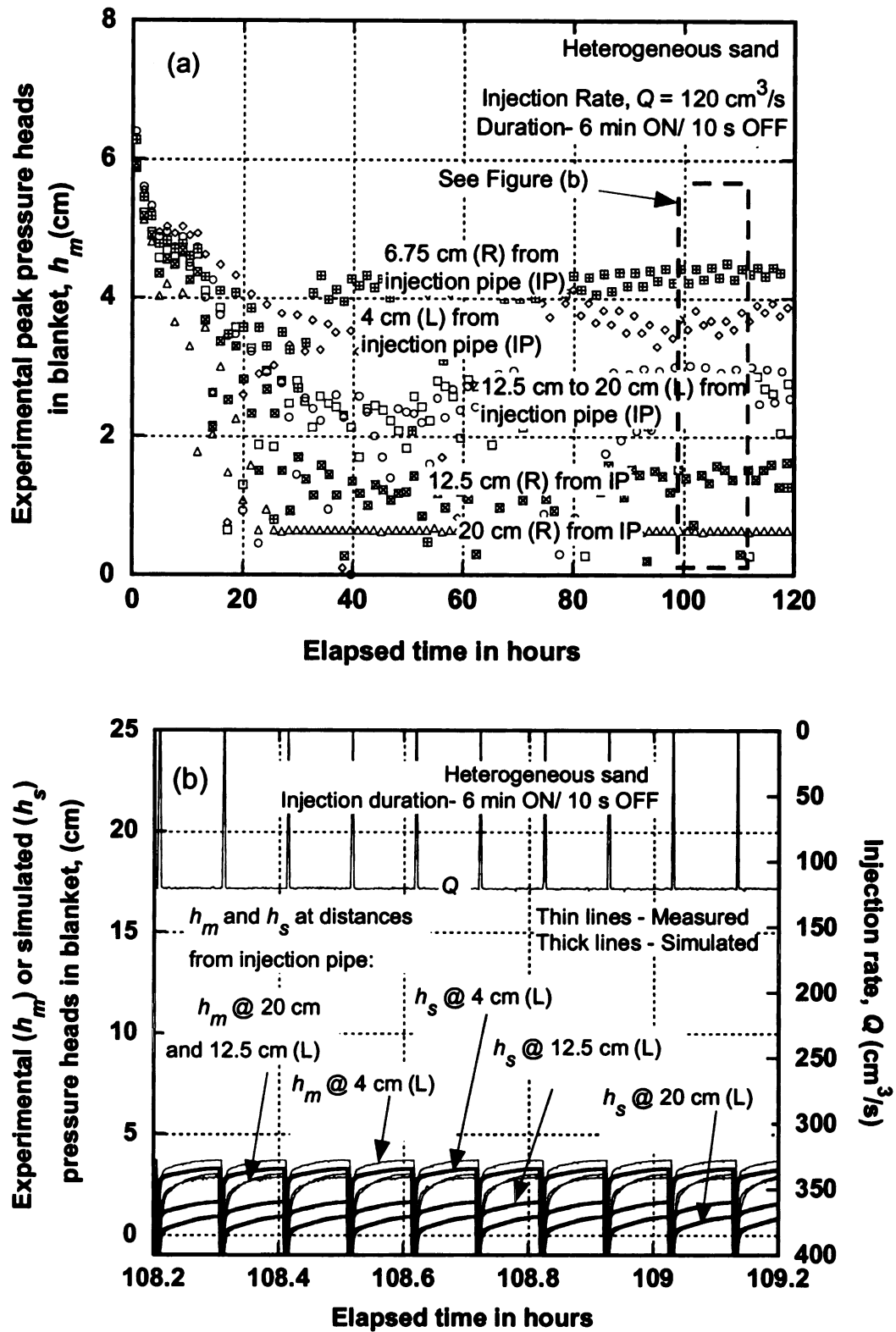


Figure 5-16: Measured and simulated: (a) peak pressure heads; and (b) snapshot of few cycles in blanket for heterogeneous sand for 6 min on and 10 s off injection.

Unlike in the homogeneous setup, the measured and simulated pressure heads matched at quasi-steady state for on/off dosing frequencies as shown in Figure 5-14b. Also, the average measured pressure heads in the blanket achieved at quasi-steady state due to intermittent injection matched exactly with the steady-state average pressure heads in blanket when water was injected at continuous rate as shown in Figure 5-7. This phenomenon was not observed in the homogeneous setup. In the homogeneous setup, the average pressure head in blanket due to on/off dosing frequencies was much higher than that obtained due to continuous injection. Less air entrapment and its compression in CS32 and CS22 blocks due to the lateral escape of air through the relatively large pores of driller sand block DS33 as discussed earlier were the reasons for more accurate match for pressure heads in heterogeneous sand. The presence of a block of highest hydraulic conductivity and low air entry value facilitated the escape of air and hence was able to reduce air entrapment.

Average Degree of Saturation of Sand Due to On/Off Injection

Homogeneous and Isotropic Sand

Figure 5-17 shows the measured water content (θ_m) and HYDRUS simulated water content (θ_s) in the underlying sand and blanket for the injection event of $120 \text{ cm}^3/\text{s}$ of dosing frequency of 6 min on/10 s off in the homogeneous setup with coarse sand. The reasons behind the discrepancies between measured and simulated water content are the air entrapment in the physical model which is not simulated in HYDRUS because it is a single phase model.

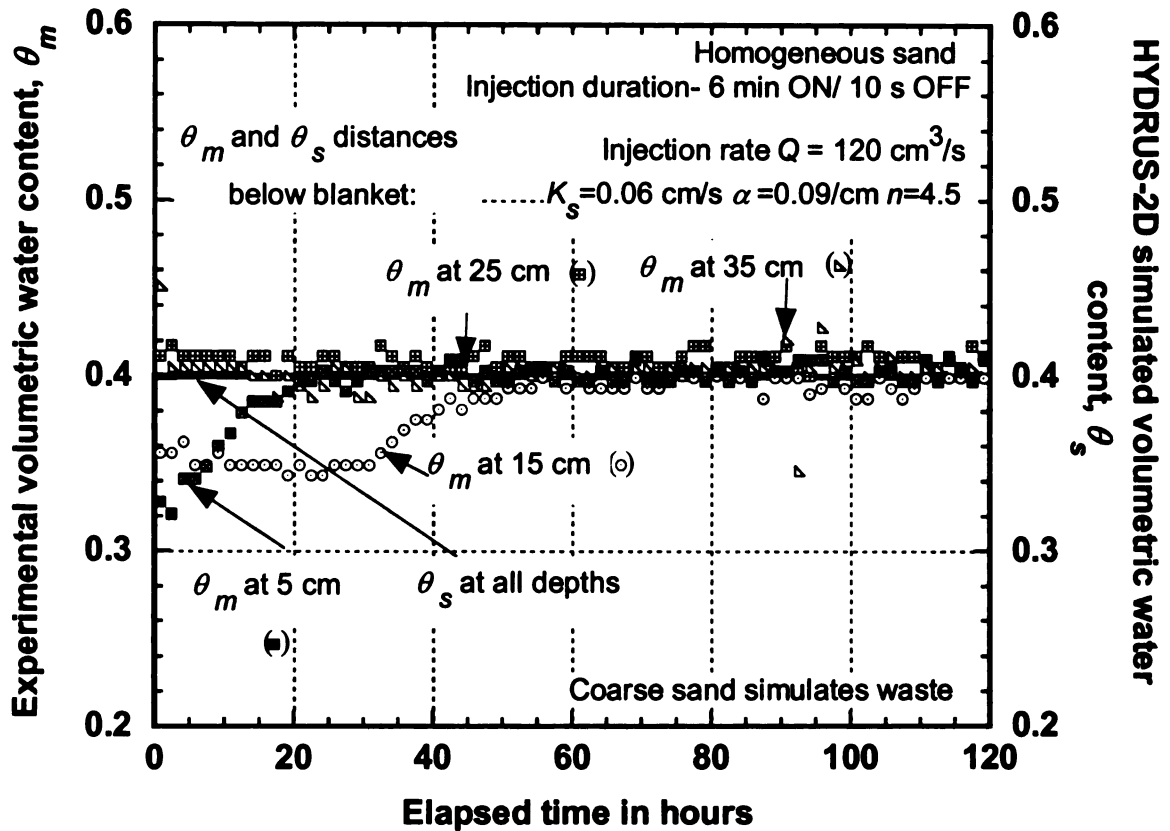


Figure 5-17: Measured and simulated water content of homogeneous sand due to 6 min on and 10 s off injection.

Heterogeneous and Isotropic Sand

Figure 5-18 show the measured water content (θ_m) and HYDRUS simulated water content θ_s in the different blocks of sand underlying the blanket. The water content at approximately depth of 15 cm below the blanket in CS22 block reached saturation 20 hours less than the saturation reached at the same depth in homogeneous sand. This finding once again proves the escape of air through DS33.

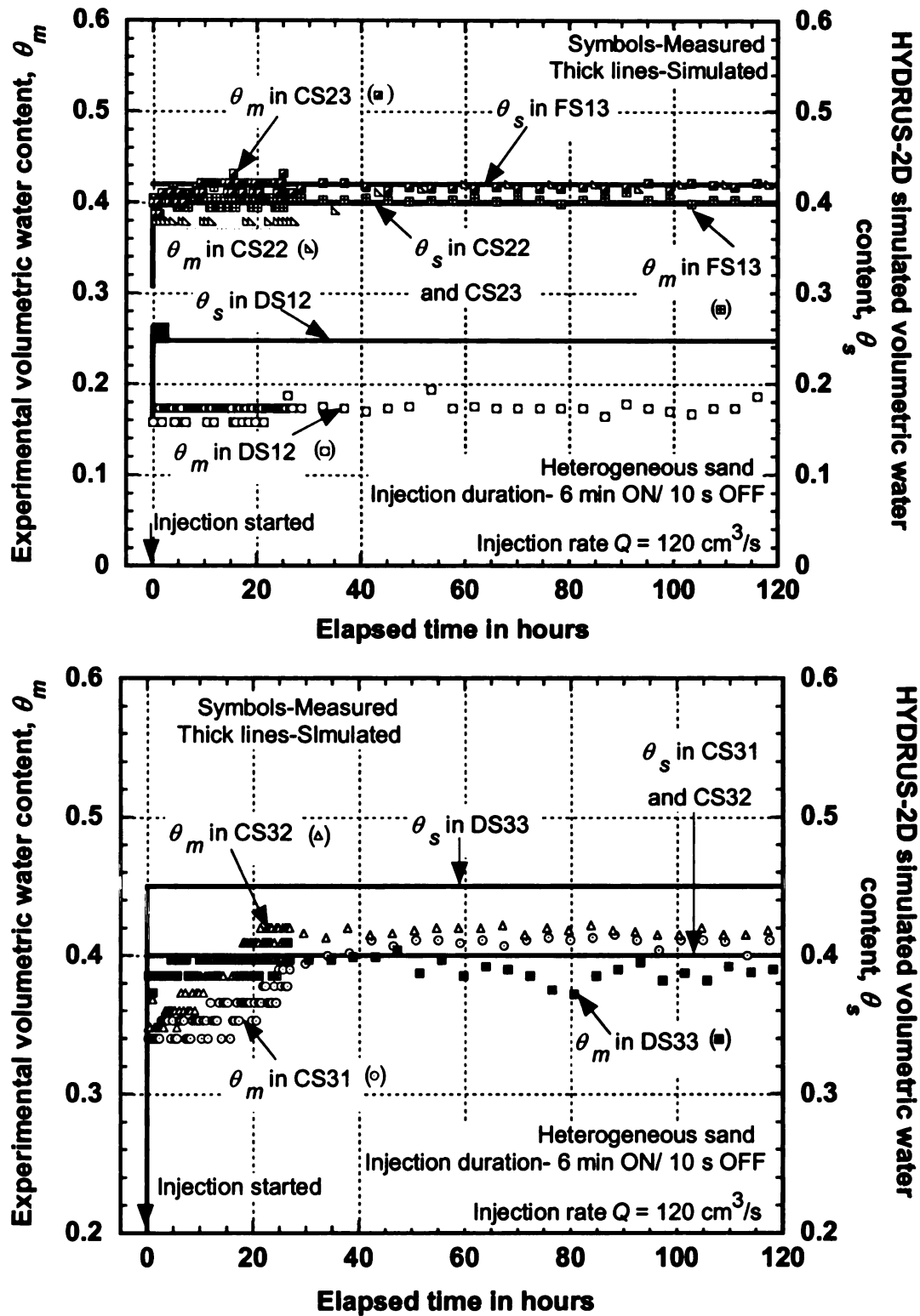


Figure 5-18: Measured and simulated water content in different blocks of heterogeneous sand due to 6 min on and 10 s off injection.

Pressure Heads in Sand Due to On/Off Injection

Homogeneous and Isotropic Sand

Figure 5-19 shows the measured pressure heads (h_m) and HYDRUS simulated pressure heads (h_s) in the homogeneous coarse sand when DI water was injected at a rate of 120 cm^3/s for a dosing frequency of 6 min on and 10 s off. The simulated and measured pressure heads did not match when the system reached quasi steady-state.

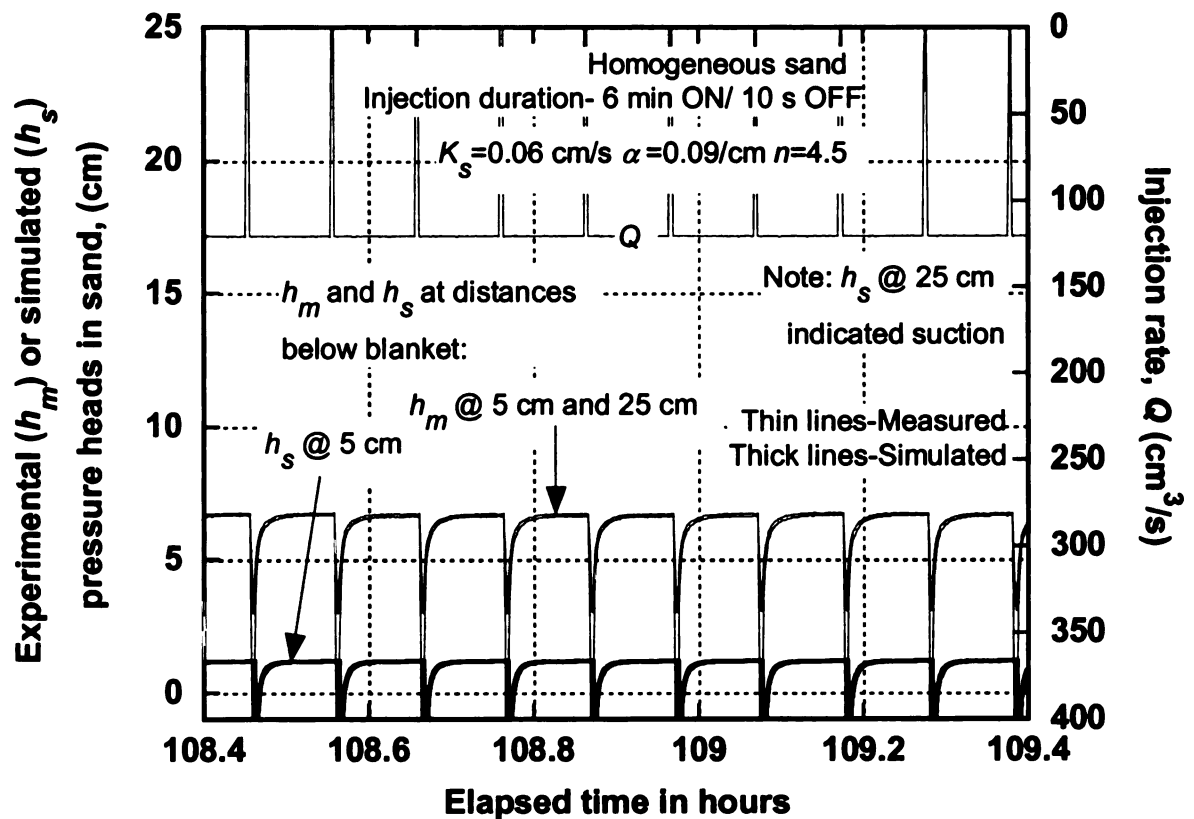


Figure 5-19: Measured and simulated pressure heads in homogeneous sand due to 6 min on and 10 s off injection.

Heterogeneous and Isotropic Sand

Figure 5-20 show the measured pressure heads and HYDRUS simulated pressure heads in various blocks of heterogeneous sand when DI water was injected at a rate of $120 \text{ cm}^3/\text{s}$ for a dosing frequency of 6 min on/10 s off. The simulated and measured pressure heads were relatively close at quasi-steady state in blocks CS32 and DS33 compared to CS23 and CS31. This was because CS32 being next to DS33, air was able to escape laterally through the large pore spaces in DS33 relatively easier than in the other blocks. The simulated pressure head in DS12 showed suction as earlier since the simulation results showed low height of water level in the bottom of DS12.

Figure 5-18 shows that the numerical model was able to confirm the pattern of increase in pressure heads within the sand.

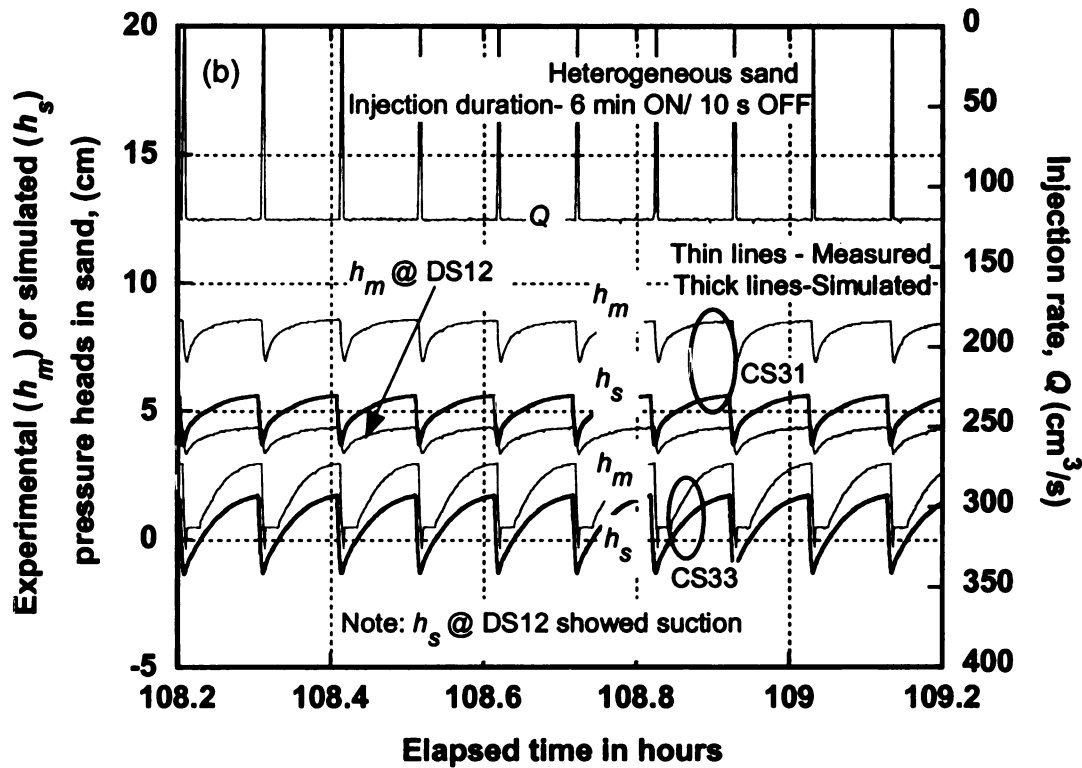
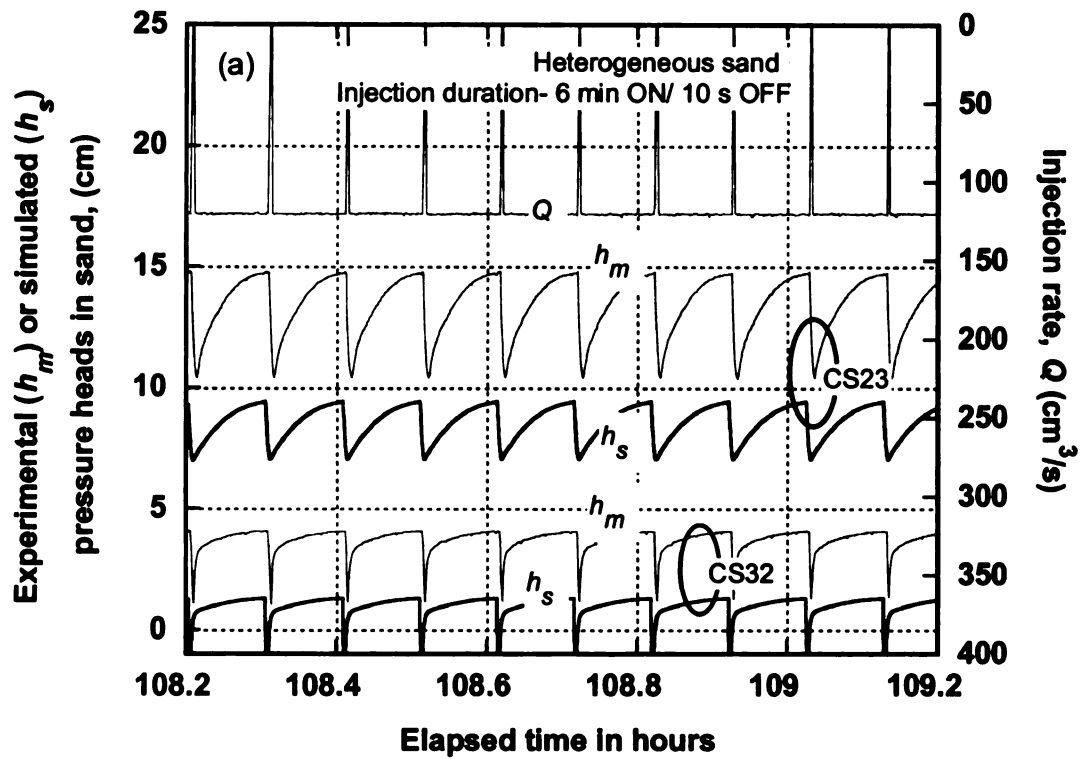


Figure 5-20: Measured and simulated pressure heads in different blocks [(a) and (b)] of heterogeneous sand due to due to 6 min on and 10 s off injection.

Hydrostatic Pressure Heads in Sand

At the end of continuous injection with $Q = 120 \text{ cm}^3/\text{s}$, water was ponded in the landfill model and the hydrostatic pressure heads were compared at different levels within blocks of heterogeneous sand. This was done to check the possibilities of entrapped air bubbles within the matrix since the air bubbles would buoy up the static water level. The ponding event would explain the difference in measured and simulated pressure heads within different blocks in heterogeneous sand.

Figure 5-21 shows the measured hydrostatic pressure heads in all the blocks within the heterogeneous sand. The open symbols represent the measured hydrostatic pressure heads at different depths within the sand due to ponding on the top carried out at the end of continuous injection. The closed symbols represent the hydrostatic pressure heads at different depths within the sand due to ponding carried out after back saturation was carried out in the sand. Water was allowed to enter the sample through one of the seepage pipes at a gradual rate and was allowed to equilibrate over a sufficient amount of time. This back saturation was carried out after a long drying period during which air was injected to dry the soil.

Except in LCS, blanket and DS33 which fell on the straight line of computed hydrostatic pressure heads, the measured hydrostatic pressure heads were higher in all other blocks. The measured hydrostatic pressure head was highest in CS23 after the back saturation event. A possible reason is that large amount of discrete air bubbles that escaped from fine sand block FS13 got entrapped in CS23 which is located directly above FS13 (Figure 5-5). The gradient at which water entered the soil was also not high to flush the bubbles up into DS33. These bubbles were unable to escape and hence contributed to

higher static pressure heads. There was no change in the pressure heads in the coarse sand blocks CS31 and CS32. The relatively accurate match for hydrostatic pressure heads in LCS, blanket and DS33 also rules out the possibilities of the pressure sensors measuring the weight due to soil skeleton. The higher than hydrostatic pressure heads in all the coarse sand blocks CS23, CS31 and CS32 (Figure 5-21) explain the higher pressure heads during dynamic flow due to air entrapment.

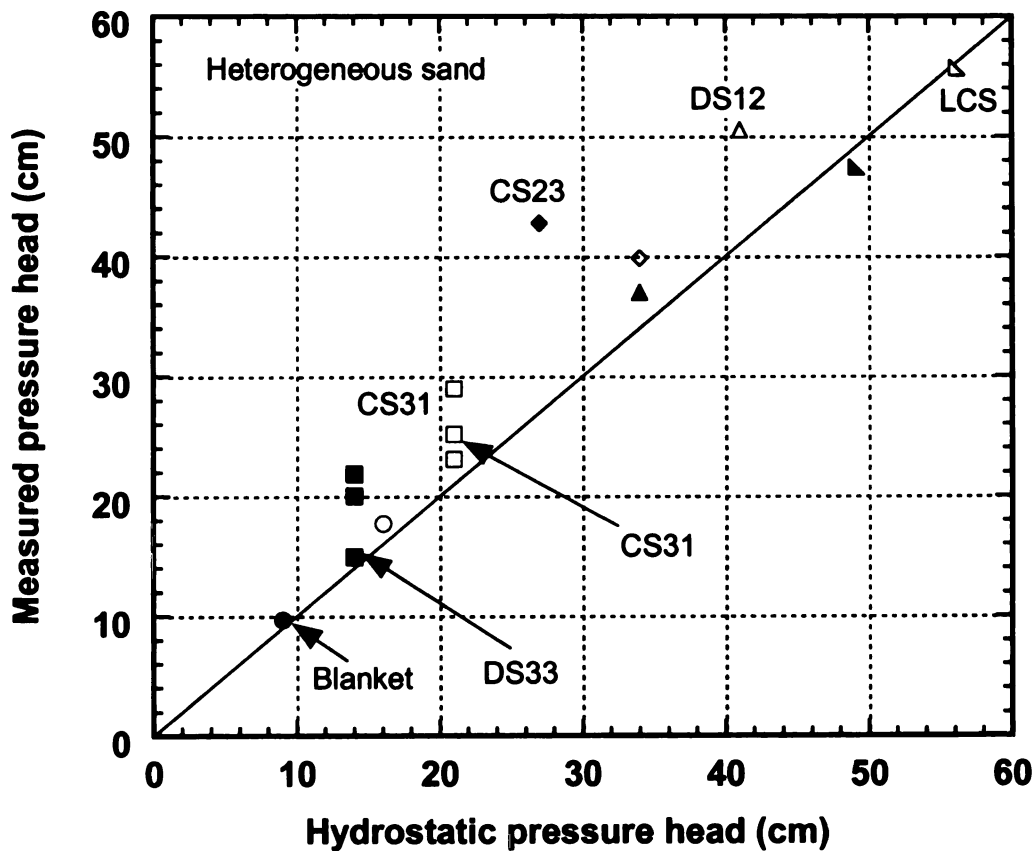


Figure 5-21: Comparison of measured versus estimated hydrostatic pressure heads at different locations in the heterogeneous sand due to static ponding.

ACRES (Analysis of Conductivity in Real-time using Embedded Sensors)

The vertical hydraulic conductivity of the sand located vertically between the blanket and the LCS for a given average degree of saturation was estimated using Equation 5-2:

$$K_{ACRES} = \frac{Q \times D}{W_w \times L \times (D + h_{av})} \quad (5-2)$$

where K_{ACRES} = average hydraulic conductivity of porous material between the blanket and LCS;

Q = Injected flow rate;

D = vertical depth of soil between the blanket and LCS;

L = Length of the blanket parallel to the length of the injection pipe;

W_w = Wetted width of the blanket; and

h_{av} = arithmetic mean of pressure heads, h_m recorded by all the pressure transducers embedded in the blanket.

For a given injection rate Q , given depth of waste D and given length of the blanket L , the wetted width W_w of the blanket and the pressure heads h_m developed in the blanket are the two important parameters which are derived from the responses of the sensors embedded in the blanket. The vertical conductivities at steady-state estimated with ACRES method for homogeneous and heterogeneous sand are compared in Table 5-3.

Table 5-3: K_{ACRES} for heterogeneous and homogeneous sand.

Experiment	Setup	K_{FH} (cm/s)	Injection rate, Q_s (cm ³ /s)	Average pressure heads in blanket , h_{av} (cm)	Wetted width, W_w (cm)	K_{ACRES} (cm/s)	
						Conti- nuous	On/Off
Continuous Injection	Hetero- geneous	0.06	120	2.75	25	0.15	-
	Homo- geneous	0.06	120	1.8	20	0.15	-
6 min on/10 s off	Hetero- geneous	0.06	120	3	25	-	0.15
	Homo- geneous	0.06	120	5.1	50	-	0.075

Analytical Equations

The overall hydraulic conductivity of the heterogeneous sand located vertically between the blanket and the LCS can also be estimated using a set of analytical equations from soil mechanics as shown below (Equations: 5-3 – Equations: 5-5):

$$K_z = \frac{d}{\sum_{i=1}^n d_i / K_i} \quad (5-3)$$

where K_z = equivalent vertical hydraulic conductivity

d = total depth of stratified layers

$$K_x = \sum_{i=1}^n \frac{K_i d_i}{d} \quad (5-4)$$

where K_x = equivalent horizontal hydraulic conductivity

d = total depth of stratified layers

$$K_{eq} = \sqrt{K_x K_y} \quad (5-5)$$

where K_{eq} = resultant hydraulic conductivity

Four cases were considered as shown in Figure 5-19a and Figure 5-19b. The hydraulic conductivity of each block has a subscript of row and column number as per its location in the grid block.

Case 1 - Each column from the original grid of 9 sand blocks was replaced with a column of equivalent horizontal and vertical hydraulic conductivities using Equations 5-3 and 5-4. These three columns were further reduced to a single equivalent soil column with equivalent horizontal and vertical hydraulic conductivities. The resultant hydraulic conductivity was then estimated using Equation 5-5.

Case 2 - Each column from the original grid of 9 sand blocks was replaced with a column of equivalent horizontal and vertical hydraulic conductivities. The resultant hydraulic conductivities for each of these 3 columns were estimated using the equivalent horizontal and vertical hydraulic conductivities. Analogous to electrical circuits, the net equivalent hydraulic conductivity was estimated by connecting them in parallel.

Case 3 - Each row from the original grid of 9 sand blocks was replaced with a row of equivalent horizontal and vertical hydraulic conductivities using Equations 5-3 and 5-4. These three rows were further reduced to a single equivalent soil layer with equivalent horizontal and vertical hydraulic conductivities. The resultant hydraulic conductivity was then estimated using Equation 5-5.

Case 4- Each row from the original grid of 9 sand blocks was replaced with a column of equivalent horizontal and vertical hydraulic conductivities. The resultant hydraulic conductivities for each of these 3 rows were estimated using the equivalent horizontal and vertical hydraulic conductivities. Analogous to electrical circuits, the net equivalent hydraulic conductivity was estimated by connecting them in series.

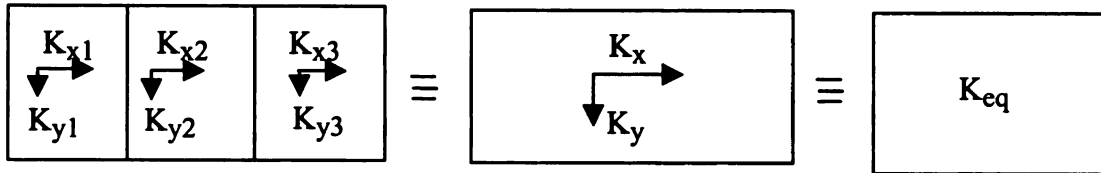
Table 5-4 shows that K_{ACRES} is greater than the range of hydraulic conductivities estimated with analytical equations considering the different cases and from falling head tests. Underestimation of the wetting width is probably the reason for the discrepancies.

Table 5-4: Comparison of hydraulic conductivities.

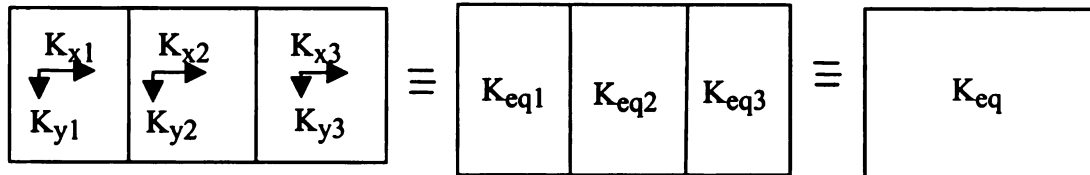
Case no.	Analytical hydraulic Conductivity (cm/s)	Falling head hydraulic conductivity (cm/s)	K_{ACRES} (cm/s)
Case 1	0.091	0.06	0.15
Case 2	0.084		
Case 3	0.062		
Case 4	0.050		

K_{31}	K_{32}	K_{33}
K_{21}	K_{22}	K_{23}
K_{11}	K_{12}	K_{13}

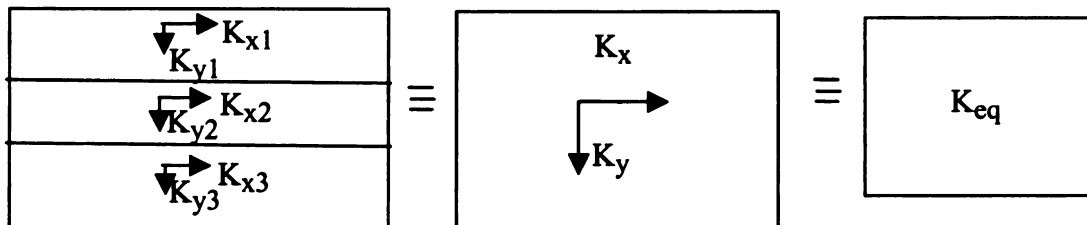
Case 1



Case 2



Case 3



Case 4

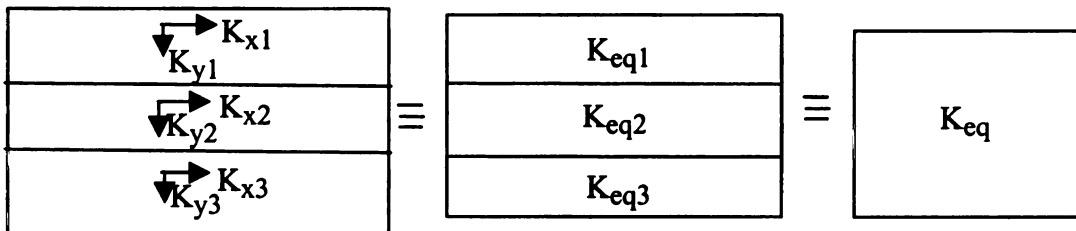


Figure 5-22: Equivalent overall hydraulic conductivity determination.

Field-Scale Simulations

In order to evaluate the effect of daily cover on field-scale implementation of ACRES method landfill cell with daily cover soil layers distributed in a structured manner was simulated. All field simulations were conducted in Vadose/W using the following parameters as input: (1) blanket width = 60 m; (2) blanket depth = 0.15 m; (3) initial degree of saturation of waste, $S = 75\%$; (4) vertical spacing between the blanket and LCS (D) = 15 m; (5) saturated and unsaturated hydraulic properties of blanket, LCS, waste and cover soil layers are presented in Table 5-3.

Figure 5-23 presents the simulated wetted width (W_w) and average pressure head (h_{av}) in the 60-m-wide blanket for liquid dosing frequencies of 2 h on/22 h off, 8 h on/16 h off and continuous, at an injection rate of $400 \text{ m}^3/\text{d}$. The pressure heads, h_{av} , reported here were those obtained when the system reached a dynamic equilibrium, a quasi steady-state for on/off dosing. At the stage of dynamic equilibrium, the outflow reached a steady value which may be lower than the inflow; the pressure heads in the blanket reached a constant value during the injection period and the total water content of the waste over a cycle remained constant although it redistributed itself within the waste mass. Greater the on to off duration ratio, greater was the magnitude of h_{av} . The wetted width W_w was also a function of the ratio of on to off leachate injection duration. The wetted width of waste was greater for a dosing cycle where the on to off times ratio was greater. The average pressure head h_{av} and the wetted widths were highest during continuous injection.

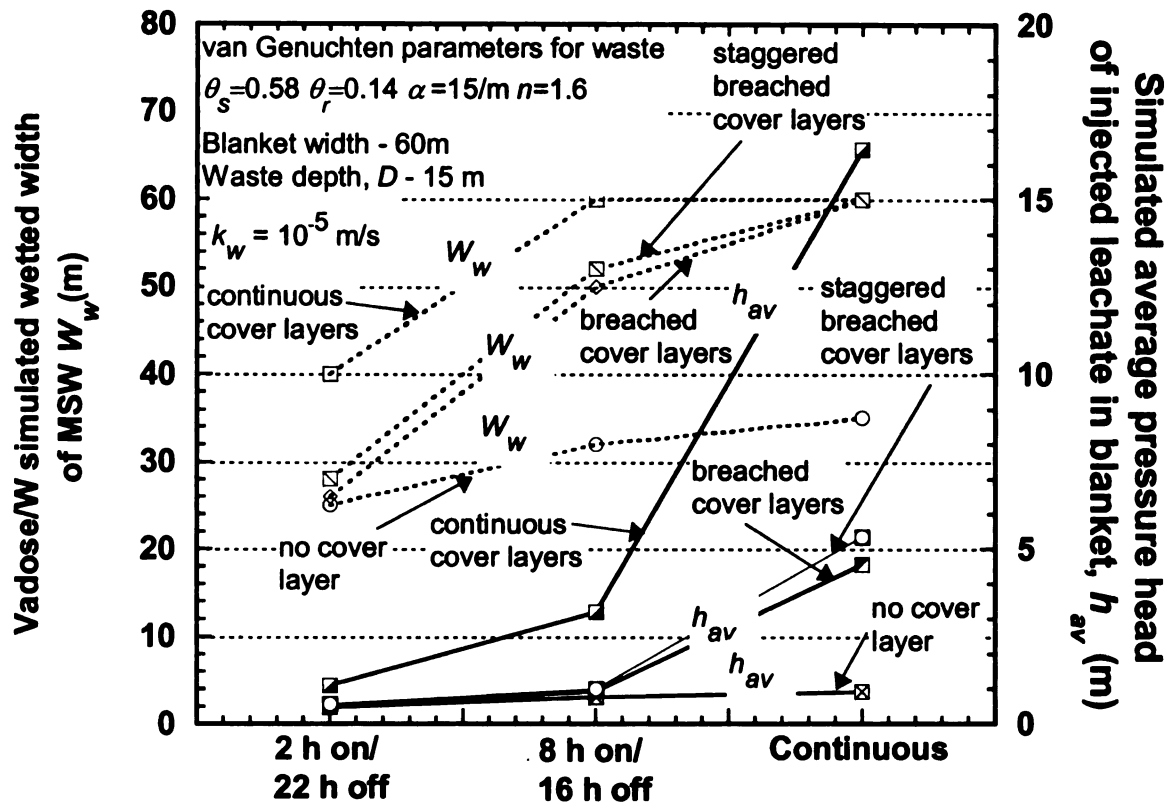


Figure 5-23: Simulated wetted width and average pressure heads of injected leachate in blanket for various dosing frequencies.

Figure 5-23 shows that the location, selection and application of daily cover soil layers affect the pressure heads and wetted widths. Low conductivity silty soil, used as a continuous daily cover impeded vertical movement of leachate resulting in relatively high pressure heads for continuous injection. The wetted width covered almost the entire domain of 100 m although the wetted width shown in Figure 5-23 was limited to 60 m.

Once the cover layer was breached at 2 m intervals, it allowed faster vertical flow in the waste and hence reducing the pressure heads in the blanket. Simulations showed that saturated lenses of leachate perched above the breached cover soil layers. Leachate channeled vertically through the breached daily cover and moved downwards. The

location of the breaches in the cover soil layer hence had an effect on leachate routing. This finding is consistent with McCreanor (1998). Perched leachate exists in landfills. Zhan *et al.* (2008) reported perched leachate mound above the intermediate cover of soils through the field measurements of pore pressures within the landfill.

K_{ACRES} was estimated using Equation 5-2 for various configuration of cover soil layers. Where the wetted width W_w was beyond the blanket width, the blanket width was considered for estimation of K_{ACRES} because it would be difficult to estimate the wetted width in field without instrumentation in the waste if it is beyond the blanket width. Estimated K_{ACRES} was lower than input waste hydraulic conductivity for all the cases. This was because the effective vertical hydraulic conductivity reduced due to the presence of daily cover layers.

Figure 5-24 presents estimated K_{ACRES} for various configurations of daily cover soil layers. It is observed that there is a range within which the equivalent ACRES estimated vertical hydraulic conductivity of a landfill with daily cover layer soils is expected to fall. The upper boundary is the hydraulic conductivity of waste only and the lower boundary depicts the hydraulic conductivity from the scenario where continuous daily cover soil layers are placed (without breaching). The vertical hydraulic conductivity estimated by ACRES for all other scenarios with breached cover soil layers, no matter how they are placed, is expected to be lower than the waste conductivity alone and would fall within the range defined by the boundaries.

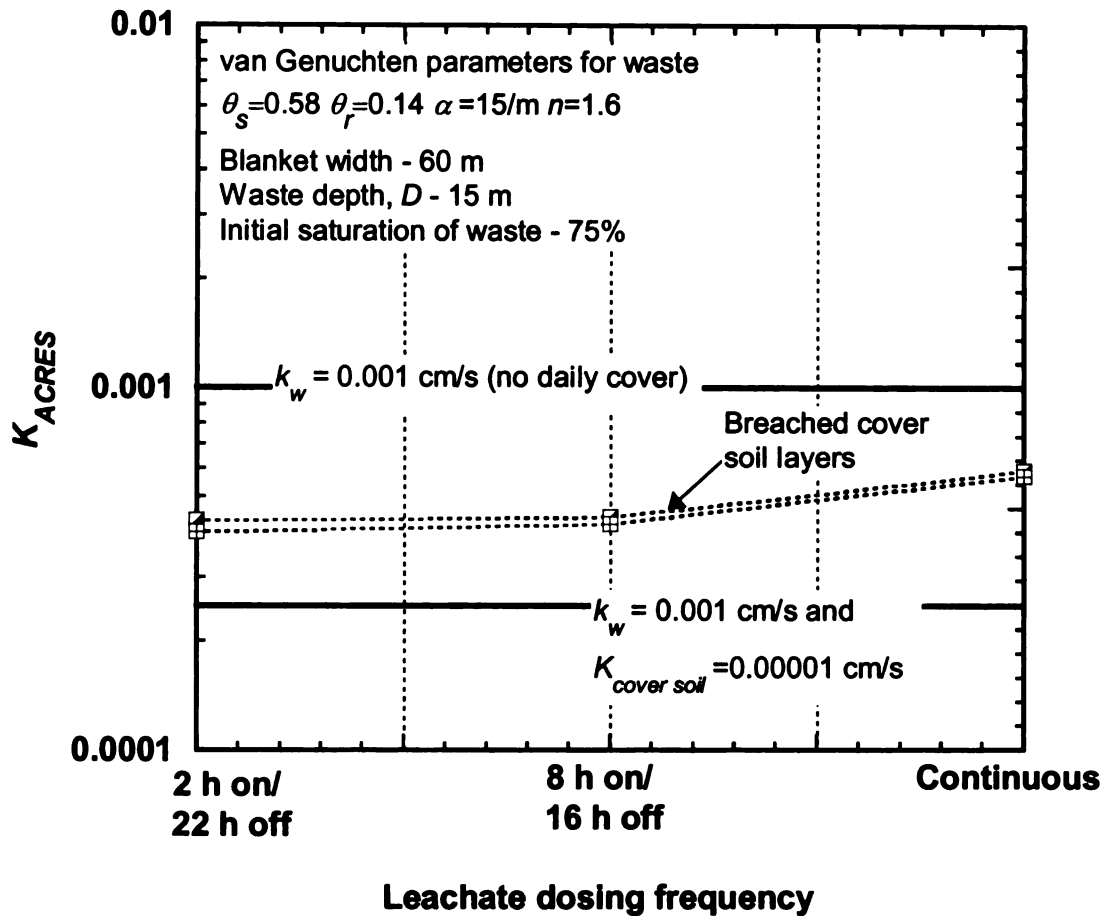


Figure 5-24: K_{ACRES} for various configurations of daily cover layers within waste for various dosing frequencies

SUMMARY AND CONCLUSIONS

The key objective of this study was to confirm the numerical models for subsurface flow within heterogeneous soil and compare the hydraulics of flow between homogeneous and heterogeneous soil when water was injected at the same rate in both. Water was injected at a continuous rate of $120\text{ cm}^3/\text{s}$ and at a dosing frequency of 6 min on/10 s off. The hydraulic pressure heads and water content in blanket and in the underlying porous media due to liquid injection were monitored by sensing system. The key conclusions of this

study are as follows:

- The pressure heads developed in the blanket depended on the vertical hydraulic conductivity of the layer of soil immediately below it. Thus, the pressure heads developed reflected the vertical hydraulic conductivity of the underlying material.
- Entrapment of air dominating the infiltration and influencing the pore water pressures was found to be more pronounced in homogeneous soil. The presence of interconnected regions of high hydraulic conductivity and low air entry suction within a heterogeneous porous medium facilitated the escape of pore air. The presence of pore air within soil influenced the hydraulic conductivity and hence dictated the pressure heads and increase in water contents within the soil.
- Presence of air in the sand that could not be completely removed during injection resulted in measured pressure heads greater than hydrostatic pressure head.
- The numerical models HYDRUS-2D and Vadose/W were able to predict pressure heads and water contents accurately when the pore air pressures were negligible.
- For a simulated field-scale landfill containing daily cover soil layers of low hydraulic conductivity, the vertical hydraulic conductivity estimated by ACRES was within the range of saturated waste hydraulic conductivity and the equivalent hydraulic conductivity of waste and stratified continuous cover soil layers.

SUMMARY AND CONCLUSIONS

The key objectives of this dissertation were to: (1) develop an instrumented landfill model with permeable blanket as liquid recirculation system to study subsurface hydraulics; (2) develop a new method for estimation of hydraulic conductivity of subsurface underlying an instrumented blanket using pressure head and flow data from sensors embedded in the blanket; and (3) test the predictive capabilities of numerical models used for subsurface injections. To achieve these objectives, a laboratory-scale model consisting of a blanket underlain by sandy soils and a liquid collection system was developed. Numerical modeling of flow through the model was carried out using saturated/unsaturated finite element models- HYDRUS-2D and Vadose/W.

The key findings of this study are as follows:

1. Liquid injection could be simulated in a 2-D lab-scale model to carry out controlled experiments. The landfill model was able to simulate steady-state and transient conditions. The landfill model was able to mimic the responses from a field-scale instrumented permeable blanket.
2. The key parameters that influence hydraulic pressure head in the blanket were: (1) liquid injection rate; (2) the vertical hydraulic conductivity of subsurface; (3) degree of saturation of the subsurface; and (4) presence of entrapped air within the subsurface.
3. The advance of saturated wetting front within the subsurface depends on the hydraulic properties of the underlying material, injection flow rate, and content of entrapped air.

4. The pressure heads in the blanket and the soil water content distributions within the sand predicted with HYDRUS-2D and Vadose/W, were in good agreement with the experimental data at steady-state. Air entrapment resulting in air pressure build up was the key reason for discrepancies between experimental and numerically simulated pressure heads and water contents. Multiphase flow approach should be adopted for simulating liquid flow in subsurface with air pressures taken into account in the flow equations.
5. Flow rate and pressure head data measured in an instrumented permeable blanket on a continuous basis can be used to estimate vertical hydraulic conductivity of waste (for landfill application) or underlying subsurface. However, the accuracy of the estimation will depend upon the rate and frequency of injection. Higher the rate and frequency, more accurate will the estimates be.
6. In field-scale waste domain with daily cover layers of low hydraulic conductivity, the estimated vertical hydraulic conductivity will be lower than the saturated waste hydraulic conductivity.

REFERENCES

- Al-Yousfi, B.A., Pohland F.G., and Vasuki, N.C. (1992). Design of landfill leachate recirculation systems based on flow characteristics. Proceedings of the 47th Purdue University Industrial Waste Conference Proceedings, Purdue University, West Lafayette, Indiana, 191-200.
- Al-Yousfi, B.A. and Pohland, F.G. (1998). Strategies for simulation, design and management of solid wastes disposal sites as landfill bioreactors. Practice Periodical of Hazardous, toxic and radioactive waste management, January 1998.
- ASTM, Standard D 2434-68, Standard test method for permeability of granular soils (Constant head), Annual Book of ASTM Standards, Vol. 4(8). ASTM International, West Conshohocken, PA.
- ASTM, Standard D 5084-03, Standard test methods for measurement of hydraulic conductivity of saturated porous materials using a flexible wall permeameter, Annual Book of ASTM Standards, Vol. 4(8). ASTM International, West Conshohocken, PA.
- ASTM, Standard D 6836-02, Standard test methods for determination of the soil water characteristic curve for desorption using a hanging column, pressure extractor, chilled mirror hygrometer, and/or centrifuge, Annual Book of ASTM Standards, Vol. 4(9). ASTM International, West Conshohocken, PA.
- Bachus, R., Jaber, J. and Harris, J. (2002). Guidance for Bioreactor Design. Proceedings of the abstracts from 2nd International Landfill Research Symposium, October, Asheville, NC, 59-60.
- Barber, C., Maris, P. J. (1983). Recirculation of leachate as a landfill management option: benefits and operational problems. Quarterly Journal of Engineering Geology, 17(1) 19-29.
- Beaven, R.P., and Powrie, W. (1995), Hydrogeological & Geotechnical Properties of Refuse Using a Large-Scale Compression Cell, Proceedings of Sardinia 95, Fifth International Landfill Symposium, Italy, Oct. 2-6.
- Beck, R.W. (2002). 2002 annual report: facility SW-376. Crow Wing County MMSW Landfill.
- Bendz, D. (1998). Generation of Leachate and the Flow Regime in Landfills. Report No 1023, Department of Water Resources Engineering, Lund University, Sweden.

- Benson, C. H., Gunter, J. A., Boutwell, G. P., Trautwein S. J., and Berzanskis, P. H. (1997). Comparison of four methods to assess hydraulic conductivity. *J. Geotech. and Geoenviron. Engrg.* 123, 929.
- Benson, C. H. (2000). Liners and covers for waste containment, *Proceedings of the Fourth Kansai International Geotechnical Forum, Creation of a New Geo-Environment*, Japanese Geotechnical Society, Kyoto, Japan. 1–40.
- Benson, C. H., Barlaz, M.A., Lane, D.T., and Rawe, J.M. (2007). Practice review of five bioreactor/recirculation landfills. *Waste Management*, 27, 13-29.
- Bleiker, D.E., McBean, E. and Farquhar, G. (1993). Refuse sampling and permeability testing at the Brock West and Keele Valley landfills. *Proceedings of the Sixteenth International Madison Waste Conference*, 548-567.
- Bleiker, D., Farquhar G., and McBean, E. (1995). Landfill settlement and the impact on site capacity and refuse hydraulic conductivity. *Waste Management and Research*, Vol. 13, 533-554.
- Bou-Zeid, E., and El-Fadel, M. (2004). Parametric sensitivity analysis of leachate transport simulations at landfills. *Waste Management*, 24(7), 681-689.
- Chang, H., and Gagnard, P. (1995). Field evaluation of leachate recirculation system. *Groundwater Quality: Remediation and Protection (Proceedings of the Prague Conference)* Publ. no. 225.
- Chen, T., and Chynoweth, D. P. (1995). Hydraulic conductivity of compacted municipal solid waste. *Bioresour. Technol.*, 51(2–3), 205–212.
- Chen, Y., Zhan, T., Ling, W. (2008). Mechanical properties of municipal solid waste from Suzhou landfill in China. *Geotechnical Special Publication no. 177, Proceedings of Geocongress 2008*, p 160.
- Childs, E. C. (1969). *An introduction to the physical basis of soil water phenomena*. John Wiley and sons ltd.
- Christiansen, J.E. (1944). Effect of entrapped air upon the permeability of soils. *Soil Sci*: 58: 355-365.
- Demetracopoulos, A. C., and Korfiatis, G. P. (1983). Modeling water movement through sanitary landfills. *Proc., Frontiers in Hydraulic Engineering*, ASCE, New York, 54–59.
- Demetracopoulos, A. C., and Korfiatis, G. P., Bourodimos, E. L., Nawy E. G. (1986) Unsaturated flow through solid waste landfills: model and sensitivity analysis. *Journal of the American Water Resources Association* 22 (4), 601–609.

- Dixon, R. M. and Linden, D. R. (1972). Soil air pressure and water infiltration under border irrigation. *Soil Sci. Soc. Am. Proc.*, Vol. 36, pp. 948-953.
- Doran, F. (1999). Lay leachate lay. *Waste Age*, April, 74-79.
- Dunnicliff, J., (1988). *Geotechnical instrumentation for monitoring field performance*, John Wiley, New York.
- Dixon, N. and Jones, D.R.V. (2005). Engineering properties of municipal solid waste. *Geotextiles and Geomembranes*, Vol 23(3) 205 - 233, ISSN 0266-1144.
- El-Fadel, M. (1999). Leachate recirculation effects on settlement and biodegradation rates in MSW landfills. *Environ. Technol.*, 20(2), 121-133.
- Ettala, M. (1987). Infiltration and hydraulic conductivity at a sanitary landfill. *Aqua Fennica*, 17(2), 231-237.
- Fayer, M.J., and Hillel, D. (1986). Air encapsulation: I. Measurement in a field soil. *Soil Sci. Soc. Am. J.* 50:568-572.
- Fellner, J., Huber, R., Döberl, G., and Brunner, P. (2003). Hydraulics of MSW landfills and its implications for water flow modeling. *Proceedings of Ninth International Waste Management and Landfill Symposium*, Sardinia, Italy, October.
- Findikakis, A., Papelis, P., Halvadakis, C., Leckie, J. (1988). Modelling gas production in managed sanitary landfills. *Waste Management and Research* 6, 115.
- Fluhler, H., Peck, A. J., and Stolzy, L. H.. (1986). Air pressure measurement. In A. Klute, (ed.) *Methods of Soil Analysis*, Part 1. 2nd Ed. *Agronomy* 9:1161-1172.
- Free, G. R. and Palmer, V. J. (1940). Inter-relationship of infiltration, air movement and pore size in graded silica sand. *Soil Sci. Soc. Am. Proc.*, Vol. 5, 390-398.
- Fredlund, D., and Xing, A. (1994). Equations for the Soil-Water Characteristic Curve. *Canadian Geotechnical J.*, 31: 521-532.
- Fredlund, D., Xing, A., and Huang, S. (1994). Predicting the Permeability Function for Unsaturated Soils Using the Soil-Water Characteristic Curve. *Canadian Geotechnical J.*, 31: 533-546.
- Fredlund, D. and Rahardjo, H. (1993). *Soil Mechanics for unsaturated soils*. John Wiley and Sons. P 31.

- Fungaroli, A., and Steiner, R. (1979). Investigation of sanitary landfill behavior. Vol. 1, Final Report, U.S. EPA 600/2-79-053a.
- Geo-Slope (2004). Vadose Zone Modeling with Vadose/W 2004: An Engineering Methodology. GEO-SLOPE International Ltd, Alberta, Canada.
- Geo-Slope (2007). Vadose Zone Modeling with Vadose/W 2007: An Engineering Methodology. GEO-SLOPE International Ltd, Alberta, Canada.
- Giroud, J., and Houlihan, M. (1995). Design of leachate collection layers. Proceedings of the Fifth Sardinia Solid Waste Conference, Cagliari, Italy, Oct. 1995, 2, 613-640.
- Giroud, J. P., Zornberg J.G., and Zhao, A. (2000a). The myth of hydraulic transmissivity equivalency between geosynthetic and granular liquid collection layers, Geosynthetics International, Special issue on liquid collection systems, 7(4-6), 381-401.
- Giroud, J. P., Zornberg J.G., and Zhao, A. (2000b). Hydraulic design of geosynthetic and granular leachate collection layers, Geosynthetics International, Special issue, Vol. 7, 4-6, 285-380.
- Grismer, M.E., Orang, M.N., Clausnitzer, V. and Kinney, K. (1994). Effects of air compression and counterflow of infiltration into soils. Journal of Irrigation and Drainage Engineering, 120 (4), 775-795.
- Gupta, R.P., and Swartzendruber, D. (1964). Entrapped air content and hydraulic conductivity of quartz sand during prolonged liquid flow. Soil Sci. Soc. Am. J. 28:9-12.
- Hammecker, C., Antonino, A. C. D., Maeght, J. L., and Boivin, P. (2003). Experimental and numerical study of water flow in soil under irrigation in northern Senegal: evidence of air entrapment. European Journal of Soil Science, Vol. 54, pp. 491-503.
- Hao C., and Gagnard, P. E. (1995). Field evaluation of leachate recirculation system. Groundwater Quality: Remediation and Protection – Proceedings of the Prague Conference, May 1995, IAHS Publ. no. 225.
- Haydar, M. M., and Khire, M. V. (2004). Numerical evaluation of heterogeneity and anisotropy of waste properties on leachate recirculation in bioreactor landfills. The Journal of Solid Waste Management & Technology, 30(4), 233- 243.
- Haydar, M. M. and Khire, M.V. (2005). Leachate recirculation using horizontal trenches in bioreactor landfills. Journal of Geotechnical and Geoenvironmental Engineering, 131(7), 837-847.

- Haydar, M. M. (2005). Leachate recirculation in bioreactor landfills: Field-scale testing and modeling. Ph.D. dissertation, Michigan State Univ., E. Lansing, Mich.
- Haydar, M. and Khire, M. (2006). Geotechnical sensor system to monitor injected liquids in landfills," *Geotechnical testing journal*, ASTM, 29(1), 37-44.
- Haydar, M. and Khire, M., (2007). Leachate recirculation using permeable blankets in engineered landfills," *Journal of Geotechnical & Geoenvironmental Engineering*. 133(4), 360-37.
- Henry, E.J., Smith, J. E. and Warrick, A. W. (2002). Two-dimensional modeling of flow and transport in the vadose zone with surfactant-induced flow. *Water Resources Research*, 38(11), 331-336.
- Hendron, D., Fernandes, G., Prommer, P., Giroud, J., Orozco, L. (1999). Investigation of the Cause of the 27 September 1997 Slope Failure of the Dona Juana Landfill. *Proceedings of the Seventh International Sardinia Waste Management and Landfill Symposium*, Cagliari, Italy, Oct, pp. 545-554.
- Hillel, D. (1998). *Environmental Soil Physics*. Academic Press, 771 pgs.
- Hossain, M.S., Gabr, M.A., Barlaz, M.A. (2003). Relationship of compressibility parameters to municipal solid waste decomposition Source. *Journal of Geotechnical and Geoenvironmental Engineering*, 129(12), p 1151-1158.
- Hossain, S., Penmestha, K., Hoyos, L. (2008). Permeability of municipal solid waste (MSW) in bioreactor landfill with degradation. *Geotechnical Special Publication no. 177, Proceedings of Geocongress 2008*, p 120.
- Hughes, G., Landon, R. and Farvolden, R. (1971). Hydrogeology of waste disposal sites in Northeastern Illinois. *EPA Solid Waste Management Series*, SW-12d.
- Hsieh, P., W. Wingle, and Healy, R. (2000). VS2DI-A graphical software package for simulating fluid flow and solute or energy transport in variably saturated porous media. *U.S. Geological Survey Water-Resources Investigations Report 99-4130*, 16 p.
- Imhoff, P. T. Jakubowitch, A., Briening, M. L., Chiu, P. C. (2003). Partitioning Gas Tracer Tests for Measurement of Water in Municipal Solid Waste. *Journal of the Air and Waste Management Association*, 53(11), p 1391-1400.
- Imhoff, P.T., Reinhart, D. R., Englund, M., Guerin, R., Gawande, N., Han, B., Jonnalagadda, S., Townsend, T. G., Yazdani, R. (2007). Review of state of the art methods for measuring water in landfills. *Waste Management*, 27, 729-745.

- Jain, P., Powell, J., Townsend, T. G., Reinhart, D. R. (2005). Moisture addition at a bioreactor landfill using vertical wells, *Journal of Environmental Engineering*, ASCE, in review.
- Jain, P., Farfour, W., Jonnalagadda, S., Townsend, T., Reinhart, D. (2005). Performance evaluation of vertical wells for landfill leachate recirculation *Geotechnical Special Publication*, n 130-142, *Geo-Frontiers 2005*, 3789-3798.
- Jain, P., Powell, J., Townsend, T. G., Reinhart, D. R. (2006). Estimating the hydraulic conductivity of landfilled municipal solid waste using the borehole permeameter test, *Journal of Environmental Engineering*, v 132, n 6, June, 2006, p 645-652.
- Jang, Y.-S. (2000). Analysis of flow behavior in a landfill with cover soil of low hydraulic conductivity. *Environmental Geology*, 39(3), p 292-298.
- Jang, Y. S., Kim, Y. W., and Lee, S. I. (2002). Hydraulic properties and leachate level analysis of Kimpo Metropolitan landfill, Korea. *Waste Management*, 22(3), 261-267.
- Kazimoglu, Y.K., McDougall, J.R., Pyrah, I.C. (2006). Unsaturated hydraulic conductivity of landfilled waste. *Geotechnical Special Publication*, n 147, *Proceedings of the Fourth International Conference on Unsaturated Soils*, p 1525-1534.
- Khire, M., Benson, C., and Bosscher, P. (1997). Water balance modeling of final covers. *Journal of Geotechnical and Geoenvironmental Engineering*, ASCE, 123(8), 744-754.
- Khire, M., Benson, C., and Bosscher, P. (1999). Field Data from a Capillary Barrier and Model Predictions with UNSAT-H. *J. Geotechnical and Geoenv. Engrg.*, 125 (6): 518-527.
- Khire, M.V. and Haydar, M. M. (2003). Numerical evaluation of granular blankets for leachate recirculation in MSW landfills. *Proceedings of the Ninth Sardinia Solid Waste Conference*, Cagliari, Italy, Oct.
- Khire, M., Haydar, M. and Mukherjee, M. 2006. Liquid head on landfill liners due to leachate recirculation. *Proceedings of Geocongress 2006*, Feb26-Mar1, Atlanta, GA.
- Khire, M. and Mukherjee, M., (2007). Leachate injection using vertical wells in bioreactor landfills. *Waste Management*, 27(9),1233-1247.
- Khire, M.V. and Haydar, M. M. (2007).Leachate recirculation in bioreactor landfills using geocomposite drainage material. *Journal of Geotechnical and Geoenvironmental Engineering*, 133(2), 166-174.

- Khire, M.V. and Mijares, R. G. (2008). Influence of the Waste Layer on Percolation Estimates for Earthen Caps Located in a Sub-humid Climate. Geotechnical Special Publication no. 177, Proceedings of Geocongress 2008, p 88.
- Kilmer, K. (1991). Leachate recycling: an alternative landfill management technology. Solid Waste & Power, December 1991.
- Koerner, R.M. and Soong, T.-Y. (2000). Leachate in landfills: the stability issues. Geotextiles and Geomembranes, 18(5), p 293-309.
- Komilis, D. P., Ham, R. K., and Stegmann, R. (1999). The effect of landfill design and operation practices on waste degradation behavior: A review. Waste Manage. Res., 17(1), 20–26.
- Korfiatis, G., Demetracopoulos, A., Boudrodimos, E. and Nawy, E. (1984). Moisture transport in a solid waste column. Journal of Environmental Engineering, 110(4), 789-796.
- Landva, A. O., Pelkey, S. G., and Valsangkar, A. J. (1998). Coefficient of permeability of municipal refuse. Proc., 3rd Int. Congress on Environmental Geotechnics, Lisbon, Portugal, 163–167.
- Leachator (2004). www.solidwaste.com.
- Lu, N. and Likos, W. J. (2004). Unsaturated soil mechanics. John Wiley and sons.
- Lugomela, G. V. (2007). Two-phase flow numerical simulation of infiltration and groundwater drainage in a rice field. Physics and Chemistry of the Earth, Vol. 32, 1023-1031.
- Maier, T. and Vasuki, N. (1996). Expected benefits of a full-scale bioreactor landfill. Proceedings of Wastecon 1996, Portland, USA, 179-185.
- McCreanor, P. (1998). Landfill leachate recirculation systems: mathematical modeling and validation. Ph.D. Dissertation, University of Central Florida, Orlando, FL.
- McCreanor, P. and Reinhart D. (1998). Hydrodynamic modeling of leachate recirculating landfills. Proceedings of Swedish Landfill Symposium, Bioreactor Technology Session, Oct.
- McCreanor, P. T., and Reinhart, D. R. (1996). Hydrodynamic modeling of leachate recirculating landfills. Water Sci. Technol., 34(7–8), 463–470.
- McCreanor, P. and Reinhart, D. (2000). Mathematical modeling of leachate routing in a leachate recirculating landfill. Water Resources. Vol. 34(4), 1285-1295.

- Meerdink, J. S., Benson, C. H. and Khire, M. V. (1996). Unsaturated hydraulic conductivity of two compacted barrier soils. *Journal of Geotechnical Engineering*. Vol. 122, no. 7, 565-576.
- Mehta, R., Barlaz, M., Yazdani, R., Augenstein, D., Bryars, M. and Sinderson, L. (2002). Refuse decomposition in the presence and absence of leachate recirculation. *Journal of Environmental Engineering*, 128(3), 228-236.
- Merry, S, Fritz, W., Budhu, M., Krzyszof, J. (2005). The effect of gas on pore pressures in wet landfills. *Journal of Geotechnical and Geoenvironmental Engineering*. 132(5), 553-561.
- Merry, S, Fritz, W., Budhu, M., Kavazanjian, E. (2005). Reconnaissance of the July 10, 2000, Payatas Landfill failure. *Journal of Performance of Constructed Facilities*, 19(2), 100-107.
- Merritt, C. A. (1992). Full scale leachate recycling at an industrial landfill. *Proceedings of 65th Annual Conference & Exposition*, Sept. 20-24, New Orleans.
- Miller, D., and Emge, S. (1997). Enhancing landfill leachate recirculation system performance. *Practice Periodical of Hazardous, Toxic, and Radioactive Waste Management*, July, 113-119.
- Moody, L.F. (1944). Friction factor for pipe flow. *ASME Transactions*, Vol. 66, 671.
- Morris, J., Vasuki, N., Baker, J., Pendleton, C. (2003). Findings from longterm monitoring studies at MSW landfill facilities with leachate recirculation. *Waste Management* 23 (7), 653–666.
- Mualem, Y. (1976). A new model for predicting the hydraulic conductivity of unsaturated porous media. *Water Resources Research*, Vol. 12, 513-522.
- Mukherjee, M., Khire, M., Qian, X. (2008). Lab-scale liquid injection model of bioreactor landfill. *Geotechnical Special Publication no. 177, Proceedings of Geocongress 2008*, p 272.
- Nastev, M., Therrien, R.; Lefebvre, R.; Gelinas, P. (2001). Gas production and migration in landfills and geological materials, *Journal of Contaminant Hydrology*, v 52, n 1-4, p 187-211.
- Noble, J. and Arnold, A. (1990). Experimental and Mathematical modeling of moisture transport in landfills. *Eng. Comm* 1991, Vol. 100, 95-111.

- Olivier, F., Gourc, J., (2007). Hydro-mechanical behavior of municipal solid waste subject to leachate recirculation in a large-scale compression reactor cell. *Waste Management*, Vol. 27, 44-58.
- Oreskes, N., Shrader-Frechette, K., and Belitz, K. (1994). Verification, validation and confirmation of numerical models in the earth sciences. *Science*, 263(4), 641-646.
- Oweis, I., Smith, D., Ellwood, R. and Greene, D. (1990). Hydraulic characteristics of municipal refuse. *Journal of Geotechnical Engineering*, 116(4), 539-553.
- Oweis, I. S. and R. P. Khera. (1990). *Geotechnology of waste management*. Butterworth & Co., London.
- Pacey, J., Augenstein, D., Morck, R., Reinhart, D. and Yazdani, R., (1999). Bioreactive landfill, *MSW Management* (Sept/Oct), pp. 53–60.
- Pang, L., Close, M., Watt, J. and Vincent, K. (2000). Simulation of picloram, atrazine, and simazine leaching through two New Zealand soils and into groundwater using HYDRUS-2D. *Journal of Contaminant Hydrol.* , 44(1), 19-46.
- Peck, A., J. (1969). Entrapment, stability, and persistence of air bubbles in soil water. *Aust. J. Soil Res.*, 1969,7,79-90
- Pohland, F., (1980). Leachate recycle as a landfill management option. *Journal of the Environmental Engineering Division* 106 (6), 1057.
- Pohland, F., Harper, S., Chang, K., Dertien, J., Chian, E. (1985). Leachate generation and control at landfill disposal sites. *Water Pollution Research Journal of Canada*, 20(3), 10-24.
- Powrie, W. and Beaven, R. (1999). Hydraulic properties of household waste and implications for liquid flow in landfills. *Proceedings of the Institution of Civil Engineers, Geotechnical Engineering Association*, 137(4), 235–247.
- Powrie, W., Hudson, A. P. and Beaven, R. (2000). Development of sustainable landfill practices and engineering landfill technology. Final report to the Engineering and Physical Sciences Research Council, February.
- Powrie, W., Beaven, R., Hudson, A., (2008). The influence of landfill gas on the hydraulic conductivity of waste. *Geotechnical Special Publication no. 177, Proceedings of Geocongress 2008*, p 264.
- Phuc, L.V. and Morel-Seytoux, H. J. (1972). Effect of soil air movement and compressibility on infiltration rates. *Soil Sci. Soc. Am. Proc.*, Vol. 36, 237-241.
- Qian, X., Koerner, R. and Gray, D. (2002). *Geotechnical aspects of landfill design and construction*. Prentice Hall, New Jersey.

- Rassam, D., and Cook, F. (2002). Numerical simulations of water flow and solute transport applied to acid sulfate soils. *J. Irrig. Drain. Eng.*, 128(2), 107-115.
- Reddy, K., Gangathulasi, J., Hettiarachchi, H., Bogner, J. (2008) Geotechnical Properties of Municipal Solid Waste Subjected to Leachate Recirculation. Geotechnical Special Publication no. 177, Proceedings of Geocongress 2008, p 144.
- Reinhart, D.R., and Carson, D. (1993). Experiences with full-scale application of landfill bioreactor technology. The 31st Annual Solid Waste Exposition of the Solid Waste Association of North America. San Jose. California, Aug 2-5.
- Reinhart, D. R., McCreanor, P. T. and Noor, Q. (1996). The hydrodynamics of leachate in recirculating landfills. Proceedings from SWANAs 1st Annual Landfill Symposium, Wilmington, Delaware, November 4-6.
- Reinhart, D., McCreanor, P., Townsend, T., (2002). The bioreactor landfill: Its status and future. *Waste Management and Research* 20 (2), 162–171.
- Reinhart, D., Al-Yousfi, A. B. (1996). Impact of leachate recirculation on municipal solid waste landfill operating characteristics. *Waste Management & Research*, v 14, n 4, 337-346.
- Richards, L. (1931). Capillary conduction of liquids in porous medium. *Journal of Physics*, 318-333.
- Rosqvist H. and Destouni G. (2000). Solute transport through preferential pathways in municipal solid waste. *Journal of Contaminant Hydrology*, Vol. 46, 39-60.
- Sakaguchi, A., Nishimura, T. and Kato M. (2005). The Effect of Entrapped Air on the Quasi-Saturated Soil Hydraulic Conductivity and Comparison with the Unsaturated Hydraulic Conductivity. *Vadose Zone Journal* 4:139–144.
- Scanlon, B., Christman, M., Reedy, R., Porro, I., Simunek, J. and Flerchinger, G. (2002). Intercode comparisons for simulating water balance of surficial sediments in semiarid regions. *Water Resources Research*, 38(12), 5901-5915.
- Schroeder, P., Lloyd, C., and Zappi, P. (1994). The Hydrologic Evaluation of Landfill Performance (HELP) Model, User's Guide for Version 3.0, U.S. Environmental Protection Agency, Cincinnati, OH.
- Seymour, R. M. (2000). Air entrapment and consolidation occurring with saturated hydraulic conductivity changes with intermittent wetting. *Irrigation Sci.*, 20(1): 9-14.

- Shank, K. L. (1993). Determination of hydraulic conductivity of the Alachua County Southwest Landfill. Master's thesis, Univ. of Florida, Gainesville, Fla.
- Simunek, J., Sejna, M. and van Genuchten, M.Th. (1999). The HYDRUS-2D software package for simulating the 2-D movement of water, heat, and multiple solutes in variably Saturated media Version 2.0, U.S. Salinity Laboratory, Agriculture Research Service, USDA, Riverside, California.
- Stoltz, G., and Gourc, J.P. (2008). Variation of fluid conductivity with settlement of domestic waste. Geotechnical Special Publication no. 177, Proceedings of Geocongress 2008, p 272.
- Straub, W., and Lynch, D. (1982). Models of landfill leaching: moisture flow and inorganic strength. Journal of Environmental Engineering, Vol. 128, 231-250.
- SWANA (2002). The solid waste manager's guide to the bioreactor landfill. SWANA, Oct.
- Thornthwaite, C.W. (1948). An approach toward a rational classification of climate. Geogr. Rev. 38, 57-94.
- Topp, G.C., Davis, J.L., and Chinnick, J.H. (1980). Electromagnetic determination of soil water content: measurements in co-axial transmission lines. Water Resources Research, Vol. 16, No. 3, pp. 574-582.
- Touma, J. and Vauclin, M. (1986). Experimental and numerical analysis of two-phase infiltration in a partially saturated soil. Transport in Porous Media 1, p 27-55.
- Townsend, T. G., Miller, W. L., and Earle, J. F. K. (1995). Leachate recycle infiltration ponds. J. Environ. Eng., 121 (6), 465-471.
- Townsend, T.G., Miller, W.L., Lee, H., Earle, J.F.K. (1996). Acceleration of landfill stabilization using leachate recycle. Journal of Environmental Engineering, 122(4), 263-268.
- Townsend, T.G. and Miller, W.L. (1998). Leachate Recycle Using Horizontal Injection, Advances in Environmental Research, 2(2), 129-138.
- Vachaud, G., Gaudet, J. P., and Kuraz, K. (1974). Air and water flow during ponded infiltration in a bounded column of soil. Journal of Hydrology, Vol. 22, 89-108.
- van Genuchten, M.Th. (1980). A closed-form equation for predicting the hydraulic conductivity of unsaturated soils. Soil Science Society of America Journal, Vol. 44, 892-898.

- Wang, Z., Feyen J., Nielsen D. R., and van Genuchten, M. T. (1997). Two-phase flow infiltration equations accounting for air entrapment. *Water Resour. Res.* 33(12):2759-2767.
- Wang, Z., Feyen J., van Genuchten M. T., and Nielsen D. R. (1998). Air entrapment effects on infiltration rate and flow instability. *Water Resour. Res.* 34(2):213-222.
- Wangemann, S. G., Kohl, R. A., and Molumeli, P.A. (2000). Infiltration and percolation influenced by antecedent soil water content and air entrapment. *Trans. ASAE*, 43(6): 1517-1523.
- Warith, M. (2002). Bioreactor landfills: Experimental and field results. *Waste Management*, 22(1), 7-17.
- Watson, R. (1993). State of Delaware's case history review: a full scale active waste management approach. Presented at the Modern Double Lined Landfill Management Seminar, March 2-4, Saratoga Springs, New York.
- Wilson, L. G. and Luthin, J. N. (1963). Effect of air flow ahead of the wetting front on infiltration. *Soil Science*, Vol. 96, 136-143.
- Zeiss, C., and Uguccioni, M. (1995). Mechanisms and patterns of leachate flow in municipal solid waste landfills. *Journal of Environmental Systems*, 23(3), 247-270.
- Zeiss, C., and Major, W. (1993). Moisture Flow Through Municipal Solid Waste: patterns and Characteristics. *Journal of Environmental Systems*, 22(3), 211-231.
- Zeiss, C. and Uguccioni, M. (1997). Modified Flow Parameters for Leachate Generation. *Water Environment Research*, 69(3), pp. 276-285.
- Zekkos, D., Bray, J. D., Stokoe, K., Kavazanjian, E., Rathje, E., Athanasopoulos, G. A., Riemer, M., Matasovic, N., Lee, J. J., Seos, B. (2008). Recent Findings on the Static and Dynamic Properties of Municipal Solid Waste. *Geotechnical Special Publication no. 177, Proceedings of Geocongress 2008*, p 176.
- Zhan, T., Ling, D., Zhang, W., Chen, Y., (2008). Hydrogeological characterization of Suzhou landfill of municipal solid wastes. *Geotechnical Special Publication no. 177, Proceedings of Geocongress 2008*, p 248.

MICHIGAN STATE UNIVERSITY LIBRARIES



3 1293 03062 4559